ERDC/CHL TR-15-15

US Army Corps
of Engineers®
Engineer Research and
Development Center

ERDC
INNOVATIVE SOLUTIONS
for a safer, better world

Coastal Inlets Research Program

Faleasao Harbor, American Samoa: Investigation of Modifications for Improving Navigation

Zeki Demirbilek, Lihwa Lin, Okey G. Nwogu,
Justin A. Goo, and Thomas D. Smith

November 2015

Coastal and Hydraulics Laboratory

The U.S. Army Engineer Research and Development Center (ERDC) solves the nation's toughest engineering and environmental challenges. ERDC develops innovative solutions in civil and military engineering, geospatial sciences, water resources, and environmental sciences for the Army, the Department of Defense, civilian agencies, and our nation's public good. Find out more at www.erdc.usace.army.mil.

To search for other technical reports published by ERDC, visit the ERDC online library at http://acwc.sdp.sirsi.net/client/default.

ERDC/CHL TR-15-15
November 2015

Faleasao Harbor, American Samoa: Investigation of Modifications for Improving Navigation

Zeki Demirbilek and Lihwa Lin

Coastal and Hydraulics Laboratory
U.S. Army Engineer Research and Development Center
3909 Halls Ferry Road
Vicksburg, MS 39180-6199

Okey G. Nwogu

University of Michigan
Department of Naval Architecture and Marine Engineering
2600 Draper Road, Ann Arbor, MI 48109-2145

Justin A. Goo and Thomas D. Smith

U.S. Army Corps of Engineers, Honolulu District
Building 230
Fort Shafter, HI 96858

Final report

Prepared for U.S. Army Engineer District, Honolulu
Building 230, Fort Shafter, HI 96858

Under Coastal Inlets Research Program

Abstract

This report describes details of a numerical modeling study conducted to evaluate impacts of infrastructure modifications for improving navigation in Faleasao Harbor in American Samoa. This small, shallow-draft harbor is located on the northwest coast of Tau Island, the largest island in the American Samoa islands chain. The existing harbor and three proposed infrastructure modifications (Alternatives) were investigated, and preliminary wave estimates were provided for design and repair of infrastructures. Navigation is affected by waves passing over reefs to the north and northwest of the harbor, and waves shoal and break on these reefs to generate unfavorable conditions to boats entering and leaving the harbor. The harbor entrance is protected on the west by a rocky natural headland, an unraveling detached west breakwater that is now a disconnected spur, and a jetty along the east side of the navigation channel. Vessels access the harbor on the north through a narrow navigation channel and the south end of the channel connects to a small turning/mooring basin where vessels turn or moor at the dock. Wave processes in exterior and interior areas of the harbor were investigated to determine benefits and consequences of the proposed infrastructure modifications for improving navigation in the harbor. These include deepening of the navigation channel and turning basin and adding structures to the tip of west peninsula. Modeling results indicated that the modifications reduced wave energy in the harbor and improved navigation in the channel, turning basin, and dock areas, thereby ensuring access by larger vessels to the harbor. Under typical weather conditions with the proposed modifications, wave estimates obtained indicated that the American Samoa Government's (ASG) largest vessel MV *Sili* would be able to access the harbor.

Contents

Figures and Tables

Figures

Tables

Preface

The Faleasao Harbor study was performed during the time period May 2014 to May 2015 by the Coastal and Hydraulics Laboratory (CHL) of the U.S. Army Corps of Engineers (USACE) Engineer Research and Development Center (ERDC) at the request of the U.S. Army Engineer District, Honolulu (POH).

Dr. Zeki Demirbilek of the Harbors, Entrances, and Structures Branch (HNH), CHL Navigation Division (HN), and Dr. Lihwa Lin of the Coastal Engineering Branch (HNC), HN, conducted the study and wrote this report with contributions by Justin A. Goo and Thomas D. Smith, POH. The USACE Coastal Inlets Research Program (CIRP) provided partial support for this study through improvement of wave processes modeling over the reefs that are important at this project site.

CIRP is administered at CHL under the USACE Navigation Research, Development, and Technology Transfer (RD&T) Program. At the time this effort was conducted, Jeffrey A. McKee was the Headquarters USACE Navigation Business Line Manager overseeing the CIRP. W. Jeff Lillycrop, CHL, was the ERDC Technical Director for Civil Works and Navigation RD&T. Charles E. Wiggins, CHL, was the ERDC Associate Technical Director for Navigation. Dr. Julie Rosati was CIRP Program Manager during the study period. Justin Goo and Tom Smith provided input and oversight for the study.

This study was conducted under the general administrative supervision of James Gutshall, Chief, HNH, and Dr. Jackie Pettway, Chief, HN. José E. Sánchez was the Director of CHL, and Dr. Kevin M. Barry was Deputy Director of CHL.

At the time of publication of this report, COL Bryan S. Green was Commander of ERDC. Dr. Jeffery P. Holland was the ERDC Director.

Unit Conversion Factors

Multiply	By	To Obtain
acres	4,046.873	square meters
cubic yards	0.7645549	cubic meters
feet	0.3048	meters
knots	0.5144444	meters per second
miles per hour	0.44704	meters per second
miles (U.S. nautical)	1.852	kilometers
miles (U.S. statute)	1.609347	kilometers

1 Introduction

Faleasao Harbor is a small, federally constructed, light- and shallow-draft harbor located on the northwestern shore of Tau Island in American Samoa. It is one of the two existing harbors on Tau Island; the other (Tau Harbor) is located at Fusi, on the west shore of Tau. Because of poor navigation conditions at the Fusi Harbor due to large swell waves from south and west during the winter and spring months, Faleasao Harbor is a relief and backup harbor for vessels using the Tau Harbor. However, the small turning basin and docking space at Faleasao Harbor have limited its use by larger vessels. Consequently, Faleasao Harbor is presently only partially accessible by the largest American Samoa Government (ASG) boat named MV *Sili*.

Faleasao Harbor was constructed in 1994 on a shallow, fringing coral reef subject to small tidal range (~0.5 m). The original harbor did not include any breakwaters or other protective structures, so it received additional improvements in the time frame between 1995 and 1999, including the construction of an eastern jetty, a western breakwater, and dredging to expand and deepen the entrance channel and turning basin areas inside the harbor. To further improve navigation at Faleasao Harbor, the Honolulu District (POH) requested that the U.S. Army Corps of Engineers (USACE) Engineer Research and Development Center (ERDC), Coastal and Hydraulics Laboratory (CHL), perform a numerical model study to investigate the existing harbor and proposed modifications. The objective of the numerical modeling was to determine how the proposed modifications to the harbor for accommodating larger vessels would impact the overall navigation and utilization of the harbor. The details of wave processes controlling wave energy in the exterior and interior of harbor, navigation channel, turning basin, and the dock (berthing) area were investigated. Harbors Division of the ASG has reported that the existing depth and dimensions of Faleasao Harbor's entrance channel and turning basin cannot presently accommodate safe ingress, berthing, and egress of the MV *Sili*. Real-time wave estimates are utilized to determine harbor access by MV *Sili* during typical weather conditions. Typical weather conditions for this study were assumed as those during which waves would not result in unsafe transit to and from Faleasao Harbor for the MV *Sili*. Low-frequency wave events were not considered since they would preclude navigation altogether.

Faleasao Harbor is protected on the west side by an elongated, rocky peninsula and also by one rubble breakwater. The peninsula is named Siuai Point. It is a natural headland that has been pounded by typhoons but still remains shore-connected, although it is overtopped by severe storms. The breakwater was built to connect to the peninsula but has since become detached due to damage from strong currents caused by waves overtopping the peninsula. There is also a rubble-mound jetty on the east side along the edge of the channel. A large body of coral fringing reef system covers the north and northwest sides of the harbor that extends to approximately the 260 ft (80 m) depth contour. Reefs transition to deeper water where offshore depths drop sharply into an extremely deep ocean canyon. Consequently, incident waves are not affected by the open ocean bathymetry until they propagate over the fringing reef systems and to the harbor entrance. The coral fringing reef system serves as natural protection for the harbor. The water depth over the reefs decreases as waves approach the entrance channel before moving into the harbor interior to interact with the protective structures and shorelines. Breaking waves over the reefs inside and outside the harbor generate wave-induced currents, which can affect navigation into/out of the harbor as well as the transport of littoral sediments into the channel and other areas in harbor.

To quantify the impacts of waves on navigation in this harbor, two wave models, Boussinesq (BOUSS)-2 Dimensional (B2D) and the Coastal Modeling System (CMS)-Wave, are used. CMS-Wave is a spectral wave model used to transform deep water waves to the project site and to develop wave estimates in the existing harbor and for alternatives. B2D is a Boussinesq-type wave model used to investigate the benefits and impacts of Alternatives on improving navigation. Alternatives included structural modifications, and deepening of the channel and turning basin in the harbor. Impacts of modifications are evaluated for improving navigation and increasing the utilization of the harbor by larger vessels. Pros and cons of modifications (Alternatives) are discussed in terms of percent of harbor usability and improved navigation within the harbor basin.

1.1 Study area

The study area is Faleasao Harbor located on a wide fringing reef on the north side of a sheltered small bay. A small-boat harbor was built in this rugged bay in the 1990s in the northwestern half of the Faleasao embayment (Figure 1-1 and Figure 1-2). Except for the dredged access channel, turning basin, boat dock, and launching areas, there are short and narrow beach segments in parts of the bay. The rest of the bay is

covered with rocks and cobbles and shallow semiexposed reefs. The adjacent beach east of the harbor contains poorly sorted coarse sand, coral rubble, shells, and some boulders. The existing harbor was constructed in the lee of Siuai Point, a natural headland. This harbor includes an entrance channel, a shore-connected short eastern jetty, a western spur detached from the land, a dock, launch ramp, and turning basin in the back side of the harbor. The harbor basin is approximately 2.3 acres in size.

Figure 1-1. American Samoa Manua Group.

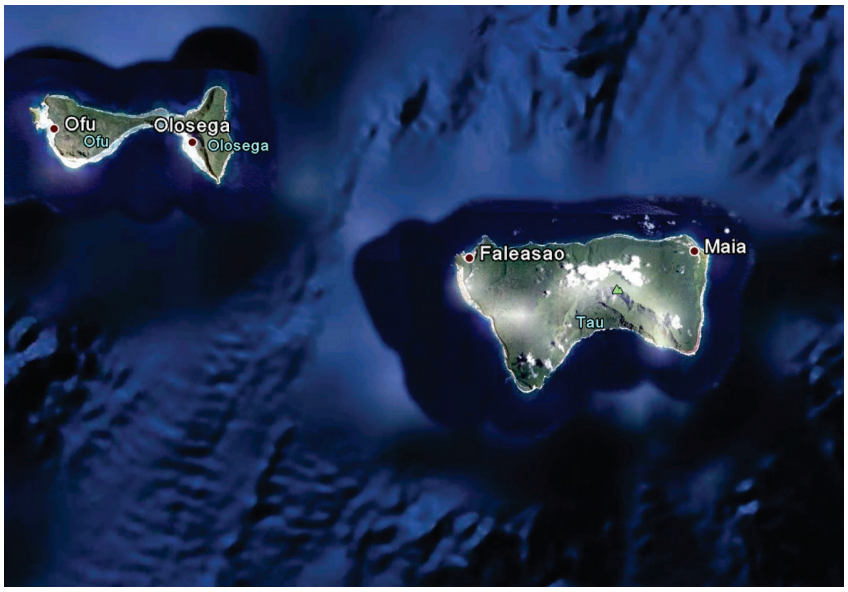

Figure 1-2. Study area location map.

Faleasao Harbor was constructed by the Federal Emergency Management Agency for the ASG in 1990 under a Department of the Army permit (PODCO-2179). In 1994, the entrance channel, turning basin, dock, and east groin were constructed for ASG by the USACE. The west breakwater was added as part of a 1995 improvement project and completed in 1999. The west breakwater was added because excessive wave energy refracted around the large rocky peninsula west of the entrance channel. During the 1995 improvement project, the turning basin was widened to the west by 50 ft (15 m).

Presently, Faleasao Harbor consists of the following navigation features. A solid pier structure has a 115 ft (35 m) long dock face. The dock in the back bay is aligned in a northeast to southwest direction, looking west toward the large rock peninsula and the unraveling landward half of west breakwater. The 380 ft (116 m) constructed length of the west breakwater has been reduced to 190 ft (58 m), and half of the breakwater is lost. The entrance channel is 13 ft (4 m) deep and 420 ft (128 m) long, and channel width varies from 100 ft (30 m) to 150 ft (45 m). The turning basin is 11 ft (3.5 m) deep, 200 ft (61 m) wide, and 220 ft (67 m) long. There is a landing craft utility (LCU) ramp adjacent to the dock, which is 50 ft (15 m) wide and 140 ft (43 m) long. It joins with a 500 ft (150 m) revetment, providing a berthing space of 11 ft (3.5 m) deep and 118 ft (36 m) long.

The modifications considered in the present study to the inner harbor are collectively referred to as *Alternatives*. Each Alternative involves a modification or change to one of the existing navigation features or the addition of a new structure. The specifics of Alternatives were determined jointly by POH and CHL study team members. These are described later in this chapter following an outline of the study plan.

1.2 Study plan

1.2.1 Purpose

There was no information available about prior field data collection or numerical modeling studies conducted for Faleasao Harbor. Because the focus of present study was limited to wave modeling at Faleasao Harbor for improving navigation, hydrodynamics and sediment transport issues were not considered in this study. Combined wave and current modeling may be necessary in the future to ascertain long-term behavior of harbor response to waves, including potential effects of hydrodynamics and

sediment processes on navigation and impacts of dredging and expansion of berthing and mooring areas on the entire harbor complex.

The most recent bathymetric, wind, and wave data available for this site were used in the numerical modeling investigation. Together with the bathymetric data, it is the magnitude and direction of forcing conditions (winds, waves, water levels) used that determine the impacts of waves on exterior and interior conditions in this harbor and how waves are affecting boats in the navigation channel, interior berthing areas, docks, and turning basin. The ultimate goal is to advise the ASG on how the proposed modifications to the harbor will affect navigation in the entrance channel and harbor interior. The wave estimates will be used to determine if harbor access by the ASG's larger vessel, the MV *Sili*, is possible during normal operational conditions. The existing depth and dimensions of the Faleasao entrance channel and turning basin cannot accommodate safe ingress, berthing, and egress of the MV *Sili*, so proposed Alternatives were selected to address these specific needs of study.

1.2.2 Approach

As noted in the previous section, it was necessary to use two wave models for developing wave estimates for this site. CMS-Wave, a spectral wind-wave transformation model for open coast and nearshore, was used for regional-scale, deep-water wave transformation and estimates of harbor access and usability. B2D, a Boussinesq-type nonlinear, time-domain wave model developed specifically for modeling waves in nearshore applications for navigation studies, channel widening, and deepening, was used for infrastructure modifications to ports, harbors, and marinas. Several improvements to CMS-Wave were made to develop inputs as well as to address this project's other needs. These additional R&D developments to improve model's predictive capabilities were funded by the Coastal Inlets Research Program (CIRP). The advances of CMS-Wave funded by CIRP included (a) analysis of wave hindcast, wind, and water level data for simulations of three tropical storms and nonstorm waves in a full-plane mode, (b) modeling of a dual-peaked wave spectrum with seas and swells from different directions,(c) development of pre- and postprocessing analysis codes for improving model setup, (d) development of Fortran and Matlab programs to provide B2D input conditions as wave parameters (height, period, direction) and two-dimensional (2D) wave spectra, (e) development of a number of Fortran and Matlab utilities to facilitate coupling of the two wave models and analyses of models results in time

and frequency domains, and (f) development of Matlab codes for comparison of wave spectra plots from solution files of both models.

The combination of the two wave models was necessary to address the needs of this project. In addition to differences between the models' theoretical and numerical formulations, different spatial extents and resolutions of model grids were necessary to model waves properly for the needs of this project, despite the stated differences between the two different classes of wave models, where possible general comparison of two models is considered.

Long-term wave climate in deep water is required to perform such numerical modeling studies for port and harbor studies. Deep-water wave data for this study were based on the Wave Information Studies (WIS) hindcast time series (1980–2011) available in the American Samoa region. Incident deep-water waves were transformed to the project site using CMS-Wave. The model result from CMS-Wave was used as input wave forcing at the boundary of the B2D model domain for evaluation of modifications (Alternatives) to infrastructures for improving navigation at Faleasao harbor.

Because no wave or water level field data were available in the harbor area, both CMS-Wave and B2D were applied using the default model settings recommended in the CMS-Wave and B2D technical reports (Lin et al. 2008; Nwogu and Demirbilek 2001). The use of default settings in both models has been demonstrated in other harbor and inlet applications with similar coral reef coast and hard bottom conditions (Demirbilek et al. 2015; Lin et al. 2011).

The modeling and analysis of predominant wave and wind conditions were utilized to determine which proposed modification(s) would allow the MV *Sili* to access the harbor during typical weather conditions. Transit into/out of the harbor during extreme conditions is not possible, but the extreme conditions were also investigated in this study to provide POH design wave estimates for the next phase of this project. Estimates of wave parameters (height, period, and direction) for operation and design works were provided at this study site using both the B2D and CMS-Wave models. These estimates may be combined with experiences of mariners to develop guidance for vessel transits and to determine infrastructure modifications which can increase operational efficiency of the harbor (i.e., improving both

access and utilization of the harbor). The B2D modeling also helps identify if potential surge problems would occur in this harbor. Ultimately, the numerical modeling predictions will help POH to determine the efficacy of proposed Alternatives for improving the navigation at Faleasao Harbor.

1.2.3 Study tasks

The main tasks of this study were (1) define regional meteorological and oceanographic conditions (e.g., winds, waves, water levels),(2) assemble bathymetric, shoreline, and structural data for interior and exterior regions of the harbor, (3) calculate waves in the existing harbor, (4) investigate how deepening of the entrance channel and turning basin, and structural modifications would affect waves for boats which access this harbor, and (5) analyze model results and summarize key findings in a technical report.

2 Data

2.1 Bathymetry and coastline data

Coastline digital data for this study were extracted from the National Geophysical Data Center (NGDC, http://www.ngdc.noaa.gov/mgg/coast/getcoast.html), and a georeferenced image file downloaded from Google Earth 5.0 (http://earth.google.com).

The bathymetry data used in this study were obtained from various sources covering the harbor, land, nearshore, and offshore area, but no new survey data were acquired for this project. The harbor area including the interior, channel, structures, and shoreline data were based on POH surveys conducted after the harbor construction. Because the harbor bottom and adjacent coast are primarily reef rock and are deprived of sediment, the previous survey data are considered to be valid and used for the present harbor study. The offshore bathymetry was based on the 16.4 ft (5 m) grid map from the Pacific Islands Benthic Habitat Mapping Center (http://www.soest.hawaii.edu/pibhmc/pibhmc_amsamoa_tau_bathy) and on 3-arc-sec bathymetry and topography of coastal digital elevation models (DEMs) by the NGDC (http://www.ngdc.noaa.gov/dem/squareCellGrid/download/647). All datasets were converted to the mean lower low water (MLLW) datum.

2.2 Water levels

Water level data for 1996–present time were available from NOAA Coastal Station 1770000 at Pago Pago, Tutuila. The tide at the study site was mixed semidiurnal, with a spring range of 2.7 ft (0.83 m) and a neap range of 1.3 ft (0.4 m). The measured mean and tidal ranges at this station are listed in Table 2-1. Figure 2-1 shows the time history of measured water levels at Pago Pago for January–June 2010 relative to the mean sea level (MSL).

Table 2-1. NOAA Station 1770000 (Pago Pago).

Station	Latitude	Longitude	Mean Tidal Range (m)	Diurnal Range (m)
1770000	14° 16.8' S	170° 41.4' W	0.77	0.83

Figure 2-1. Measured water levels at Pago Pago for Jan–Jun 2010.

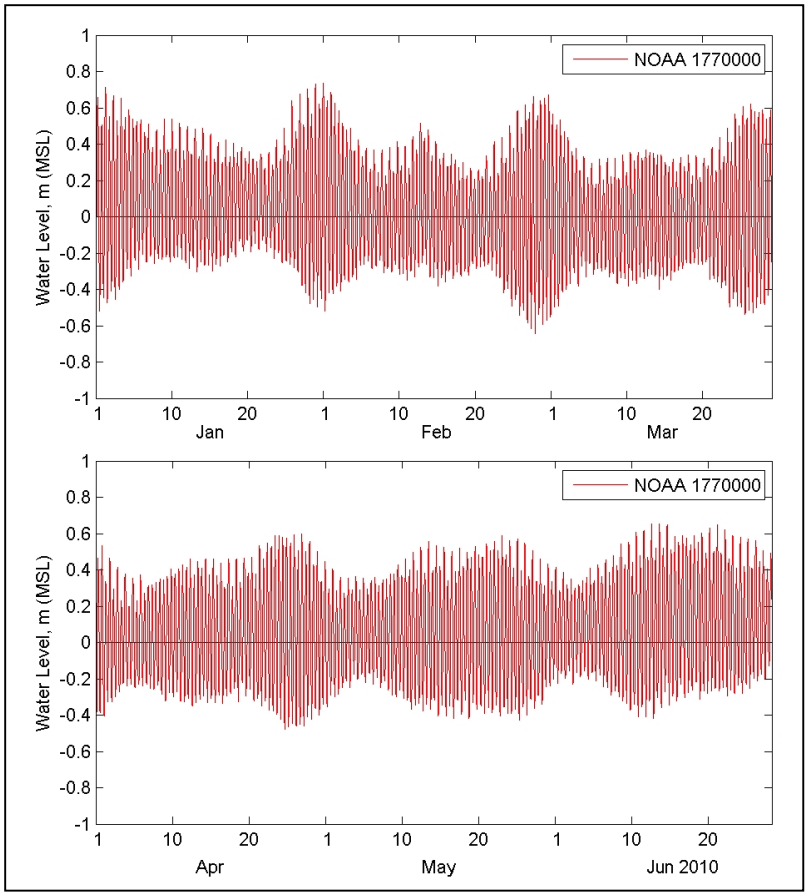

2.3 Wind and wave data

Coastal wind data available at Pago Pago station (1770000) for 2008–present time were used in this study. In this region of the southern hemisphere, trade winds from the east are moderate during the months of May to November, and winds are variable for the rest of the year. The cyclonic typhoon/hurricane season is during the winter months, and strong tropical storms have caused coastal damage every 3 to 5 years. Figure 2-2 shows the wind speed and direction measured at Pago Pago for 2010.

Waves at American Samoa and vicinity include wind seas generated by the easterly trade winds and the ocean swells from the south or north. There are no wave measurements at Tau and nearby Ofu and Olosega islands. Offshore wave hindcast data for 32 years (1980–2011) are available from the WIS. Figure 2-3 shows the nearest WIS stations north and west of Tau. In the present modeling study, WIS Sta 81137 (13.5° S, 169.5° W) was used for the incident wave conditions.

Figure 2-2. Measured wind speed and direction at Pago Pago for 2010.

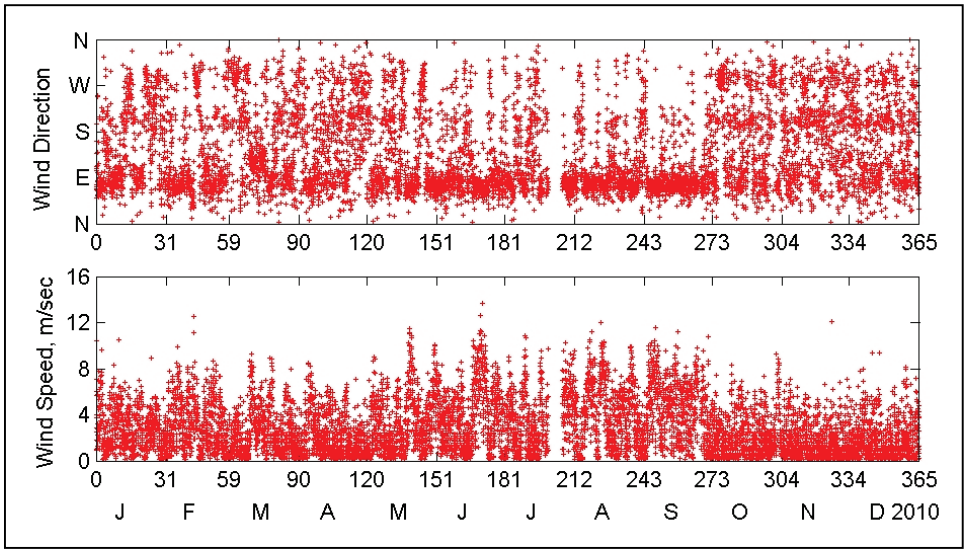

Figure 2-3. The WIS stations near Faleasao Harbor.

Figures 2-4 and 2-5 show the wind and wave rose diagrams for WIS 81137, respectively. Figure 2-6 shows the time history of hindcast wind and waves at WIS 81137 for 2010. The maximum wave condition with significant wave height H_s = 5.1 m, and spectral peak period T_p = 9.7 sec occurred on 13 February 2010, which was produced by the Category 3 Hurricane Rene.

Figure 2-4. Wind rose at WIS 81137.

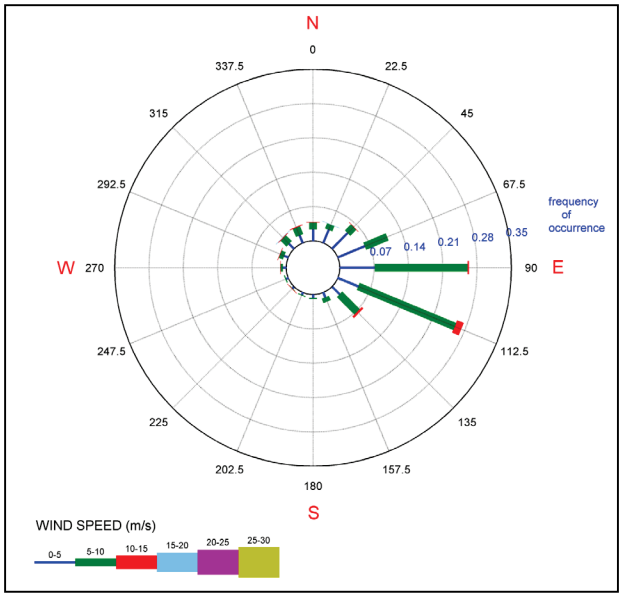

Figure 2-5. Wave rose at WIS 81137.

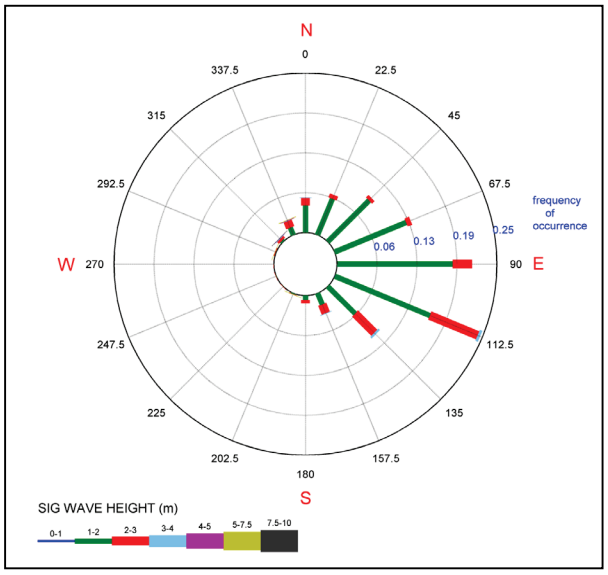

Figure 2-6. Year 2010 hindcast wind and wave data at WIS 81137.

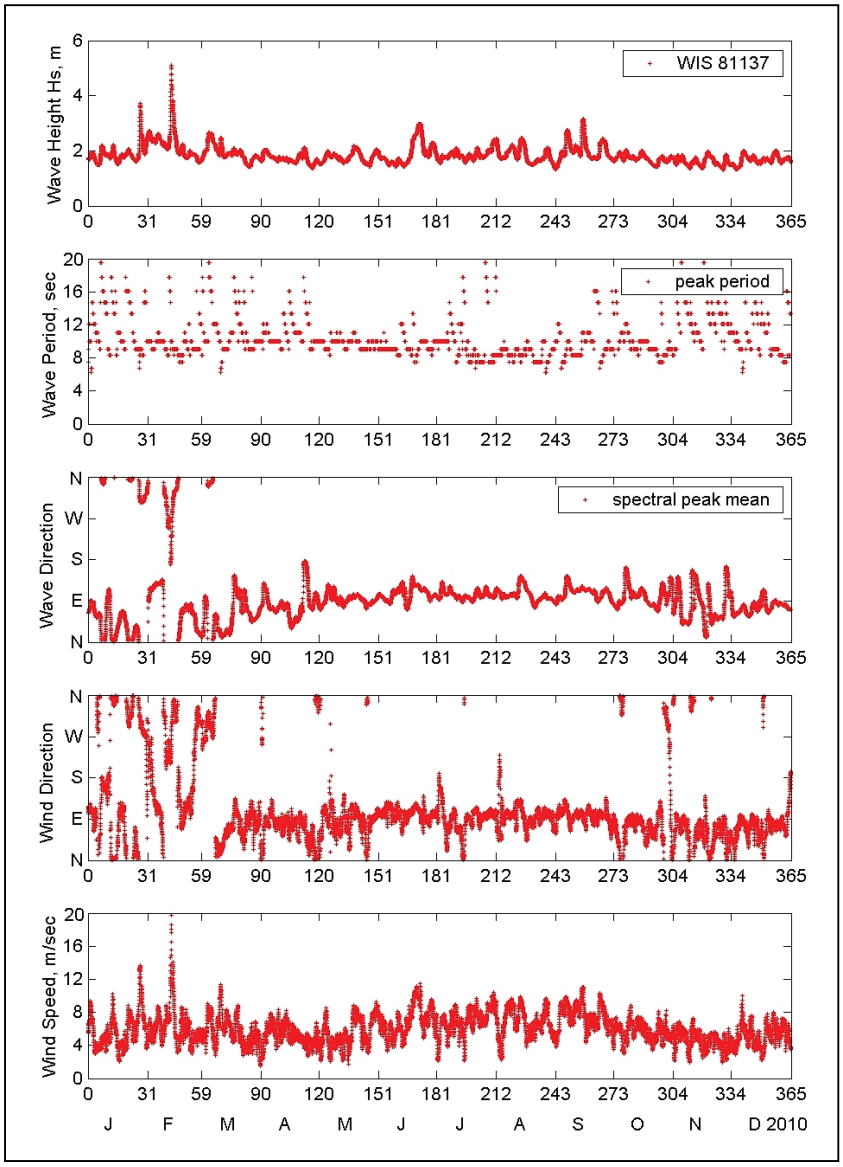

Analysis of the wave data at WIS Sta 81137 indicated seasonality in the average wave height and wind speed, with annual mean significant wave height and mean wave period of approximately 1.6 m and 10.5 sec, respectively. The corresponding annual average wind speed was 6 m/sec, and majority of the wind and waves from the east sector are caused by the trade winds.

Chapters 3, 4, and 5 describe details of two types of wave modeling performed using the data summarized in Chapter 2.

3 CMS-Wave Modeling

Two classes of wave models, BOUSS-2D (B2D) and CMS-Wave, were used to investigate improvement of navigation at Faleasao Harbor. B2D is a Boussinesq type 2D wave model (Demirbilek et al. 2007b; Demirbilek et al. 2005a, 2005b; Nwogu and Demirbilek 2001). This model is used in this study to investigate proposed Alternatives at Faleasao Harbor, which represent different infrastructure changes. CMS-Wave is a steady-state 2D spectral wave model CMS-Wave (Lin and Demirbilek 2012; Lin et al. 2011; Demirbilek and Rosati 2011; Lin et al. 2008; Demirbilek et al. 2008). It is used to transform deep-water incident waves to nearshore to develop input conditions for B2D. CMS-Wave is part of an integrated Coastal Modeling System (CMS) for coastal inlet navigation and regional sediment modeling applications. A short description of CMS is provided in Appendix A.

As a nonlinear, time-domain wave model capable of representing various wave processes occurring from deep to shallow water, B2D is a computationally resource-demanding model. Large domain modeling around this harbor was not possible with B2D because a large number of wave conditions affecting navigation in this harbor had to be simulated. It was necessary to augment B2D modeling with a spectral wave model capable of providing wave estimates over a large domain for many wave conditions. Because of complementary features of B2D and CMS-Wave, these two models are frequently used in tandem in coastal studies. CMS-Wave was used to transform the deep-water waves to seaward boundary of B2D. A short summary of B2D model and its capabilities is presented in Appendix B. Chapter 4 describes details of the B2D modeling effort.

CMS-Wave can be used in half-plane or full-plane mode to transform deep water waves to project sites nearshore. The half-plane is the default mode for CMS-Wave, and the model runs efficiently in this mode as waves are transformed primarily from deep water toward shore. CMS-Wave is based on the wave-action balance equation that includes wind-wave generation and growth, wave propagation, refraction, shoaling, diffraction, reflection, breaking, and dissipation. The computational efficiency of CMS-Wave and recent improvements to the capabilities of the model (Lin and Demirbilek 2012; Lin et al. 2011; Demirbilek and Rosati 2011) allow for simulating large spatial domains and a large number of wave conditions in coastal engineering applications. The reminder of this chapter is focused on detailed information about CMS-Wave modeling for Faleasao Harbor.

3.1 Description of Alternatives

The main features of Faleasao Harbor configurations investigated in this study are listed in Table 3-1. The existing harbor is Alternative 0 (Alt-0), and three Alternatives with specific infrastructure modifications to the existing harbor are Alternative 1 (Alt-1), Alternative 2 (Alt-2), and Alternative 3 (Alt-3). See Table 3-1 for a list of key features of each alternative.

Table 3-1. Four harbor configurations.

ID	Configuration	Features
Alt-0	Existing Harbor	Existing harbor geometry.
Alt-1	Deepen channel and turning basin	Deepen navigation channel and navigable parts of turning basin from -10.5 ft (-3.2 m) to -19 ft (-5.8 m), MSL.
Alt-2	Alt-1 with 230 ft west breakwater	A 230 ft (70 m) long breakwater from the tip of the peninsula eastward toward the channel is added to Alt-1.
Alt-3	Alt-1 with 280 ft west breakwater	A 280 ft (85 m) long breakwater from the tip of the peninsula eastward toward the channel is added to Alt-1.

3.1.1 Alternative 0 (Alt-0)

The Alt-0 configuration represents the existing harbor. The present harbor geometry (Figure 3-1) is different than the original harbor as designed and modified in 1990s. One key difference is an isolated spur structure on the west side of the harbor. This short and shallow-crest spur structure previously was connected to the west headland, but it is presently a disconnected structure at MSL. The channel and turning basin are comparatively shallower due to natural sedimentation occurring in the harbor. Figure 3-1 depicts the present geometry of the existing harbor. Depth contours in the vicinity of the entrance channel and interior harbor and the structures are color coded, with land boundaries shown in orange lines. Depths in the present channel vary from -10 to -13 ft (-3 to -4 m) MSL, and in other areas of the harbor, the depths are shallower. The channel width varies at the north and south ends, where it is approximately 150 ft (46 m) and 135 ft (41 m), respectively. Water depths over the coral fringing reefs to the north and northwest before the start of the entrance channel are comparatively much deeper than depths in the channel . Depths in the open ocean beyond the reefs drop sharply into a canyon, becoming very deep. These and other characteristics of the existing harbor are represented in model grids.

Figure 3-1. The geometry of existing harbor (Alt-0).

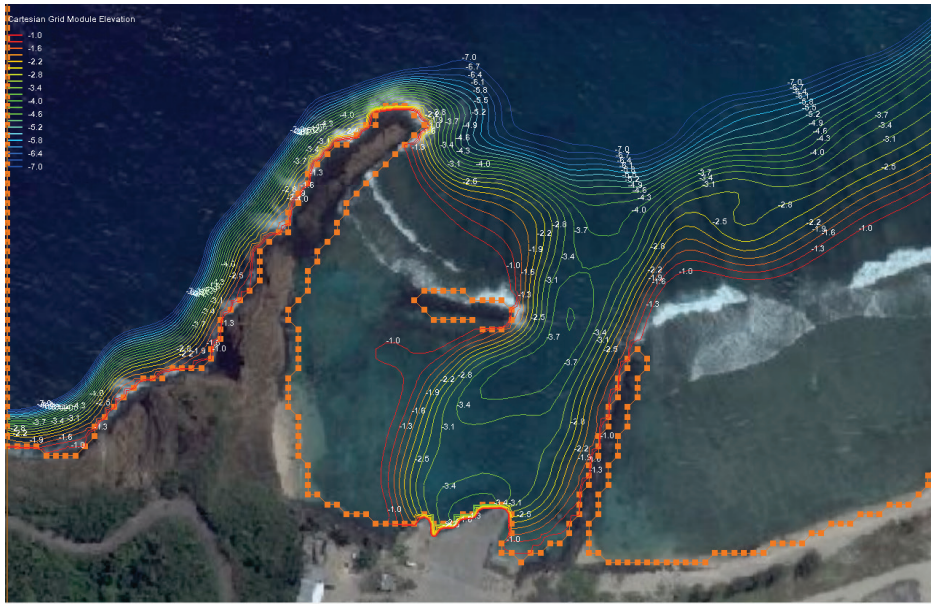

3.1.2 Alternative 1 (Alt-1)

Alt-1 configuration is shown in Figure 3-2, showing the infrastructure modifications and extent of changes made. Alt-1 involved deepening the navigation channel from -13 ft to -19 ft (MSL) and the turning basin from -10.5 ft to -19 ft (MSL). For comparison, the average depth of these areas is -10.5 ft (MSL) in Alt-0. The boundaries of deepened polygon area are shown in green color in Figure 3-2. The channel widths at the north and south ends remain as in Alt-0, which are 150 ft (46 m) and 135 ft (41 m), respectively. Channel widening was not considered due to concerns that more wave energy may get into the channel, turning basin, and dock areas.

3.1.3 Alternative 2 (Alt-2)

The Alt-2 configuration included one additional modification to Alt-1 by adding a 230 ft (70 m) long west breakwater to the tip of the west peninsula. Figure 3-3 shows a sketch of the added structure that extends northeast toward the channel entrance. This added breakwater is a rubble-mound structure with a crest elevation of 6.6 ft (2 m) (MSL) and side slopes 2 on 3 (2:3).

Figure 3-2. The geometry of Alt-1.

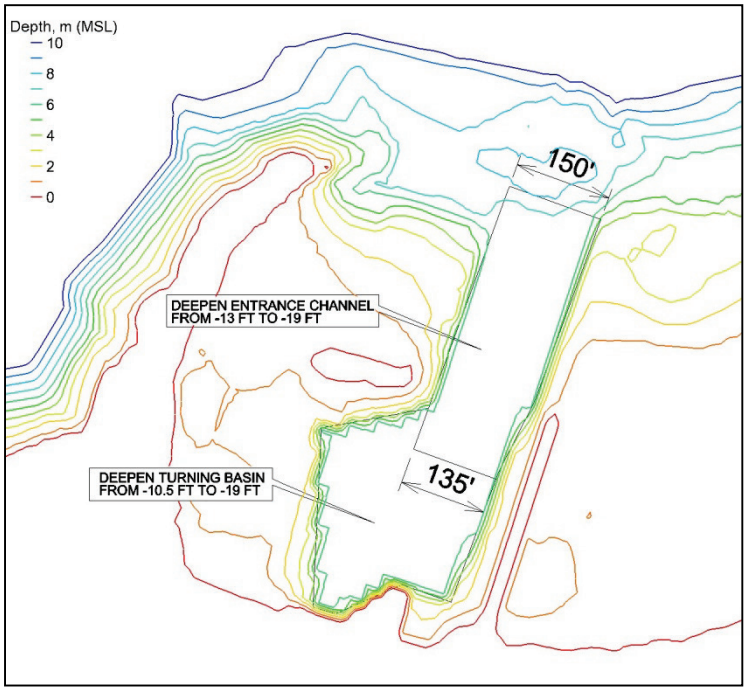

Figure 3-3. The geometry of Alt-2.

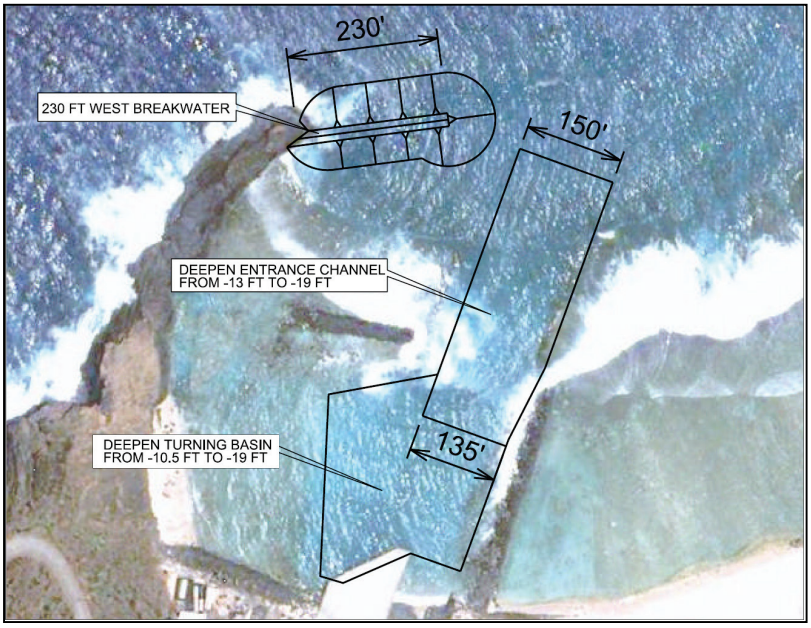

3.1.4 Alternative 3 (Alt-3)

This Alternative is similar to Alt-2 and required making one more modification to Alt-1 by adding a 280 ft (85 m) long west breakwater to the tip of the west peninsula. Therefore, the added breakwater in Alt-3 is a longer version of the structure in Alt-2. Figure 3-4 shows a sketch of the

added structure that extends northeast toward the channel entrance. The breakwater is a rubble-mound structure with a crest elevation of 6.6 ft (2 m) (MSL) and sloping sides 2 on 3 (2:3).

Figure 3-4. The geometry of Alt-3.

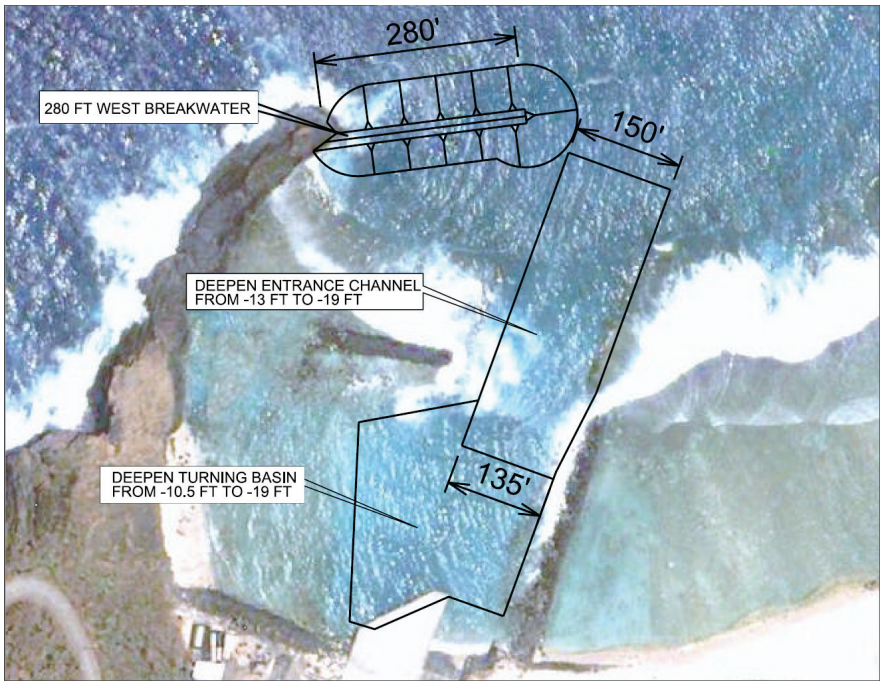

3.2 Model domain

Numerical model grids were developed for four harbor geometries, the existing configuration (Alt-0), and three Alternatives (Alt-1, Alt-2, and Alt-3). These four grids had the same seaward bathymetry but different harbor interior areas and bathymetric changes specific to each Alternative (Figures 3-1 to 3-4). Because CMS-Wave was forced with deep-water incident waves, the modeling domain was extended farther into the ocean at greater depths. The BOUSS-2D model domain was comparatively smaller, covering the harbor and coral reefs to the north and northwest of the harbor. Details of the CMS-Wave model domains and simulations are provided in the remainder of this chapter, and BOUSS-2D modeling is described in Chapter 4.

The CMS-wave grid covered a large rectangular area approximately 21 miles × 24 miles (13 km × 15 km). It included the eastern coast of Olosega and northwest coast of Tau. The grid cell size in the model varied from 20 to 1,640 ft (6 to 500 m) and water depths 0 to 7,550 ft (0 to 2,300 m). The model grid was used to transform offshore incident wave

conditions to the project site nearshore to develop wave conditions for B2D. Figure 3-5 shows the CMS-Wave model domain with incident waves applied to the north, northeast, and northwest boundaries of the grid

Figure 3-5. CMS-Wave model domain.

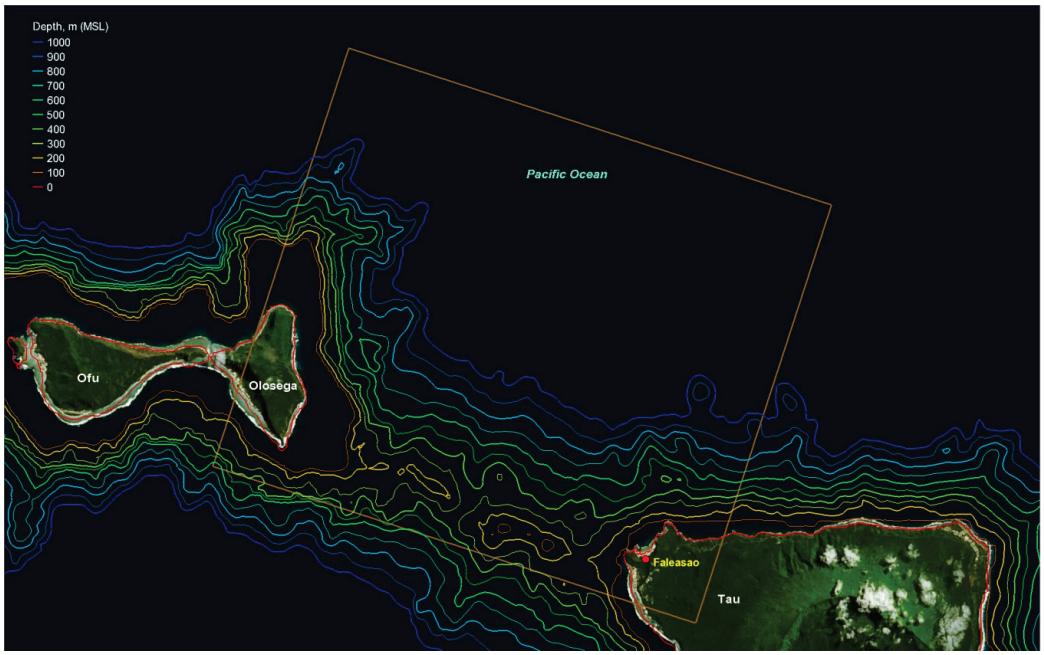

3.3 Incident wave conditions

Storm and average waves affecting Faleasao Harbor were selected as incident waves for CMS-Wave modeling. The extreme wave analysis results at the WIS Sta 81137 are shown in Figure 3-6. Storm events were selected from the top 10 events based on maximum significant wave height. Three wave conditions representing storms from north and northwest directions were selected. Two conditions corresponded to recent powerful Category-5 cyclones, Heta in January 2004 and Olaf in February 2005. Note that Olaf passed almost directly over Tau, causing substantial damage to properties and reefs. The third storm in January 1987 was the Category-1 Hurricane Tusi, which made a direct hit on the island of Tau. Table 3-2 presents wind and wave conditions for the three storms modeled with CMS-Wave at two different water levels, 0 m and 0.5 m (MSL).

Figure 3-6. Extreme wave height analysis results for WIS Station 81137.

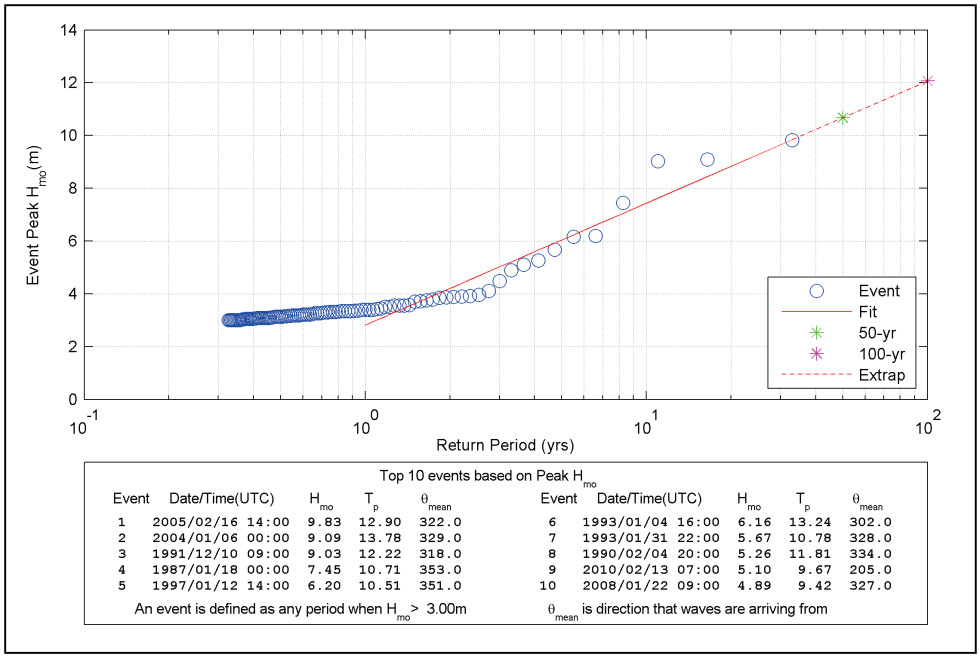

Table 3-2. Storm wind and wave conditions simulated with CMS-Wave.

Date/Time (UTC)	Storm Wind and Wave Condition*	Water Level (m, MSL)	Label
2005/02/16 14:00	H_s=9.83 m, T_p=13 sec, θ_m=320 deg, U_w=30 m/sec, θ_w=315 deg	0	H9.8T13D320W0
		0.5	H9.8T13D320W0.5
2004/01/06 00:00	H_s=9.09 m, T_p=14 sec, θ_m=330 deg, U_w=23 m/sec, θ_w=350 deg	0	H9.1T14D330W0
		0.5	H9.1T14D330W0.5
1987/01/18 00:00	H_s=7.45 m, T_p=11 sec, θ_m=0 deg, U_w=29 m/sec, θ_w=340 deg	0	H7.5T11D0W0
		0.5	H7.5T11D0W0.5

* Mean wave direction θ_m and wind direction θ_w are based on the meteorological convention (from). Wind speed U_w is from WIS 81137 at 10 m above the water surface.

Three wave directions (θ_m = 0°, 320°, and 340°) were used to transform the annual mean height and period data at WIS Sta 81137 to the project site. The effect of tides in these simulations was considered by running CMS-Wave for the two water levels (0 m and 0.5 m, MSL) that correspond to approximately low and high water levels, respectively. Figure 3-7 shows the joint probability distribution of significant wave height and peak wave period for 2010 at WIS Sta 81137. Excluding tropical events, the annual mean significant height and peak period are 1.5 m and 10 sec, respectively. These values were applied to the CMS-Wave grid north boundary. Average wave conditions selected for CMS-Wave modeling are provided in Table 3-3.

Figure 3-7. Joint distribution of wave height and period at WIS Sta 81137 for 2010.

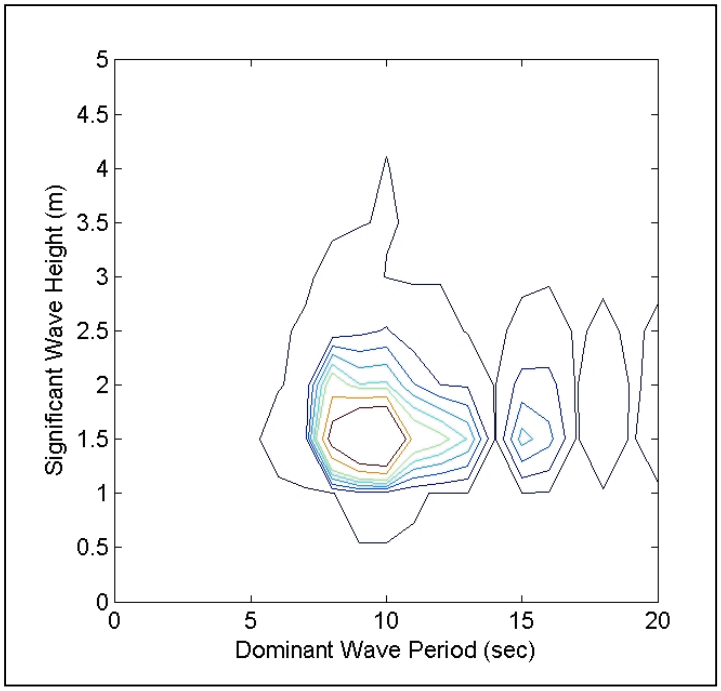

Table 3-3. Average wave conditions simulated with CMS-Wave.

Average Wave Condition*	Design Water Level (m, MSL)	Label
H_s=1.5 m, T_p=10 sec, θ_m=320 deg	0	H1.5T10D320W0
	0.5	H1.5T10D320W0.5
H_s=1.5 m, T_p=10 sec, θ_m=340 deg	0	H1.5T10D340W0
	0.5	H1.5T10D340W0.5
H_s=1.5 m, T_p=10 sec, θ_m=0 deg	0	H1.5T10D0W0
	0.5	H1.5T10D0W0.5

* Mean wave direction θ_m is based on the meteorological convention (coming from).

3.4 Alt-0 results for storm waves

Modeling results are provided in this section for storm waves, which may be used in design and repair of structures for protection of Faleasao Harbor. Description of model output transects and saved output locations are presented in this section. Modeling results for average (i.e., typical) operational conditions are provided in the next section.

CMS-Wave was run for six incident wave storm conditions with wind input (Table 3-2). Default lateral and backward reflection coefficients of

0.5 and 0.3, bottom friction (Darcy-Weisbach coef = 0.01), were used in these simulations. Calculation of infragravity wave forcing was activated for potential long-period swell effects. Model results were saved over the entire computational domain, including three engineering wave parameters (significant wave height, peak period, and mean direction). Calculated directional spectra were saved at 70 output locations (i.e., save stations) along nine transect lines (T1–T9) shown in Figure 3-8 that cover the areas of interest inside and outside the harbor.

Figure 3-8. Output transects T1 to T9 used in CMS-Wave modeling.

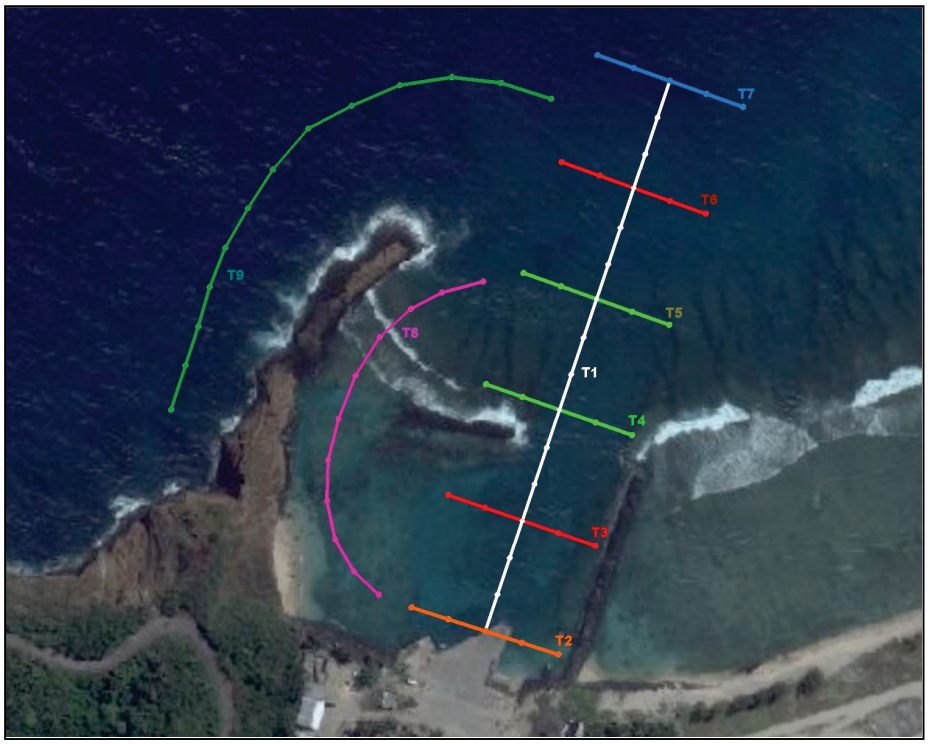

Transect T1 is a 984 ft (300 m) straight line along the entrance channel centerline. Transects T2 to T7 are each 262.5 ft (80 m) long and perpendicular to T1 (Figure 3-8). Transect T8 along the west side of harbor interior is 690 ft (210 m) long. Transect T9 along the west side of the harbor exterior (ocean side of Siuai Point) is 984 ft (300 m) long. Figures 3-8 and 3-9 display the nine transects (T1 to T9) and 70 output locations along these transects, respectively. Some transects are not straight lines. Transects T2 to T7 are nearly perpendicular to the channel centerline and oriented northwest to southeast whereas T1, T8, and T9 are oriented southwest to northeast.

Figure 3-9. Output locations (70) along transects (9) used for CMS-Wave modeling.

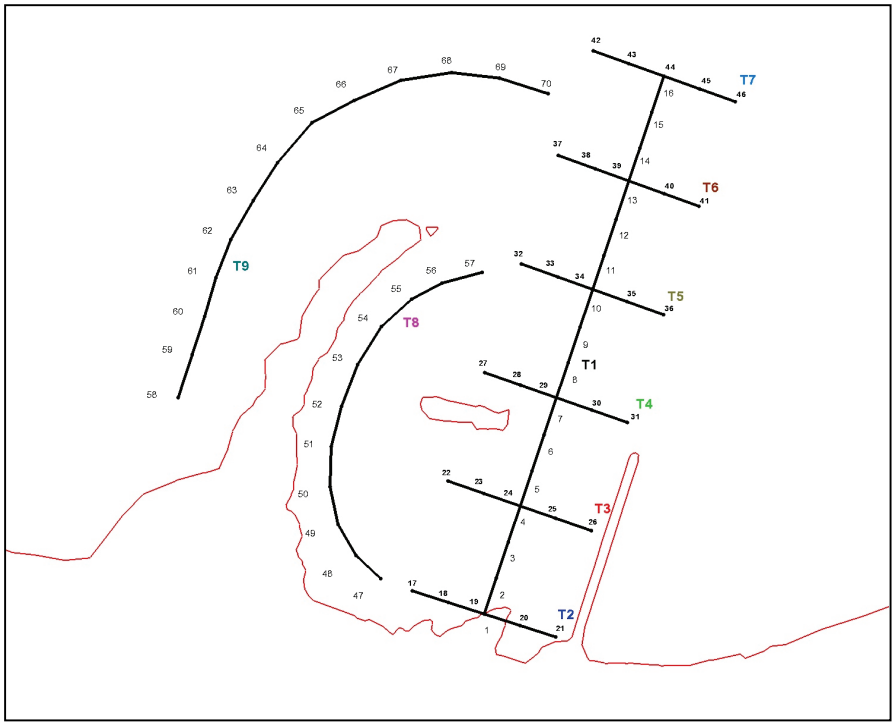

Examples of calculated storm wave field (storm event H9.1T14D330W0.5) snapshots for the entire model domain and local harbor area are provided in Figures 3-10 and 3-11, respectively. Figures 3-12 to 3-20 show wave heights calculated along T1 to T9 for six storm conditions (three incident waves at two water levels). In these figures, the horizontal axis is the distance along a transect line.

Overall, CMS-Wave results indicate storm wave heights decrease by 10% to 30% between the offshore incident wave boundary located in deep water and the most seaward transect (T7) at the harbor entrance. After waves pass over the reefs located north and northwest of the harbor, the variation in wave height along the transect that passes through the center of the channel (T1) shows that wave heights reduce and wave energy dissipates while propagating into harbor. This is because waves inside the channel are depth limited in this relatively shallow channel. Wave heights at the dock (T2) range from 0 to 1.8 m for all simulated storms and thus do occasionally exceed the wave height threshold of 1.5 m requirement for boats to stay safely inside the harbor. Wave heights are greater in the turning basin (see results for transects T3 and T4), ranging from 0.2 to 2.2 m at low water level (0 m, MSL), and 0.7 to 3 m at high water level (0.5 m, MSL).

Figure 3-10. Regional wave field for storm event 9.1T14D330W0.5 (Alt-0).

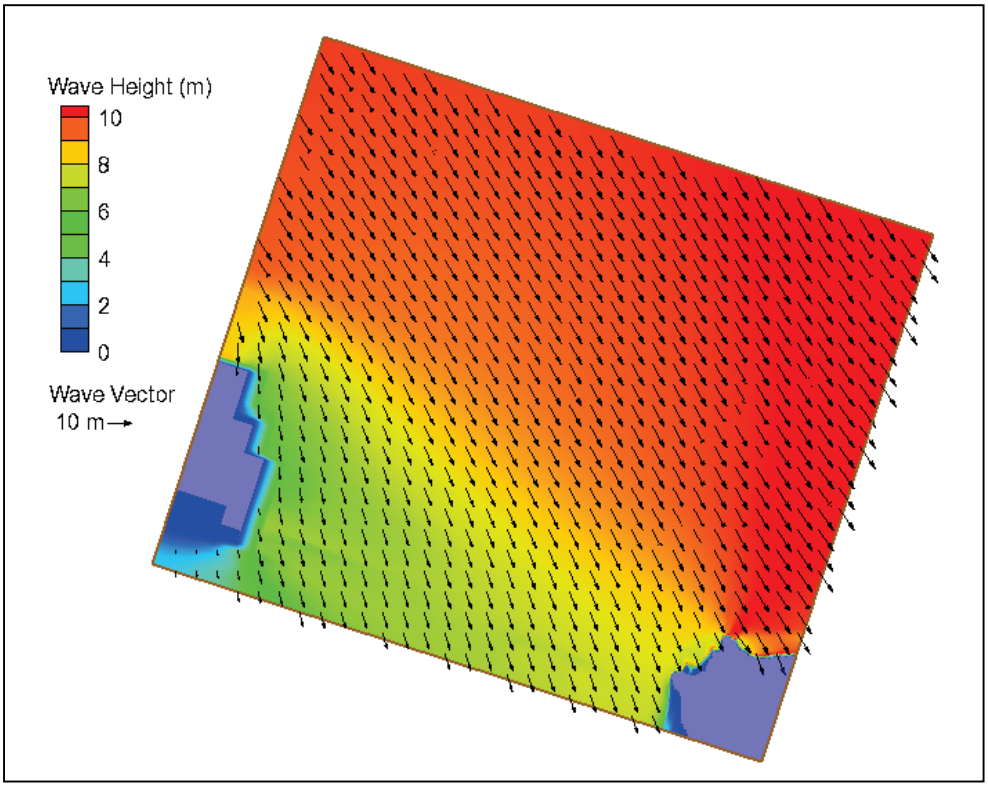

Figure 3-11. Harbor wave field for storm event 9.1T14D330W0.5 (Alt-0).

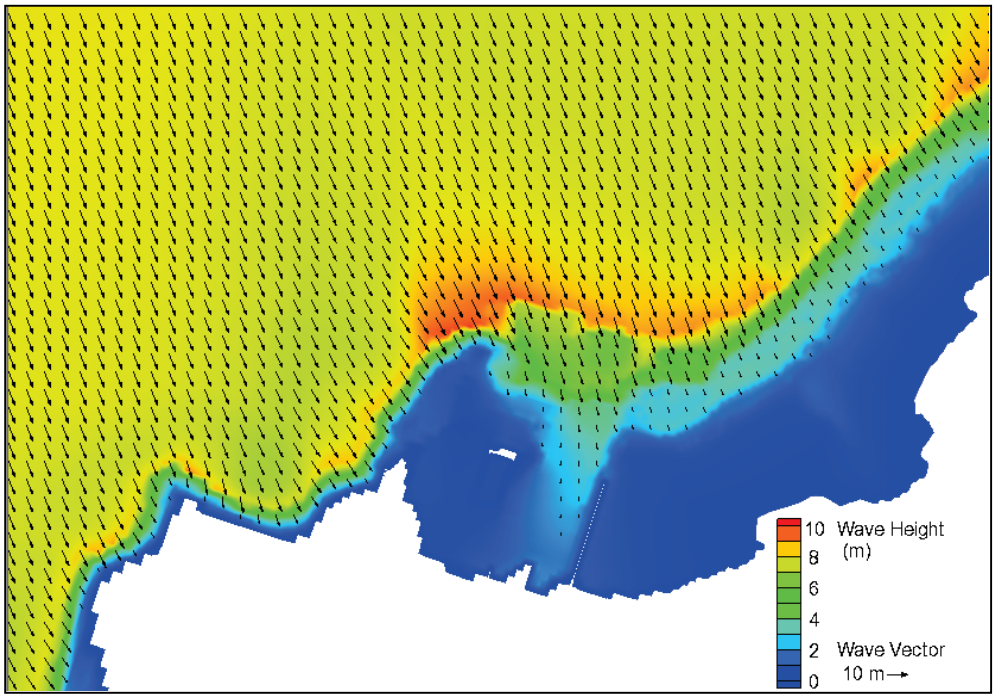

Figure 3-12. Wave height variation along T1 for three storms at two water levels (Alt-0).

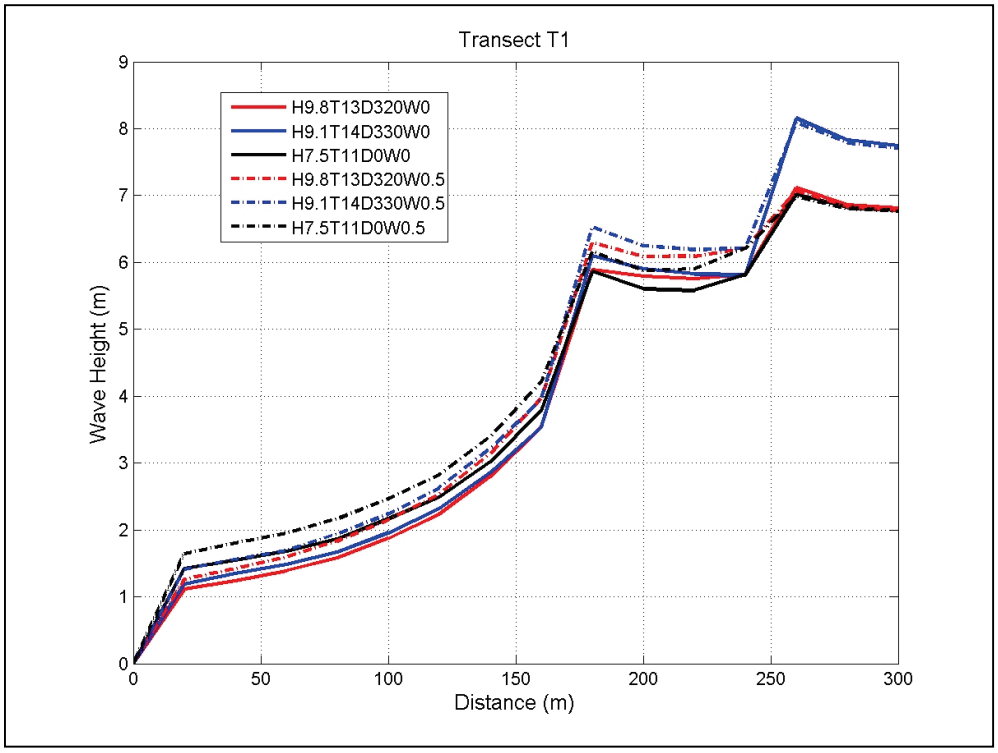

Figure 3-13. Wave height variation along T2 for three storms at two water levels (Alt-0).

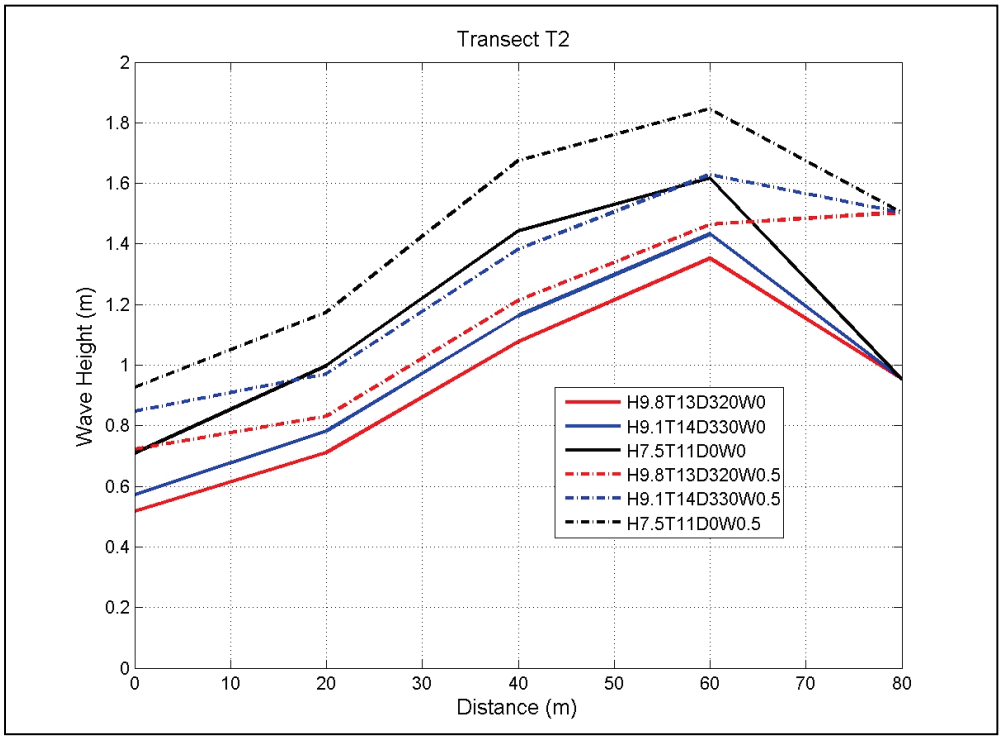

Figure 3-14. Wave height variation along T3 for three storms at two water levels (Alt-0).

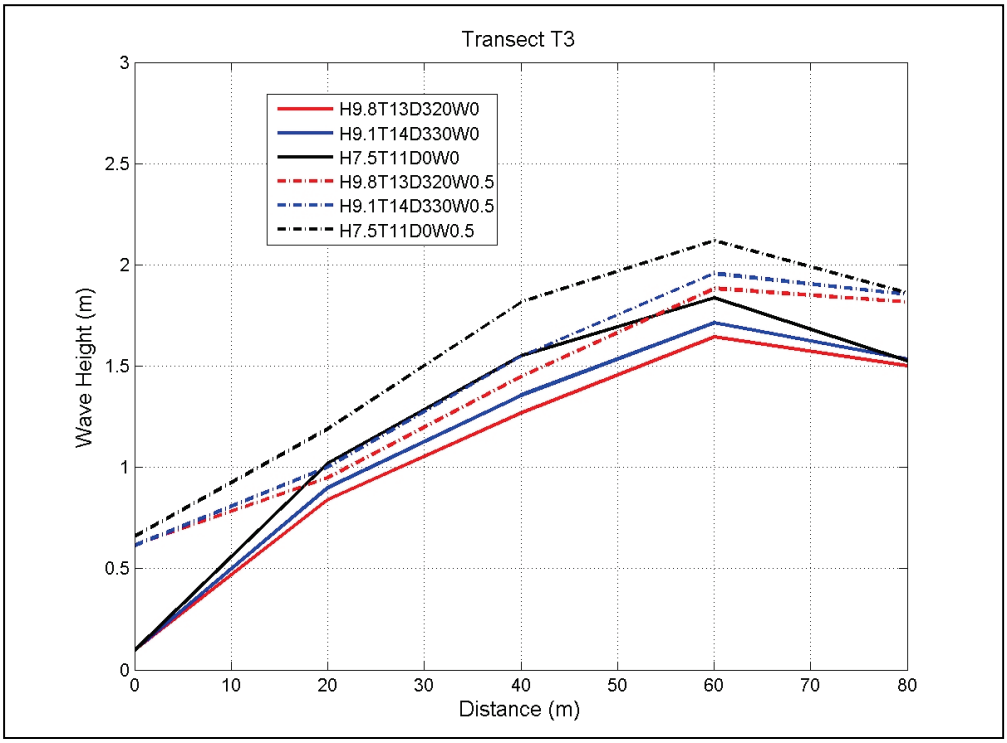

Figure 3-15. Wave height variation along T4 for three storms at two water levels (Alt-0).

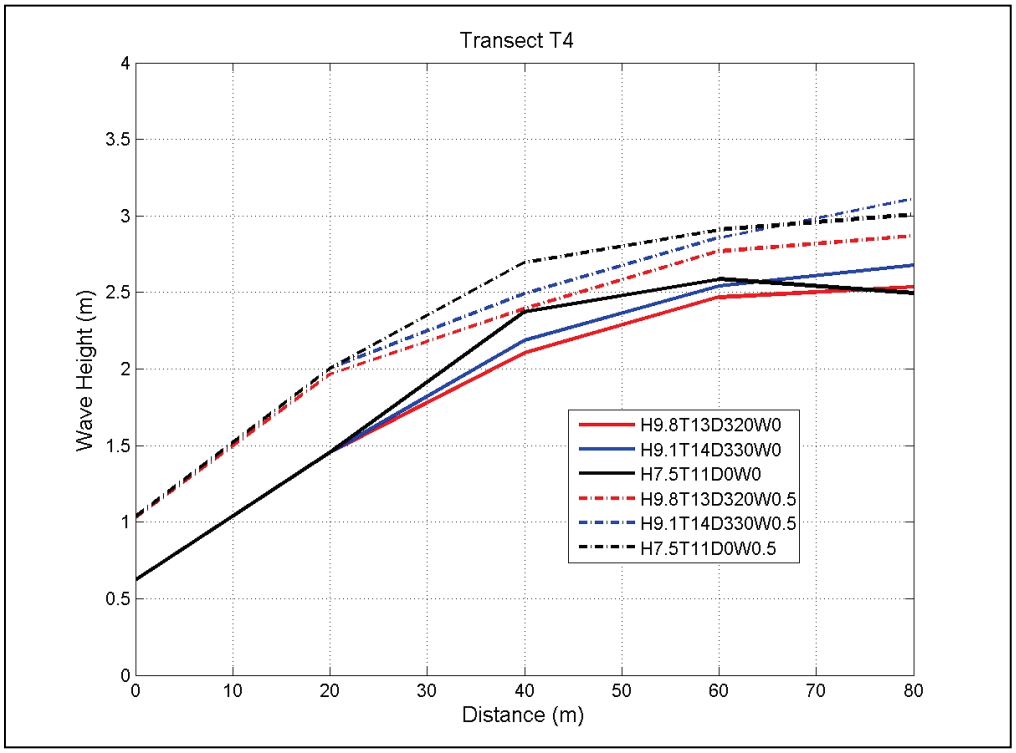

Figure 3-16. Wave height variation along T5 for three storms at two water levels (Alt-0).

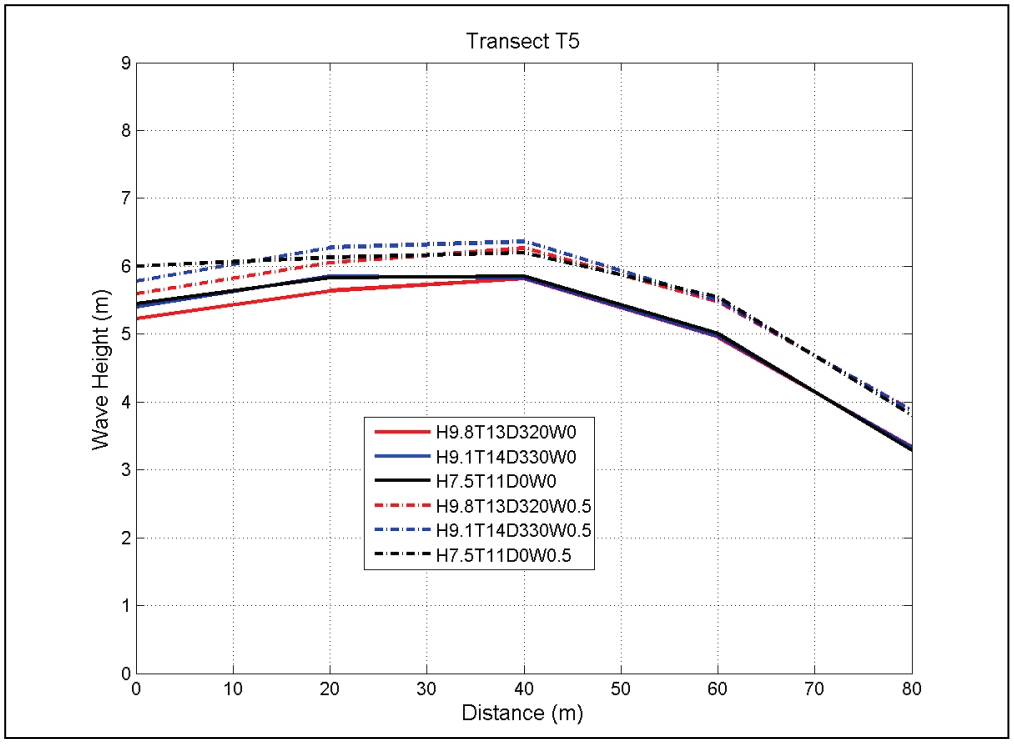

Figure 3-17. Wave height variation along T7 for three storms at two water levels (Alt-0).

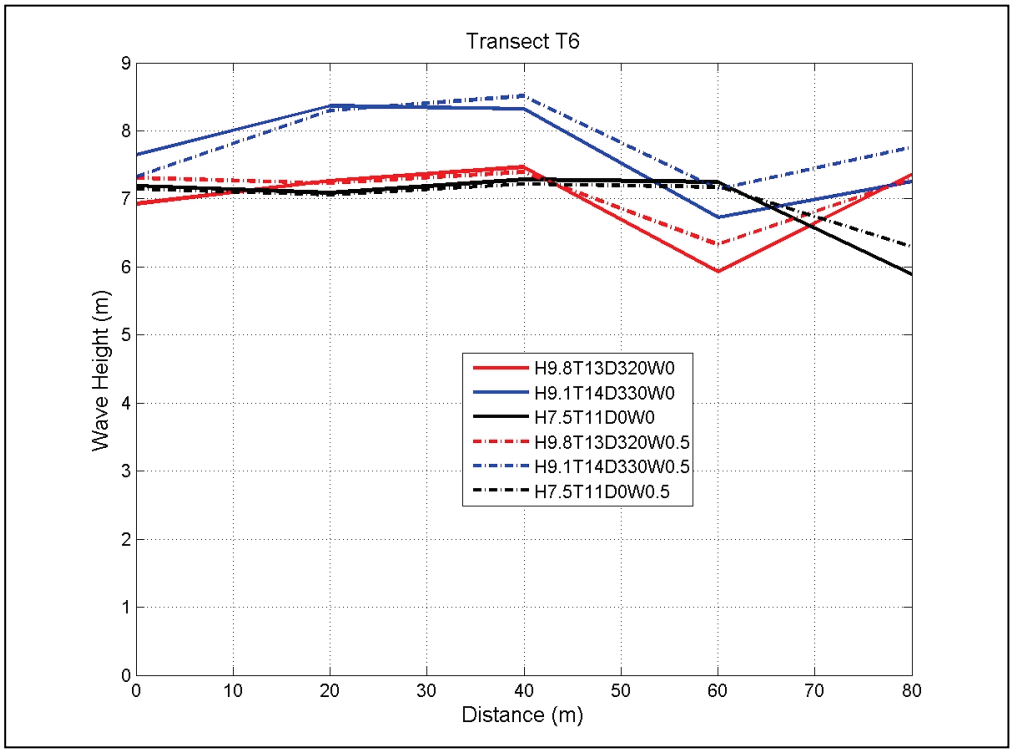

Figure 3-18. Wave height variation along T7 for three storms at two water levels (Alt-0).

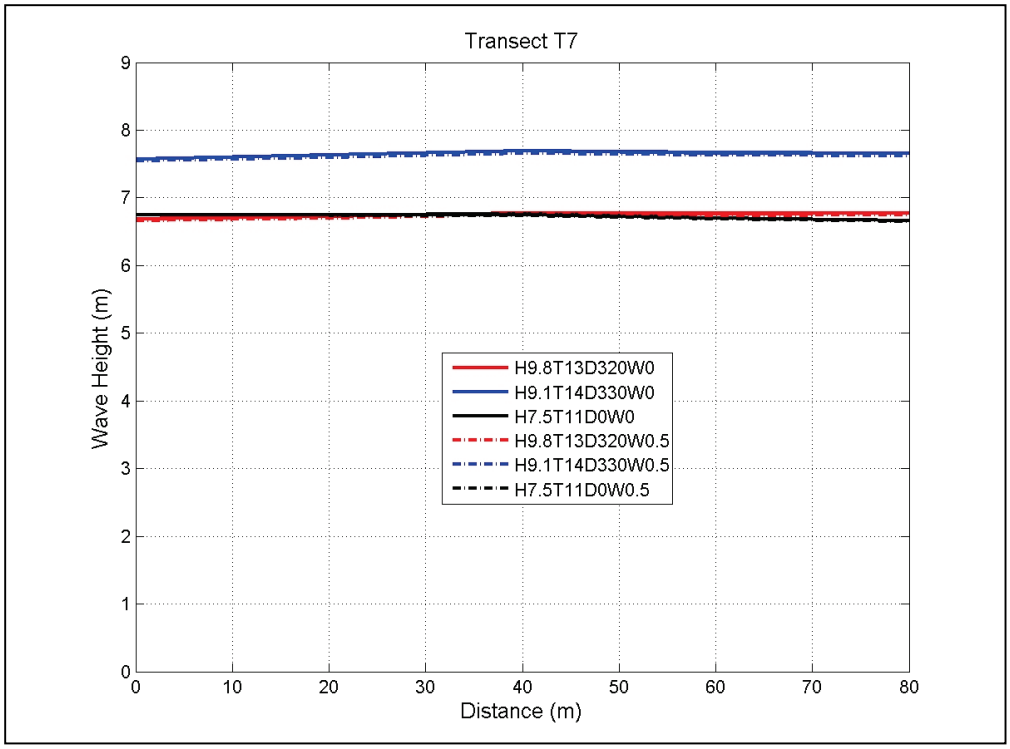

Figure 3-19. Wave height variation along T8 for three storms at two water levels (Alt-0).

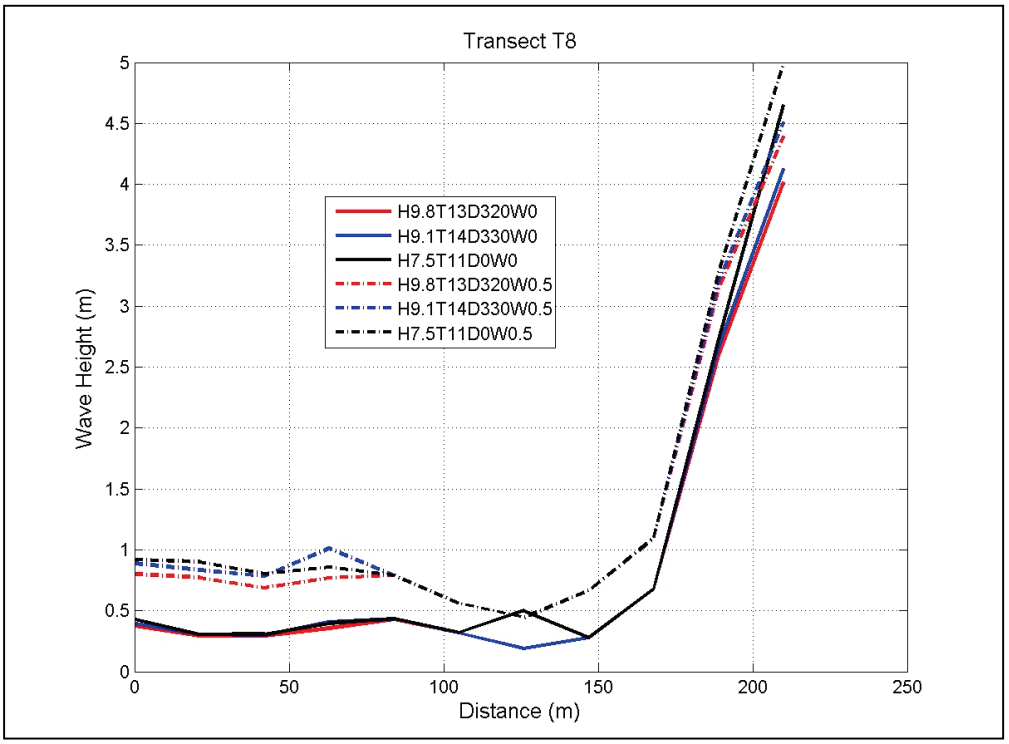

Figure 3-20. Wave height variation along T9 for three storms at two water levels (Alt-0).

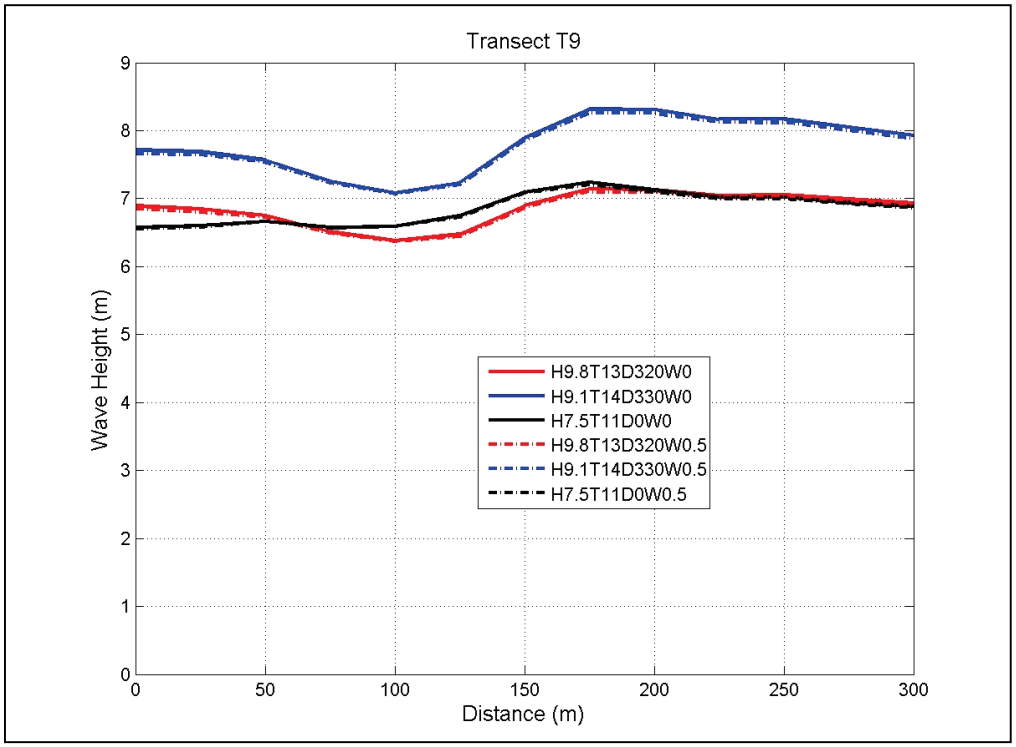

Model results indicated wave heights increased in some areas along the channel and perpendicular transects (T4-T7). Among the simulated six storm conditions, the events H9.1T14D330W0 and H9.1T14D330W0.5 produced the largest wave heights in the harbor entrance (T7) at the two simulated water levels. The storms H7.5T11D0W0 and H7.5T11D0W0.5 yielded the largest wave heights at the dock and in the turning basin.

3.5 Alt-0 results for average wave conditions

In Section 3.4, wave estimates for storm waves were developed for design and repair of structures to protect the harbor. In this section, estimates are provided for typical (routine) conditions for day-to-day operational needs in the harbor.

CMS-Wave simulations were performed for six average wave conditions shown in Table 3-3, with one wave height (H_s = 1.5 m), one peak wave period (T_p = 10 sec), three directions (θ_m = 320°, 340°, 0°), and two water levels (WL = 0 and 0.5 m, MSL). Lateral and backward wave reflection coefficients of 0.5 and 0.3 and a bottom friction coefficient (Darcy-Weisbach) of 0.01 were used in these simulations. Model results were saved over the entire grid, including significant wave height, peak period,

and mean wave direction. Directional wave spectra were saved at the 70 output locations on the 9 transects shown in Figures 3-8 and 3-9.

Wave heights calculated along transects T1 to T9 are shown in Figures 3-21 to 3-29. Results indicate waves approaching the harbor entrance are shoaling over the reef outside the harbor, and some waves break before propagating into the interior harbor through the channel along T1. Some waves can reach the dock and turning basin areas situated in the back of the harbor. During the transformation from deep water to the harbor, average wave height decreases 5% to 15% from the incident condition offshore to the most seaward transect T7 located at the start of the harbor entrance. Wave heights at the dock along T2 and in the turning basin (T3, T4, south segment of T8) are less than waves entering the channel. Values along T3 range between 0.5 to 0.95 m at the mean water level of 0 m (MSL), and 0.6 to 1.2 m at the higher water level of 0.5 m (MSL). Overall, model estimates inside the harbor (T2, T3, T4, and part of T8) for two different water levels indicate wave heights at high water level (0.5 m) are slightly greater than wave heights calculated at low water level (0 m).

Greater wave heights occur along the channel section that lies between transects T7, T6, and T5 while waves are moving into the harbor interior. Among the six average wave conditions simulated, the two wave conditions (H1.5T10D0W0 and H1.5T10E0W0.5) from the north produced the greatest wave height at the dock (T2) and in the turning basin (T3, T4, and south half-segment of T8). Based on these results for nonstorm conditions, waves coming with ±10° from north have the greatest effect on the day-to-day boating operations in Faleasao Harbor. These waves are the most consequential to safety of boats coming into and going out of the harbor. The spatial variation of wave height along the nine transects in Figures 3-21 to 3-29 provides detailed information on how waves change along these transects that cover different areas of the harbor. Overall, approximately 95% of wave heights are less than the 1.5 m maximum wave height, the limit assumed by mariners for safe boating operations in the Faleasao Harbor.

Figure 3-21. Wave heights along T1 for average wave condition at two water levels (Alt-0).

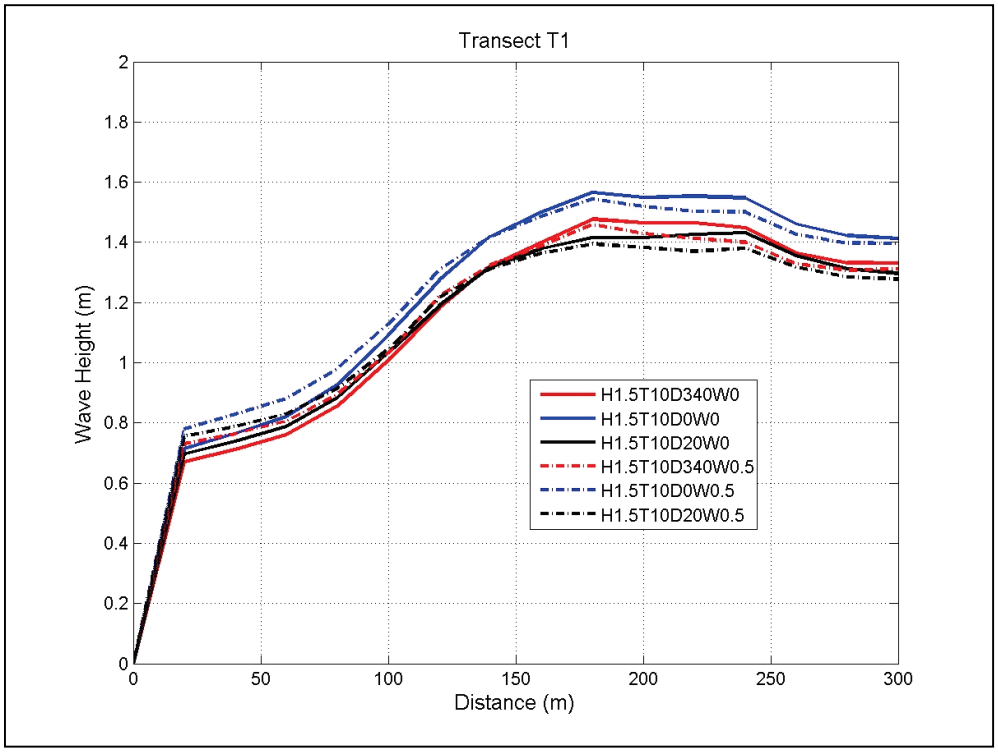

Figure 3-22. Wave heights along T2 for average wave condition at two water levels (Alt-0).

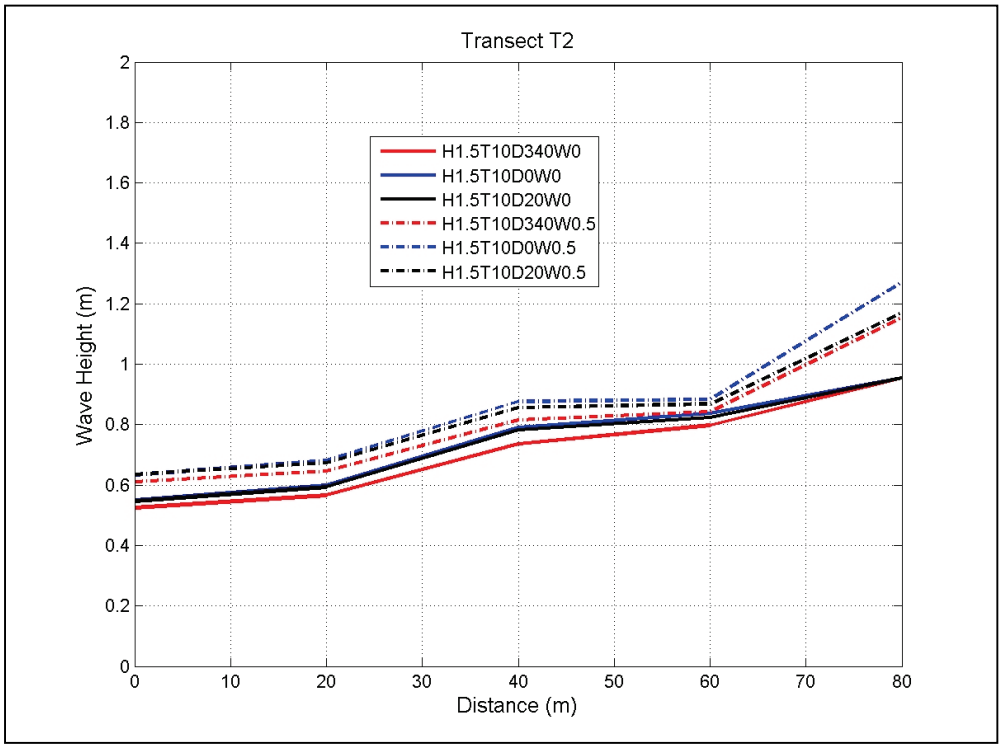

Figure 3-23. Wave heights along T3 for average wave condition at two water levels (Alt-0).

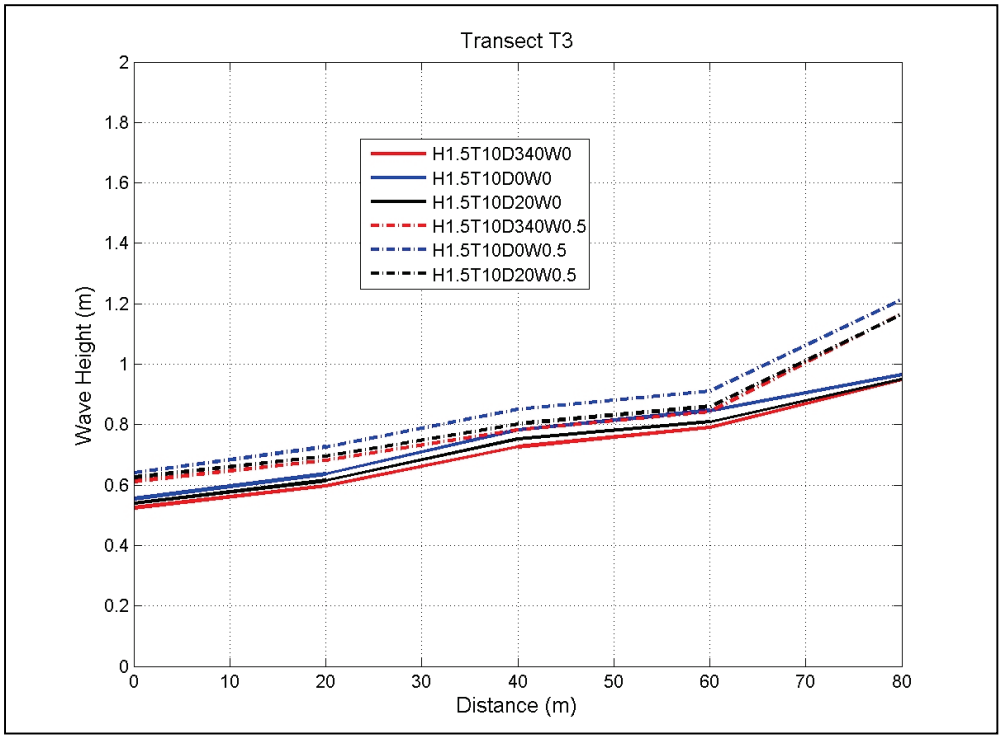

Figure 3-24. Wave heights along T4 for average wave condition at two water levels (Alt-0).

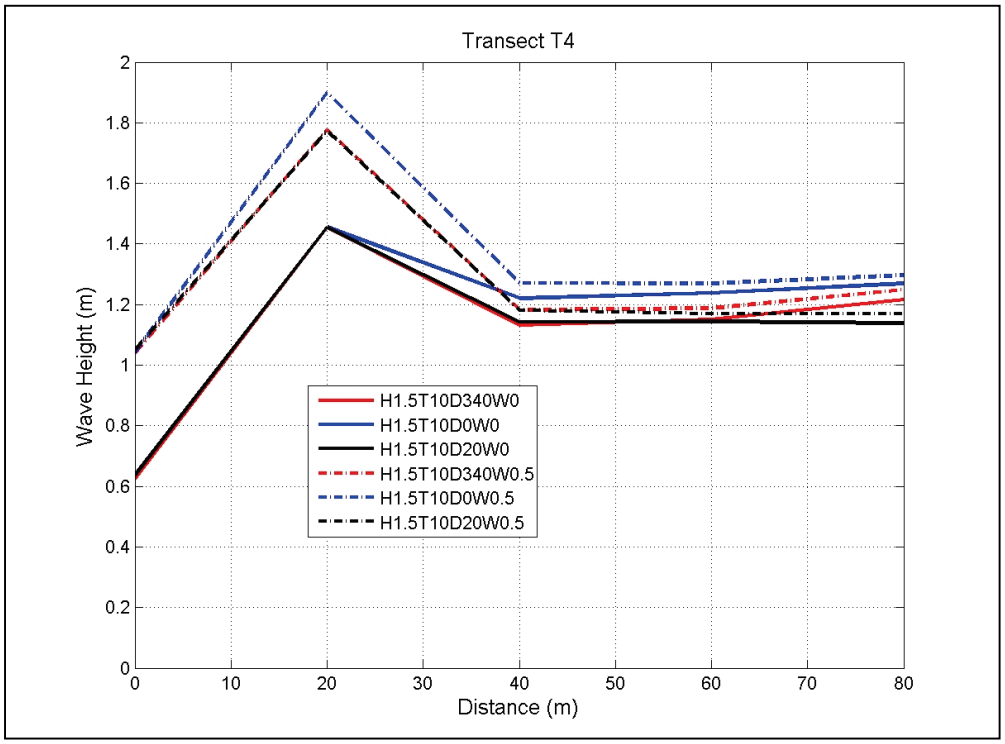

Figure 3-25. Wave heights along T5 for average wave condition at two water levels (Alt-0).

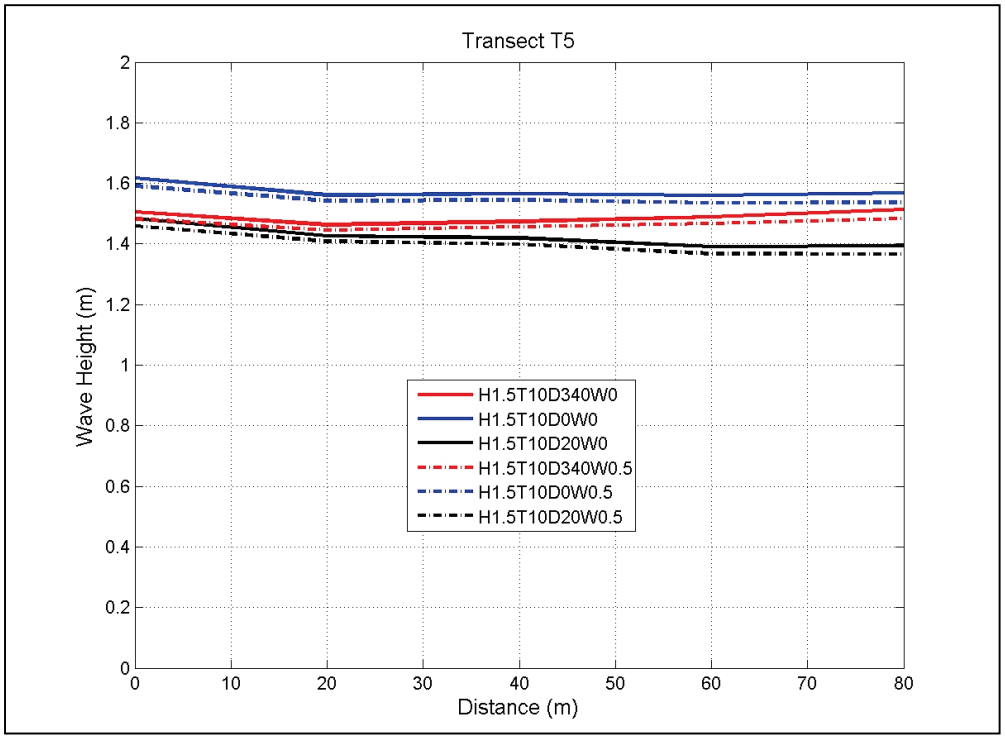

Figure 3-26. Wave heights along T6 for average wave condition at two water levels (Alt-0).

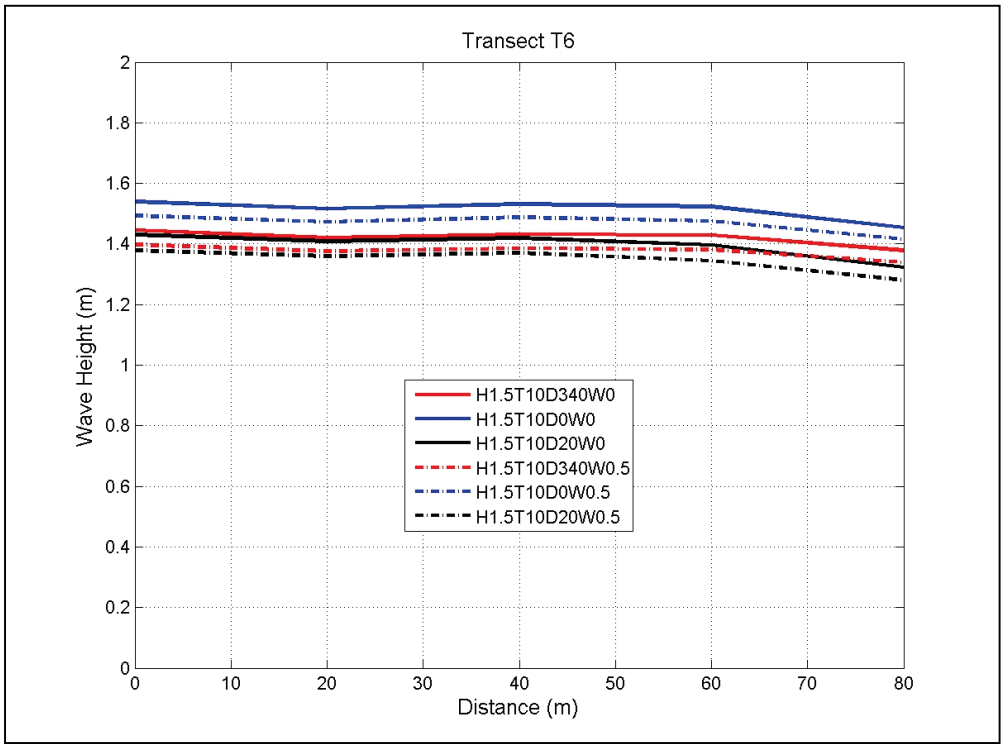

Figure 3-27. Wave heights along T7 for average wave condition at two water levels (Alt-0).

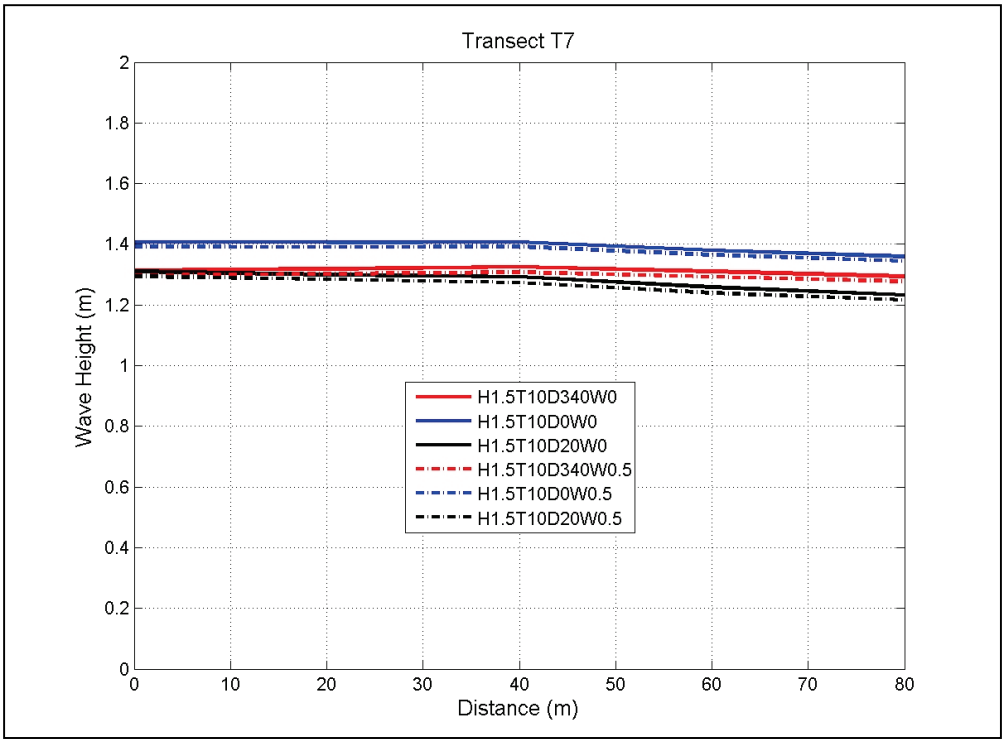

Figure 3-28. Wave heights along T8 for average wave condition at two water levels (Alt-0).

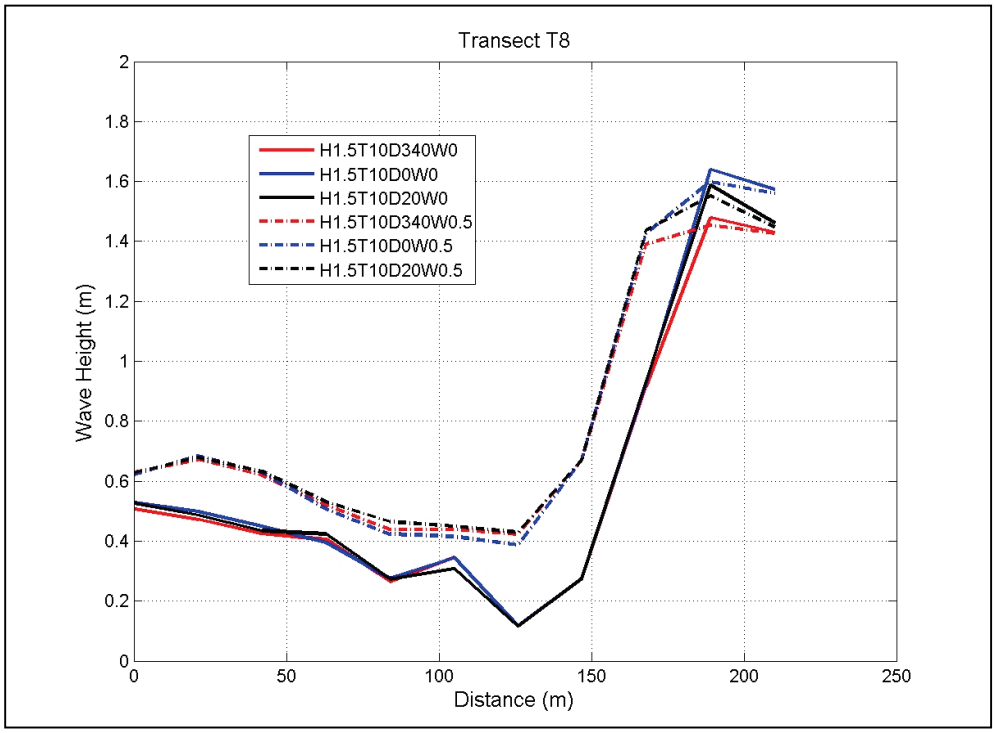

Figure 3-29. Wave heights along T9 for average wave condition at two water levels (Alt-0).

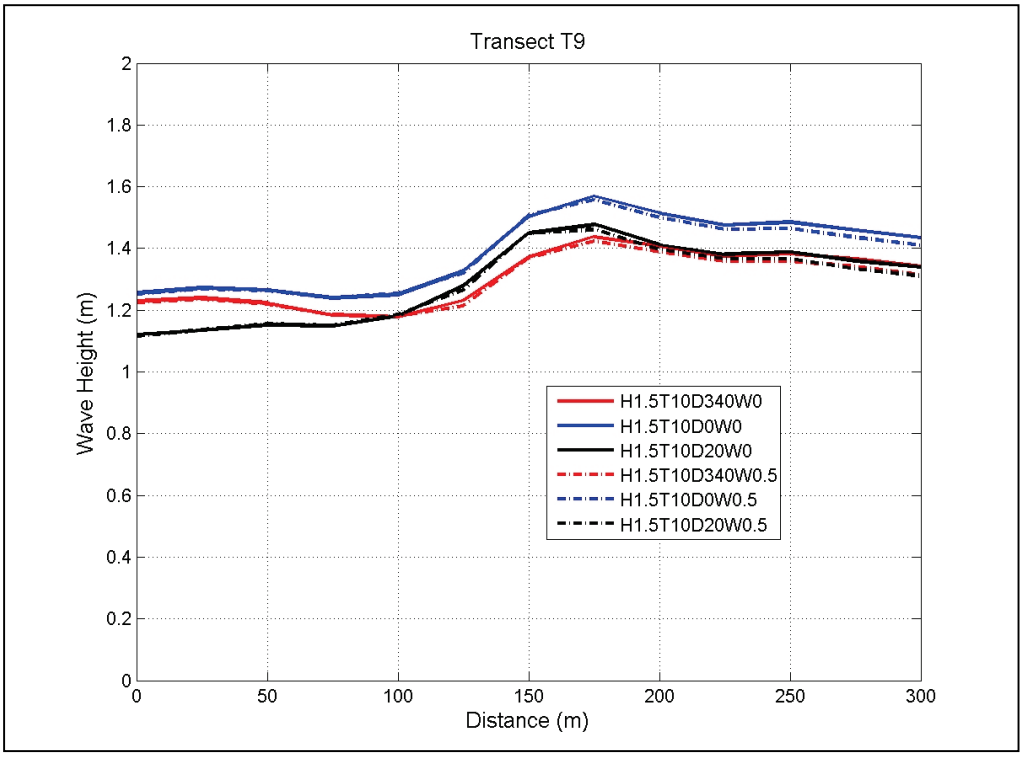

3.6 Results for Alternatives

Based on the findings of storms and nonstorm wave conditions for the existing harbor (Alt-0) described in Section 3.5, simulations for three Alternatives (Alt-1, Alt-2, and Alt-3) were performed for one average and one storm condition at two water levels. A storm wave condition was selected from Table 3-2 at two water levels (H9.1T14D330W0 and H9.1T14D330W0.5). For the average wave condition at two water levels, H1.5T10D0W0 and H1.5T10D0W0.5 were used (Table 3-3).

Figures 3-30 to 3-49 provide a comparison of the calculated wave heights for the four harbor configurations investigated (e.g., Alt-0, Alt-1, Alt-2, and Alt-3). Figures 3-30 to 3-34 provide model results along T1, T2, T3, T5, and T8 for the storm condition at low water level (H9.1T14D330W0). Figures 3-35 to 3-39 provide results for the same storm at high water level (H9.1T14D330W0.5). For the average wave condition, results along the same transects are presented in Figures 3-40 to 3-44 at low water level (H1.5T10D0W0) and in Figures 3-45 to 3-49 at high water level (H1.5T10D0W0.5).

Figure 3-30. Comparison of wave height variation for Alternatives along T1 for a storm wave (H9.1T14D330W0).

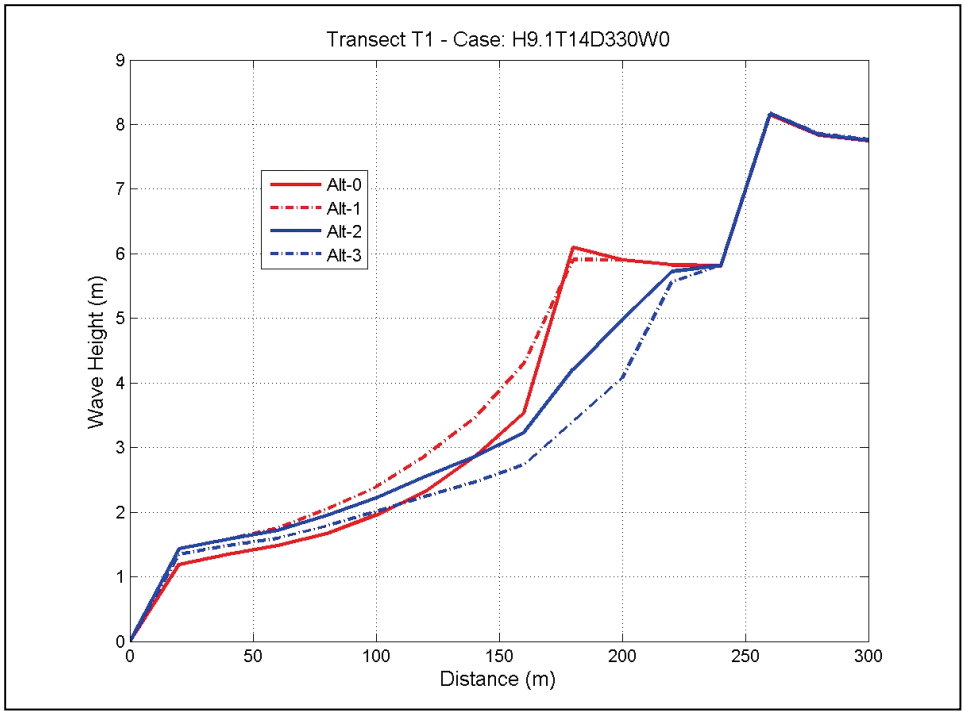

Figure 3-31. Comparison of wave height variation for Alternatives along T2for a storm wave (H9.1T14D330W0).

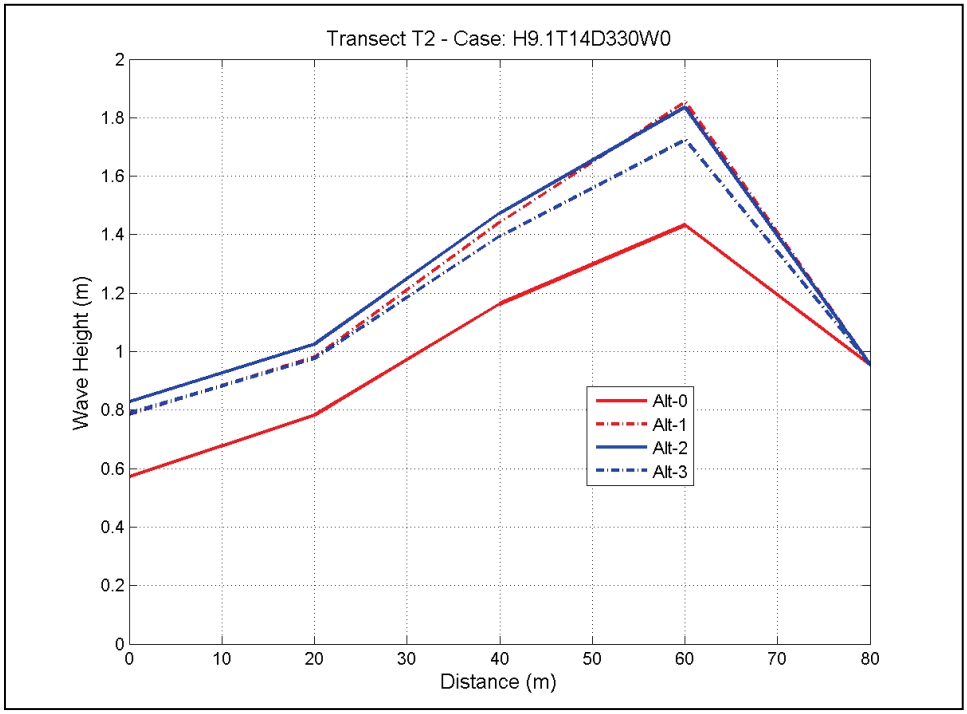

Figure 3-32. Comparison of wave height variation for Alternatives along T3 for a storm wave (H9.1T14D330W0).

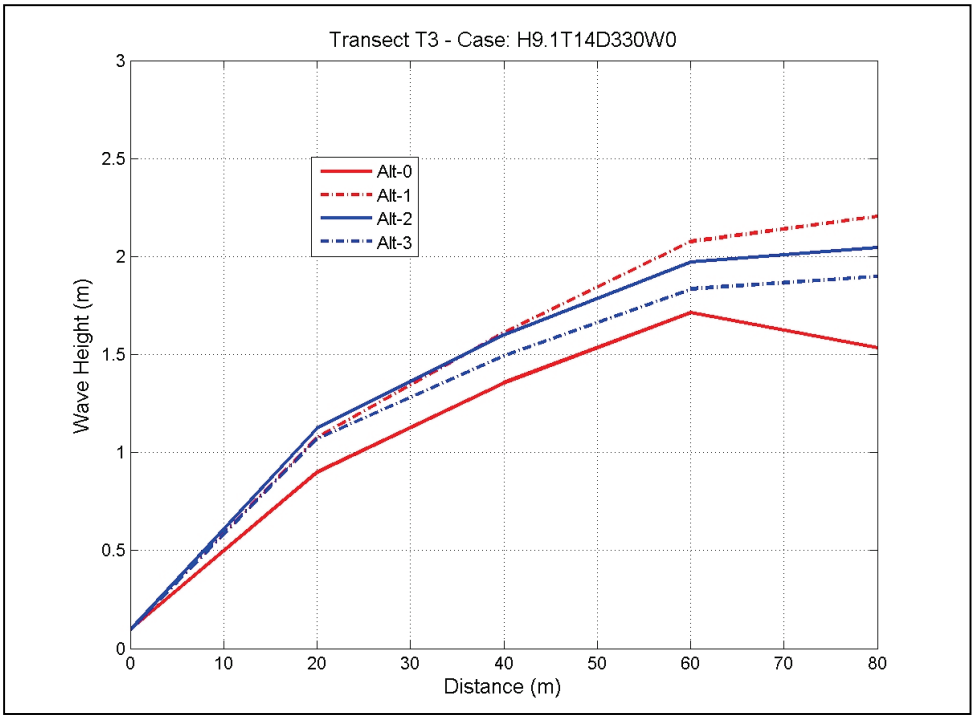

Figure 3-33. Comparison of wave height variation for Alternatives along T5 for a storm wave (H9.1T14D330W0).

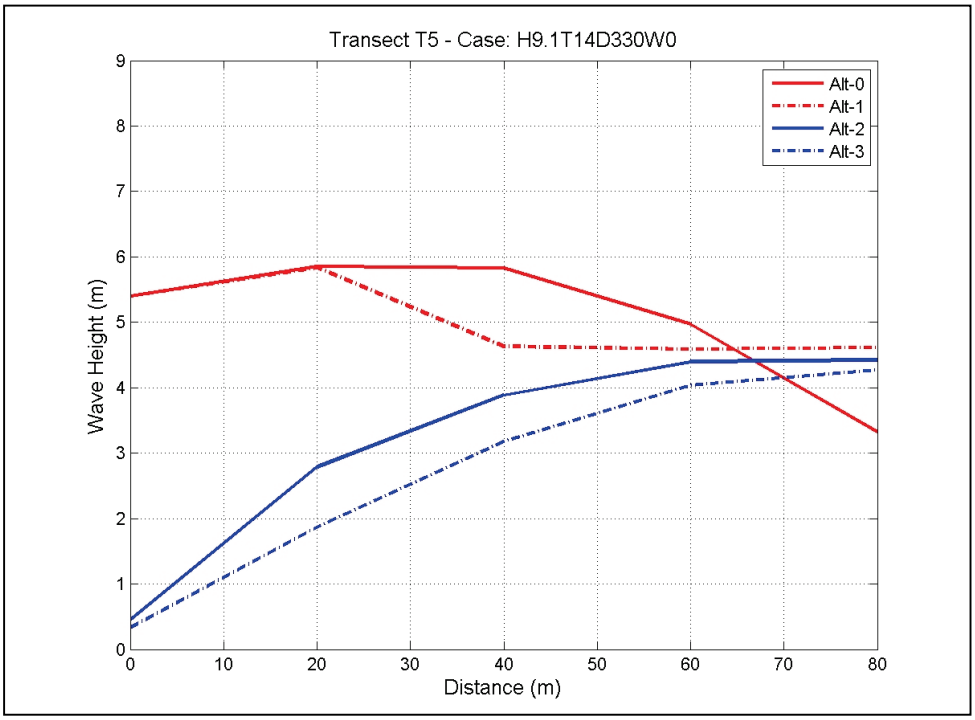

Figure 3-34. Comparison of wave height variation for Alternatives along T8 for a storm wave (H9.1T14D330W0).

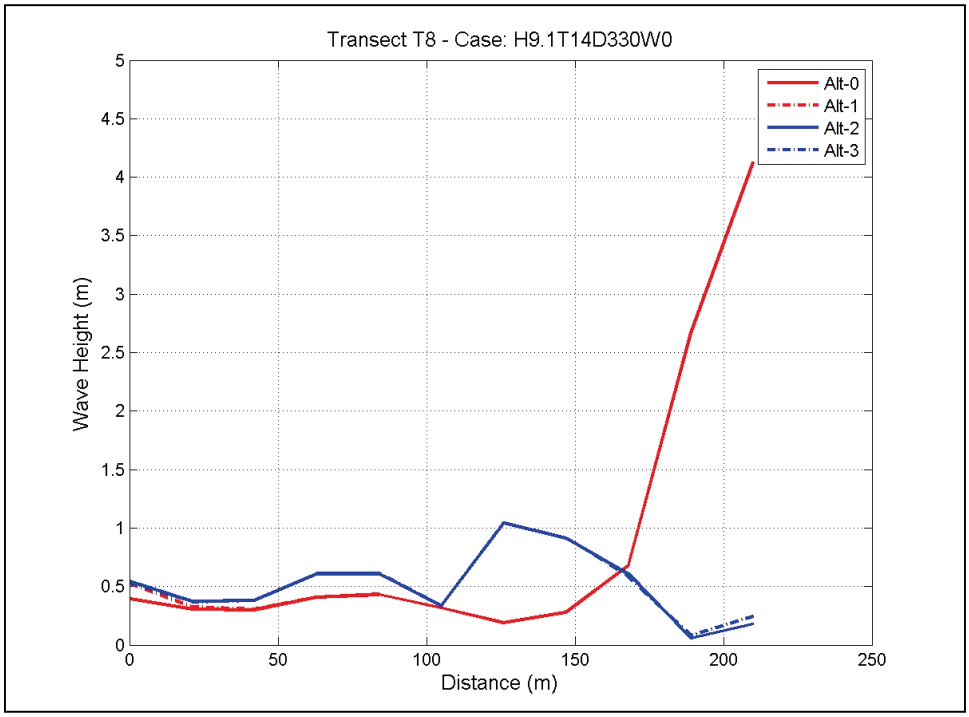

Figure 3-35. Comparison of wave height variation for Alternatives along T1 for a storm wave (H9.1T14D330W0.5).

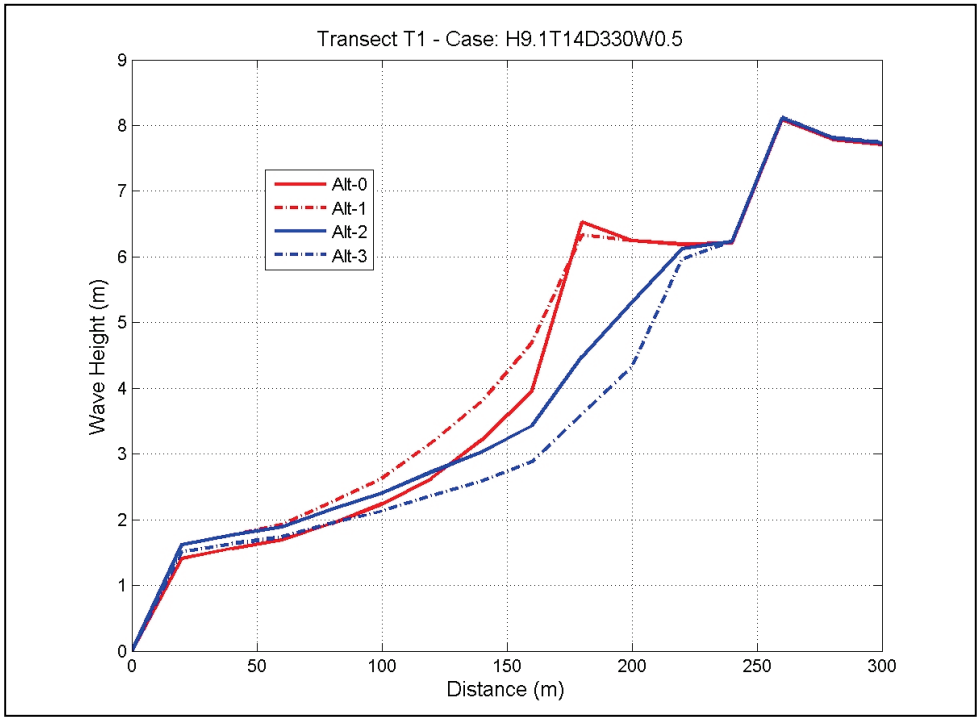

Figure 3-36. Comparison of wave height variation for Alternatives along T2 for a storm wave (H9.1T14D330W0.5).

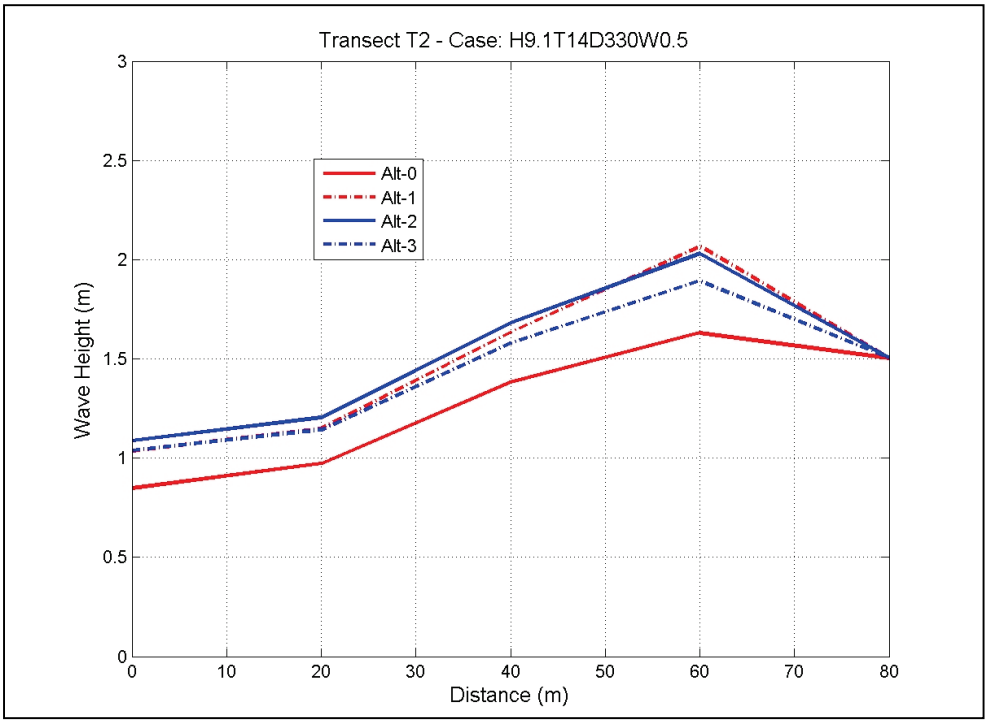

Figure 3-37. Comparison of wave height variation for Alternatives along T3 for a storm wave (H9.1T14D330W0.5).

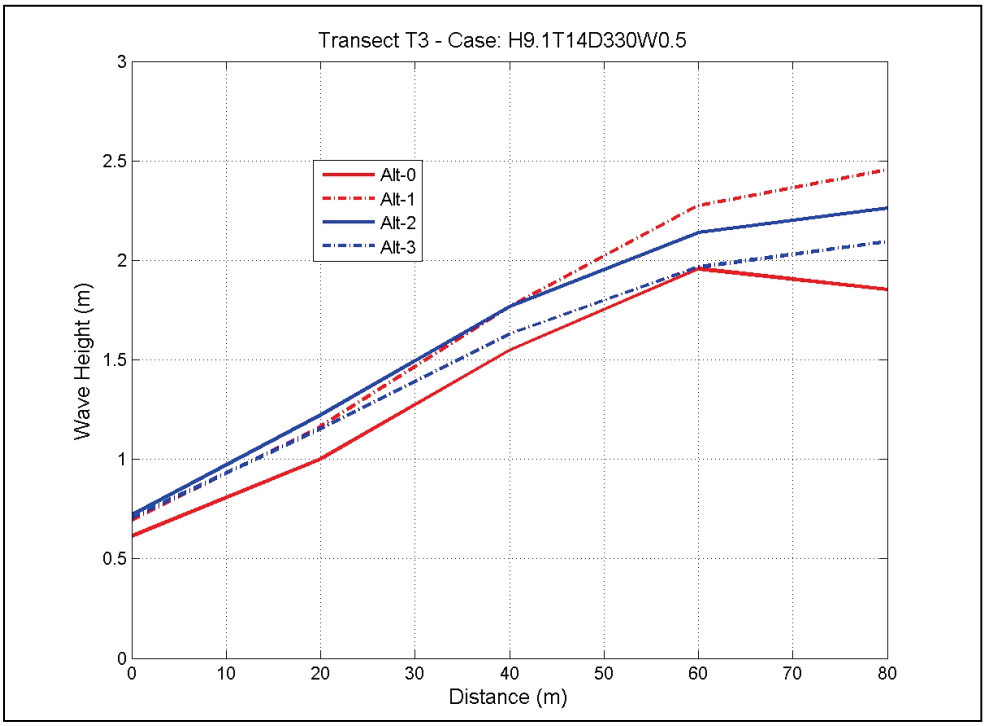

Figure 3-38. Comparison of wave height variation for Alternatives along T5 for a storm wave (H9.1T14D330W0.5).

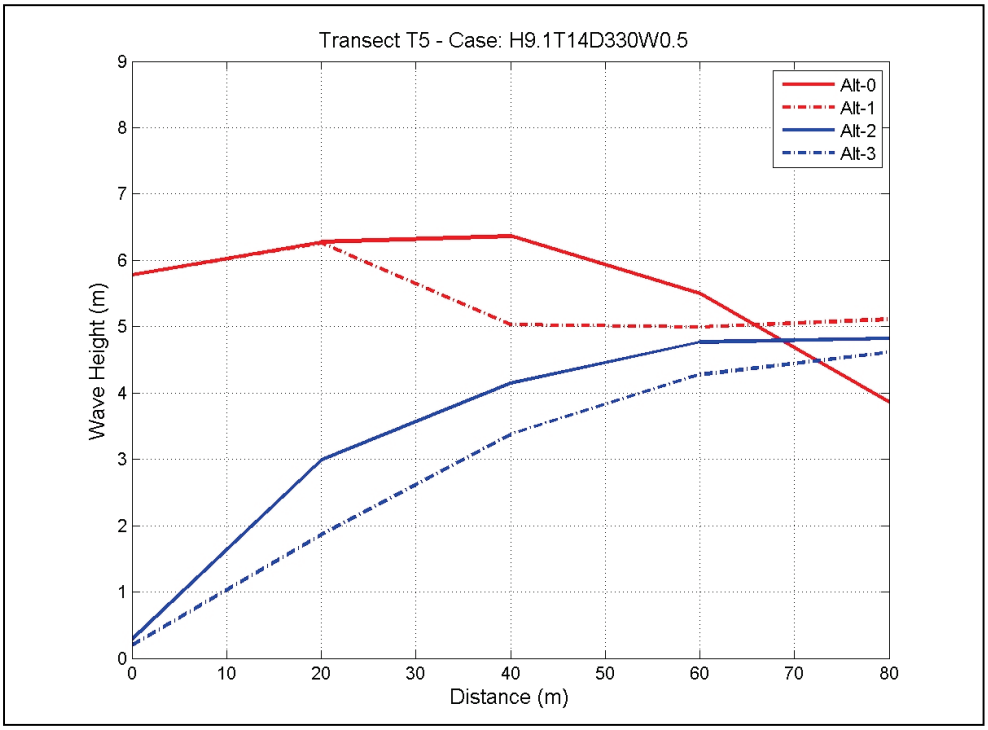

Figure 3-39. Comparison of wave height variation for Alternatives along T8 for a storm wave (H9.1T14D330W0.5).

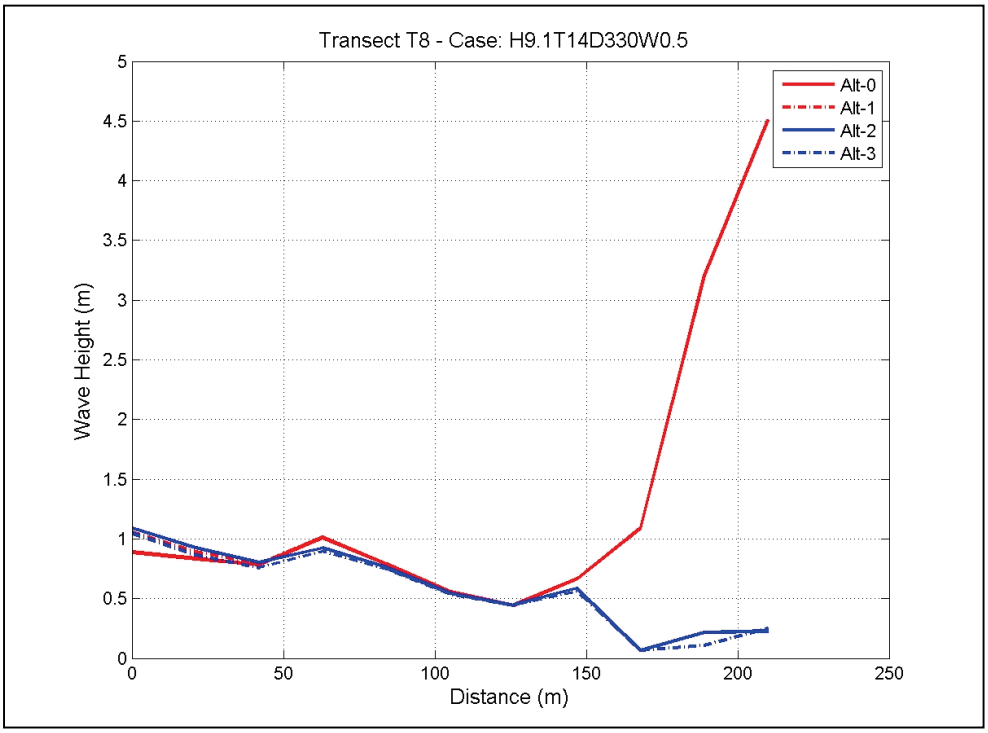

Figure 3-40. Comparison of wave height variation for Alternatives along T1 for an average wave H1.5T10D0W0.

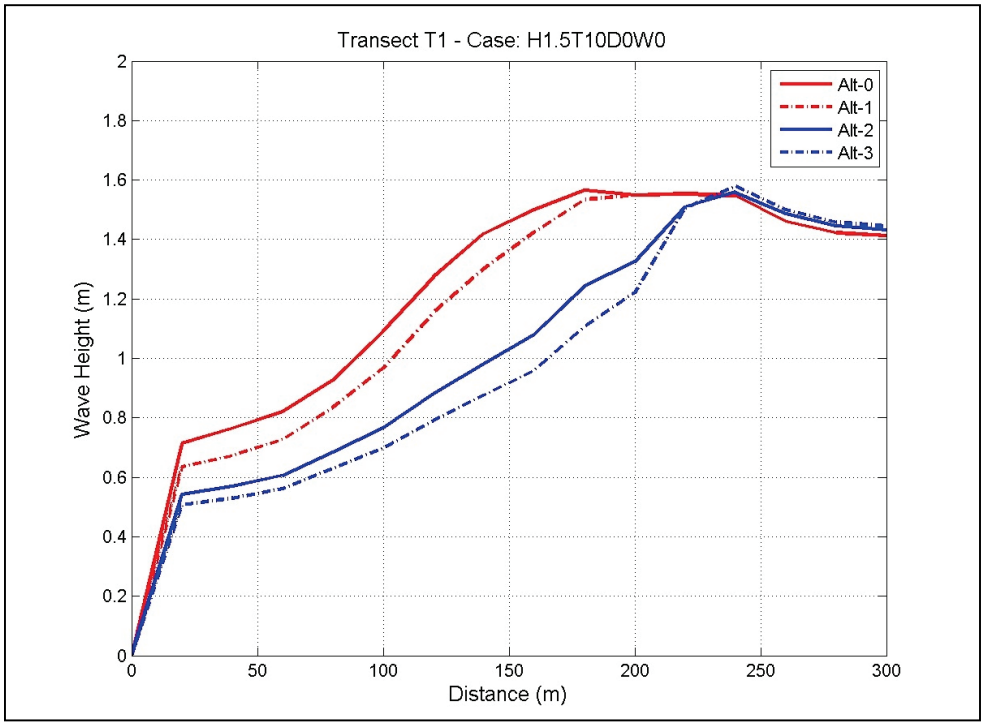

Figure 3-41. Comparison of wave height variation for Alternatives along T2 for average wave H1.5T10D0W0.

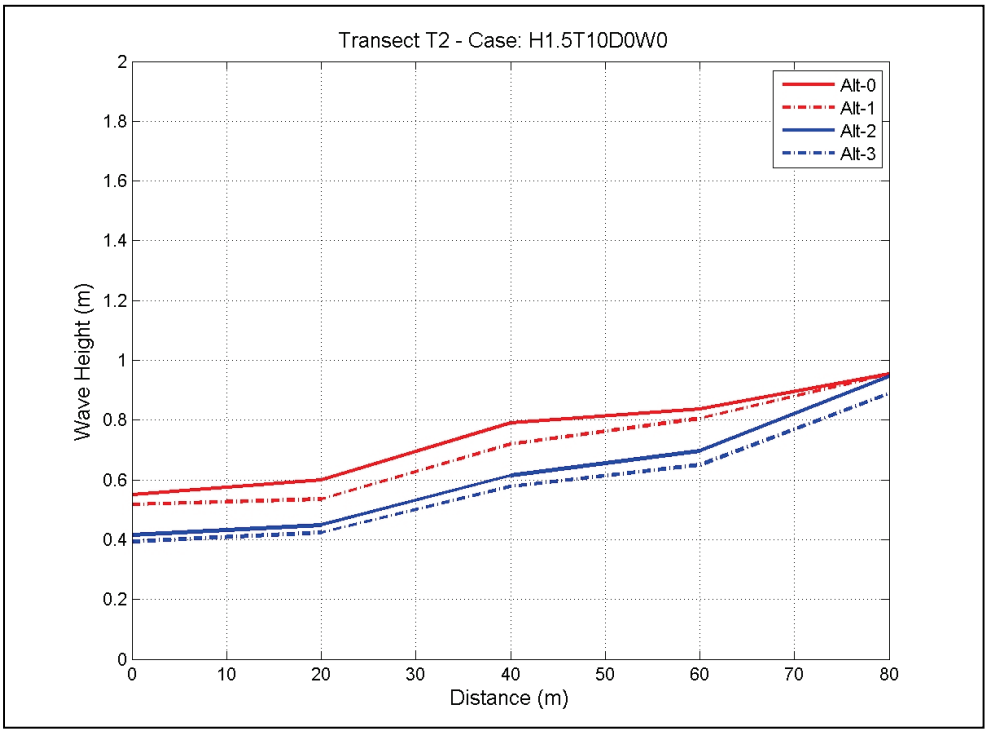

Figure 3-42. Comparison of wave height variation for Alternatives along T3 for average wave H1.5T10D0W0.

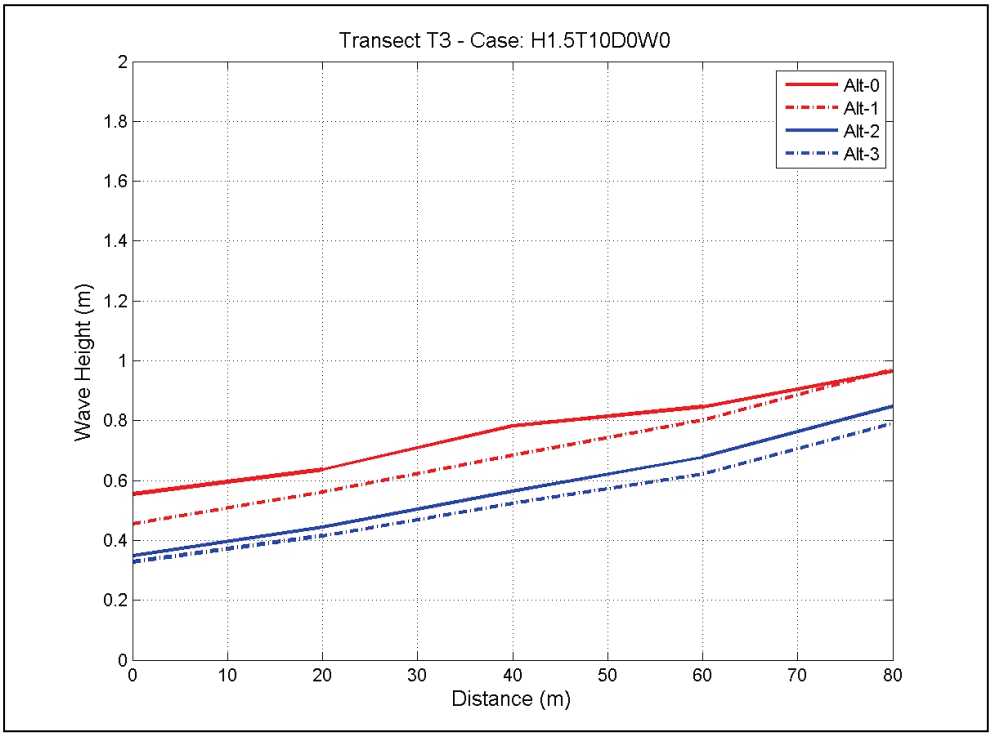

Figure 3-43. Comparison of wave height variation for Alternatives along T5 for an average wave H1.5T10D0W0.

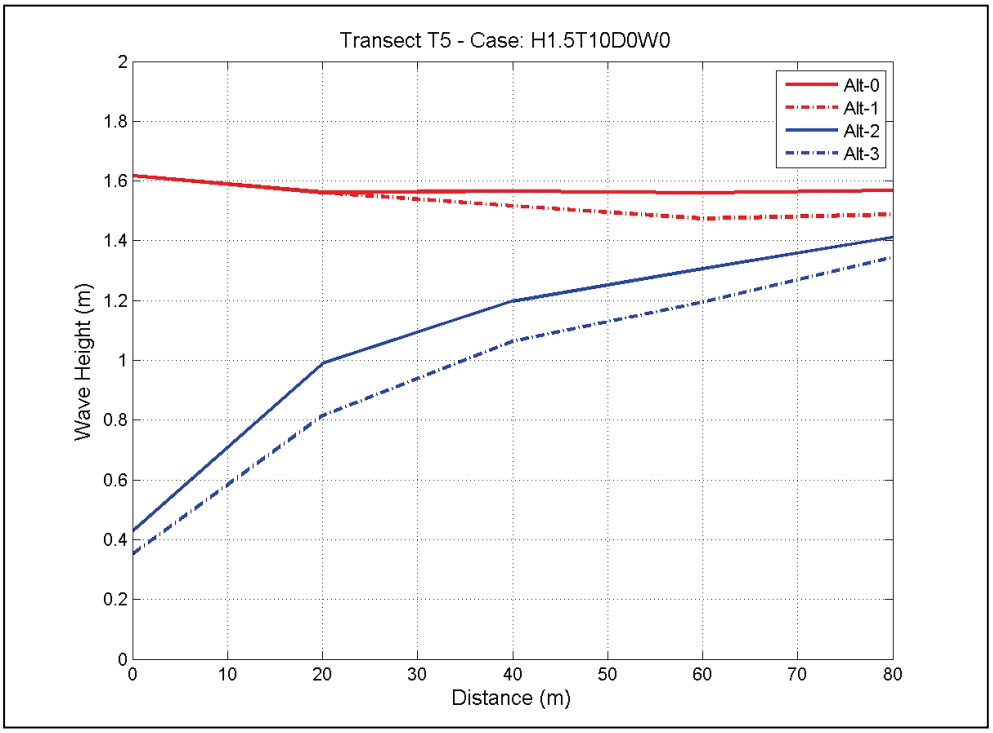

Figure 3-44. Comparison of wave height variation for Alternatives along T8 for average wave H1.5T10D0W0.

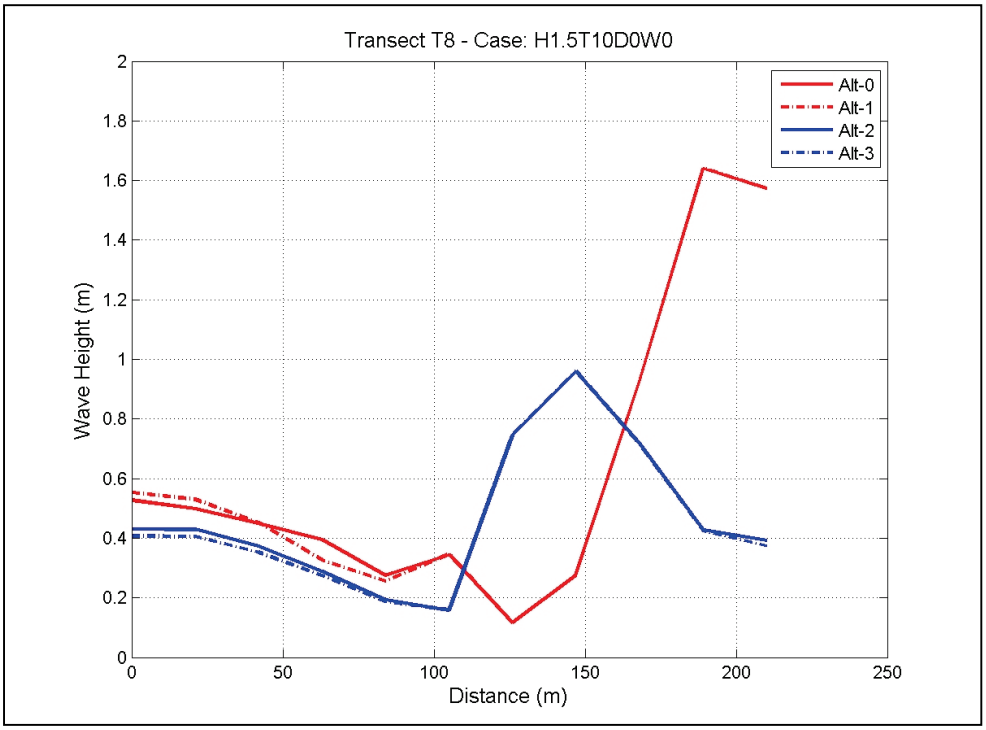

Figure 3-45. Comparison of wave height variation for Alternatives along T1 for an average wave H1.5T10D0W0.5.

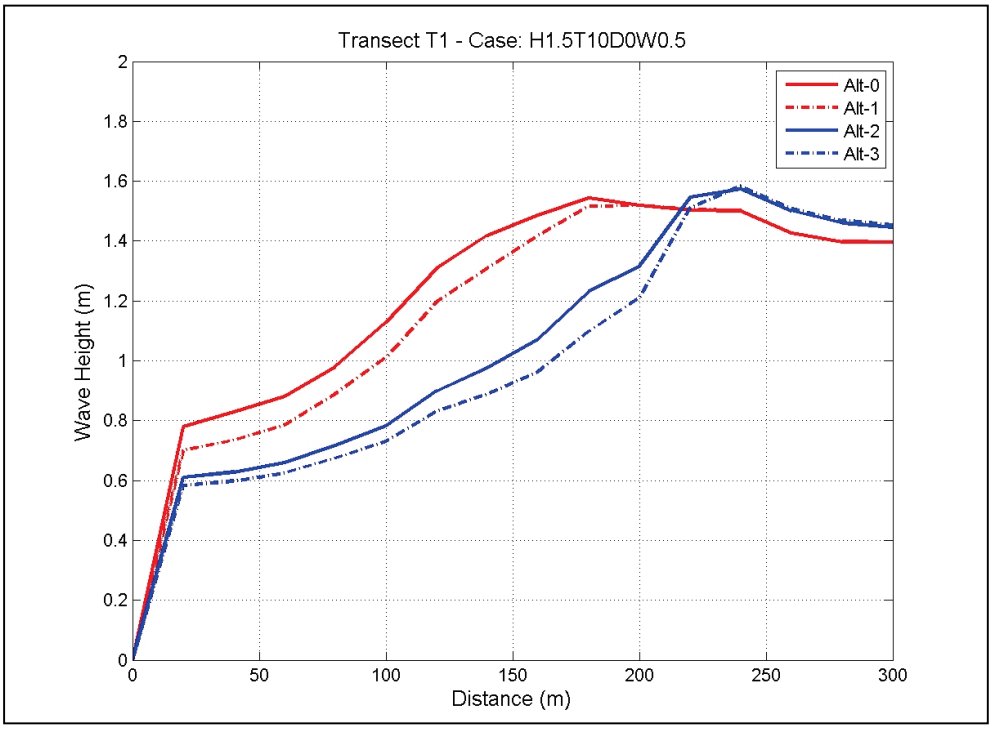

Figure 3-46. Comparison of wave height variation for Alternatives along T2 for an average wave H1.5T10D0W0.5.

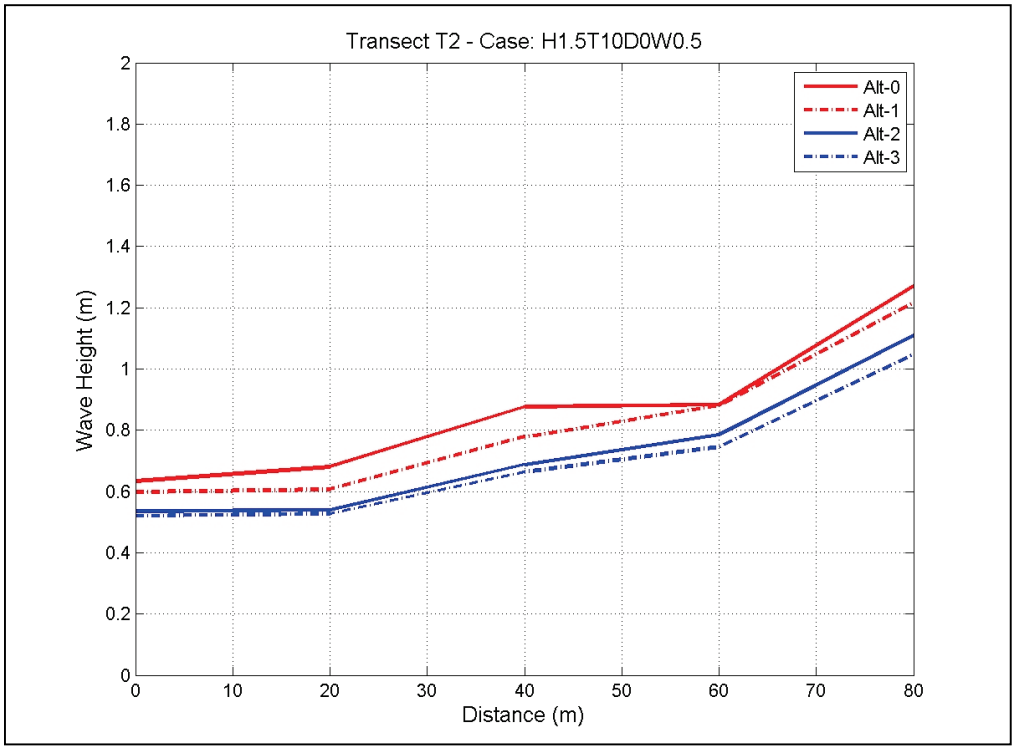

Figure 3-47. Comparison of wave height variation for Alternatives along T3 for an average wave H1.5T10D0W0.5.

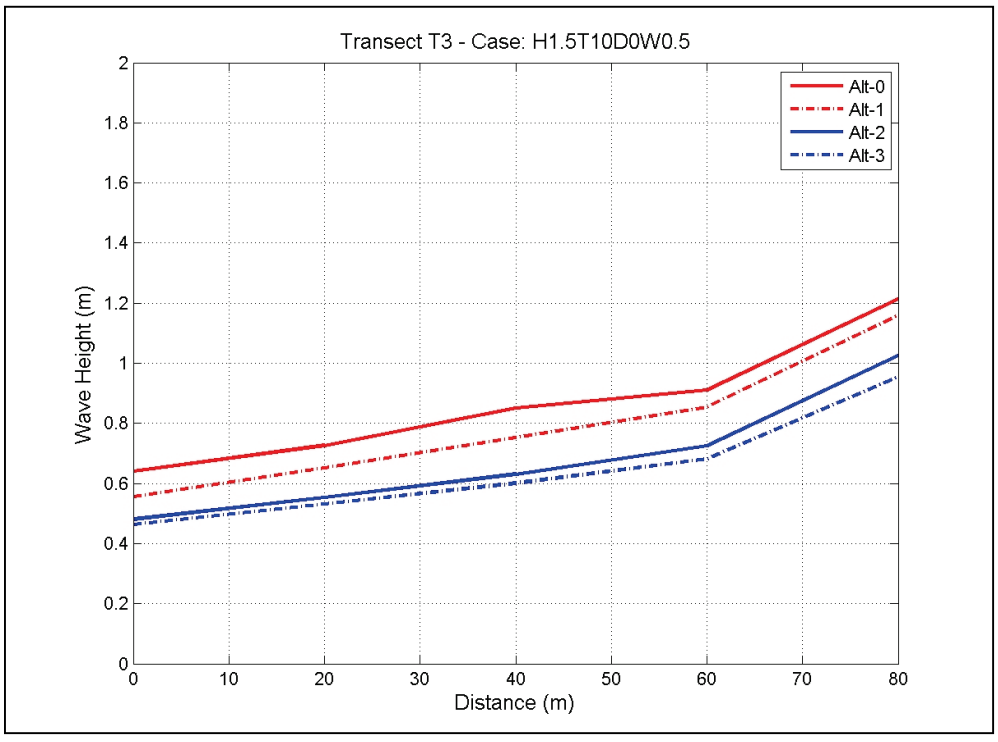

Figure 3-48. Comparison of wave height variation for Alternatives along T5 for an average wave H1.5T10D0W0.5.

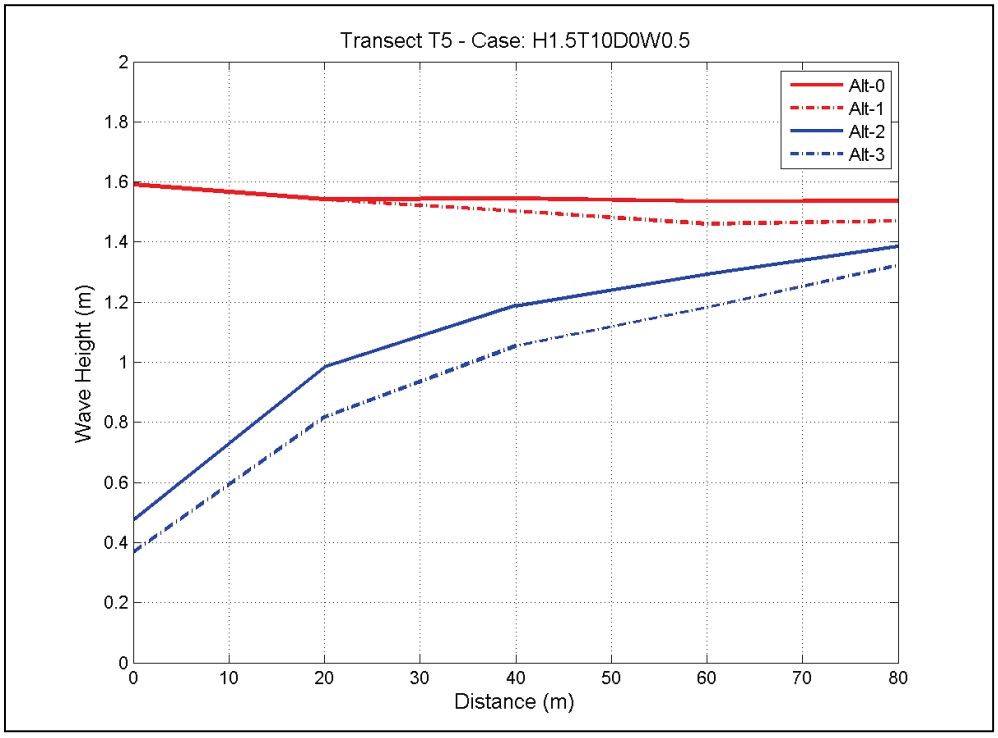

Figure 3-49. Comparison of wave height variation for Alternatives along T8 for an average wave H1.5T10D0W0.5.

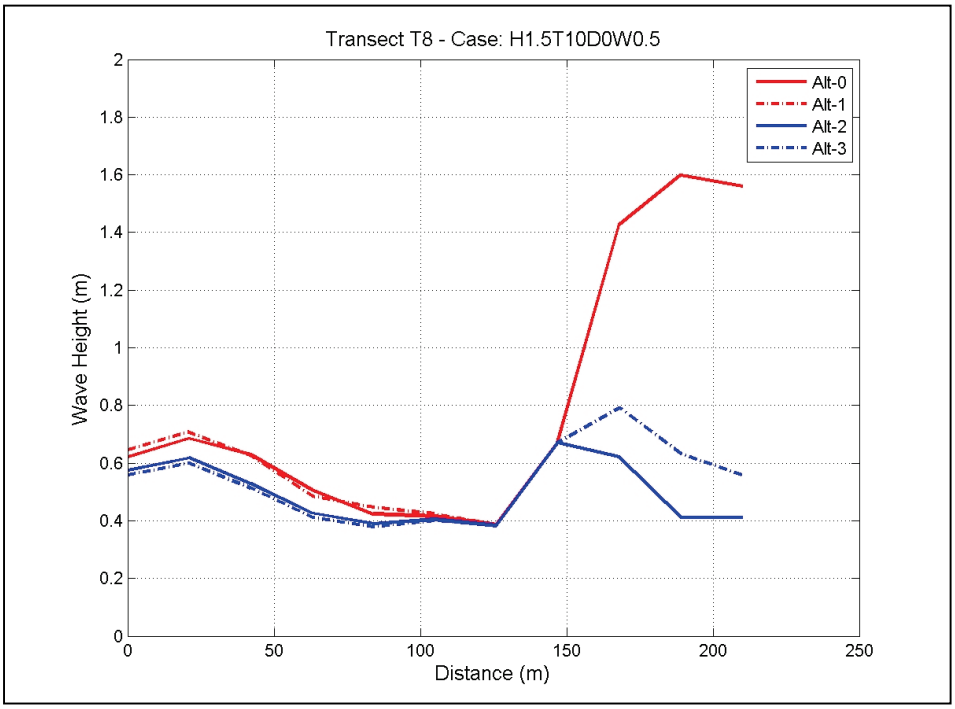

Model results for H9.1T14D330 show storm wave heights for Alt-1, Alt-2, and Alt-3 are generally greater than for the existing configuration (Alt-0) at the dock (T2) and turning basin (T3, T4, and south segment of T8). Wave heights along T1 at high water level are greater than the calculated heights at mean water level (0 m, MSL). Alt-3 yielded the smallest wave heights at the dock and turning basin. Wave heights for Alt-1, Alt-2, and Alt-3 for the storm condition H9.1T14D330 along T2 vary from 1 to 2 m at high water level and 0.8 to 1.8 m at mean water level. Maximum wave heights along T3 for H9.1T14D330 for Alt-1, Alt-2, and Alt-3 range between 2.1 and 2.5 m at high water level and 1.85 and 2.25 m at mean water level. These results indicate that a 0.5 m water level increase gives rise to approximately a 10% increase in wave height in the back areas of Faleasao Harbor, which is a minor change and within the range of uncertainty for any wave model that solves the wave action equation.

Figures 3-40 to 3-49 provide results for the average wave condition at two water levels (H1.5T10D0W0 and H1.5T10D0W0.5 for Alt-1, Alt-2, and Alt-3). Wave heights are generally smaller at the dock (T2) and turning basin (T3, T4, and south part of T8) than those for the existing configuration (Alt-0). Among the three Alternatives (Alt-1, Alt-2, and Alt-3) investigated, Alt-3 produced the smallest calculated wave heights at the dock and in the turning basin. Values of calculated wave heights along T2 for Alt-1, Alt-2, and Alt-3 for the average wave condition range between 0.5 and 1.2 m at the higher water level (0.5 m) and between 0.4 and 0.8 m at the mean water level (0 m). The maximum wave heights for three Alternatives along T3 vary between 0.95 and 1.15 m at high water level and between 0.8 and 1 m at the mean water level.

These results show the effect of water level on wave height to be similar to those for the storm waves (e.g., a 10% increase in wave height for 0.5 m increase in water level). Results show the calculated wave heights for average conditions in the back side of the harbor and through most of the entrance channel remain under the threshold operational wave height limit of approximately 1.5 m (~ 5 ft). This implies that modifications made to the harbor (channel deepening and adding breakwaters) would not produce significant changes to wave energy getting into the harbor. Results indicate that for the three Alternatives considered, there is a small increase in wave height occurring near the harbor entrance channel (T5, T6, and T7) in comparison to the existing configuration (Alt-0). Because this increase is limited to the local channel entrance area, it was concluded that this represents the combined effects of adding the west breakwater structures and channel deepening in Alt-1, Alt-2, and Alt-3.

4 Boussinesq Wave Modeling

Boussinesq wave modeling for Faleasao Harbor is described in this chapter. As noted in Chapter 3, two numerical wave models, CMS-Wave and BOUSS-2D (B2D), were used in this study. CMS-Wave was applied to a large domain covering deep-water offshore areas up to the shorelines. The computational efficiency of CMS-Wave permits simulation of many wave conditions. B2D is capable of handling short- and long-period waves by solving nonlinear, shallow-water wave processes and is designed for nearshore wave processes in intermediate and shallow water depths, which are computationally demanding. Consequently, this model is appropriate for smaller modeling domains and simulation of a limited number of wave conditions. Computational constraints of B2D require the use of a combination of spectral and Boussinesq type wave models when addressing a broad range of wave modeling needs of this and other USACE projects.

Wide fringing coral reefs are present in the ocean north and northwest of Faleasao Harbor. These offer a natural protection to the harbor from incident storm waves. Because the exterior reefs affect waves that can get into Faleasao Harbor, it was necessary to include part of the offshore (deep water) and details of the nearshore (shallow water) areas in the B2D grids. The B2D model domain covered the exterior reefs, the entrance channel that leads into the interior harbor, extended to the adjacent shorelines, and covered all the main features present in the entire interior harbor. Because there were no field data available, numerical models could not be calibrated and validated with data. This chapter describes B2D modeling performed for the existing harbor (Alt-0) and three Alternatives (Alt-1, Alt-2, Alt-3) at two water levels (0 m and 0.5 m MSL). The wave estimates obtained for the existing (Alt-0) and three Alternatives (Alt-1, Alt-2, Alt-3) are discussed.

B2D model considers the effects of shallow-water wave processes such as wave diffraction, reflection, refraction, shoaling, breaking, and nonlinear wave-wave and wave-current interactions but not the wind generation and growth effects. Wave height, period, and direction are the three primary wave parameters of interest for navigation issues in this harbor. The wave parameters which are used to characterize waves at any water depth are widely used in coastal engineering practice:

- significant wave height, (m)
- spectral peak period, (sec)

- mean wave direction, (deg).

The "Wave Mechanics" chapter in *Coastal Engineering Manual* (CEM) by Demirbilek and Vincent (2010) provides additional information about how these parameters are measured or calculated and how they are used in numerical models for practical applications. Generally speaking, a steady-progressive wave train can be defined using these and some other nondimensional parameters derived from them. For example, mean water depth (h), wave crest-to-trough height (H), and wavelength (L), which is related to wave period, suffice to define a progressive wave. Nonlinear shallow-water waves may be characterized by three dimensionless quantities, H/h, L/h, and H/L. In most practical applications, the wave period is known rather than the wave length. It is noted that waves in a prototype coastal environment often travel on a finite current, and consequently, the wave speed and hence the measured wave period vary with the background current (i.e., waves travel faster with the current than against it). B2D takes into consideration the nonlinear effect of currents on waves.

The parameters H/L and H/h represent the nonlinearity of waves and are used in Boussinesq wave theory to define nonlinear features of shallow-water waves. Wave nonlinearity increases with the wave height as depth decreases, which leads to increase in wave skewness and asymmetry. The B2D model represents these wave characteristics and other nonlinear shallow-water wave processes, which affect waves inside the shallow-draft Faleasao Harbor.

4.1 Model grids

The B2D modeling domain extended to approximately 160 ft (50 m) depth offshore and included nearshore reefs fronting the harbor entrance and the rugged and irregularly shaped rocky shorelines present on both sides of the harbor. Four B2D grids were used to simulate waves which could potentially affect the harbor. The coastline and bathymetric data described in Chapters 2 and 3 were used to generate the four B2D grids. Figure 4-1 shows the four B2D model grids for the existing harbor (Alt-0) for simulation of the incident waves from 0° (N), 20° (NNE), 340° (NNW), and 320° (WNW), respectively. Each grid covered approximately a 40° sector of incident waves due from 0° (N), 20° (NNE), 340° (NNW), and 320° (WNW).

Figure 4-1. N, NNE, NNW, and WNW grids of Alt-0.

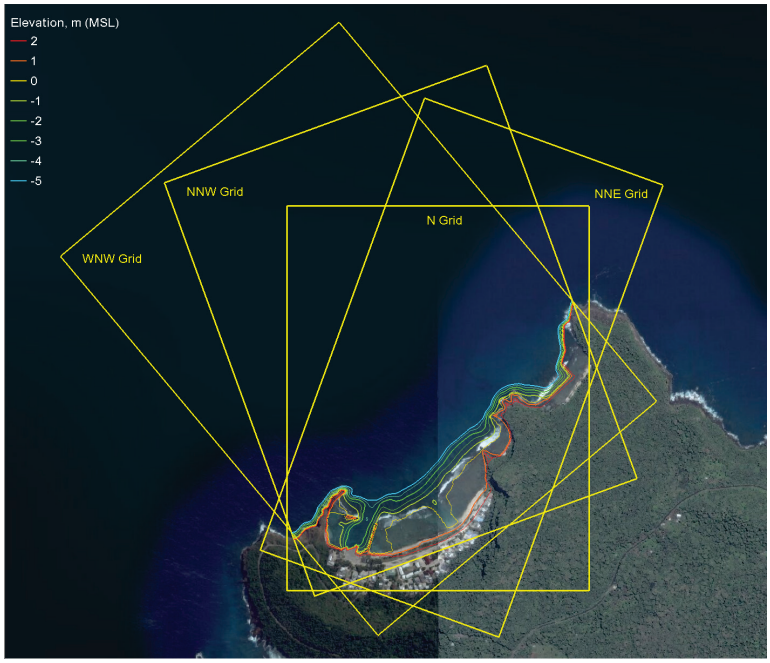

Because there was a wide range of incident wave directions along the B2D model offshore boundary, which is also referred to as the *wavemaker* boundary, it was not possible to use only one grid for all simulations. If large, oblique incident waves are used at the wavemaker boundary, loss of wave energy can occur through the lateral boundaries. This would reduce the wave energy that should be coming into the harbor. Hence, four grids were used to handle all wave directions. Each grid was designed for a ±20° incident wave direction sector centered on that grid's orientation angle (e.g., the 20° grid was used for incident wave from 0° to 40° sector centered on this grid's angle while the 340° grid was used for incident waves from 320° to 360° sector). The bathymetry of harbor exterior, reefs, shorelines, structures, navigation channel, turning basin, and other prominent features in the interior harbor was included in these grids. These custom grids were developed initially for the existing harbor and modified later for each Alternative. A brief description of the grids follows.

The grids developed initially for the existing harbor (Alt-0) were subsequently modified and adapted to Alternatives. This was done by incorporating specific changes for each Alternative at the channel, turning basin, and west breakwater.

The origin of the four grids is at the lower left corner of the grid domains. The modeling domain of the N-grid (0° grid) was 1.8 miles by 2.2 miles

(1.1 km by 1.4 km) and was oriented in N-S direction with a 0° grid angle. The computational domain of the 20° grid was 1.5 miles by 2.8 miles (0.93 km by 1.76 km), and was oriented 20° clockwise with respect to north. The area covered in the 340° grid was 2 miles by 2.6 miles (1.26 km by 1.61 km), and the grid angle was 20° counter clockwise. The 320° grid was rotated 40° counter clockwise and covered a 2.1 miles by 2.9 miles (1.33 km by 1.81 km) area. A 5 m cell size was used in all grids. The offshore wavemaker boundary of the four grids was placed at 160 ft (50 m) depth contour.

Exterior and interior wave-makers were tested with the four grids to check sensitivity of model results to the location of the forcing boundary. Model results were not affected by the type of wavemaker. The wavemaker that was most favorable to computational stability was used in production runs. Wavemakers were placed at 50 m constant water depth along each grid's offshore boundary. Depending on the characteristics of the specified incident waves, sensitivity tests were performed for input parameters influencing the computational stability of the model. These included the Chezy (bottom friction) and Smagorinsky (turbulence) coefficients and damping layer characteristics (width and strength of damping or sponge layers) used to represent reflectivity of boundaries. For oblique waves, preliminary tests indicated selection of appropriate lateral damping layers (location, width, and coefficient) was important for numerical stability of the computations. Partially absorbing lateral damping layers with varying width (5 to 25 m) along parts of the lateral grid boundaries were used in the simulations.

Test runs were used to determine proper values of the damping layers to represent land and structural boundaries. Weak reflection was due to mild slopes of harbor interior shorelines and presence of reefs, rocks, and gravel throughout the harbor interior. Insensitivity of model results confirmed low reflection in the harbor interior. For the range of wave parameters used in the test runs, wave reflection from harbor interior boundaries was weak, ranging from 0% to 5%, except at the man-made structures and dock area where reflection was stronger.

Water depths outside the navigation channel and turning basin are relatively shallow throughout the harbor. The land-water interface areas of the harbor are fronted by gently sloping areas which are mostly dry or partially wet. For these reasons, the interior land boundaries of the harbor

were treated as absorbing. For wave periods up to 20 sec, damping coefficients of 0, 0.05, and 0.1 and damping widths 5 m to 25 m were assigned to boundaries. These parameters were used for the existing harbor and Alternatives. Wave damping varies with the water level, requiring the use of different damping layer types at two water levels (0 m and 0.5 m MSL). The dark brown lines in Figure 4-1 show the location of damping layers assigned to shorelines, structures, and lateral boundaries of the grid. The four grids of the existing harbor (Alt-0) are presented first, followed by four grids for each Alternative (Alt-1, Alt-2, and Alt-3).

Test runs for the existing harbor indicated that long-period infragravity waves (IG) were extremely small in three areas of interest (e.g., channel, turning basin, and dock/pier). Since the periods of IG waves were not close to the natural periods of the harbor, they were ruled out as concern to navigation in the existing harbor. However, after an Alternative is selected for improving navigation and increasing harbor access by larger vessels, an IG wave analysis should be conducted for potential effects on navigation, mooring lines, and moored vessels at the dock.

Figures 4-2, 4-3, and 4-4 show grids for Alt-1, Alt-2, and Alt-3, respectively. These custom-designed grids for the Alternatives had the same spatial extent as its corresponding grid for the existing harbor (Alt-0). However, the grids are different in the interior harbor where Alternative-specific modification(s) were incorporated.

For extraction and comparison of modeling results for all harbor geometries investigated, the same output stations and transects were used. General features of the grids for Alt-1 are depicted in Figure 4-2, for Alt-2 in Figures 4-3, and for Alt-3 in Figures 4-4.

Figure 4-2. N, NNE, NNW, and WNW grids of Alt-1.

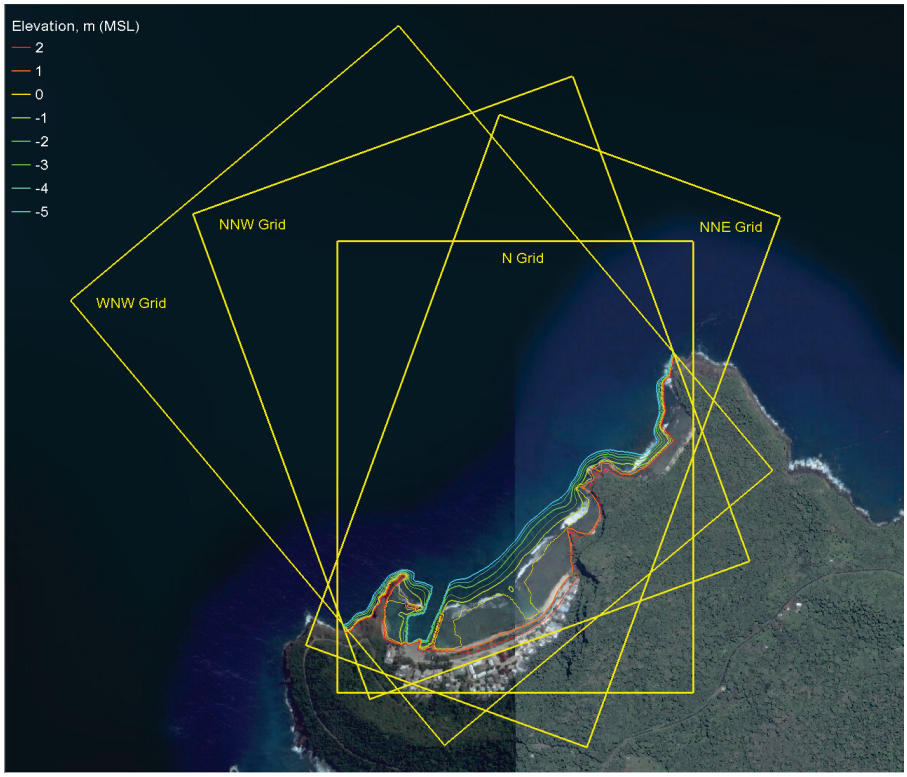

Figure 4-3. N, NNE, NNW, and WNW grids of Alt-2.

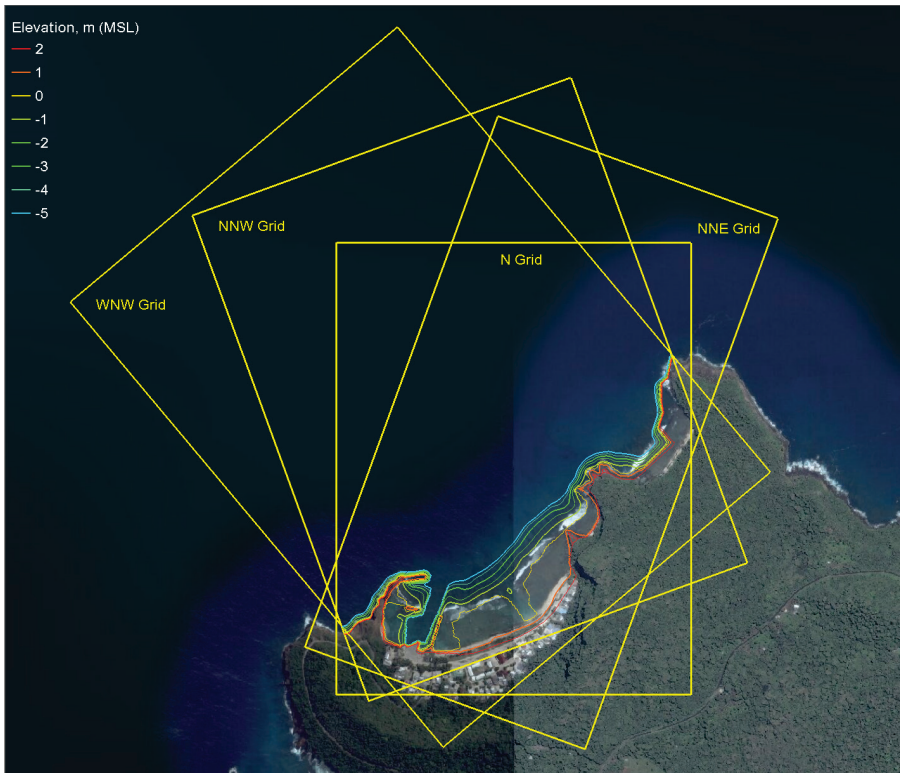

Figure 4-4. N, NNE, NNW, and WNW grids of Alt-3.

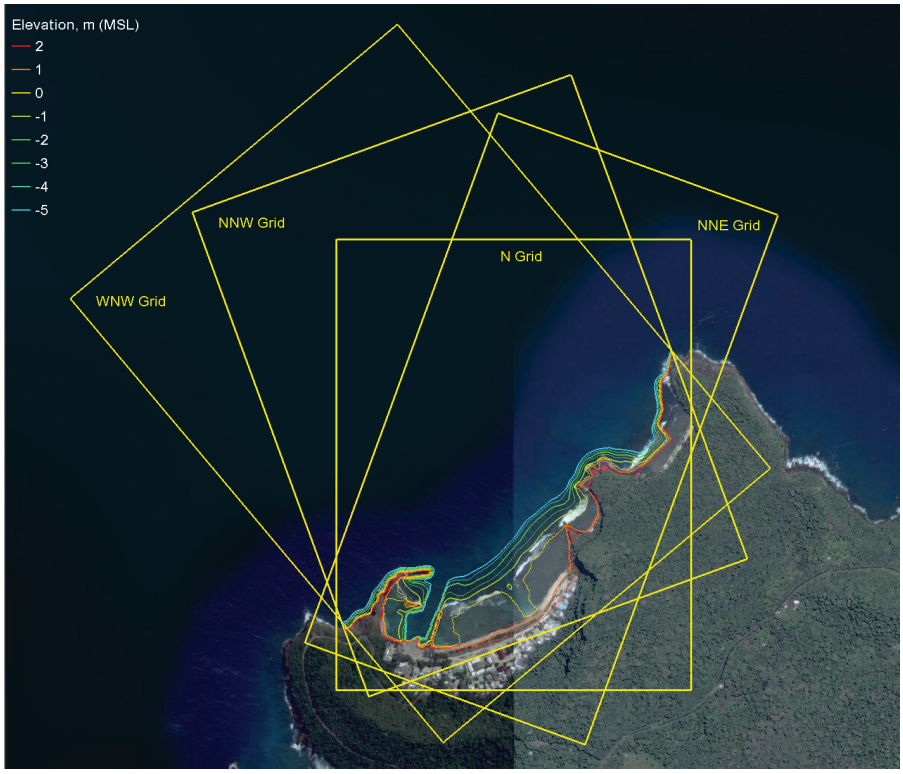

4.2 Input conditions

Incident wave inputs for B2D simulations were specified based on directional wave estimates obtained from CMS-Wave modeling described in Chapter 3. The WIS hindcast for deep-water incident wave conditions (Tables 3-1 and 3-2) was transformed to the project site with CMS-Wave. Calculated CMS-Wave wave height, period, and direction parameters at the seaward boundaries of B2D grids were used in the harbor modeling.

The input conditions used in B2D simulations are summarized in Tables 4-1 and 4-2. The first group of wave inputs in Table 4-1 represents the average or normal operational sea state that allows boats to safely access the harbor. This average wave condition has a significant wave height H_s = 1.5 m and a peak period T_p = 10 sec at the offshore boundary of the B2D grids. It represents the majority of waves affecting the harbor from different directions and is the condition used for investigating navigability and utilization of the harbor. This average wave condition was used with 0°, 20°, 340°, and 320° grids at two water levels (0 m and 0.5 m MSL).

Table 4-1. Average wave conditions in B2D simulations.

ID	*Hs* (m)	*Tp* (sec)	Θ (deg)	Water Level (m)	Used in grid
1	1.5	10	0	0	0°
2	1.5	10	20	0	20°
3	1.5	10	340	0	340°
4	1.5	10	320	0	320°
5	1.5	10	0	0.5	0°
6	1.5	10	20	0.5	20°
7	1.5	10	320	0.5	320°
8	1.5	10	340	0.5	340°

Table 4-2. Storm wave conditions in B2D simulations.

Runs	*Hs* (m)	*Tp* (sec)	Θ (deg)	Water Level (m)	Used in grid
1	7.5	11	0	0	0°
2	9.8	13	320	0	320°
3	9.1	14	320	0	320°
4	7.5	11	0	0.5	0°
5	9.8	13	320	0.5	320°
6	9.1	14	320	0.5	320°

The second wave input group in Table 4-2 includes large storm wave conditions during which navigation and harbor access do not occur. Three severe storms were selected from historical typhoons/hurricanes which had impacted Faleasao Harbor and vicinity areas. The values of model inputs (significant wave heights, peak wave periods, and directions) associated with these storm events are listed in Table 4-2. Because severe storms affect Faleasao Harbor from west and northwest directions, storms were simulated for only two incident wave directions (0° and 320°) and two water levels (0 m and 0.5 m MSL). Results from both categories of incident wave conditions (average and storm waves) are used in evaluation of Alternatives.

4.3 B2D modeling of existing harbor (Alt-0)

4.3.1 Model calibration

Because field data were unavailable to calibrate and validate the B2D model, computational parameters used in the B2D simulations were based on values used in similar previous studies. The Kikiaola Harbor wave modeling study was recently completed (Demirbilek et al. 2015); it was

similar to Faleasao Harbor in several ways. Both harbors are shallow-draft harbors, both are fronted by fringing reefs, and incident wave conditions and water levels affecting both harbors are very similar. Consequently, the values of Chezy coefficient (bottom friction) and Smagorinsky coefficient (turbulent eddy viscosity) used in Faleasao Harbor study were the same values of these input parameters determined in the Kikiaola Harbor project based on model-field data calibration. Similar values of calibration parameters were used in Alt-0, Alt-1, Alt-2, and Alt-3 simulations.

4.3.2 Output files

For user-specified output fields, temporal and spatial solution files are generated by B2D over the entire grid. These may include surface elevation, significant wave height, mean wave direction, mean velocity or current, mean water level or wave setup, pressure, wave force, etc. In addition, optional outputs are available such as water surface elevation time series, pressure, and wave forces at the user-specified output locations, referred to as *probes* or save stations. Time-domain solution files saved can then be postprocessed to develop a variety of engineering design wave parameters such as wave spectra, infragravity wave estimates, statistical wave conditions for risk-based engineering design works, wave forces, wave runup and overtopping, and flood inundation excursion limits, just to name a few.

Model results were saved over the entire grid domain of each of the four harbor geometries. The B2D interface in the Surface-water Modeling System (SMS) was used to view, extract, and postprocess model results (i.e., wave height, period, direction, water level, and wave-induced current). A user-friendly model interface in SMS allows users to perform additional analyses of time series solution files saved at specified probes. Both time-domain and frequency-domain analyses codes exist in the interface for users interested in statistical estimates of wave parameters of interest for engineering applications. Modeling results provided later in this chapter were obtained by postprocessing model solution files using the analyses tools available in the SMS interface of B2D.

4.3.3 Average and storm wave simulations

Eight wave conditions in Table 4-1 represent *average* or *typical* multidirectional sea states at Faleasao Harbor. These were simulated to determine if boat transits into/out of Faleasao Harbor are possible during

average wave conditions from four primary directions (0°, 20°, 340°, and 320°). Values of H_s = 1.5 m and T_p = 10 sec were used in these simulations at two water levels to evaluate proposed improvements to navigation.

For the small boats presently using Faleasao Harbor, calculated wave height estimates determine if safe boat transit into/out of the harbor is possible. According to boat captains, a safe transit in this shallow-draft small boat harbor is possible if wave heights are less than 2 ft in the access channel. Model results indicated input waves to B2D with heights greater than 1.5 m and periods greater than 10 sec would exceed this 2 ft (0.61 m) wave height limit in the channel. Local seas and short-period swells with 1.5 m wave height and 10 sec peak period occur commonly outside the Faleasao Harbor. Four incident wave directions relative to true north (20°, 0°, 340°, and 320°) were used. These represent waves from the NNE, N, NNW, and WNW, respectively. It was noted that incident waves from the N sector come straight into the harbor while waves from NNE and NNW sectors are oblique to the harbor entrance. The most oblique waves to harbor are from the WNW sector (320°).

Six storm conditions were simulated with B2D only for Alt-0 for two wave directions, N (0°) and WNW (320°). Storms were not simulated in B2D for the Alternatives but were modeled with CMS-Wave (see Chapter 3 for details). Model results for storms indicated harbor response was relatively insensitive to water level and also incident wave direction approaching the harbor entrance from deep water. Because no transits are possible during storms, modeling results for storms are not appropriate for navigation but may be used for other purposes such as structural design and repair works. As shown in Table 4-2, selected storms had 7.5 m to 9.8 m significant wave heights (H_s) and 11 sec to 14 sec peak periods (T_p). These significant wave heights and peak periods were simulated with CMS-Wave. These were specified inputs to B2D at two water levels, MSL (0 m) and mean high higher water (MHHW) (0.5 m), for the existing harbor.

4.3.4 Output locations

B2D results were saved over the entire grid and at the special locations of interest in the navigation channel, turning basin, and near harbor protection structures. These were extracted from the global solution files along the nine transects (T1 through T9) shown in Figures 4-5 and 4-6 and postprocessed using the SMS interface of B2D.

Figure 4-5. Output transects T1-T9 for Faleasao Harbor.

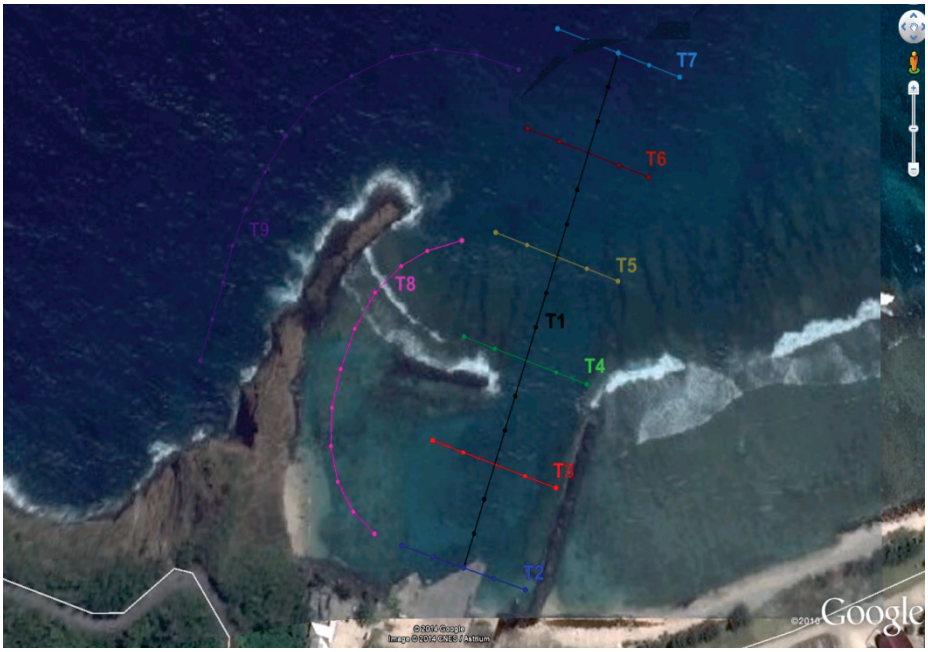

Figure 4-6. Output transects T1-T9 for extraction of B2D results in SMS.

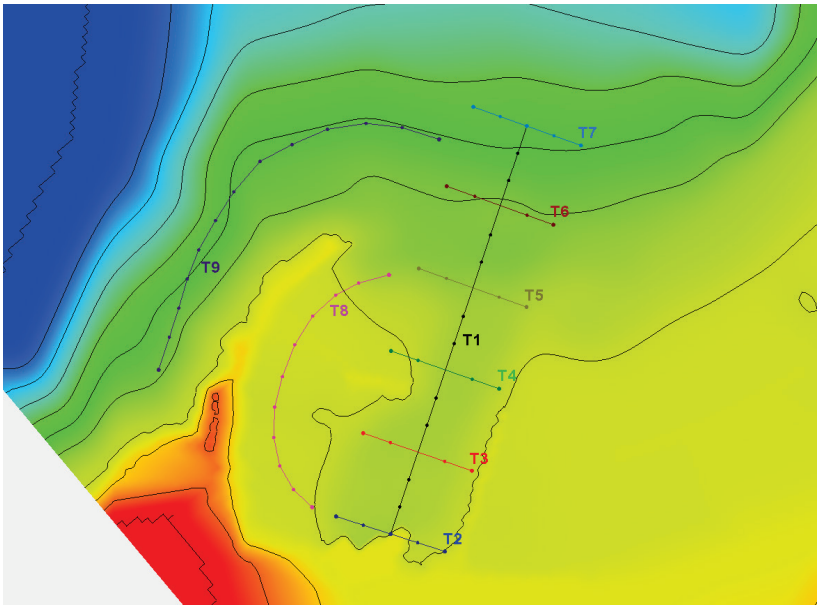

Transects T1 to T9 in Figures 4-5 and 4-6 were placed in three areas of interest. As shown in Figure 4-6, transect T1 is a 300 m straight line along the entrance channel centerline that extends through the turning basin, ending at the dock. Transects T2 to T7 each are 80 m long perpendicular to T1 (Figure 4-6). Transects T8 is approximately 210 m long and runs through the west side of the interior harbor. The 300 m long transect T9 is placed outside the harbor west of the Siuai Point.

4.3.5 Snapshots of wave fields

Calculated wave fields for average wave conditions from four directions are provided in Figures 4-7 through 4-14. These model results over the entire four grids depict wave height variation outside and inside the harbor, showing how the deep water waves transform as they propagate over the outside reefs before entering the harbor. These spatial variations of waves and resulting wave-induced currents by breaking waves are visible in shallower parts of grids. The zoomed snapshots provide additional information on the wave fields in areas of interest.

Figure 4-7. Wave height and wave-induced current fields (N grid).

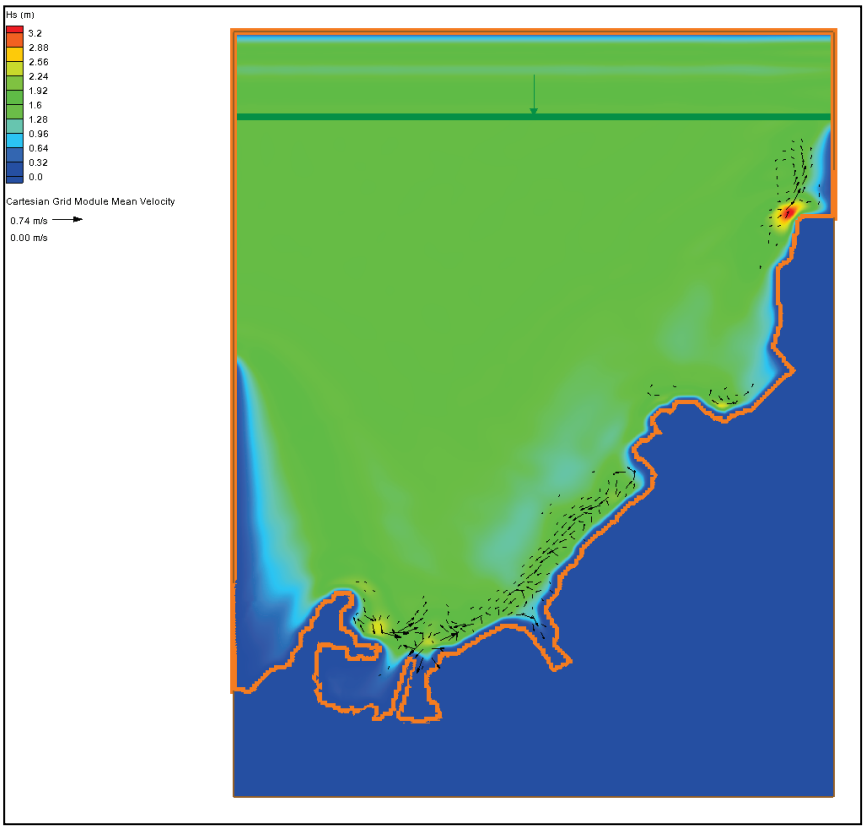

Figure 4-8. Zoomed image of wave height and current fields (N grid).

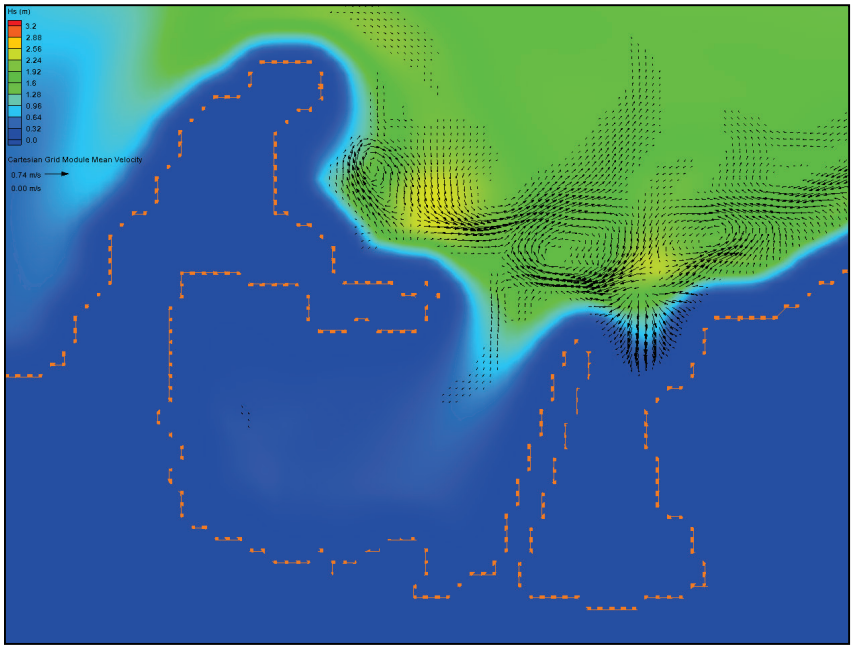

Figure 4-9. Wave height and current fields (NNE grid).

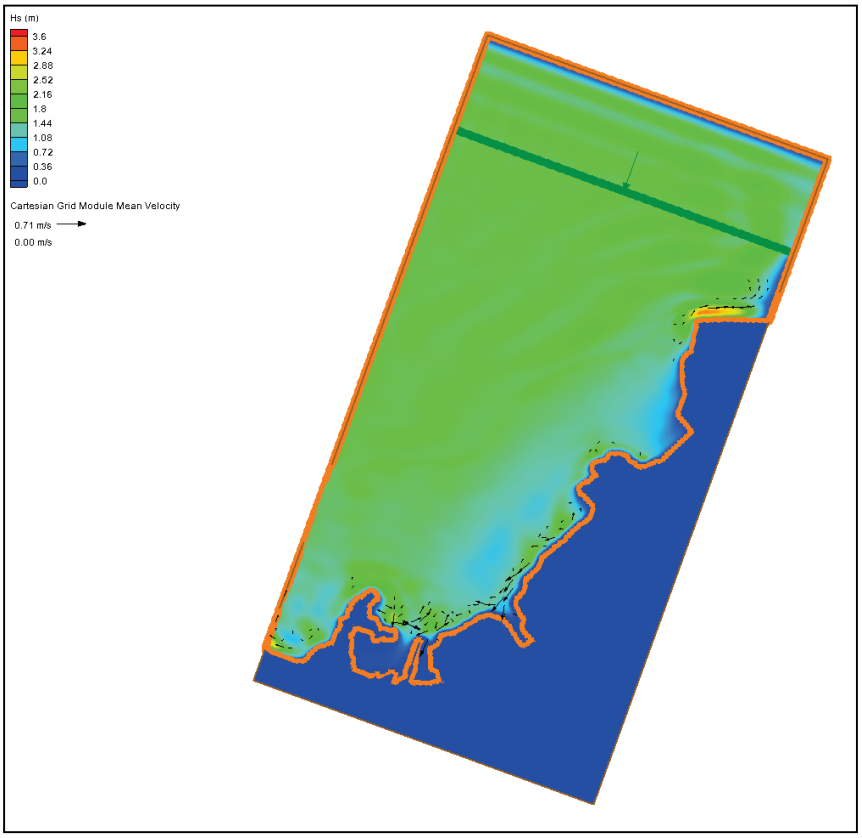

Figure 4-10. Zoomed image of wave height and current fields (NNE grid).

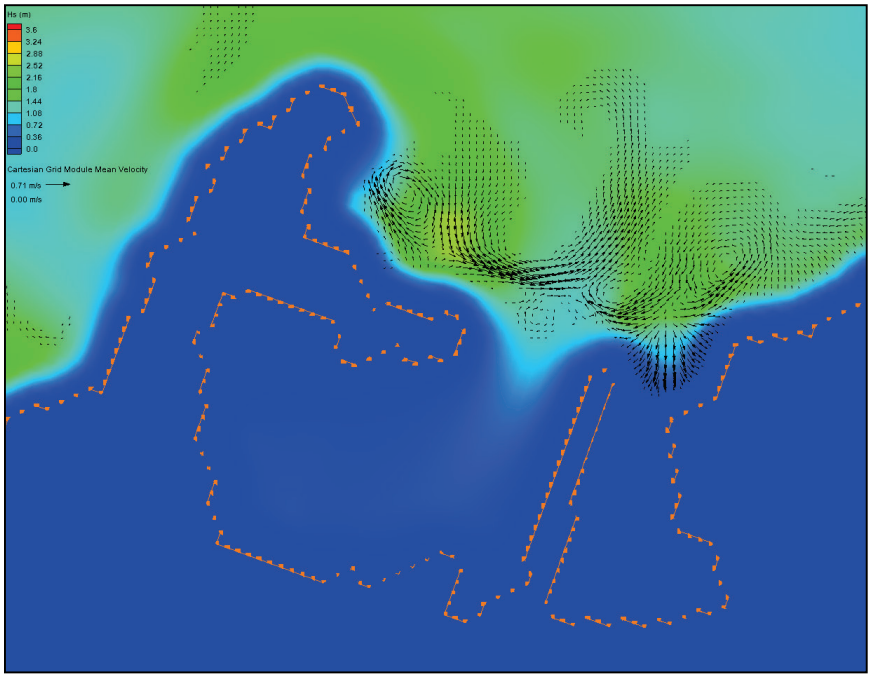

Figure 4-11. Wave height and current fields (NNW grid).

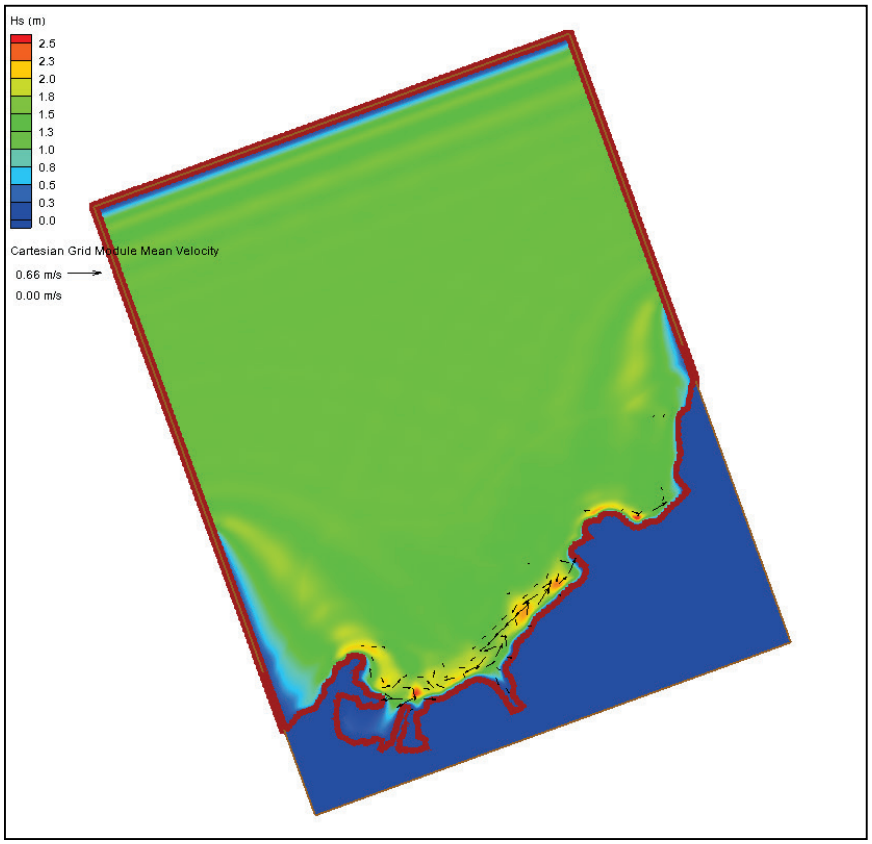

Figure 4-12. Zoomed snapshot of wave height and current fields (NNW grid).

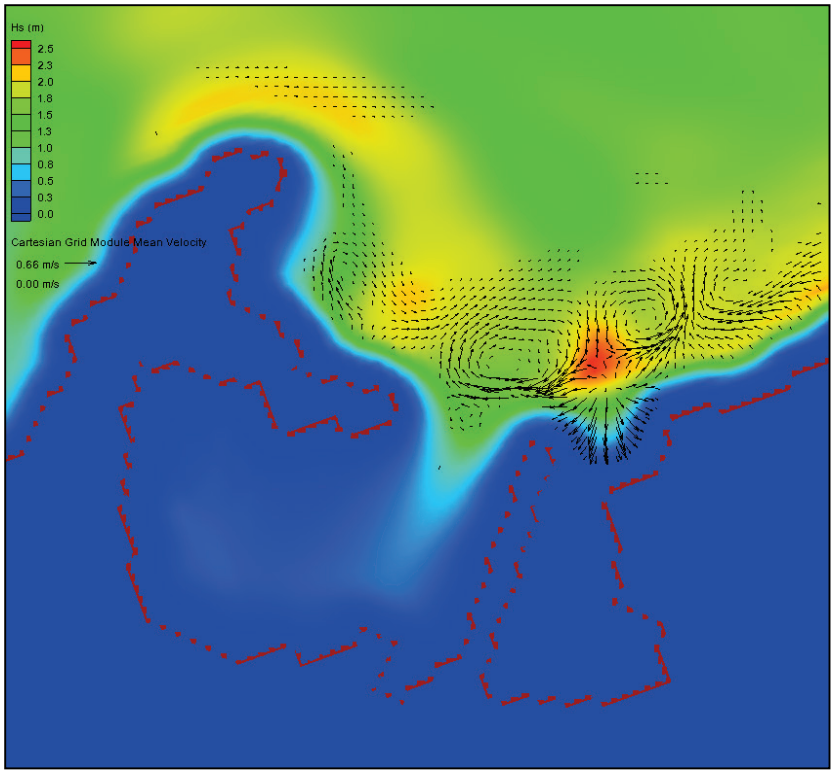

Figure 4-13. Wave height and current fields (WNW grid).

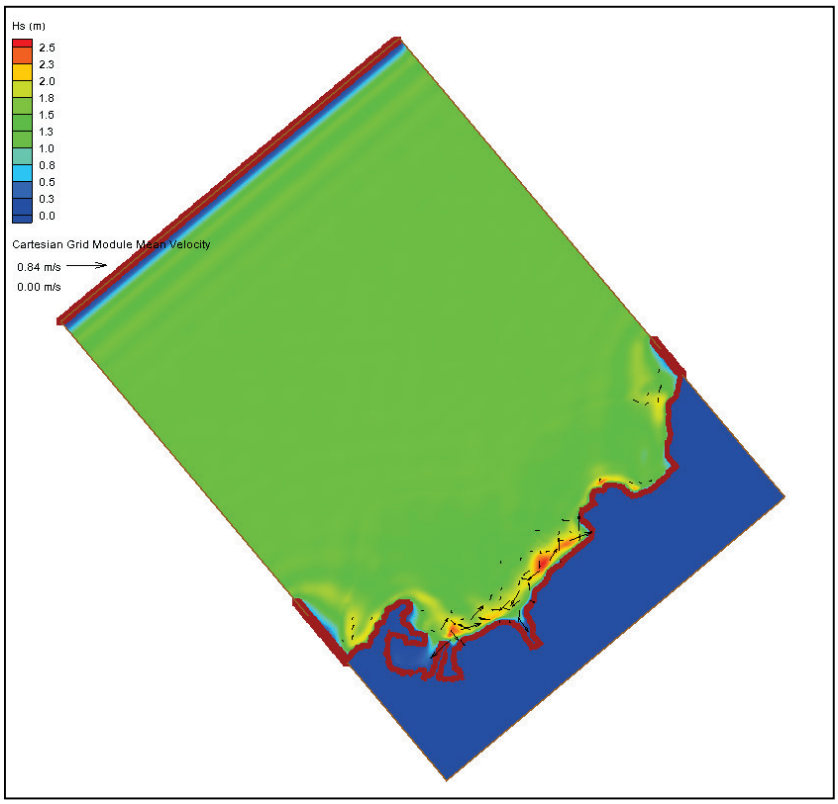

Figure 4-14. Zoomed snapshot of wave height and current fields (WNW grid).

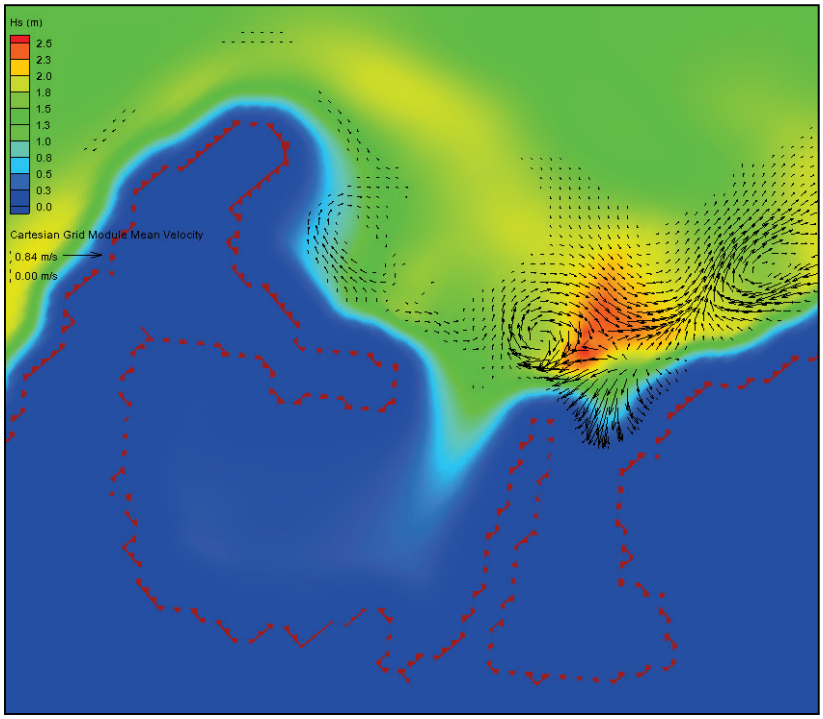

4.3.6 Results for average wave condition

Calculated wave heights in the existing harbor (Alt-0) for average wave conditions were extracted along Transects T1-T9. These spatial variations in the wave height are indicators of the change experienced by waves in different areas of this harbor. Figures 4-15 to 4-19 show an average wave condition from the north at two water levels. Wave heights are slightly greater at the higher water level but less dependent on water level in the northern half of channel. Maximum wave height (~1.8 m) occurs in Figure 4-15 approximately 150 m from the start of T1 near the west spur. The increase in wave height at the channel centerline is due to wave reflection and diffraction effects by the spur at this location. A structure placed close to the west edge of the channel may affect waves in the channel, and this effect depends on size and orientation of the structure and incident wave conditions. Results indicate values of the wave height remain close to the 1.5 m incident wave height in the initial 300 m distance along T1 in the north navigation channel. In the turning basin area along T2, wave heights at both water levels are small, generally less than 7 cm.

Figure 4-15. Wave height variation along T1 and T2 for average wave condition from N.

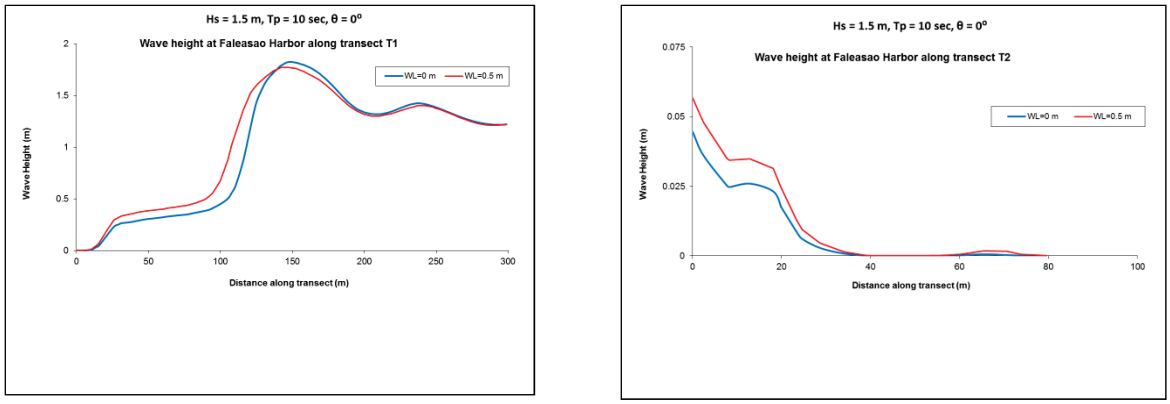

Figure 4-16 shows wave heights along T3 and T4, which are two 80 m long transects perpendicular to the channel in the south part of the harbor. The maximum wave height (~1.5 m) occurs midway (~40 m) along T4 near the west spur. Wave heights decrease rapidly past the spur along T3, and the maximum wave height is 0.5 m midway along T3. Calculated wave heights are smaller at the low water level along T3 and T4.

Figure 4-16. Wave height variation along T3 and T4 for average wave condition from N.

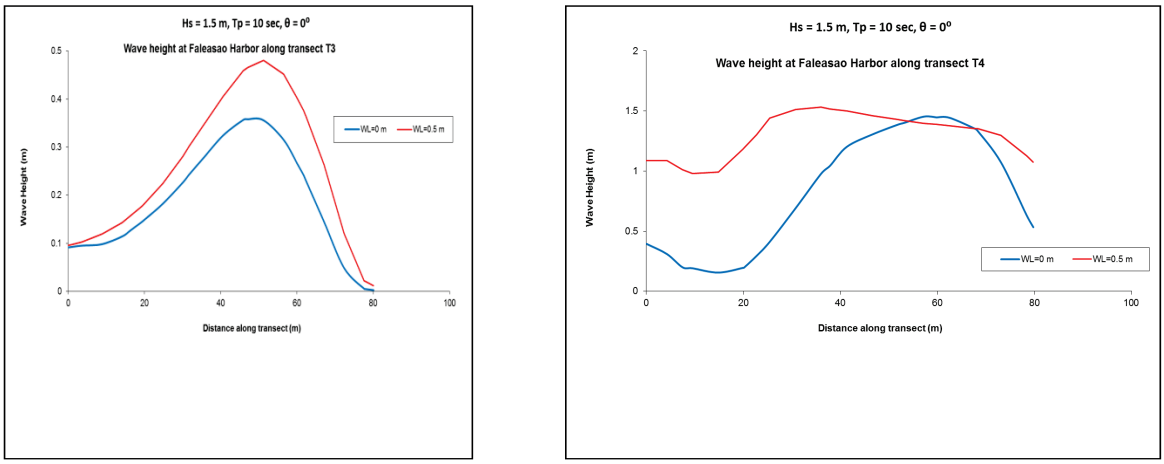

Wave heights along T5 and T6 are provided in Figure 4-17. These 80 m long transects are perpendicular to the north channel. T5 is within the range of potential influence of the spur, causing the wave height to increase over the initial 40 m length of this transect. Calculated wave heights along these transects at the two water levels fluctuate approximately 1.5 m and remain similar to the input incident wave height.

Figure 4-17. Wave heights along T5 and T6 for average wave condition from N.

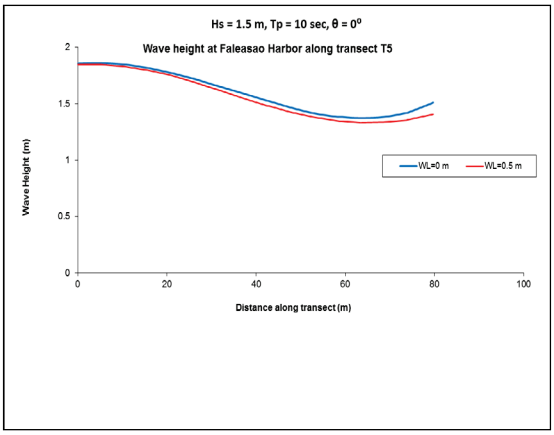

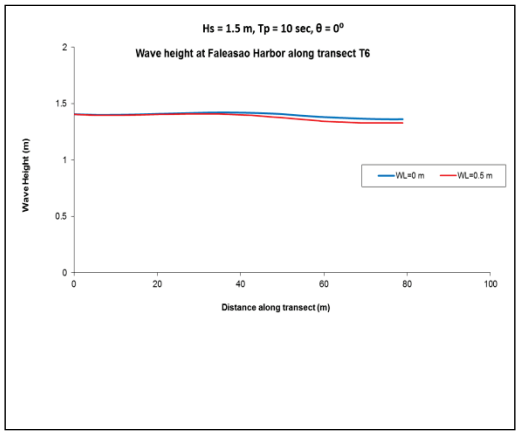

Wave heights along T7 and T8 are displayed in Figure 4-18, where T7 is 80 m long and is perpendicular to the north entrance channel. T8, a curved transect, starts in the south side of the harbor and ends near T5. Wave heights are flat along T7, remain 1.3 m for both water levels, are small (less than 0.2 m) the first 170 m of T8, and gradually increase to 1.5 m near the termination point of T8. Wave heights along T9 located outside the harbor vary; values range from 0.4 m at the south end to 1.6 m at the north side (Figure 4-19). Water level does not appear to affect wave heights along T9.

Figure 4-18. Wave heights along T7 and T8 for average wave condition from N.

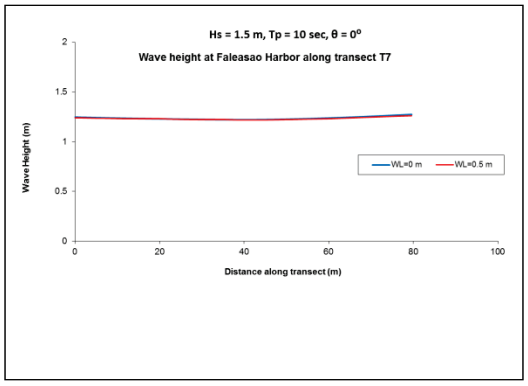

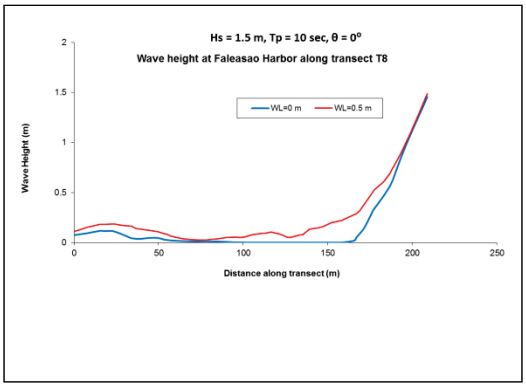

Figure 4-19. Wave heights along T9 for average wave condition from N.

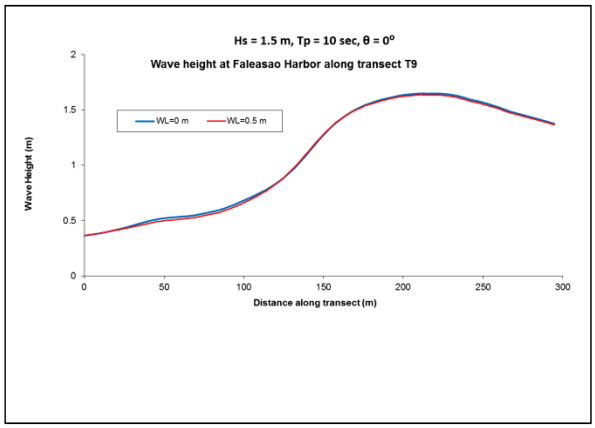

Calculated wave heights along the nine transects are compared for the average wave condition to determine how waves from the different incident directions (0°, 20°, 340°, and 320°) impact navigation and access to Faleasao Harbor. Wave heights along transects T1 to T9 at both water levels are compared in Figures 4-20 through 4-28. Each figure has two panels to display model results along one of the nine transects for four incident wave directions. B2D results for low and high water levels are shown in the left and right panels, respectively. There are four curves in each panel comparing model results for four incident wave directions. These side-by-side panels illustrate the effect of water level on calculated wave heights for different incident wave directions.

Maximum wave heights are seen on T1 for an incident wave from 0° (N), followed by waves from 340° (NNW), 320° (WNW), and 20° (NNE), respectively. The effect of water level is overall weak. Calculated wave heights along T1 generally increase at high water level but decrease at some directions. For example, wave heights along T1 decrease for incident wave from 20° (NNE). Similar observations apply to other transects (T2 through T9) with different trend of wave height variation for each transect. For example, wave heights along T4 for incident wave from 340° (NNW) decrease at high water level. This is not surprising because of minor effect of the west spur at high water level on waves along transects near the spur. Figures 4-20 to 4-28 depict the effects of water level and directionality of incident waves simulated. These results collectively provide important guidance about the local effects of waves on navigation in different areas of Faleasao Harbor.

Figure 4-20. Comparison of wave heights along T1.

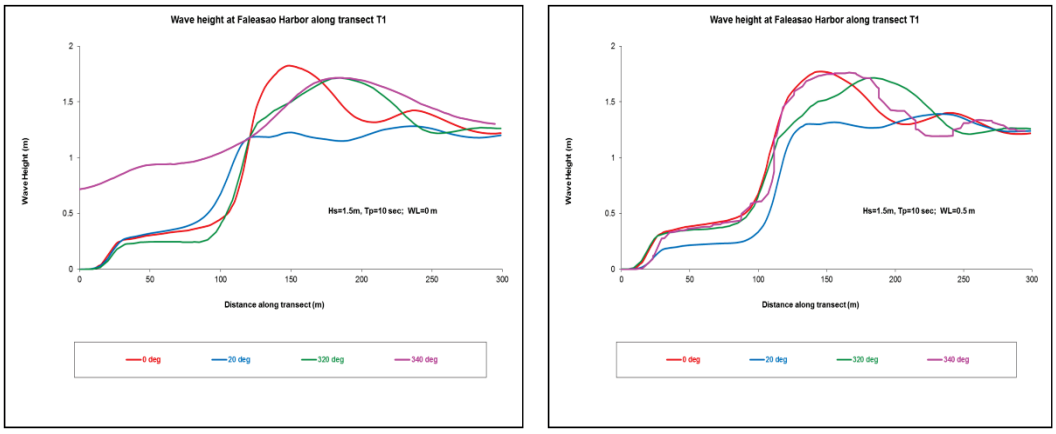

Figure 4-21. Comparison of wave heights along T2.

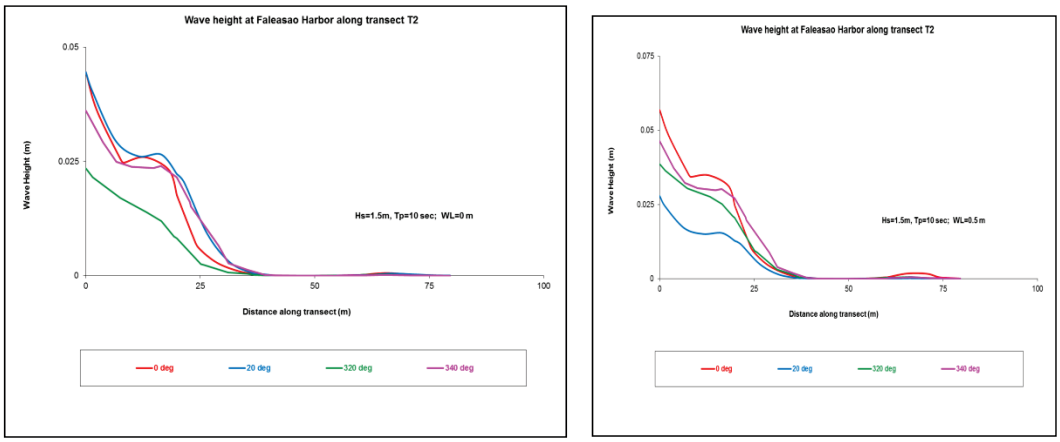

Figure 4-22. Comparison of wave heights along T3.

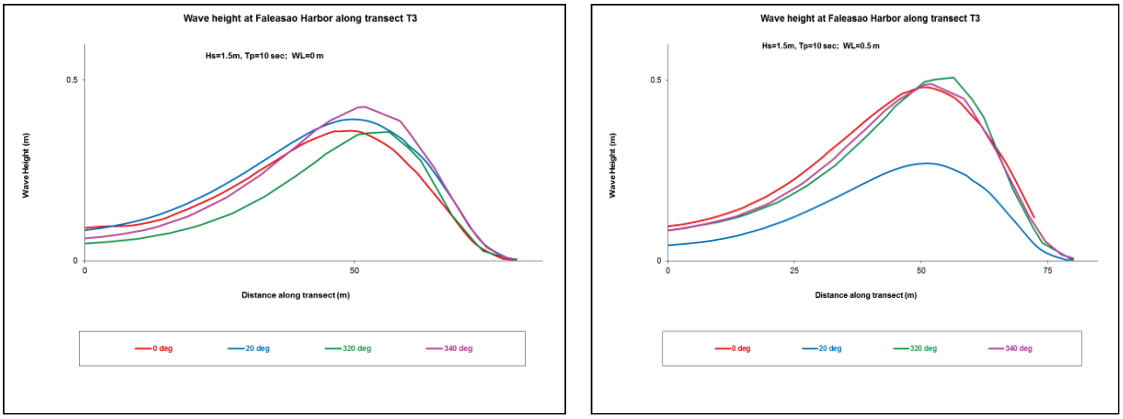

Figure 4-23. Comparison of wave heights along T4.

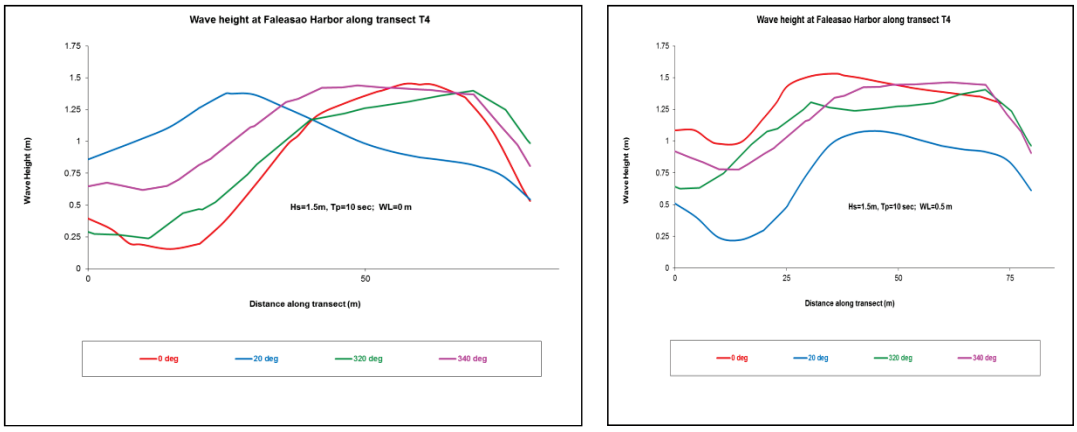

Figure 4-24. Comparison of wave heights along T5.

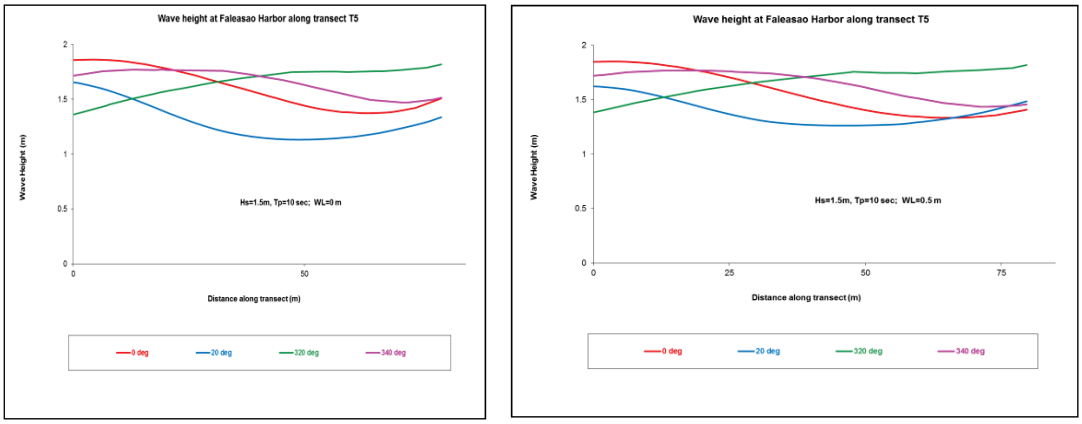

Figure 4-25. Comparison of wave heights along T6.

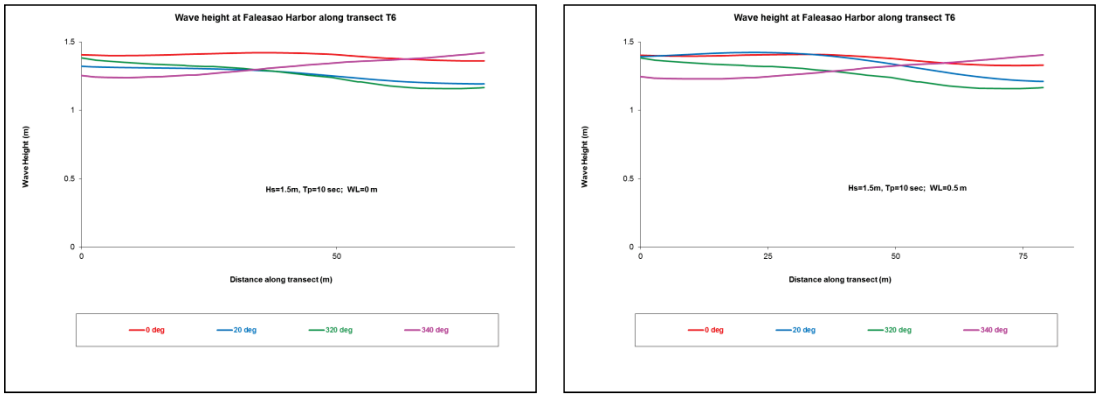

Figure 4-26. Comparison of wave heights along T7.

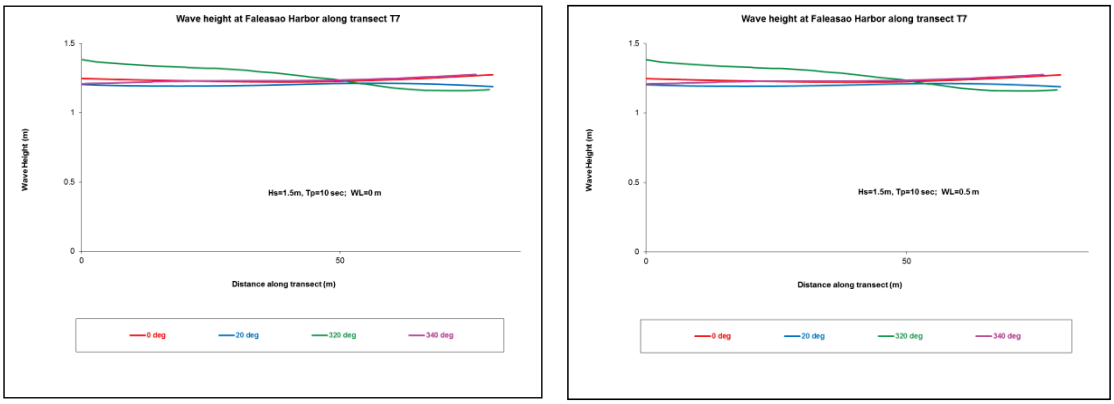

Figure 4-27. Comparison of wave heights along T8.

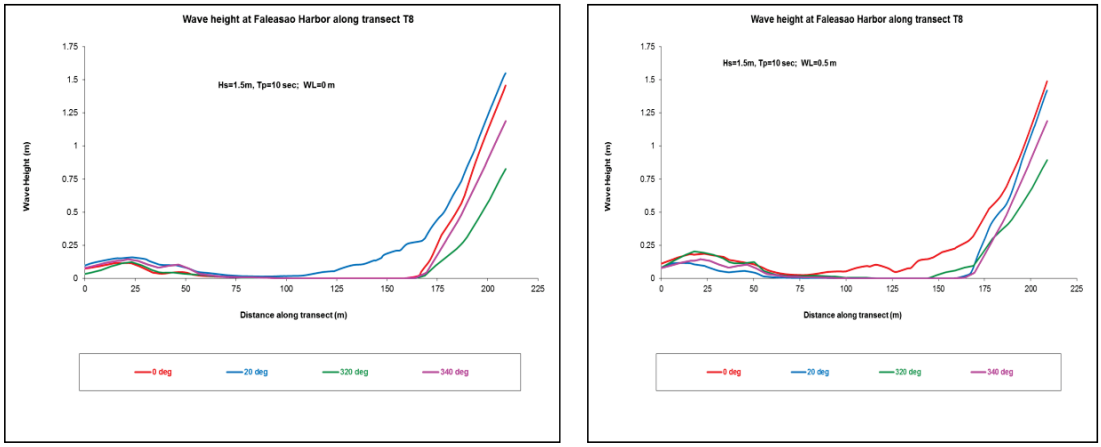

Figure 4-28. Comparison of wave heights along T9.

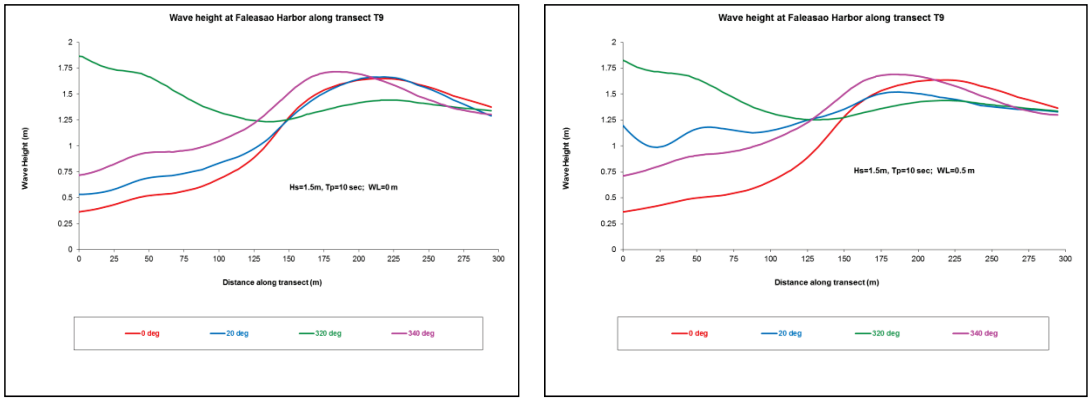

4.3.7 Results for storm wave conditions

Storms approach Faleasao Harbor from the norther, northwestern, and western directions. B2D simulations of three storms from various directions (Table 4-2) indicated wave estimates inside the harbor were proportional to the incident wave height. The three storms had similar

wave periods. Since calculated wave heights for three simulated storms were similar, results are presented in Figures 4-29 through 4-33 for one of the storm conditions (H_s = 7.5 m, T_p = 11 sec incident from north). These figures display the spatial variation of wave heights along the nine transects. Results indicate that waves reaching the navigation channel and harbor interior have similar heights because such waves are depth limited.

The west peninsula and spur block the majority of storms coming into the harbor from the west and northwest, thus sheltering the turning basin and dock areas very effectively. Results suggest that adding new structure(s) to the west side of the harbor and repairing existing structures would greatly improve navigation in the Faleasao Harbor. Results for storms are useful in evaluation and selection of Alternatives.

Wave heights of approximately 9 m in Figure 4-29 along T1 in the north channel are large, but these are associated with past typhoon conditions. Wave heights along T2 in the turning basin are below 0.4 m, less than 2 m along T3, and increase in the north channel, reaching 4 m to 8 m along transects T4 through T7. Based on the values of large wave heights obtained in the most protected south side of harbor, this harbor would be risky for boats to remain in or seek shelter in during hurricane-level severe storm events.

Figure 4-29. Wave heights along T1 and T2 for a storm (H_s =7.5 m, T_p = 11 sec) from N.

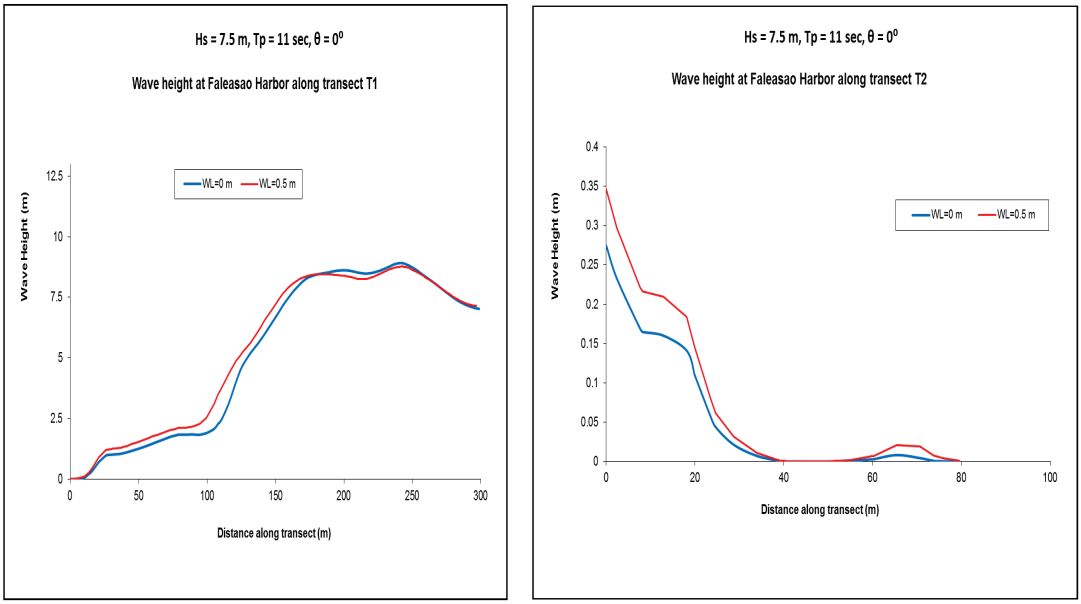

Figure 4-30. Wave heights along T3 and T4 for a storm (Hs =7.5 m, Tp = 11 sec) from N.

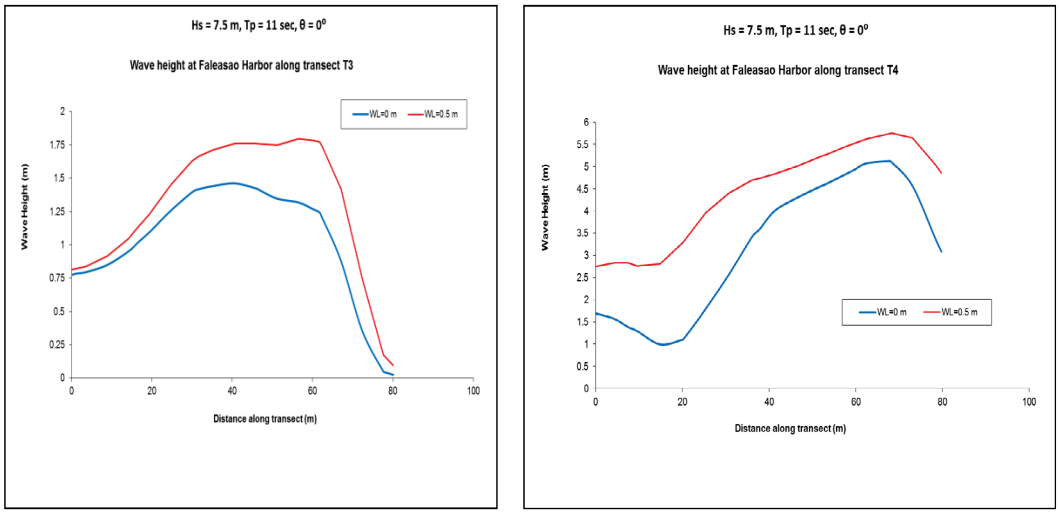

Figure 4-31. Wave heights along T5 and T6 for a storm (H_s =7.5 m, T_p = 11 sec) from N.

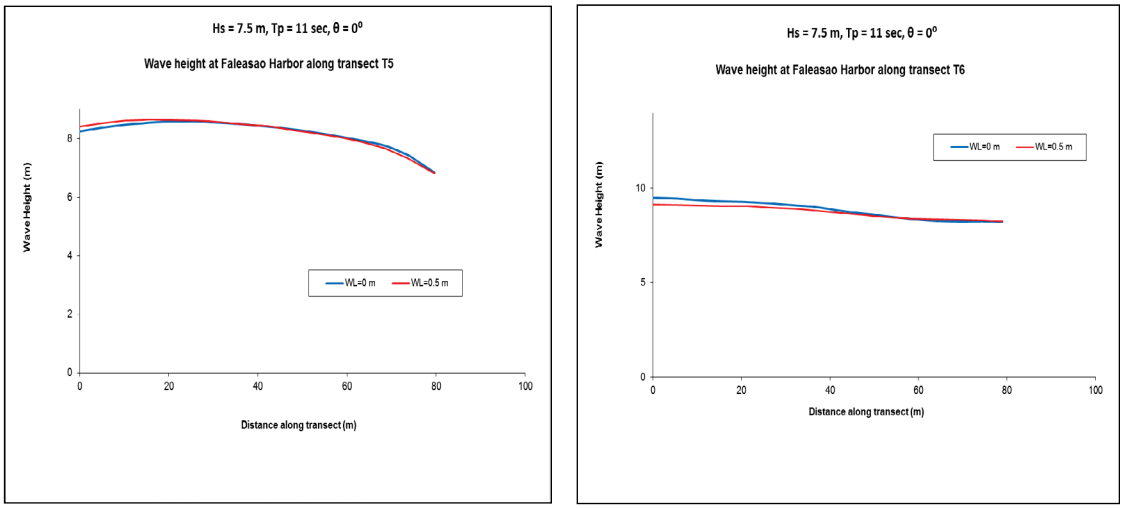

Figure 4-32. Wave heights along T7 and T8 for a storm (H_s =7.5 m, T_p = 11 sec) from N.

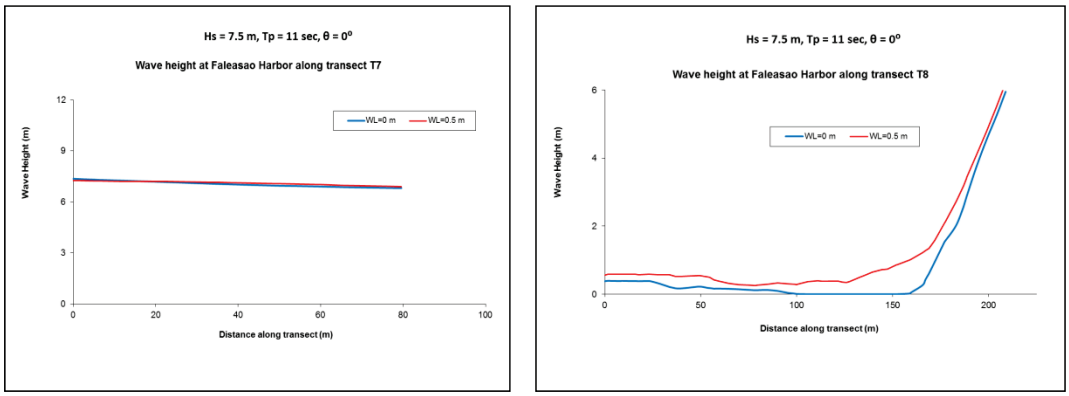

Figure 4-33. Wave heights along T9 for a storm (Hs =7.5 m, Tp = 11 sec) from N.

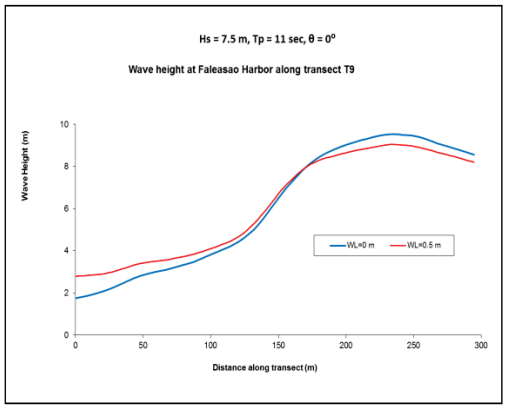

4.3.8 Discussion of existing harbor (Alt-0) results

Wave heights for the average wave condition in Figures 4-20 through 4-28 are greater in the the northern part of navigation channel (T1) and less in the southern. Wave heights are greater along the three northern transects perpendicular to the channel (T5, T6, T7) than those along the three southern transects (T2, T3, T4). The largest wave heights calculated are outside the harbor, occurring along the transect T9 in the north and west.

Comparison of calculated wave heights along the nine transects indicates wave heights are generally greater at high water level (0.5 m, MSL) than at low water level (0 m, MSL). However, wave heights along the 100 m south segment of T1 are less than the 2 ft threshold for safe transit in shallow-draft navigation channels. Wave heights are also less than the threshold along T2 and T3 at the dock and in the turning basin areas. Wave heights are also less than the safe transit limit along most of transect T8 but only over a small part of transect T4. The threshold wave height limit is exceeded along T4, T5, T6, and T7, part of T8, and all of T9. These observations apply to all simulated incident waves from all four directions.

There was little or no change in CMS-Wave results for Alt-0 in the offshore incident conditions up to T7. This is expected since the water depths outside Faleasao Harbor are deep. A reduction in wave height outside the harbor may not occur until waves move over the fringing coral reefs since the water depths over the reefs range from 100 m to 10 m. Extreme storm waves may also break over the reefs, and consequently, incident waves of height up to 5 m or less may not be affected by the reefs just outside the harbor entrance. This was confirmed by CMS-Wave calculated wave heights, and also by B2D results for all four incident wave directions at the

two water levels (Figures 4-24 to 4-28). B2D results indicate wave heights decrease in the channel and turning basin. Wave heights keep decreasing from the start of the channel as waves move through the channel to reach the turning basin and dock. The reduction occurs in part because waves are moving into the harbor through a narrow and shallow channel. Additional reduction in wave heights occurs once waves get into the much shallower interior harbor areas where waves eventually break.

Alt-0 results for a storm wave condition (H_s = 7.5 m, T_p = 11 sec) from the north are presented in Figures 4-29 through 4-33. Because the general trend of model results was similar for the three other storms, results are provided only for one storm. Note that the wave height reduction inside the harbor for storm waves is not as severe as the reduction occurring for average wave conditions. Wave heights of storm waves which lose less energy in some areas of the four grids can increase in parts of harbor due to wave shoaling, reflection, and diffraction. For the three storm events simulated, wave heights at the dock and turning basin remained below the 2 ft threshold along T2 and along the south segment of T8. Wave heights far exceeded the 2 ft limit along all other transects. Calculated wave heights were consistently greater at the high water level (0.5 m) compared to the low water level (0 m). Based on calculated wave heights inside and outside the harbor, B2D results indicate vessels cannot access Faleasao Harbor or seek refuge in the harbor during extreme events. If moored properly, boats might stay in the southwest side of the mooring area and also at the dock.

4.4 Model results for Alt-1

Alt-1 includes deepening of the channel and mooring basin in an attempt to improve navigation to allow larger boats access to Faleasao Harbor. With this goal in mind, it then suffices to evaluate the Alternatives based on analysis of average wave condition results during which navigation can occur. Because vessels cannot access Faleasao Harbor during storm conditions, results from storm simulations can only be used as design conditions. Each Alternative will be assessed by comparing its performance relative to the existing harbor (no-project condition).

For an Alternative to be considered viable, it has to provide a significant reduction in wave energy (wave height) in one of the three areas that is critical to navigation. The three areas are the navigation channel, turning basin, and dock/pier. Although it is not required, evaluation of each

Alternative can consider (for completeness) average and storm wave conditions. Even though no boat traffic is possible during extreme storms, it was decided to consider storms as well in determining the effectiveness of Alternatives. This allows providing information for future design and repair of harbor infrastructures. For Alt-1, the variation of wave heights along the nine transects at the two water levels is described for average wave conditions. This is followed by a comparison of Alt-1 and Alt-0 results for one selected storm event.

Alt-1 results for the average incident wave from the north are shown in Figures 4-34 through 4-42. These are compared to Alt-0 results to assess the effectiveness of Alt-1. At the same water level, the solid lines represent Alt-0, and the dash lines with the same color are for Alt-1. This notation is used throughout this chapter when comparing results of an Alternative to those of the existing harbor. Based on this notation, results for an Alternative in red/blue dash lines should be less than solid lines of the same color for the existing harbor (Alt-0). This notation is easily visible, a sign of wave height reduction by an Alternative. It is possible for an Alternative to reduce wave heights along some transects but not all of them. It is also possible for an Alternative to reduce wave heights along part of a transect but not over the entire transect.

The efficiency of an Alternative increases if there are large reductions along parts or an entire transect or along multiple transects. One or more of these outcomes are indicators of the partial or strong effectiveness of an Alternative relative to the existing harbor. Consider Figure 4-34, where the dash lines (Alt-1) remain below the solid line counterparts (Alt-0) in the first 150 m. This trend reverses between 150 m and 200 m, but then dash and solid lines become identical or overlap. To emphasize the uncertainty in the model results due to lack of field data, it is emphasized to note that this trend could change if different values of modeling parameters were used in simulations. This is because certain input parameters in B2D (e.g., Chezy and Smagorinksy coefficients) influence the global solution while others (e.g., damping layers) affect more the localized results. Alt-1 (or Alt1) results are compared to Alt-0 (Alt0) in Figures 4-34 to 4-42.

Figure 4-34. Comparison of Alt-0 and Alt-1 wave heights along transect T1 ($\theta = 0^0$).

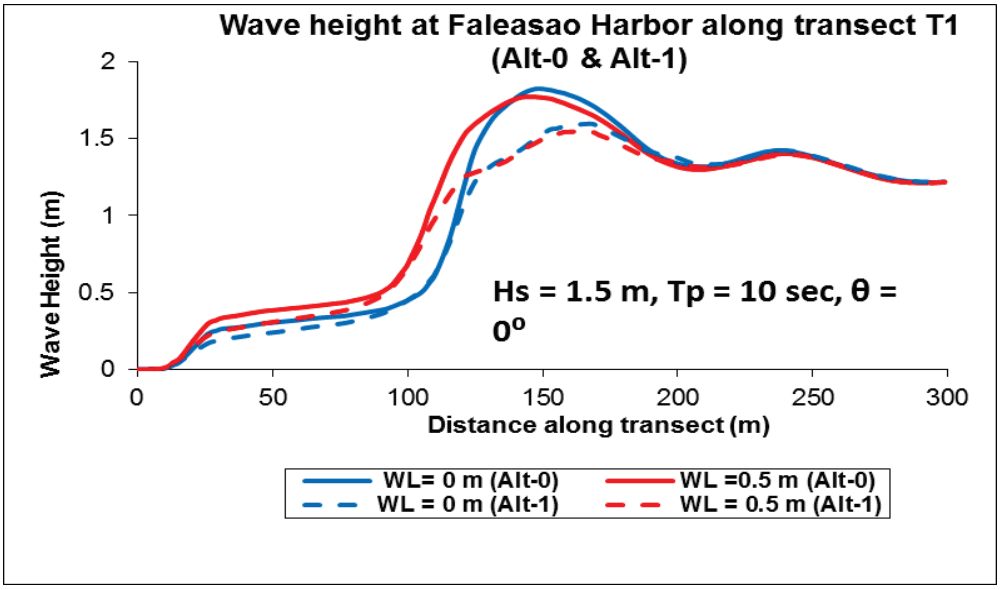

Figure 4-35. Comparison of Alt-0 and Alt-1 wave heights along transect T2 ($\theta = 0^0$).

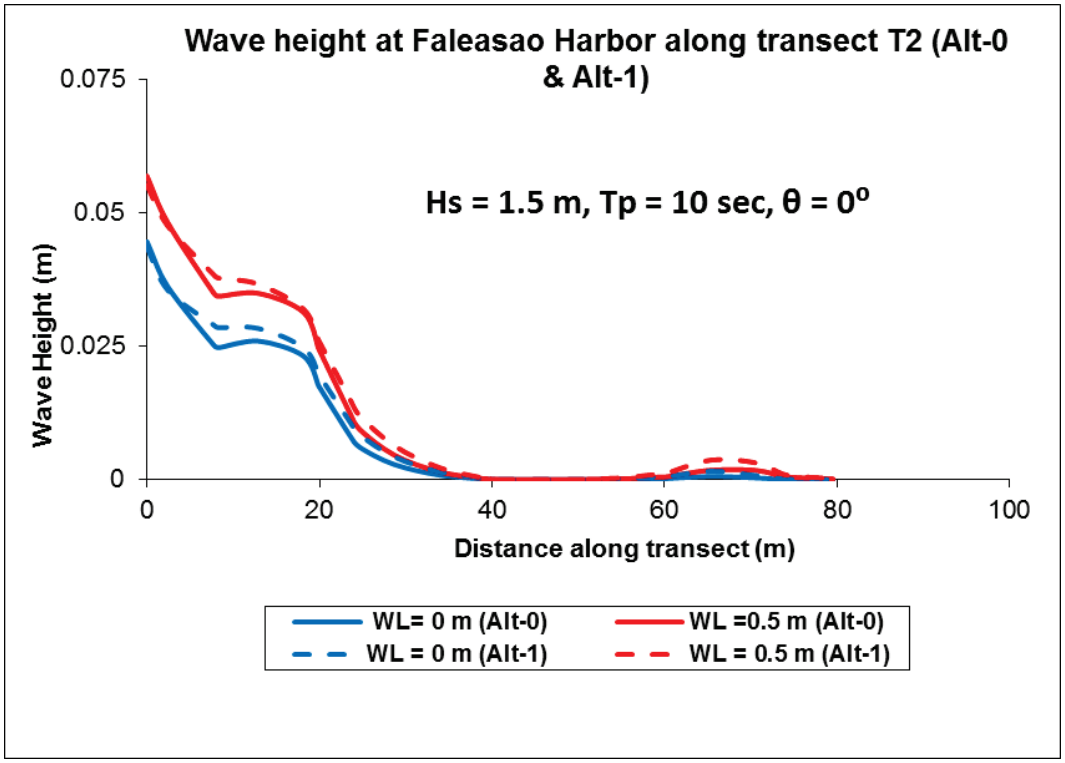

Figure 4-36. Comparison of Alt-0 and Alt-1 wave heights along transect T3 (θ = 0°).

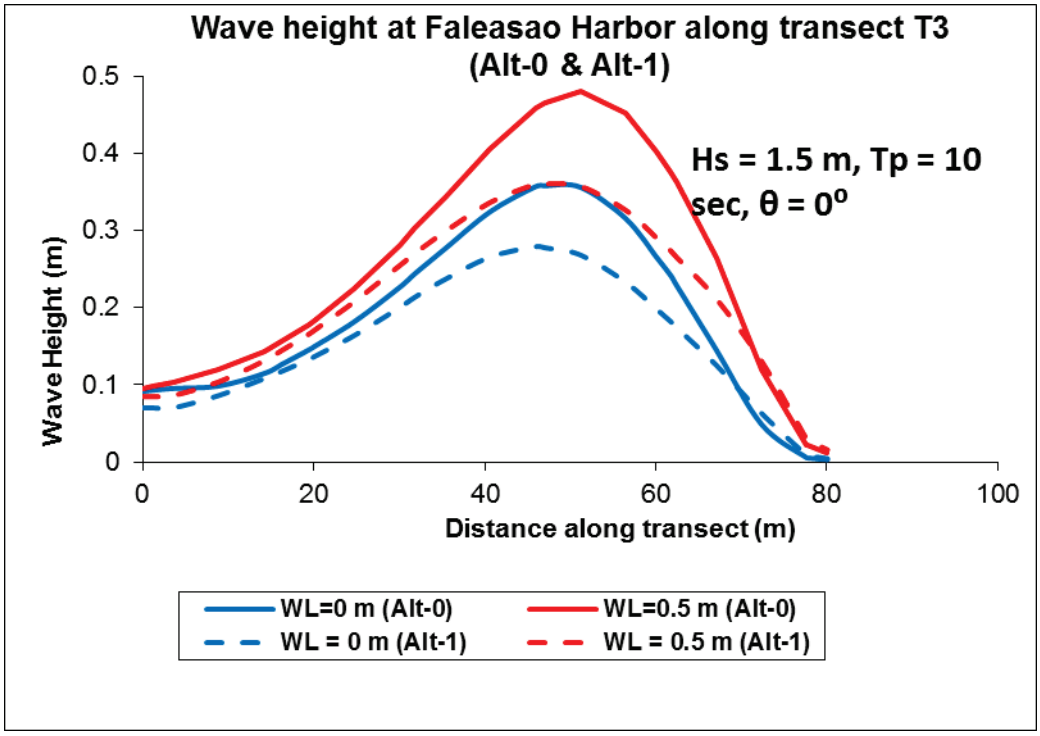

Figure 4-37. Comparison of Alt-0 and Alt-1 wave heights along transect T4 (θ = 0°).

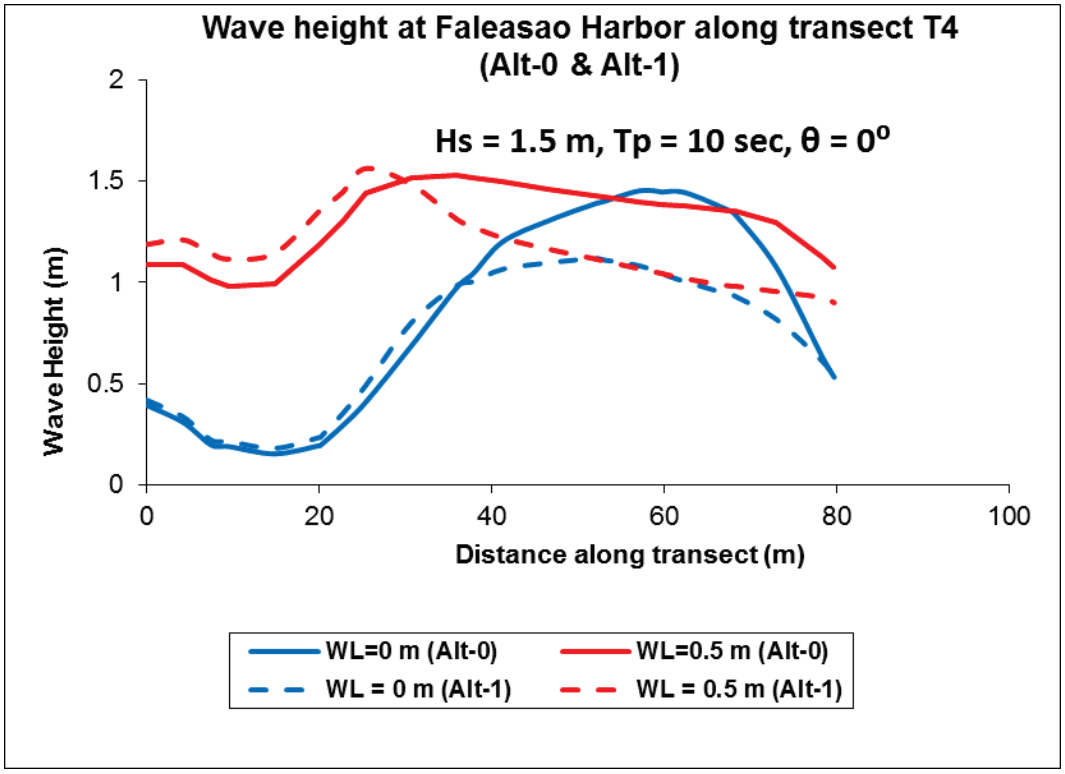

Figure 4-38. Comparison of Alt-0 and Alt-1 wave heights along transect T5 ($\theta = 0^0$).

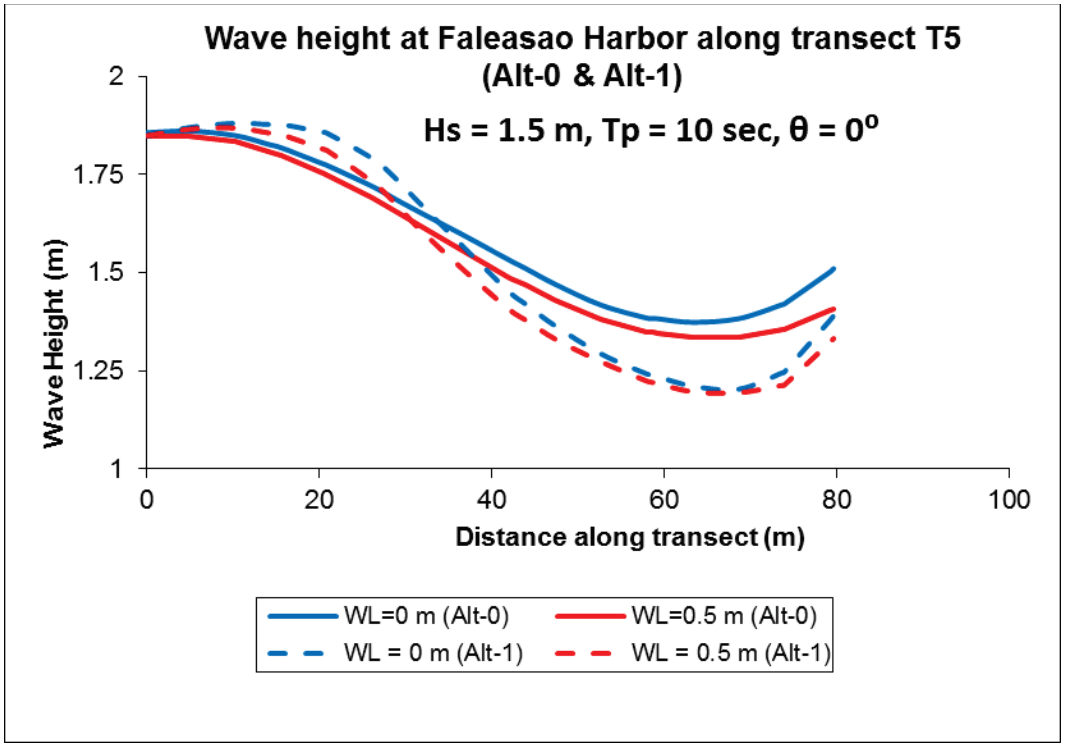

Figure 4-39. Comparison of Alt-0 and Alt-1 wave heights along transect T6 ($\theta = 0^0$).

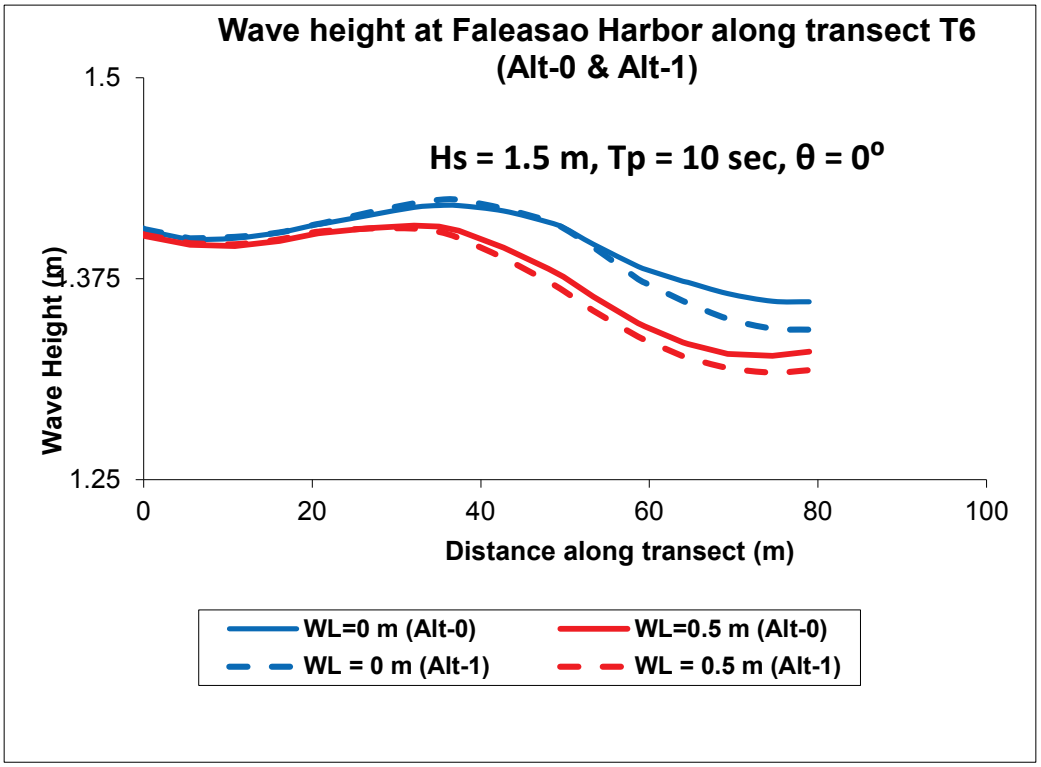

Figure 4-40. Comparison of Alt-0 and Alt-1 wave heights along transect T7 ($\theta = 0^0$).

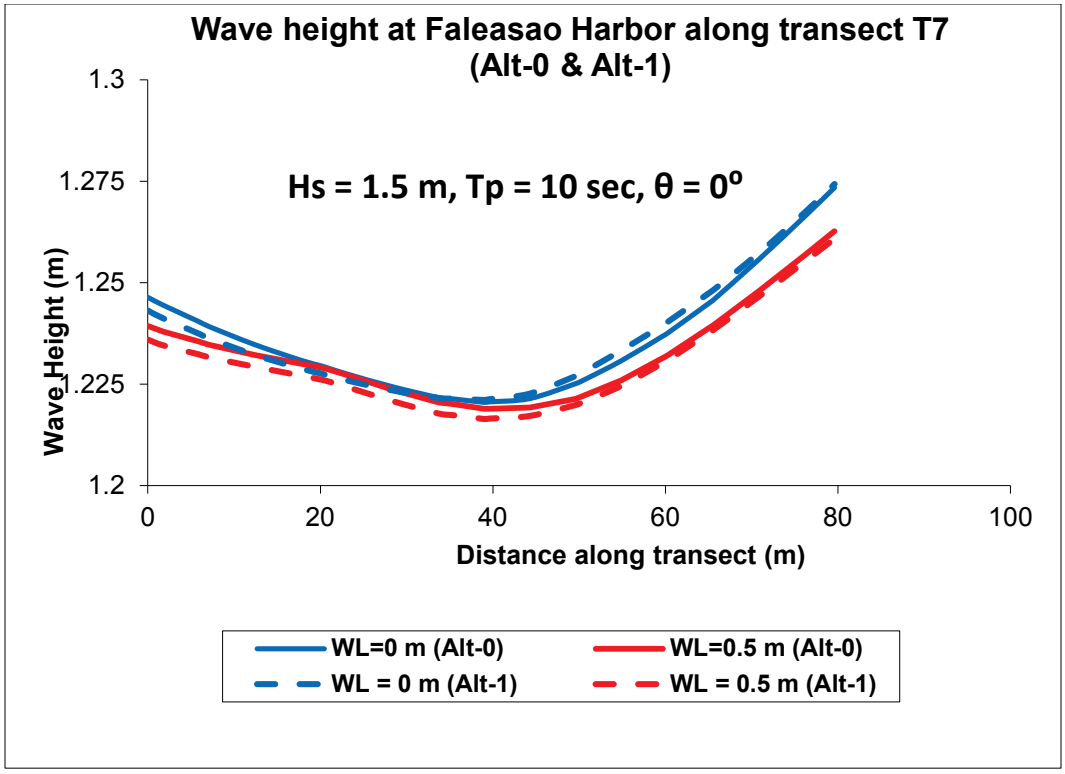

Figure 4-41. Comparison of Alt-0 and Alt-1 wave heights along transect T8 ($\theta = 0^0$).

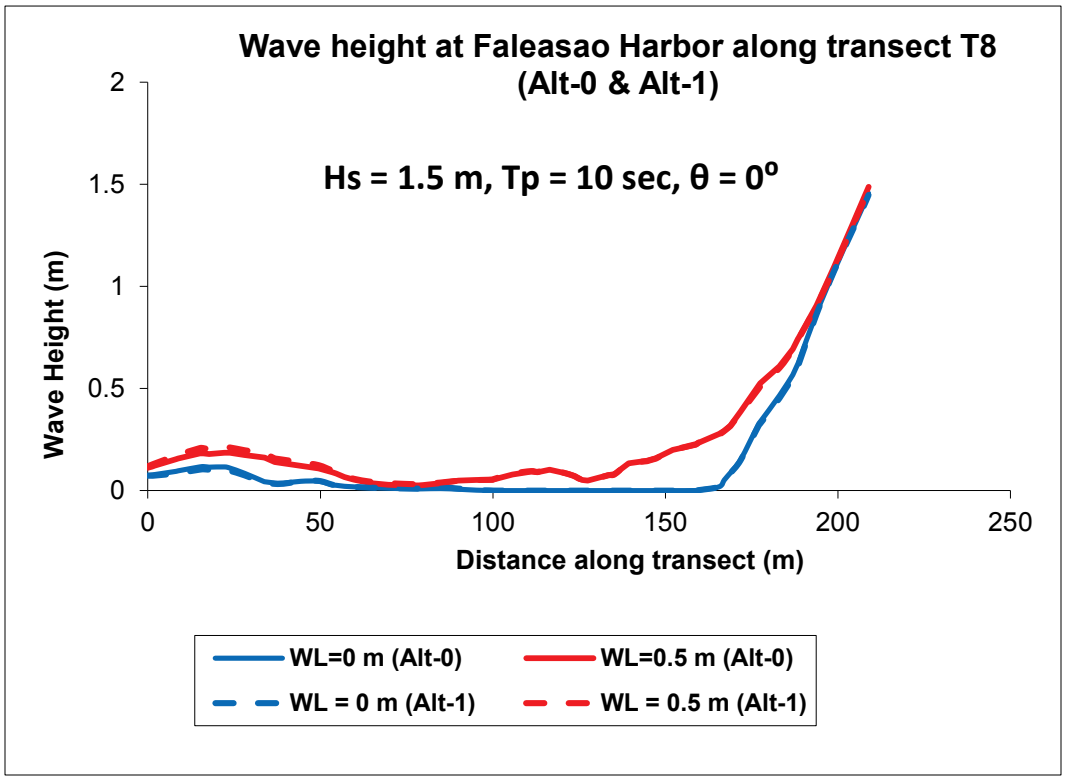

Figure 4-42. Comparison of Alt-0 and Alt-1 wave heights along transect T9 ($\theta = 0^0$).

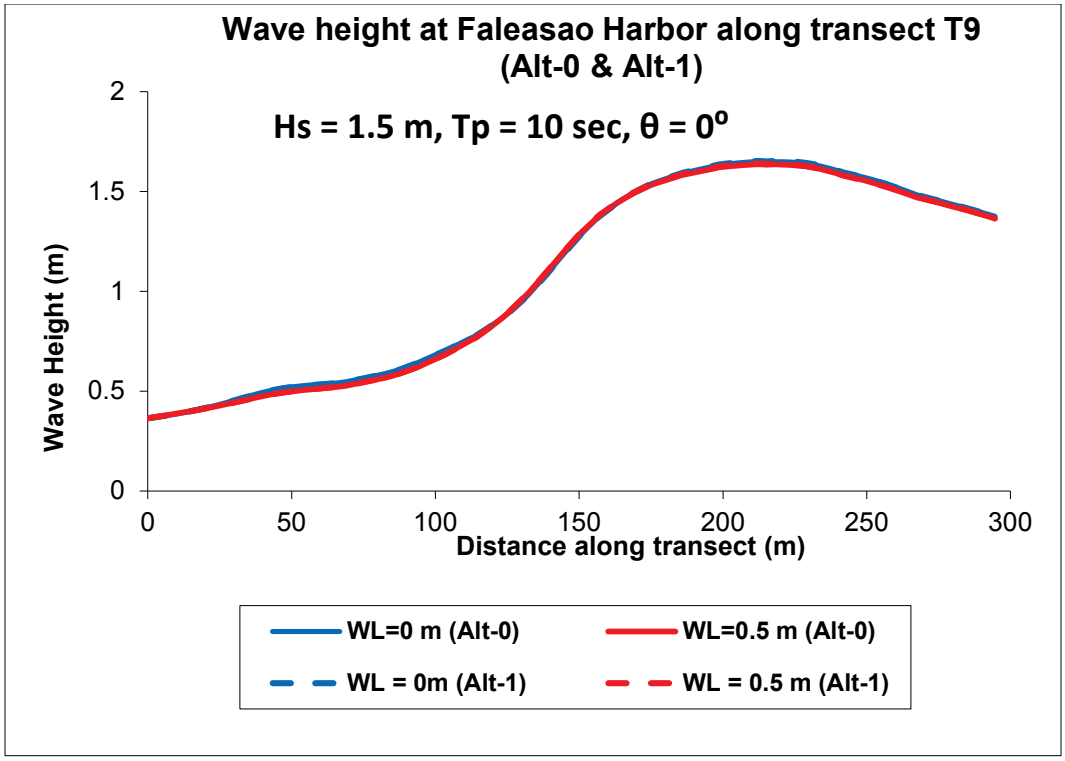

Alt-1 and Alt-0 results from the 20° grid (NNE grid) are compared in Figures 4-43 through 4-51, showing the local variation of wave heights along nine transects at two water levels. The dredged channel (Alt-1) results in dash lines are generally less than Alt-0 results (solid lines), indicating no increase in wave energy in the harbor by deepening the channel and turning basin areas. A figure for each transect shows the local change in wave heights resulting from deepening of the channel and mooring areas.

Figures 4-52 through 4-60 show comparison of Alt-0 (solid lines) and Alt-1 results (dashed lines) for incident waves from 340°. Results indicate that, except in a few local areas, wave heights for Alt-1 along each transect are generally less than Alt-0 results.

Alt-1 results for incident waves from 320° (WNW grid) are compared to Alt-0 results in Figures 4-61 through 4-69. Results do not show a significant increase of wave heights caused by deepening of the channel and mooring areas.

Figure 4-43. Comparison of Alt-0 and Alt-1 wave heights along transect T1 (θ = 20°).

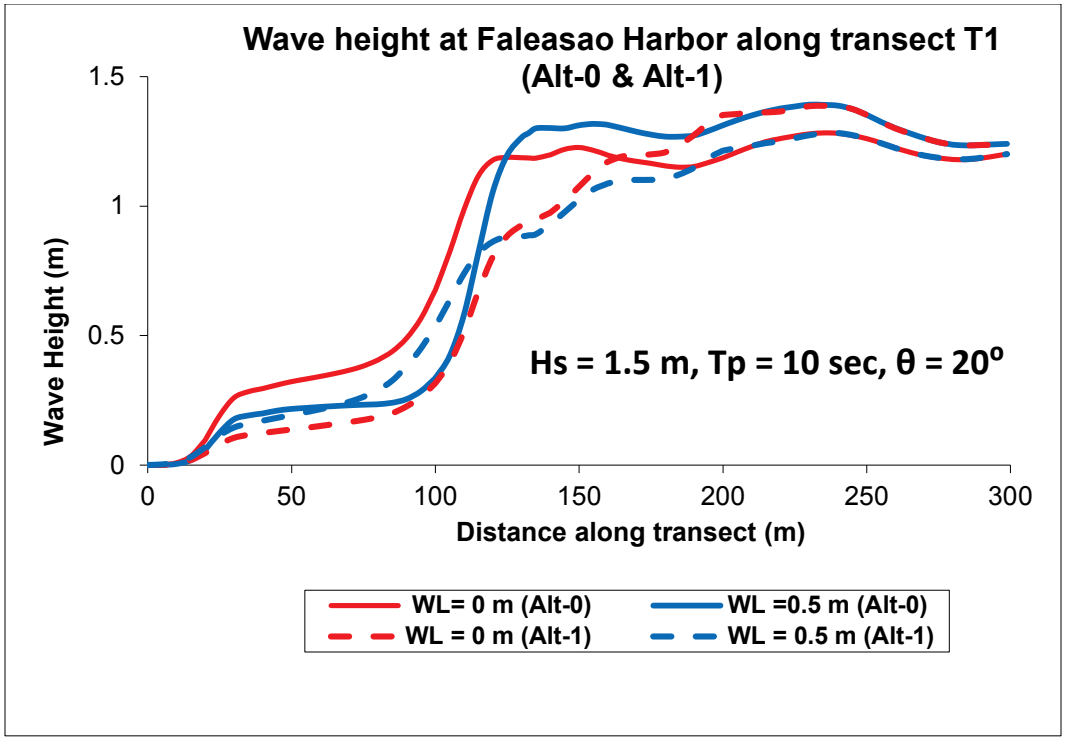

Figure 4-44. Comparison of Alt-0 and Alt-1 wave heights along transect T2 (θ = 20°).

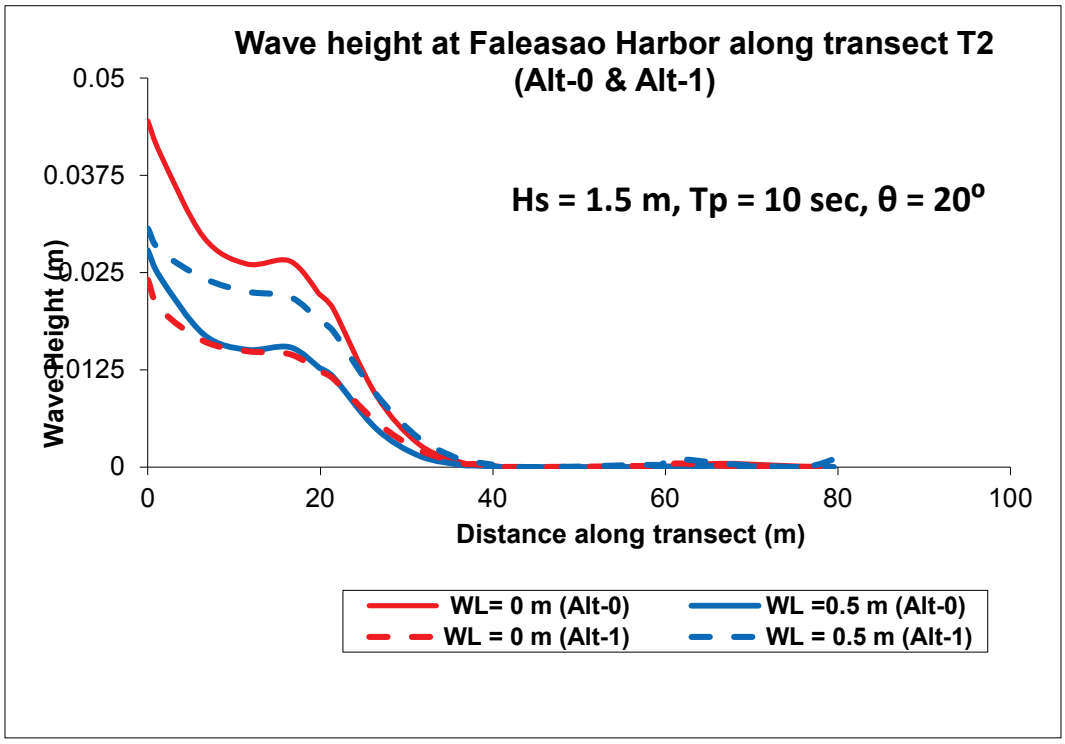

Figure 4-45. Comparison of Alt-0 and Alt-1 wave heights along transect T3 ($\theta = 20^o$).

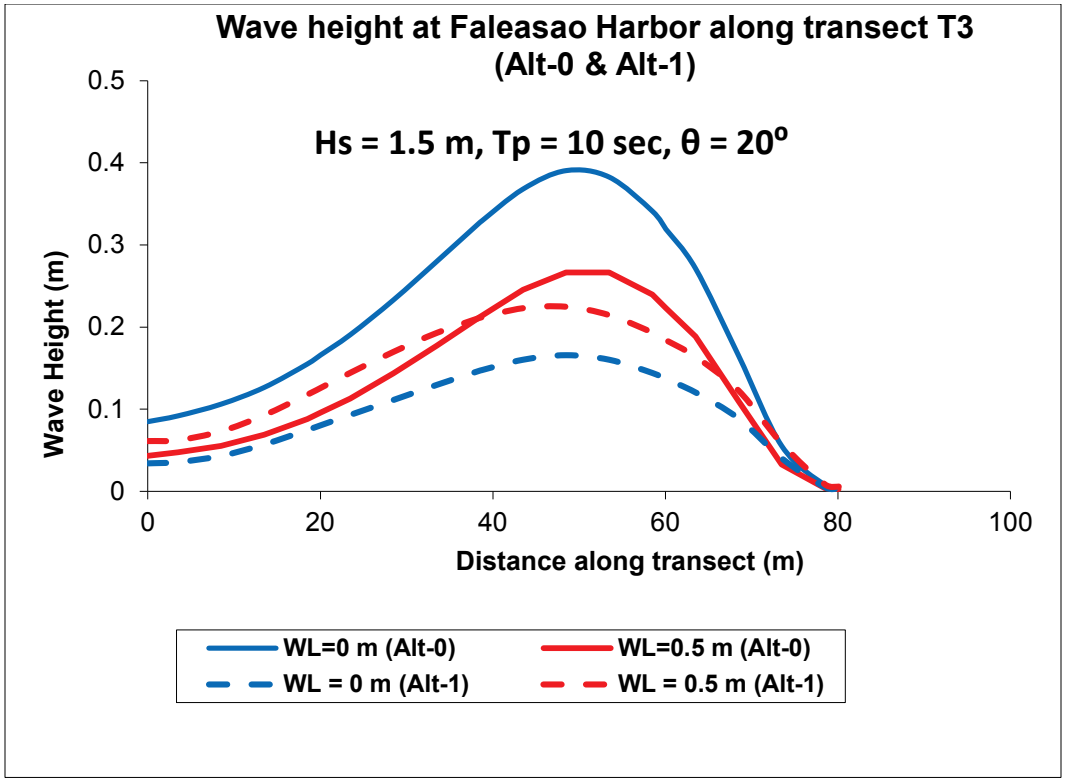

Figure 4-46. Comparison of Alt-0 and Alt-1 wave heights along transect T4 ($\theta = 20^o$).

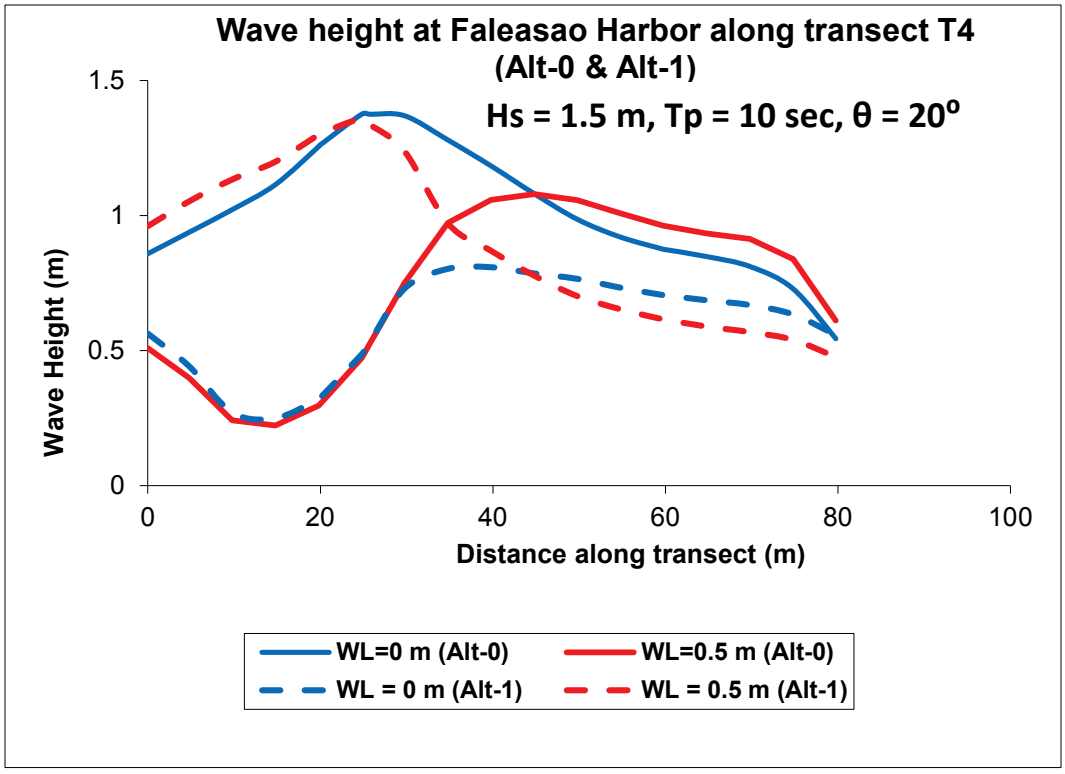

Figure 4-47. Comparison of Alt-0 and Alt-1 wave heights along transect T5 (θ = 20°).

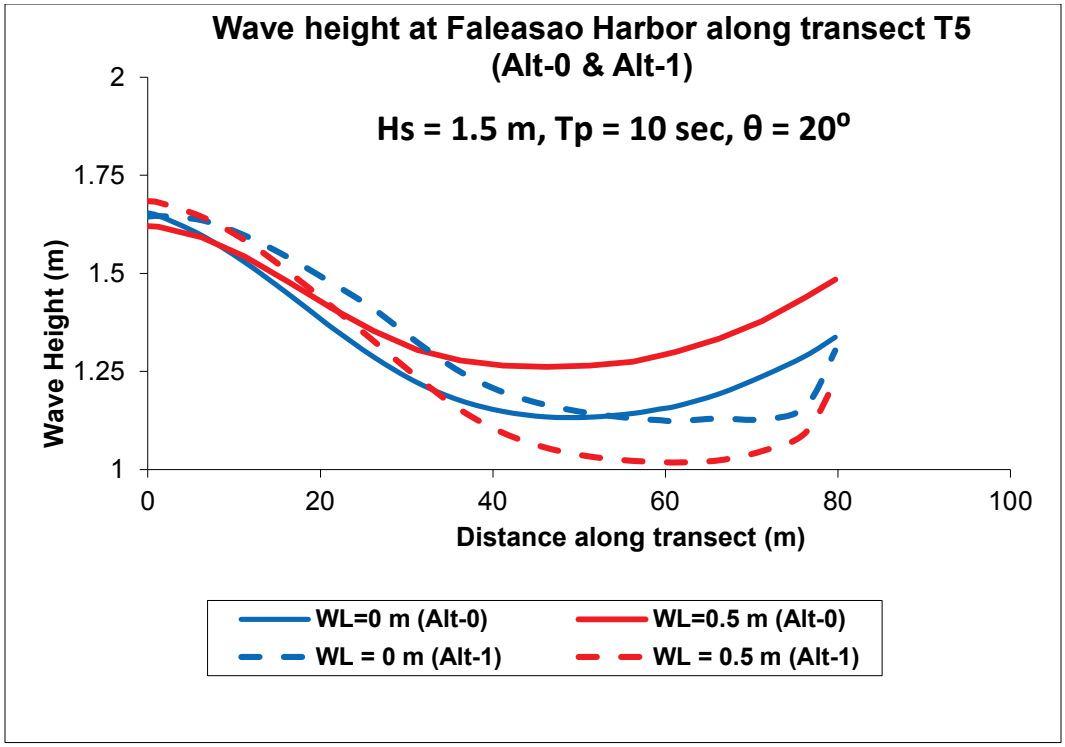

Figure 4-48. Comparison of Alt-0 and Alt-1 wave heights along transect T6 (θ = 20°).

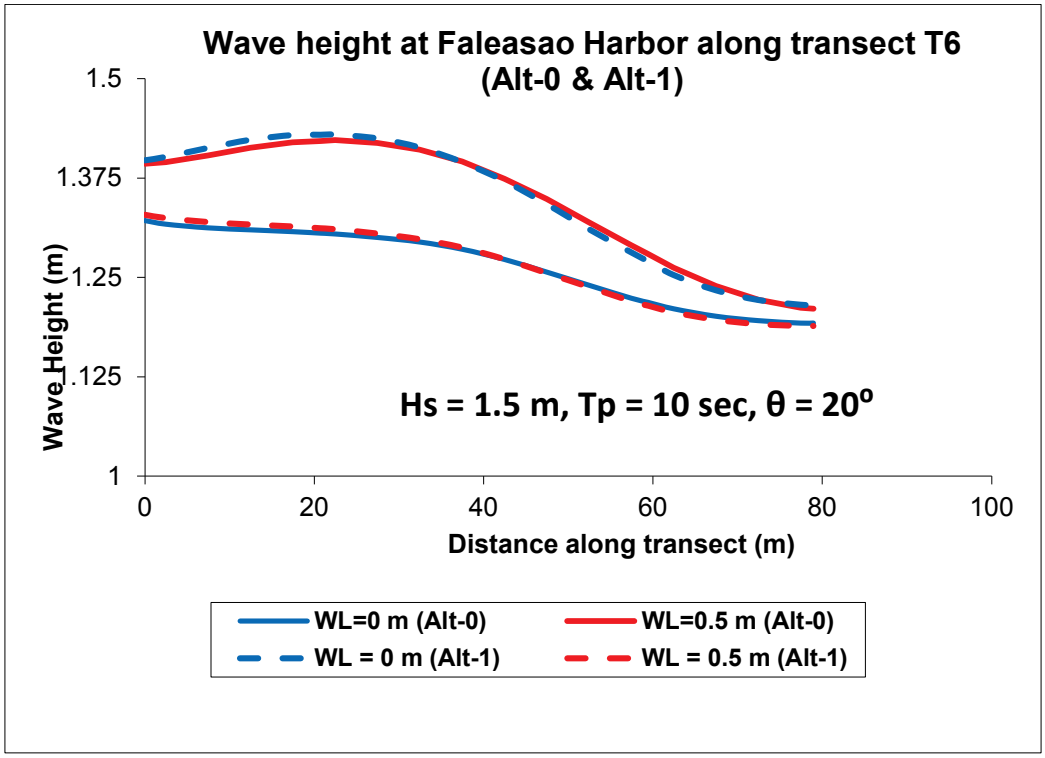

Figure 4-49. Comparison of Alt-0 and Alt-1 wave heights along transect T7 (θ = 20°).

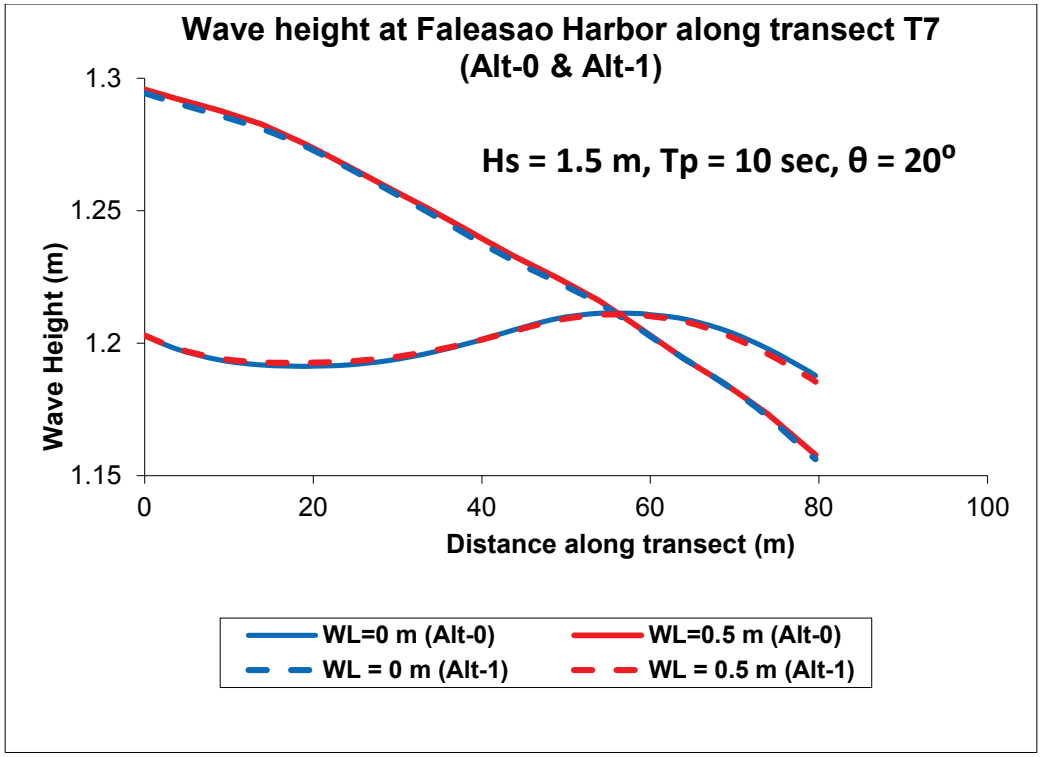

Figure 4-50. Comparison of Alt-0 and Alt-1 wave heights along transect T8 (θ = 20°).

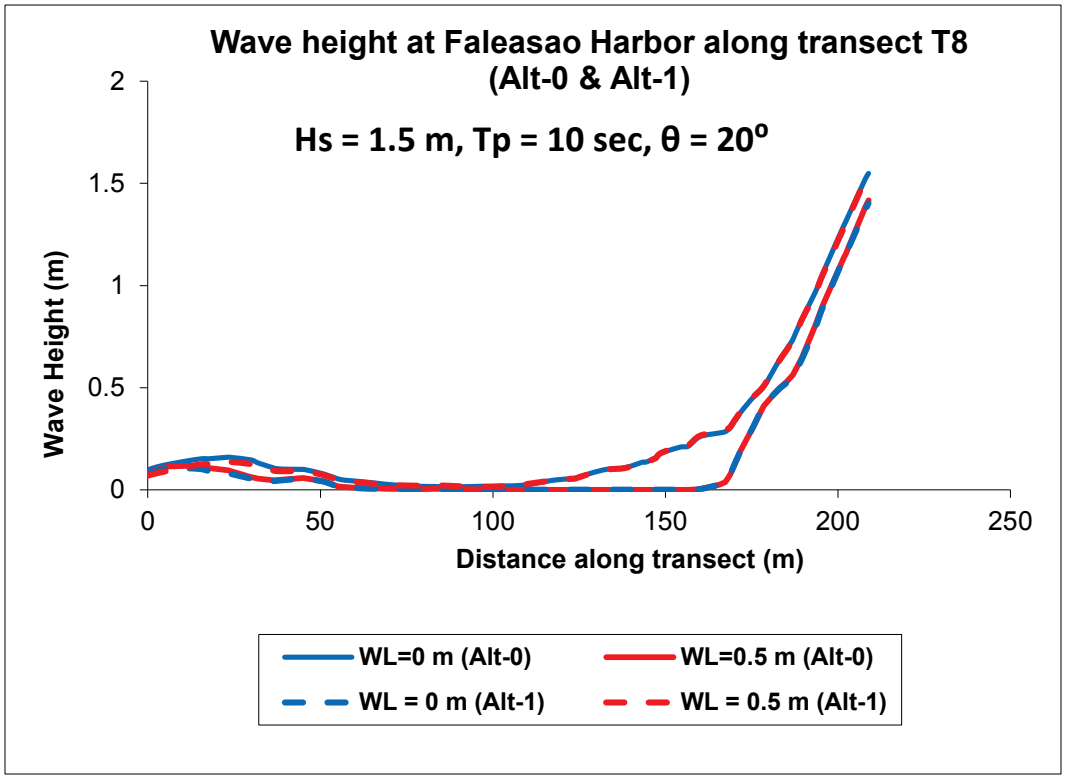

Figure 4-51. Comparison of Alt-0 and Alt-1 wave heights along transect T9 (θ = 20°).

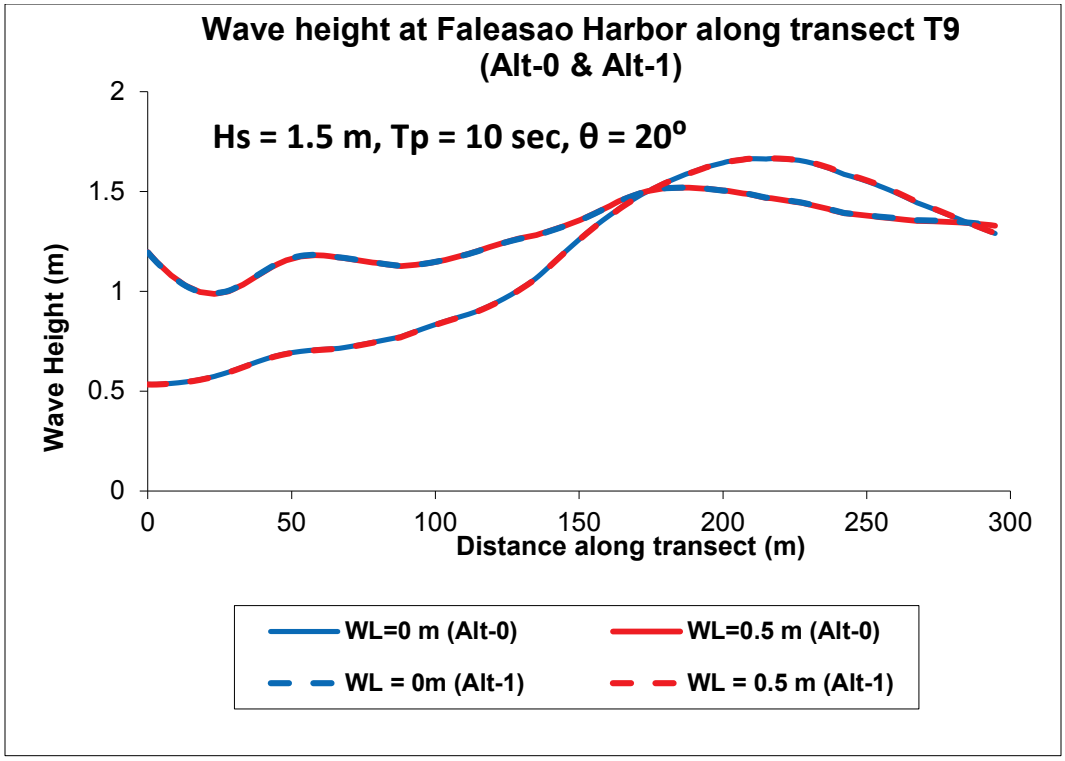

Figure 4-52. Comparison of Alt-0 and Alt-1 wave heights along transect T1 (θ = 340°).

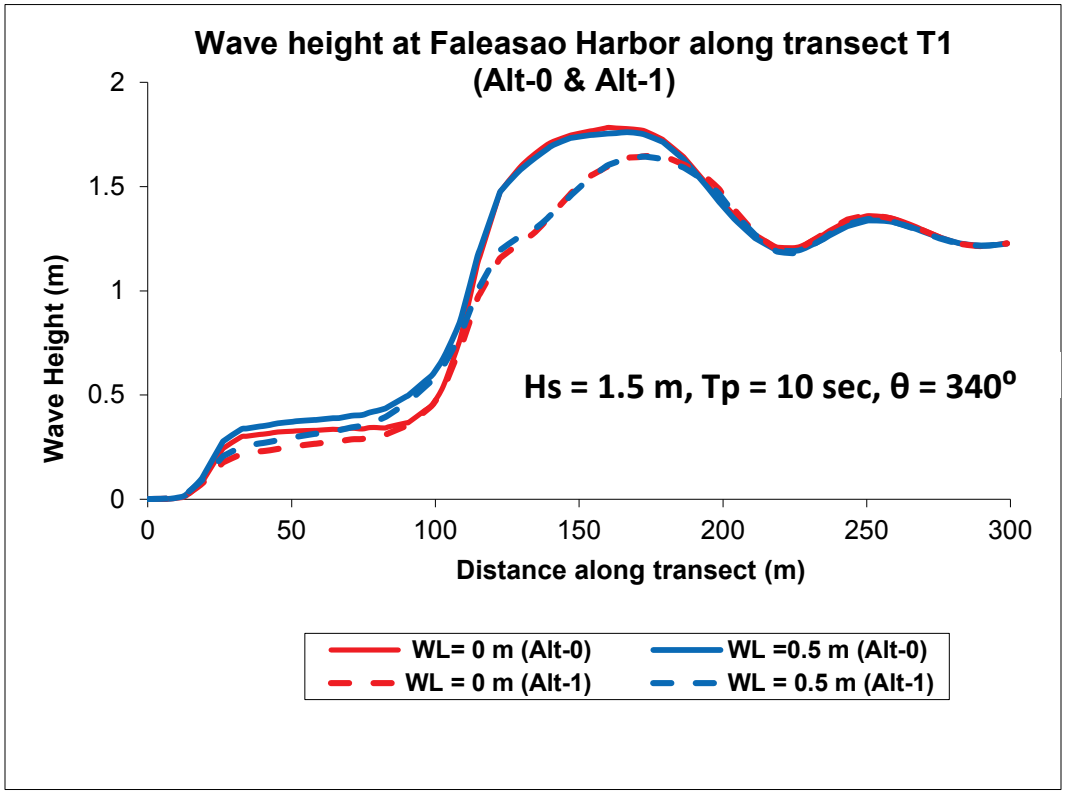

Figure 4-53. Comparison of Alt-0 and Alt-1 wave heights along transect T2 (θ = 340°).

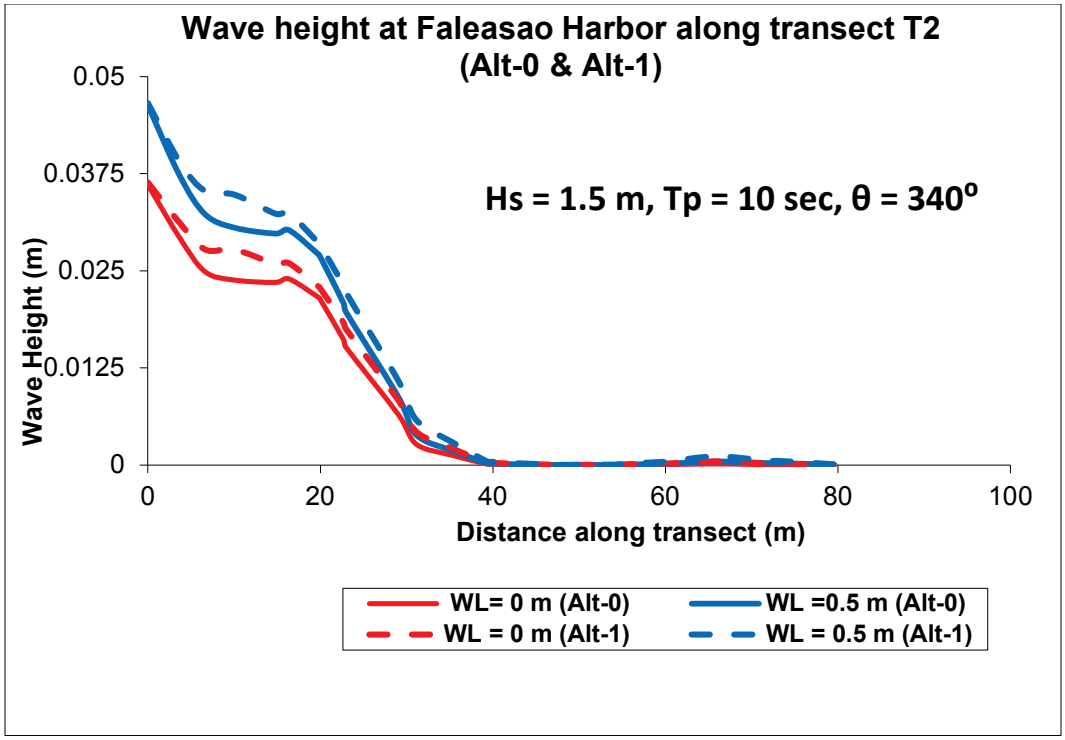

Figure 4-54. Comparison of Alt-0 and Alt-1 wave heights along transect T3 (θ = 340°).

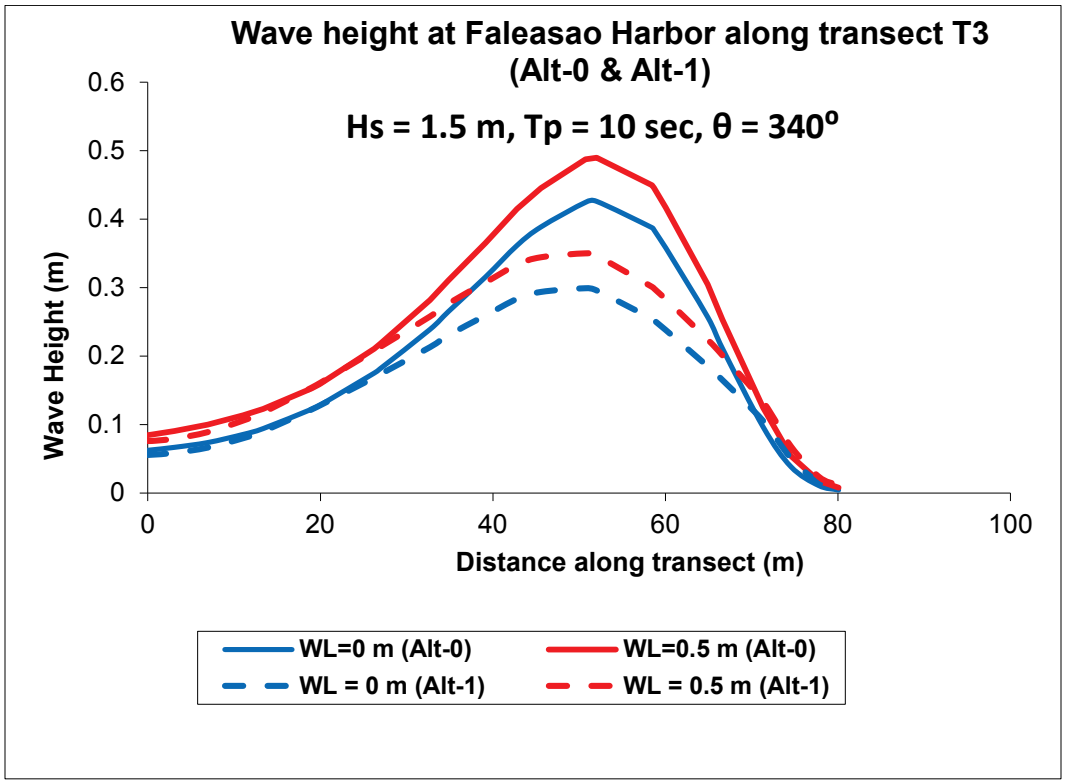

Figure 4-55. Comparison of Alt-0 and Alt-1 wave heights along transect T4 (θ = 340°).

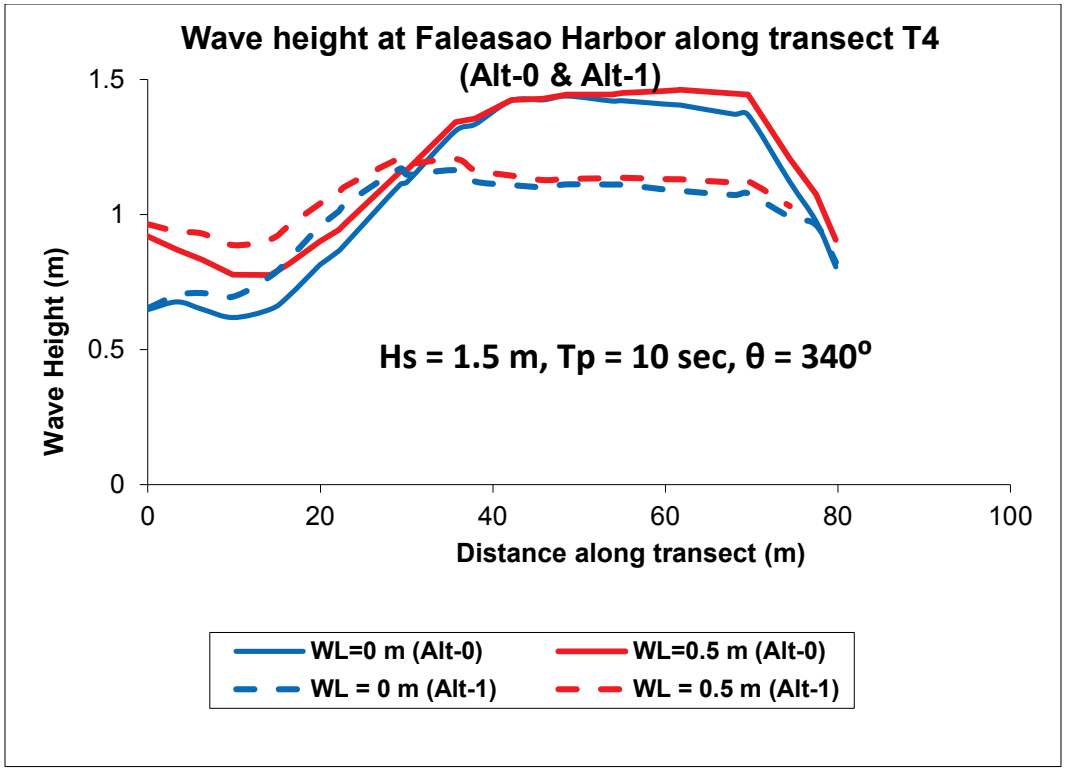

Figure 4-56. Comparison of Alt-0 and Alt-1 wave heights along transect T5 (θ = 340°).

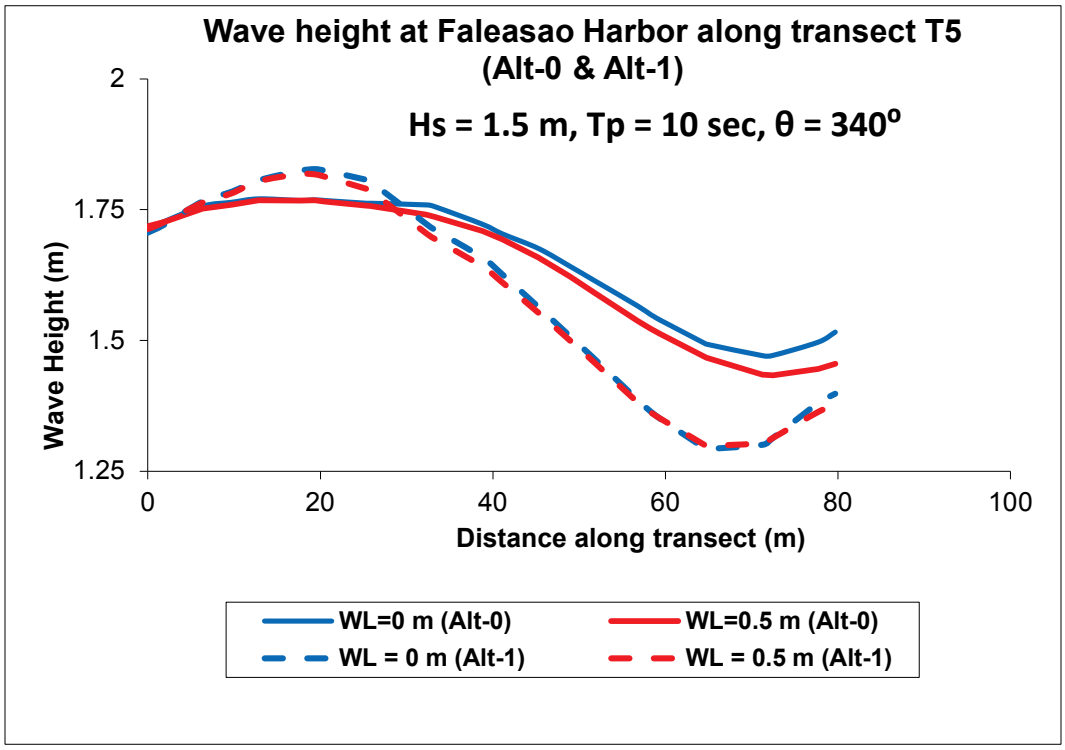

Figure 4-57. Comparison of Alt-0 and Alt-1 wave heights along transect T6 (θ = 340°).

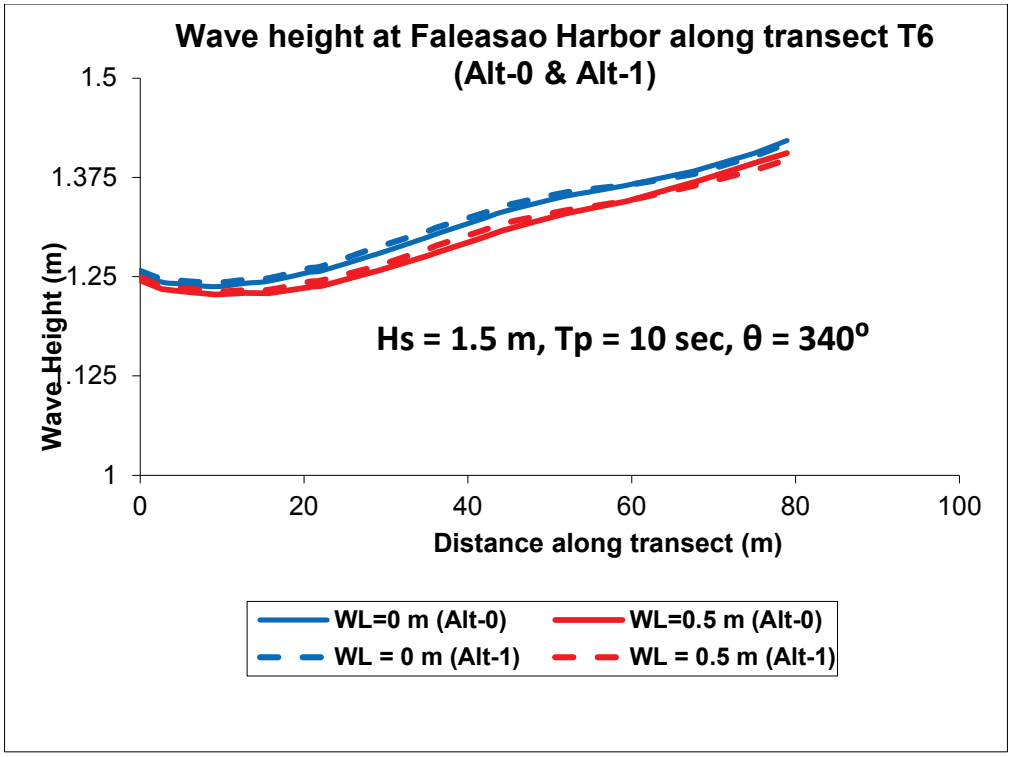

Figure 4-58. Comparison of Alt-0 and Alt-1 wave heights along transect T7 (θ = 340°).

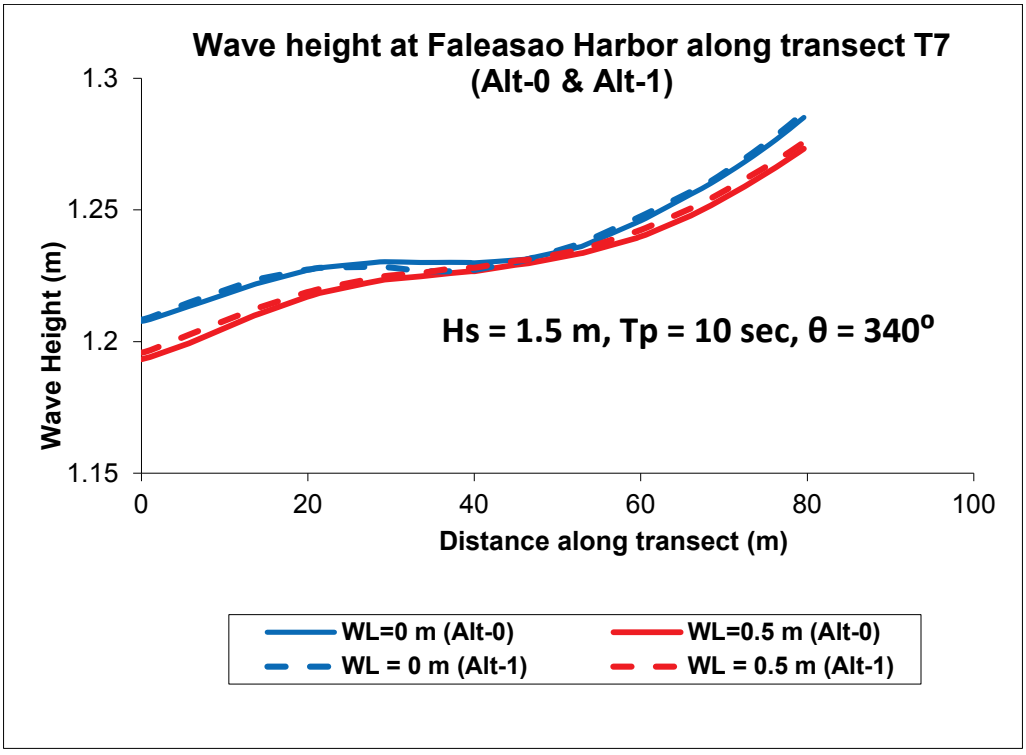

Figure 4-59. Comparison of Alt-0 and Alt-1 wave heights along transect T8 (θ = 340°).

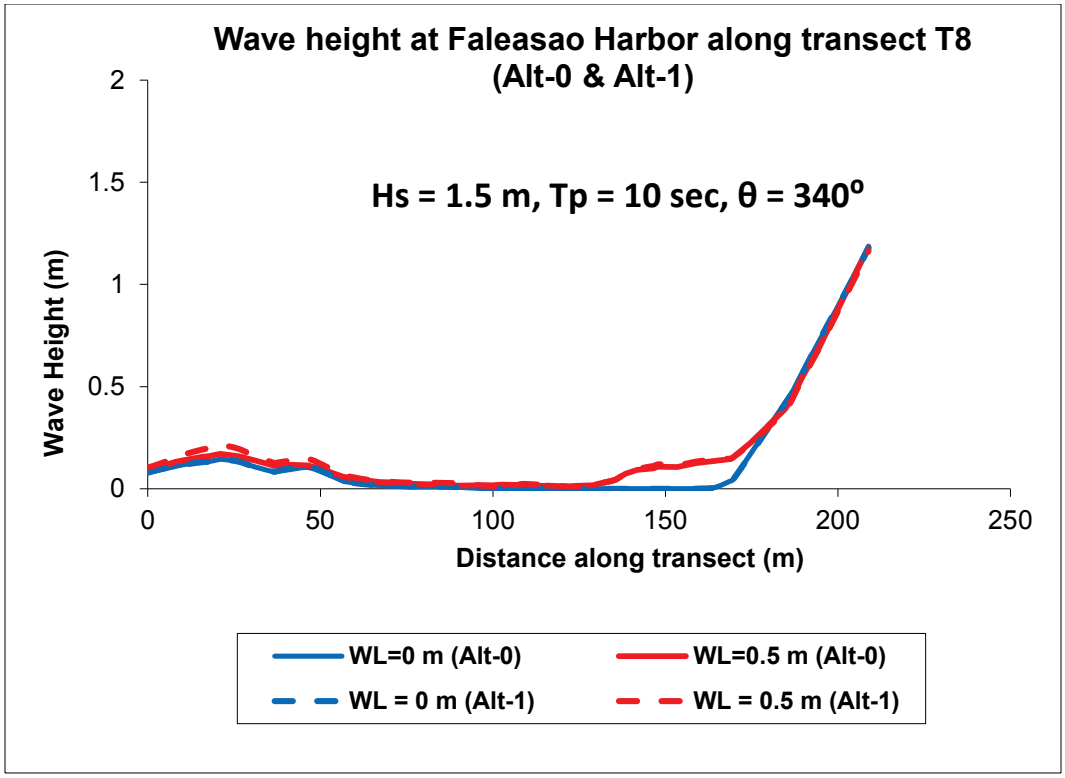

Figure 4-60. Comparison of Alt-0 and Alt-1 wave heights along transect T9 (θ = 340°).

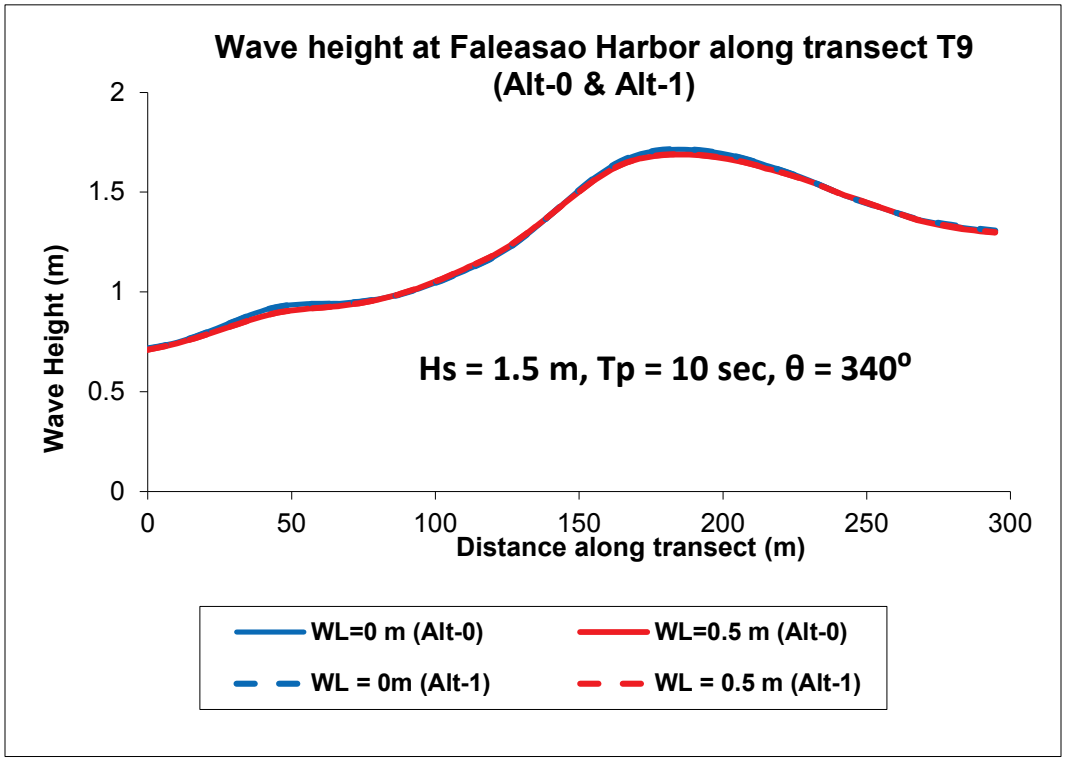

Figure 4-61. Comparison of Alt-0 and Alt-1 wave heights along transect T1 (θ = 320^0).

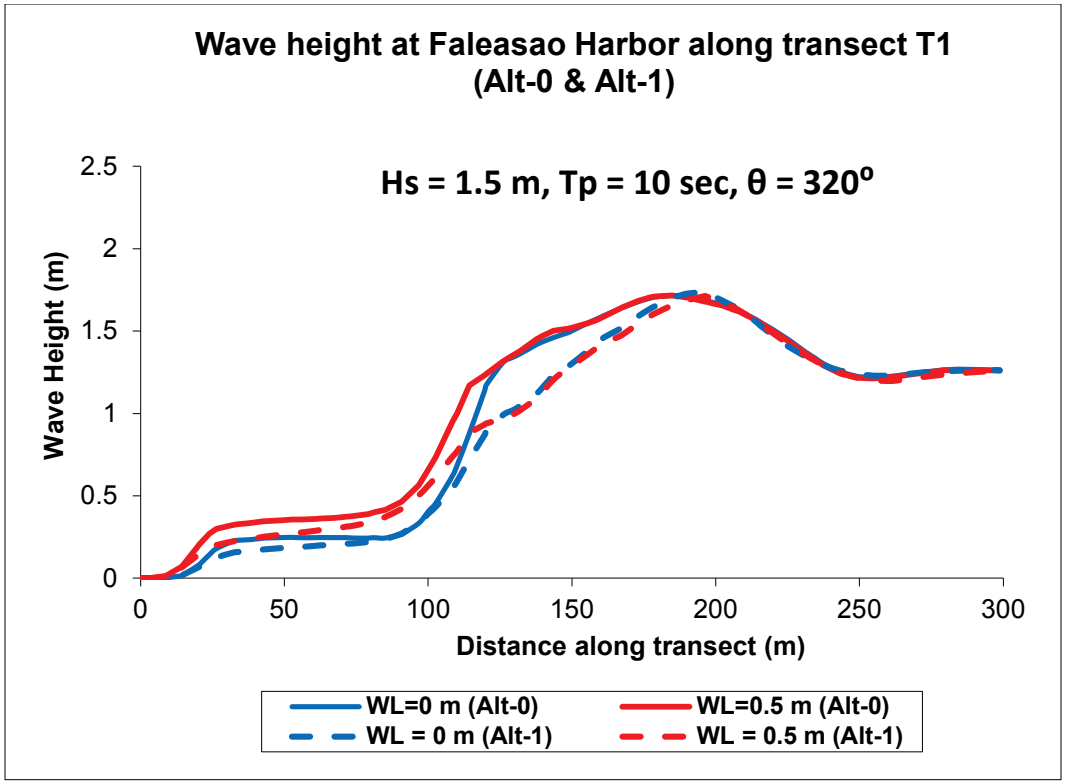

Figure 4-62. Comparison of Alt-0 and Alt-1 wave heights along transect T2 (θ = 320^0).

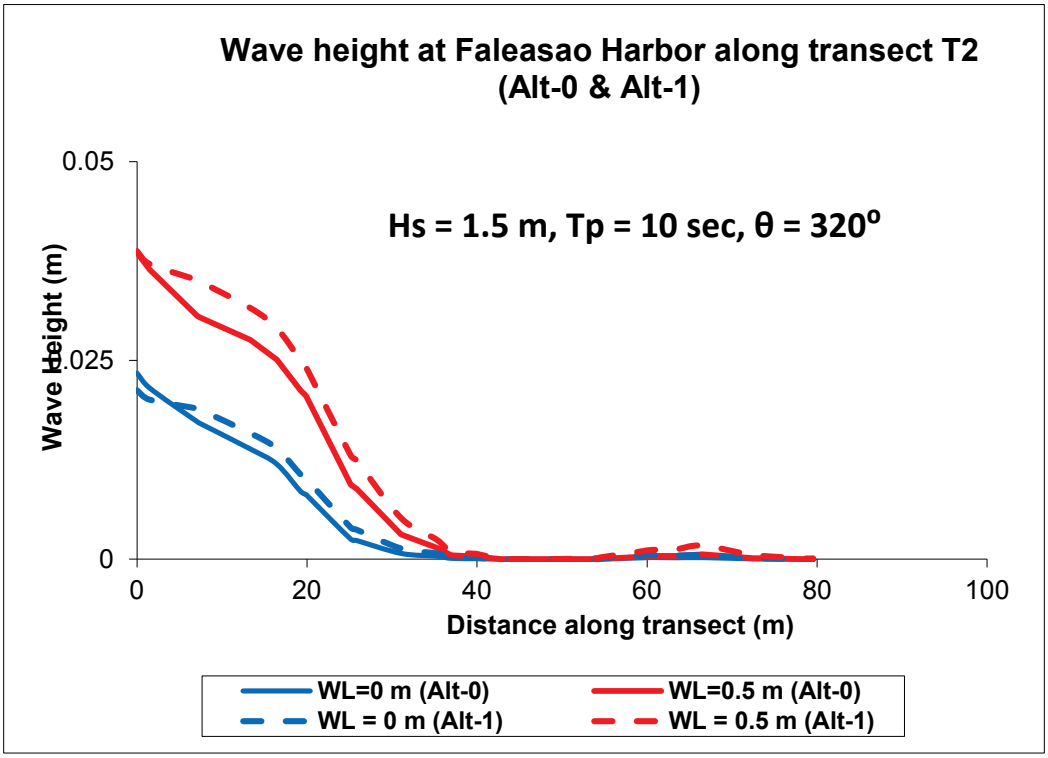

Figure 4-63. Comparison of Alt-0 and Alt-1 wave heights along transect T3 (θ = 320°).

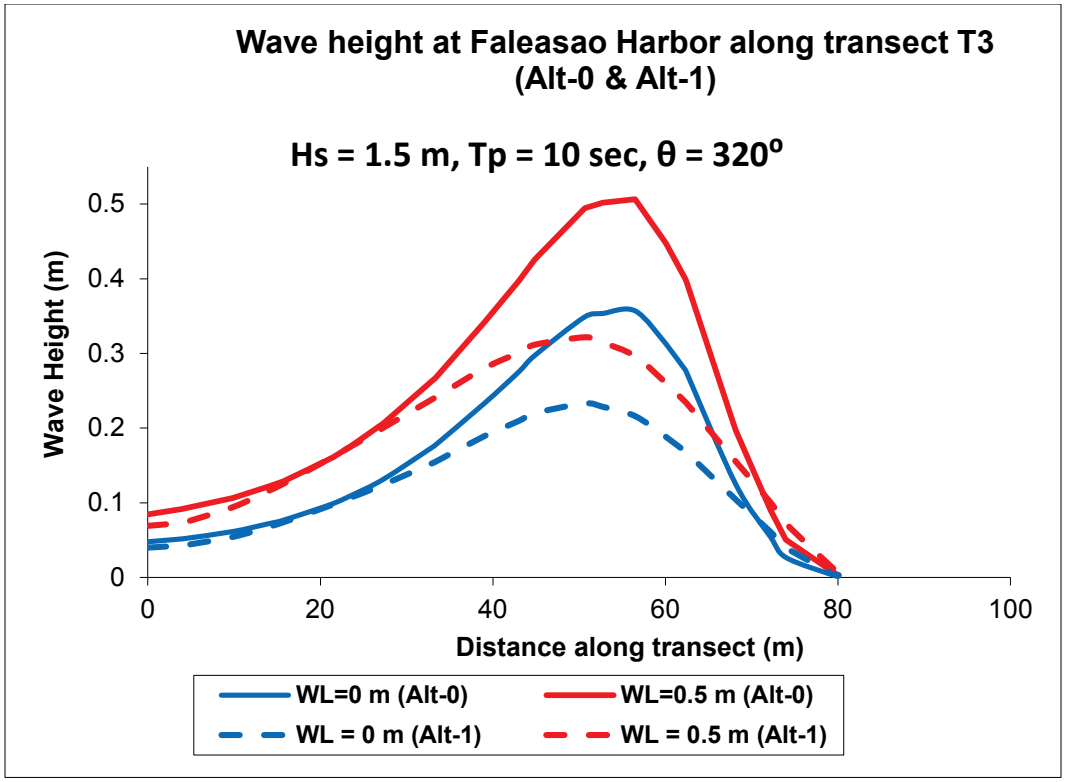

Figure 4-64. Comparison of Alt-0 and Alt-1 wave heights along transect T4 (θ = 320°).

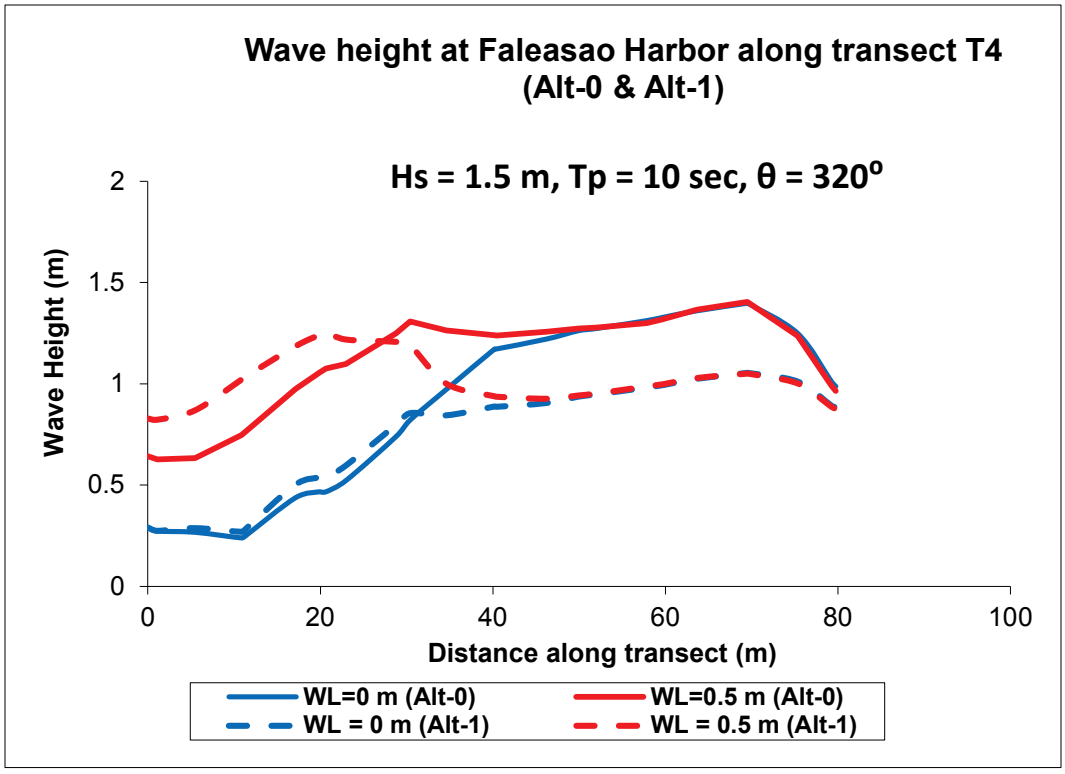

Figure 4-65. Comparison of Alt-0 and Alt-1 wave heights along transect T5 (θ = 320^0).

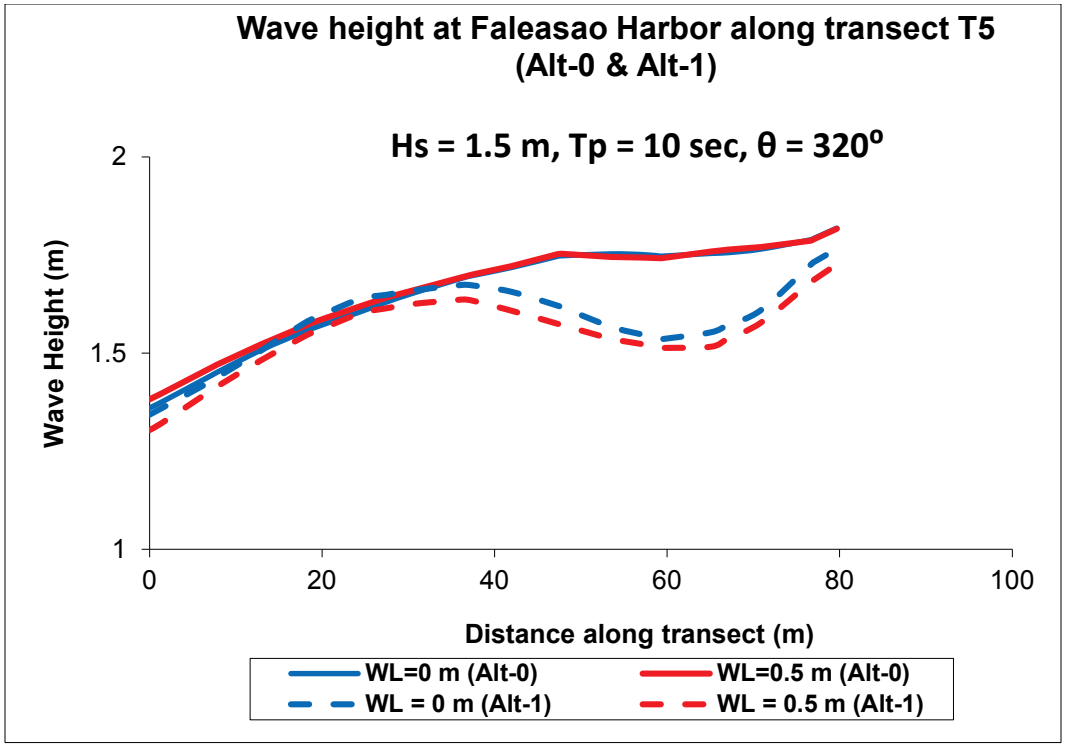

Figure 4-66. Comparison of Alt-0 and Alt-1 wave heights along transect T6 (θ = 320^0).

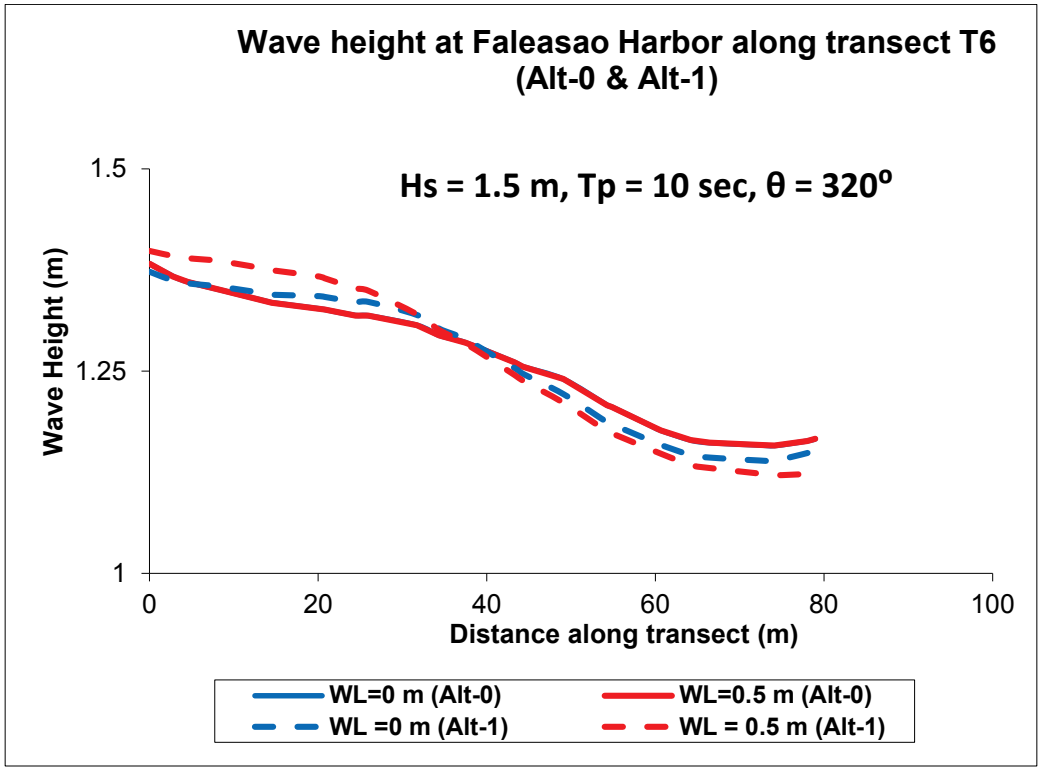

Figure 4-67. Comparison of Alt-0 and Alt-1 wave heights along transect T7 (θ = 320°).

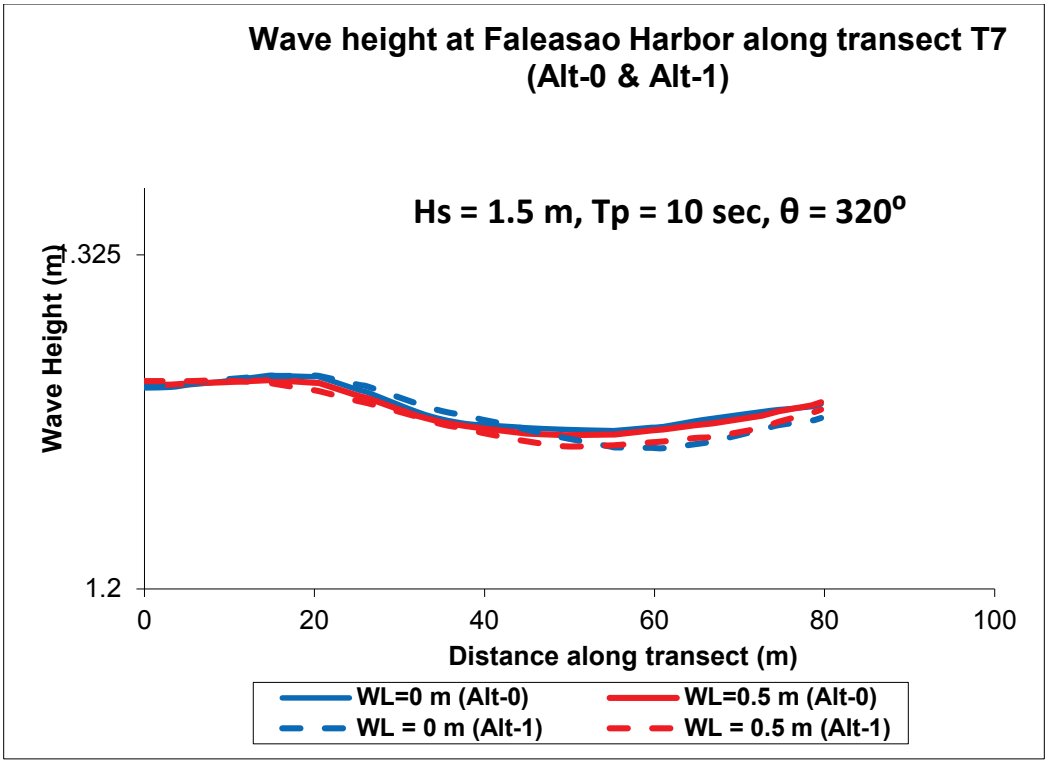

Figure 4-68. Comparison of Alt-0 and Alt-1 wave heights along transect T8 (θ = 320°).

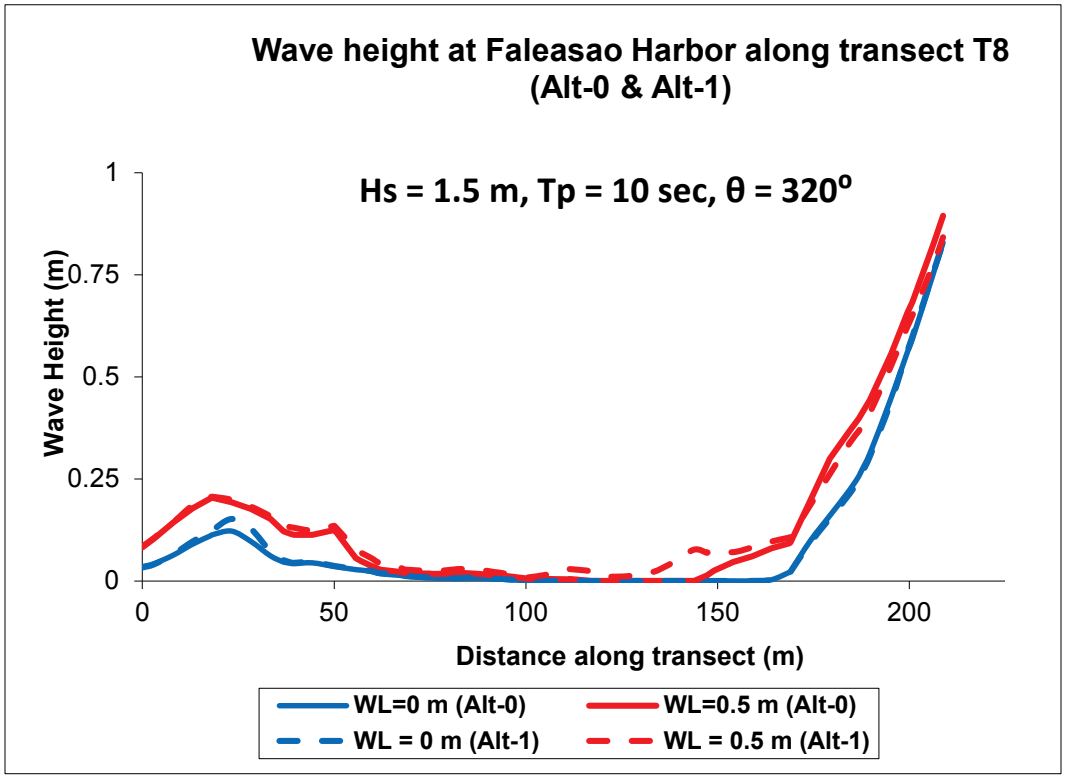

Figure 4-69. Comparison of Alt-0 and Alt-1 wave heights along transect T9 (θ = 320°).

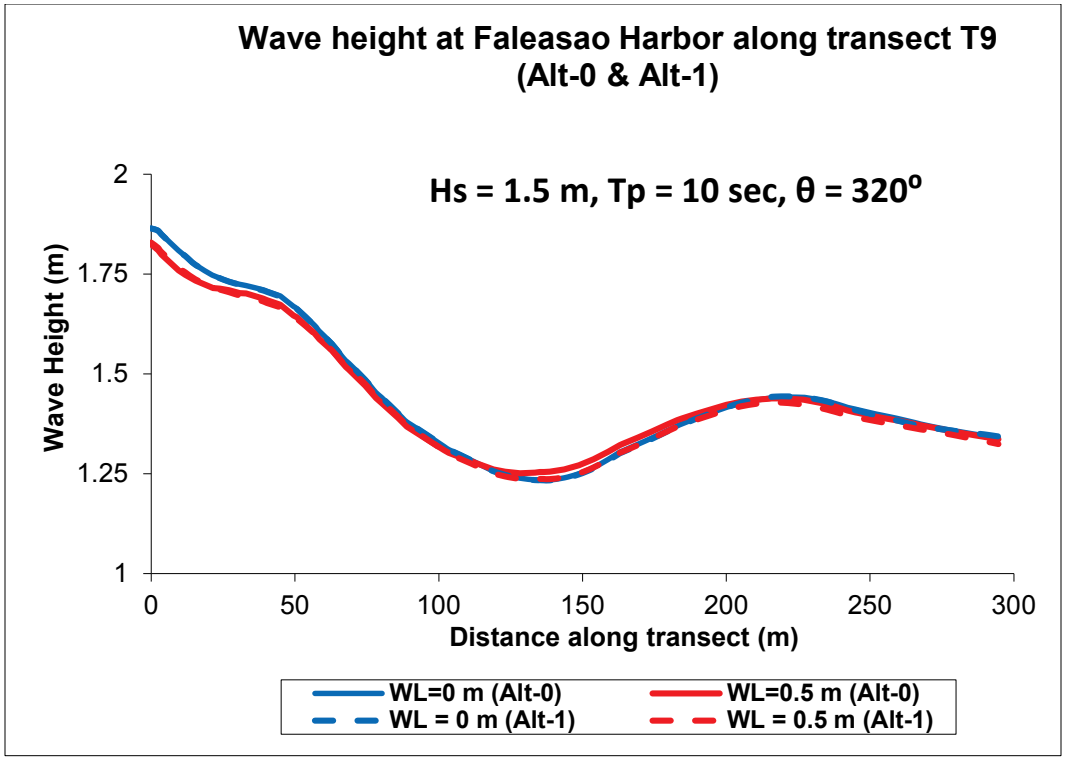

4.5 Model results for Alt-2

The second Alternative (Alt-2) represents a 230 ft long breakwater attached to the tip of the west peninsula in an attempt to provide improved conditions to vessels transiting into the harbor through the deepened navigation channel. It is approximately 50 ft shorter than Alt-3 and includes the deepened channel and mooring areas of Alt-1. Vessels reaching the south side of the harbor may either use the mooring or dock areas. Results for Alt-2 are provided in this section for 0° average incident wave direction and are compared to the existing harbor (Alt-0) in Figures 4-70 through 4-78. These are followed by results for 20° incident wave in Figures 4-79 to 4-87, for 340° incident wave in Figures 4-88 to 4-96 and for 320° incident wave in Figures 4-97 to 4-105. These comparative results indicate Alt-2 provides a reasonable reduction in wave heights in the areas of interest, but not as well as Alt-3.

Figure 4-70. Comparison of Alt-0 and Alt-2 wave heights along transect T1 (θ = 0^0).

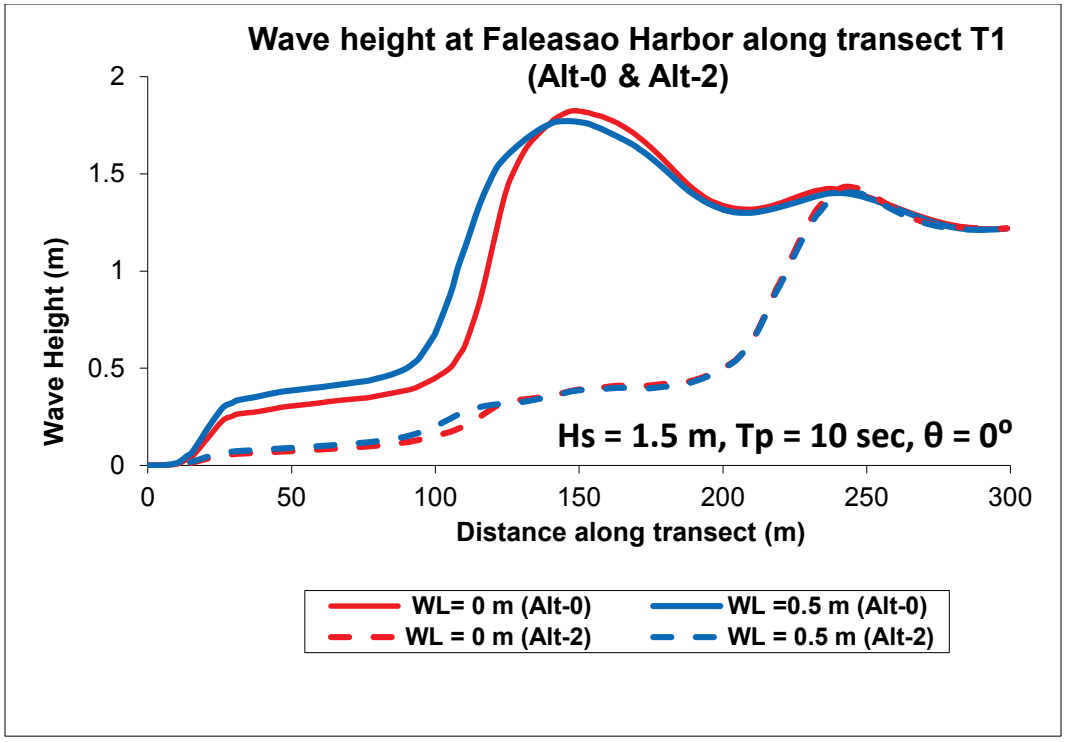

Figure 4-71. Comparison of Alt-0 and Alt-2 wave heights along transect T2 (θ = 0^0).

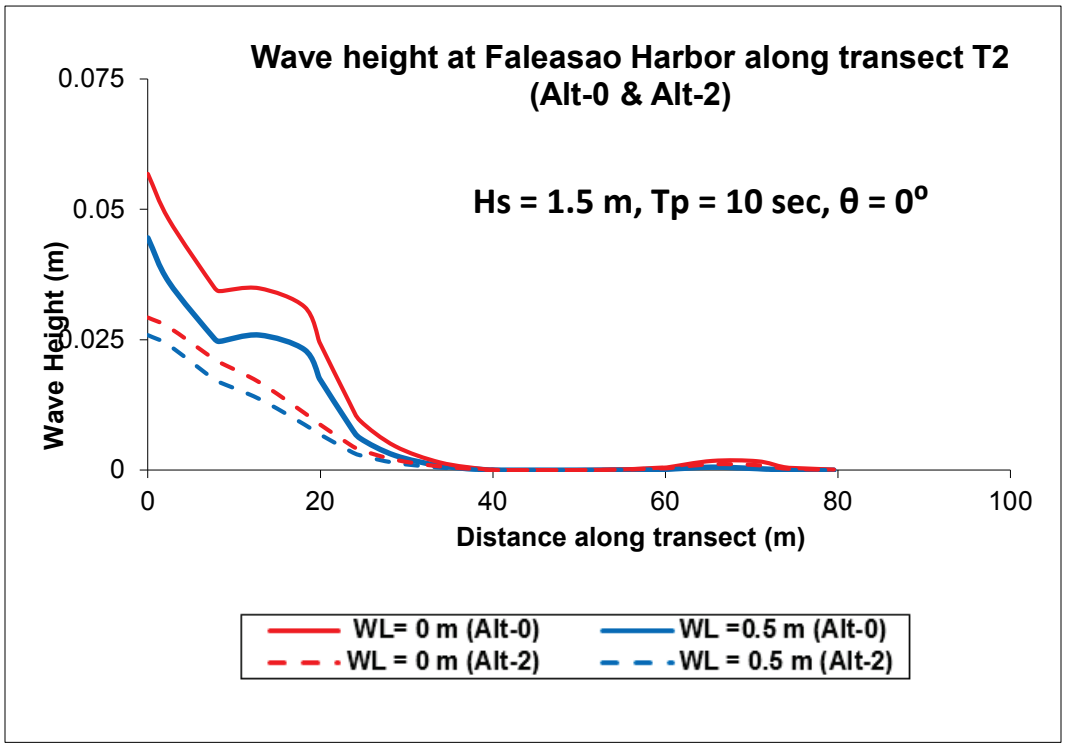

Figure 4-72. Comparison of Alt-0 and Alt-2 wave heights along transect T3 (θ = 0°).

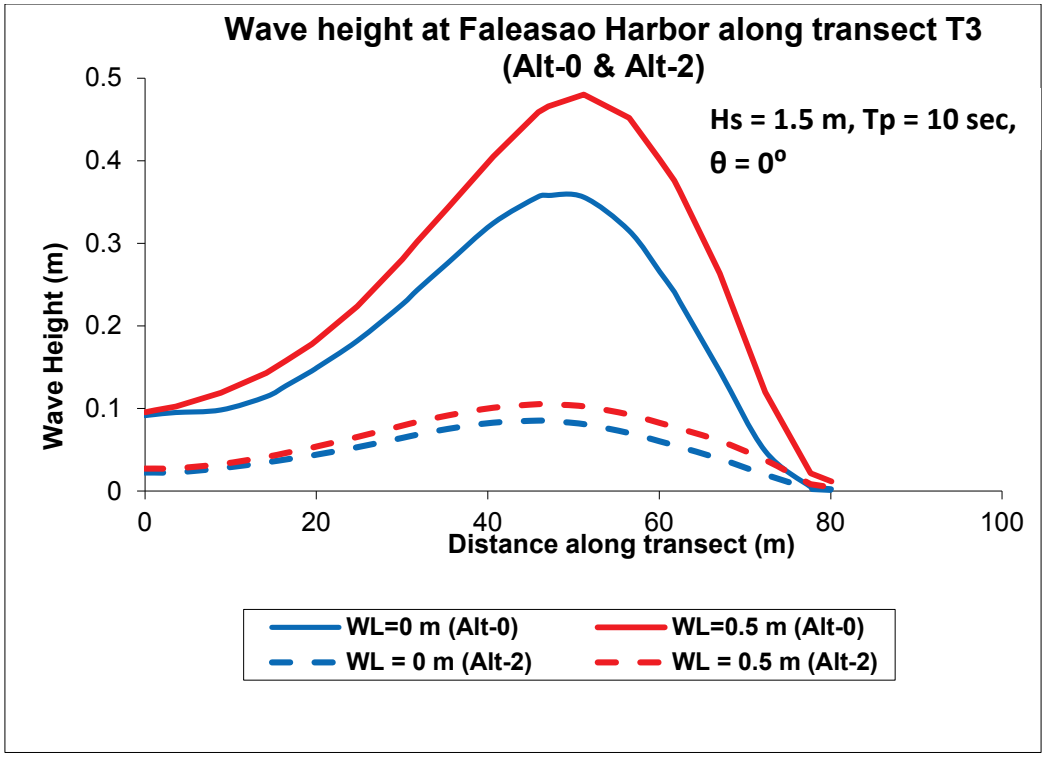

Figure 4-73. Comparison of Alt-0 and Alt-2 wave heights along transect T4 (θ = 0°).

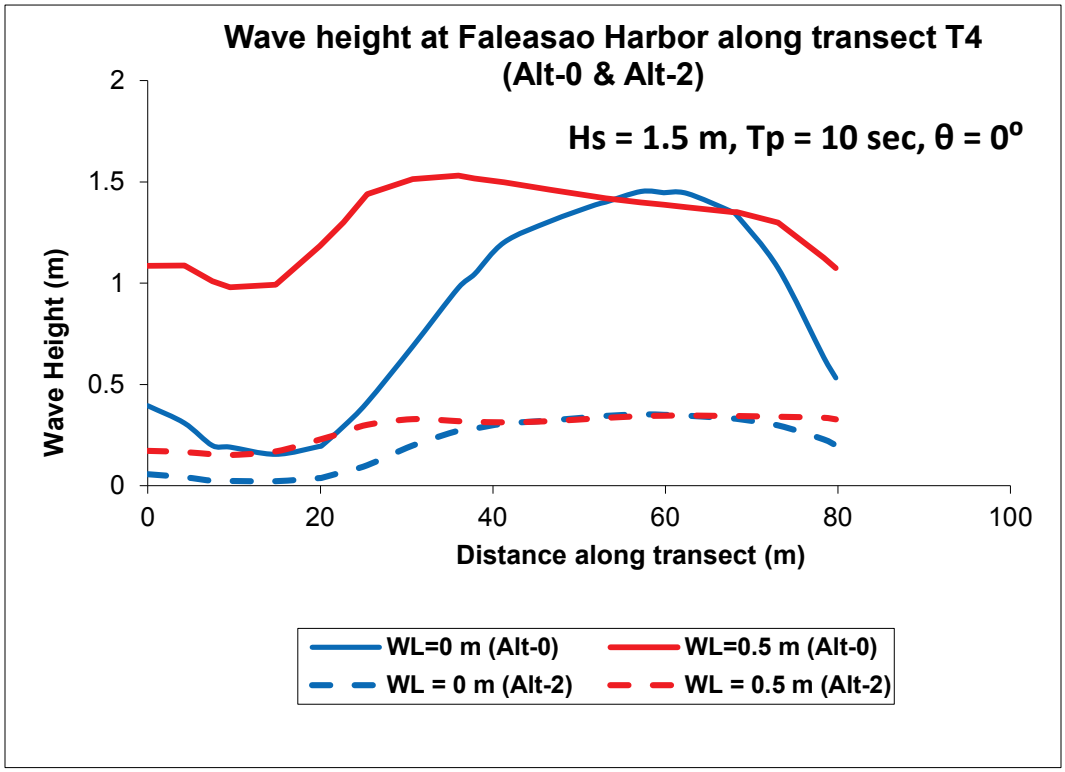

Figure 4-74. Comparison of Alt-0 and Alt-2 wave heights along transect T5 (θ = 0°).

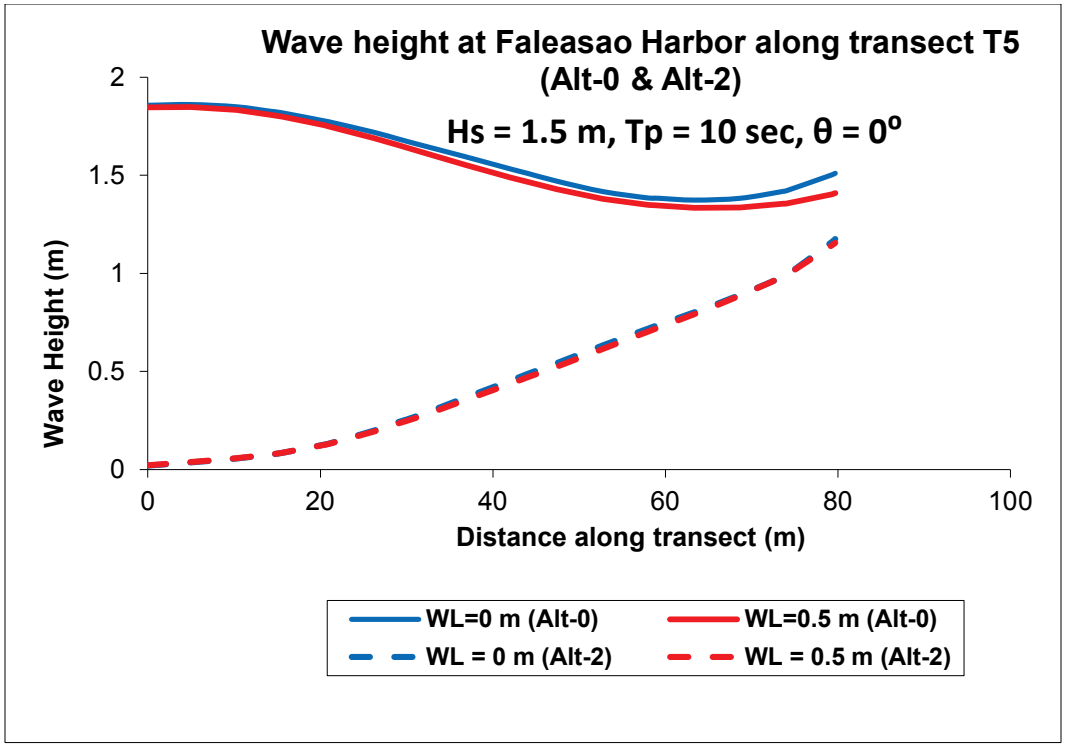

Figure 4-75. Comparison of Alt-0 and Alt-2 wave heights along transect T6 (θ = 0°).

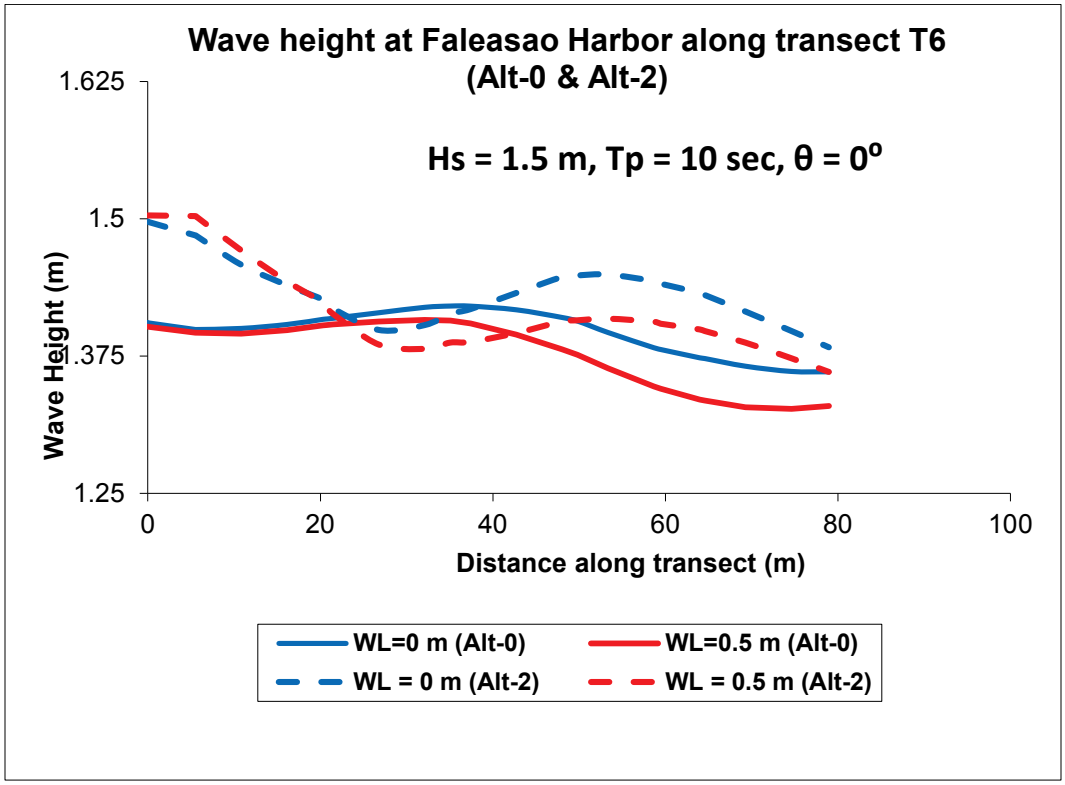

Figure 4-76. Comparison of Alt-0 and Alt-2 wave heights along transect T7 ($\theta = 0^0$).

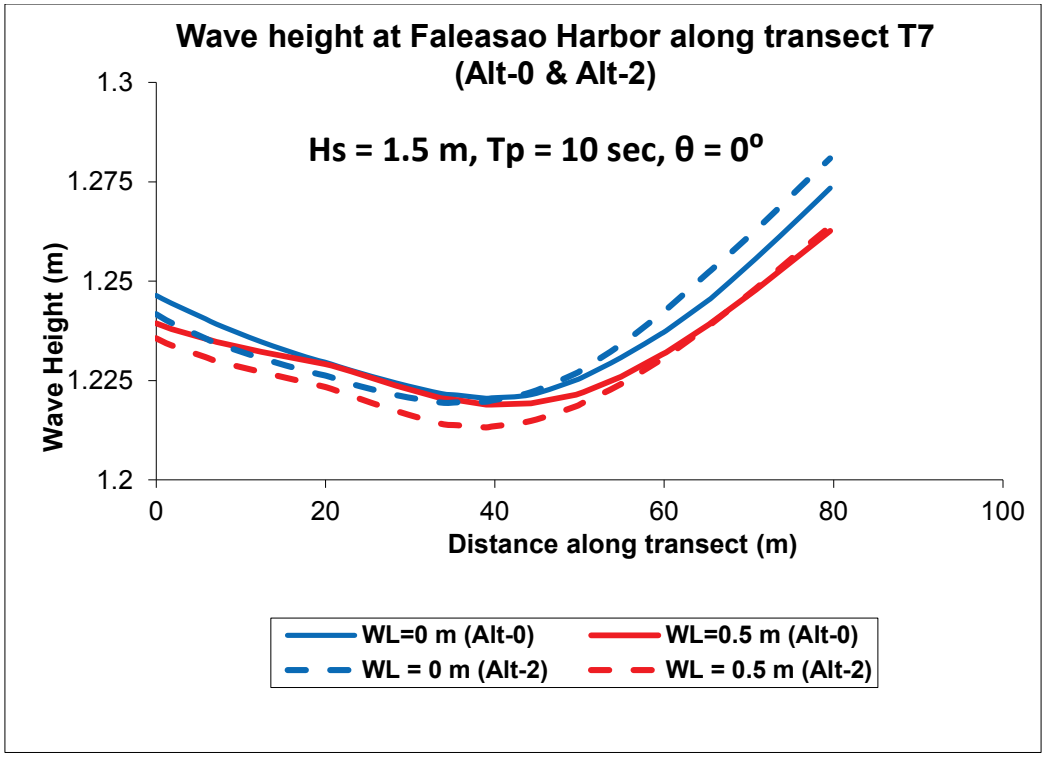

Figure 4-77. Comparison of Alt-0 and Alt-2 wave heights along transect T8 ($\theta = 0^0$).

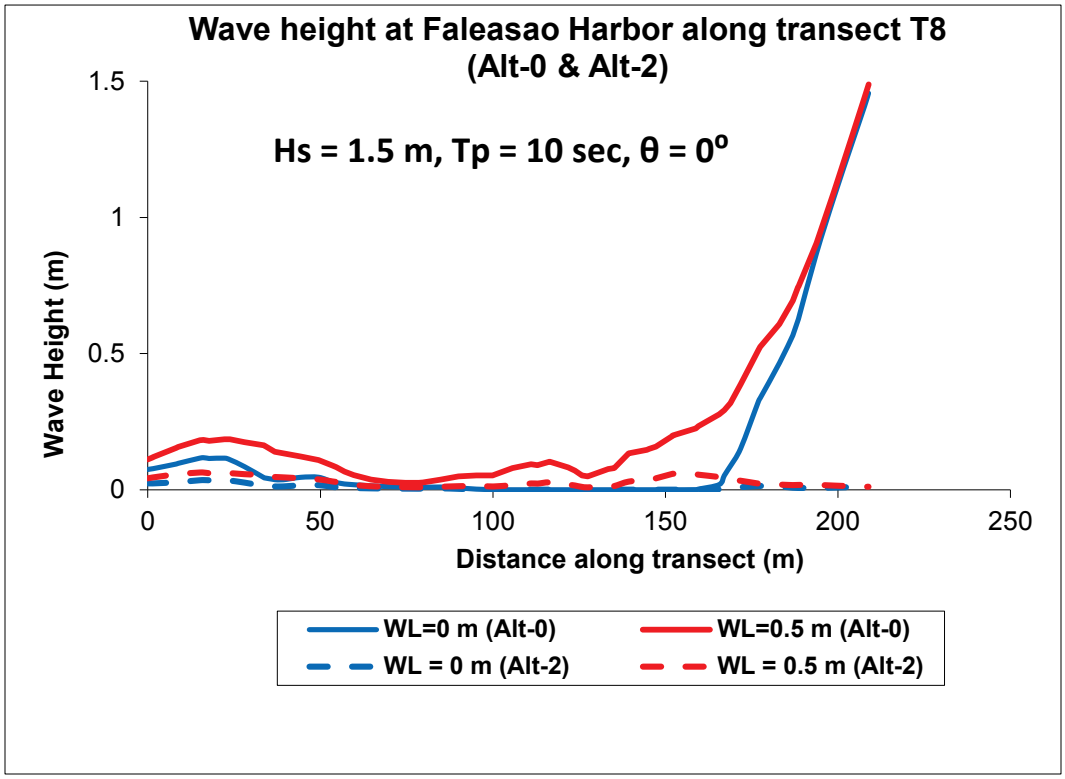

Figure 4-78. Comparison of Alt-0 and Alt-2 wave heights along transect T9 ($\theta = 0^0$).

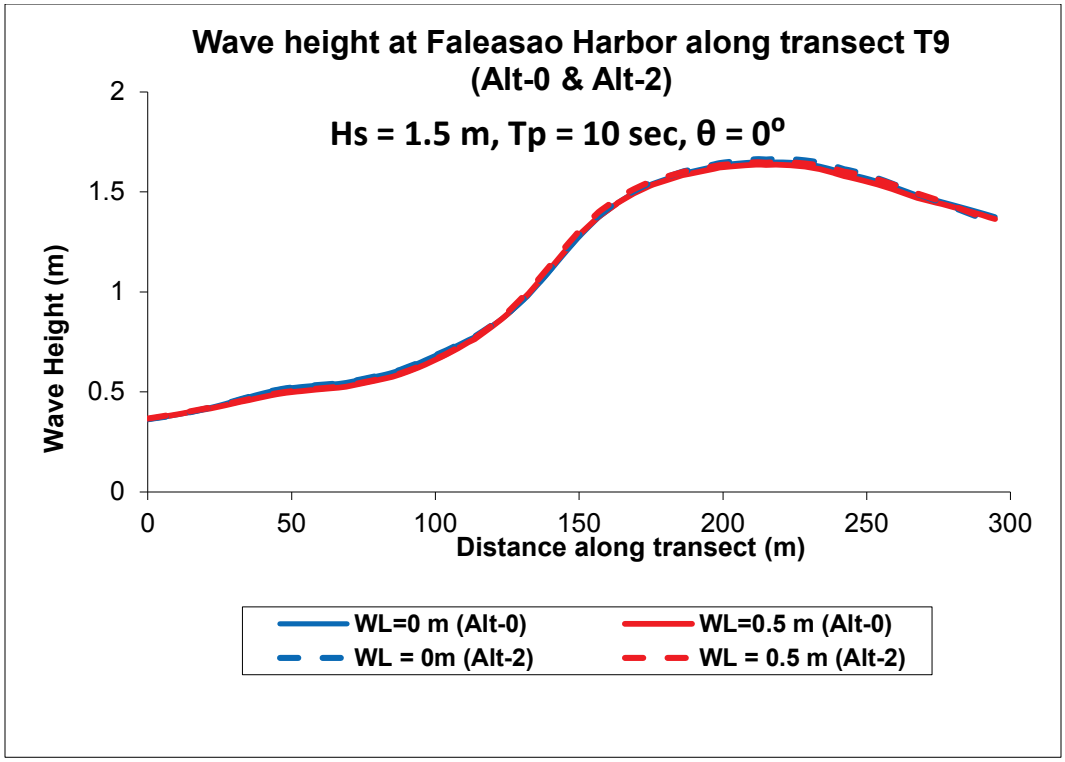

Although the geometries of Alt-1 and Alt-2 were different, the same numerical parameters were used in Alt-2 simulations for control of numerical stability and convergences of model solutions Alt-2 results suggest this short breakwater is reasonably effective in sheltering the harbor and reduces wave height along several transects located both inside and outside the harbor. The local variations in wave height along the nine transects for the two different water levels for incident waves from four directions are described next.

Values of the average wave height along T1 for Alt-2 and Alt-0 (Figure 4-70) are approximately 0.6 m and 1.2 m, respectively, indicating a 50% wave height reduction by Alt-2. Sensitivity tests indicated the change in wave height reduction was less than 4% using different values of damping or friction or turbulence parameters in model simulations. Tests were also conducted to determine the change in wave height reduction for two other incident wave conditions (H_s = 1.25 m and 1.75 m, and T_p = 9 sec and 11 sec). These test showed a 6% maximum change in wave height reduction along T1 that was proportional to H_s. The Alt-2 results are compared to the existing harbor (Alt-0) to quantify the local wave height variation along the nine transects.

Alt-2 results for a 20° incident average wave condition are compared to the existing harbor (Alt-0) in Figures 4-79 to 4-87. These show local wave height variation along the nine transects which cover the areas of interest in the harbor.

Figure 4-79. Comparison of Alt-0 and Alt-2 wave heights along transect T1 (θ = 20°).

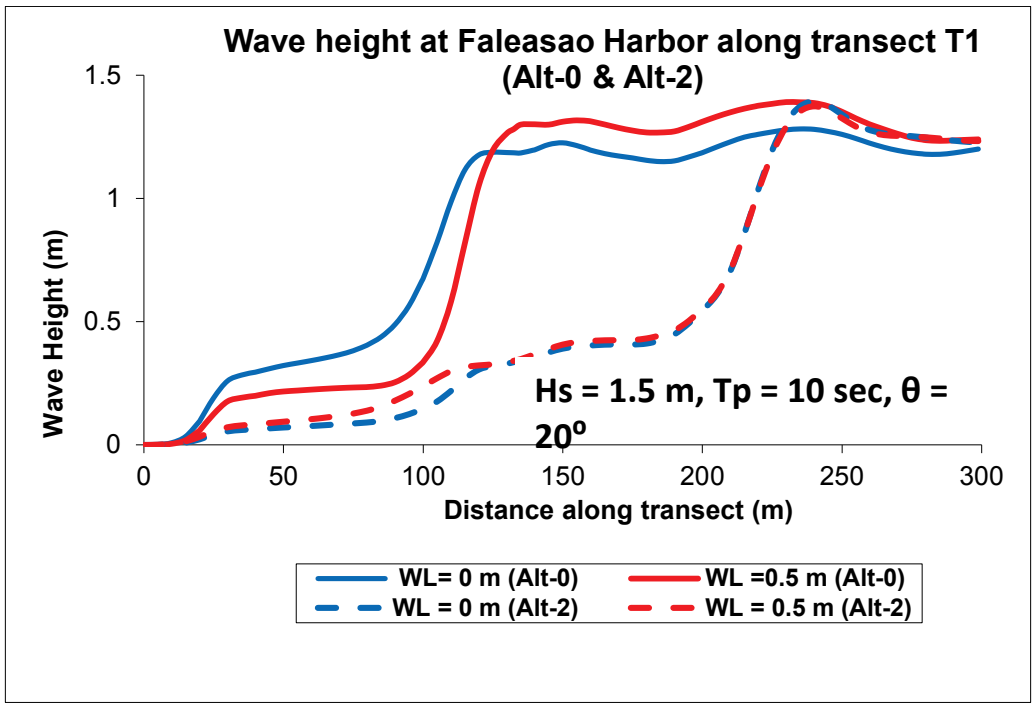

Figure 4-80. Comparison of Alt-0 and Alt-2 wave heights along transect T2 (θ = 20°).

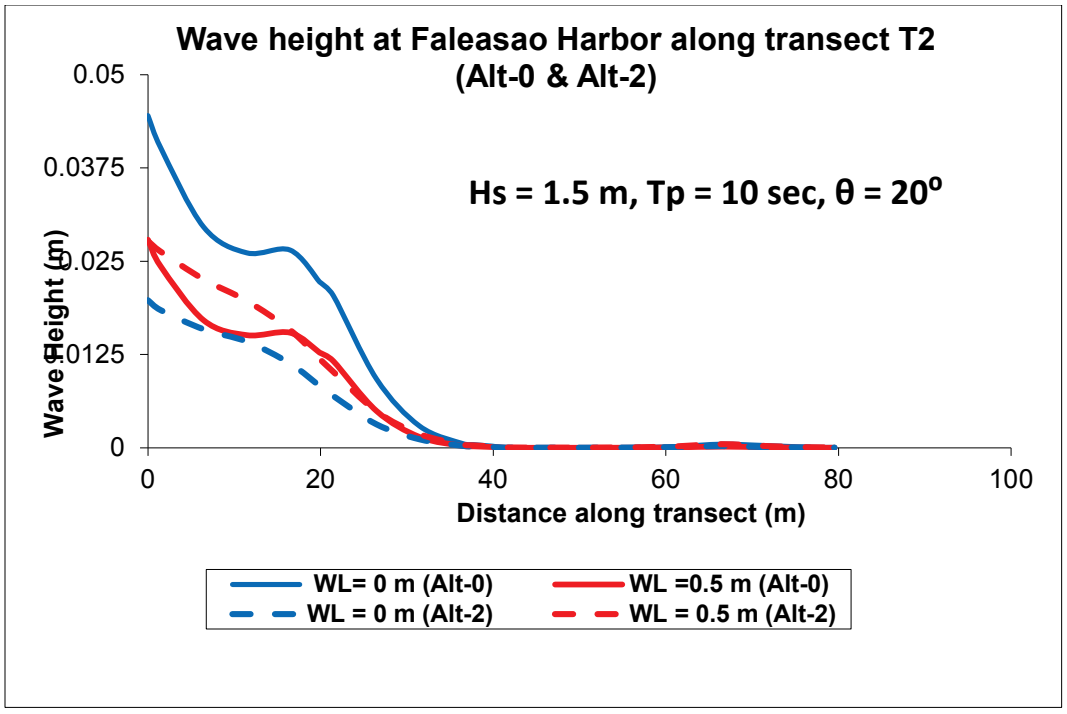

Figure 4-81. Comparison of Alt-0 and Alt-2 wave heights along transect T3 (θ = 20°).

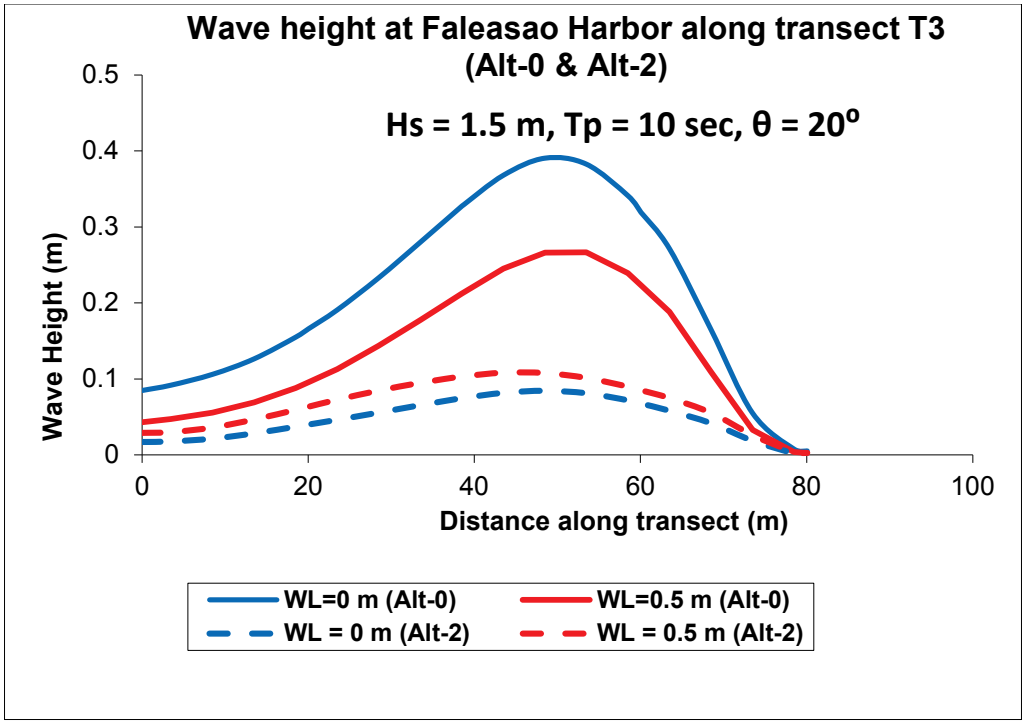

Figure 4-82. Comparison of Alt-0 and Alt-2 wave heights along transect T4 (θ = 20°).

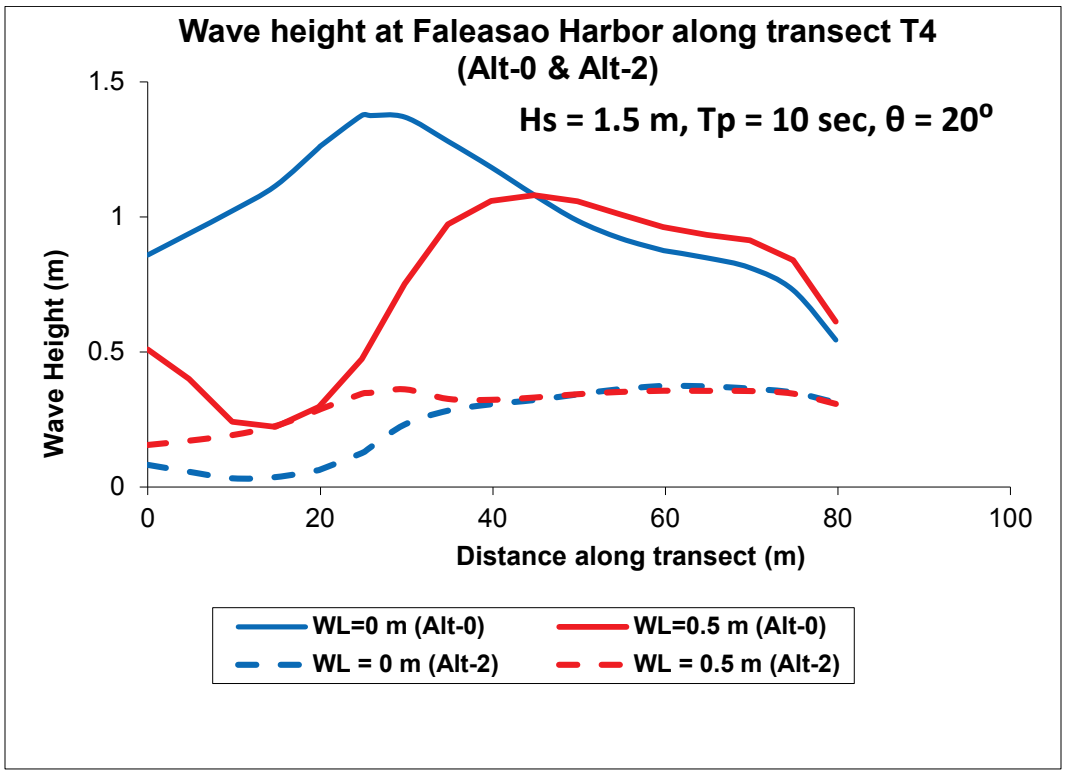

Figure 4-83. Comparison of Alt-0 and Alt-2 wave heights along transect T5 (θ = 20°).

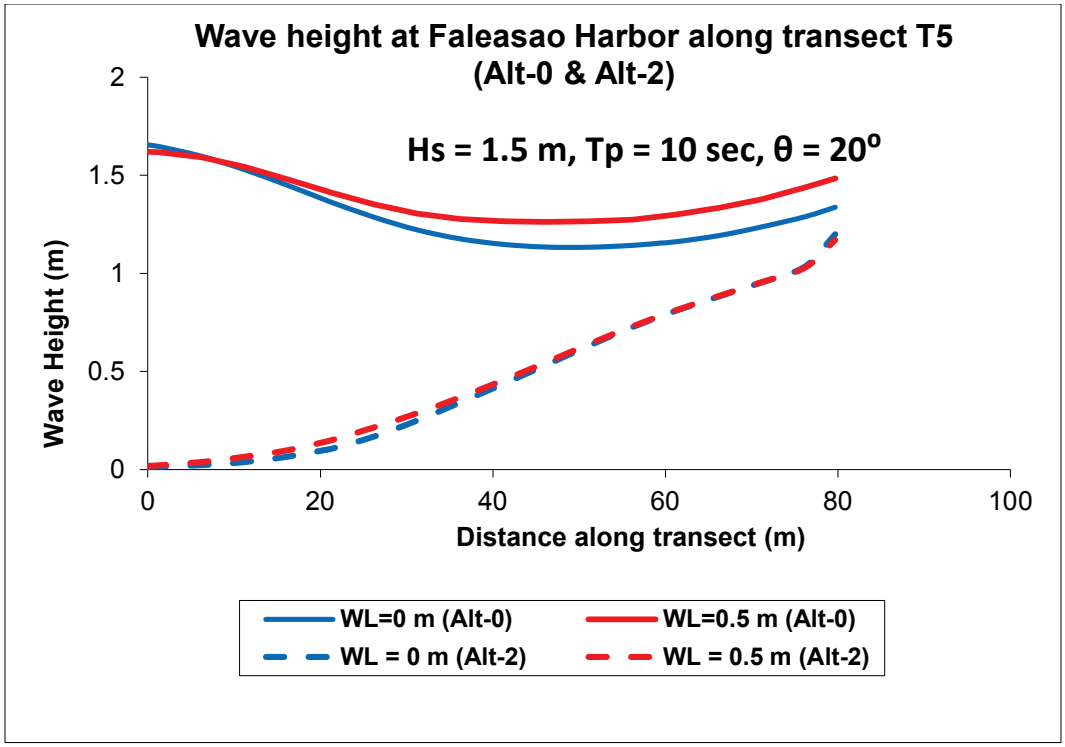

Figure 4-84. Comparison of Alt-0 and Alt-2 wave heights along transect T6 (θ = 20°).

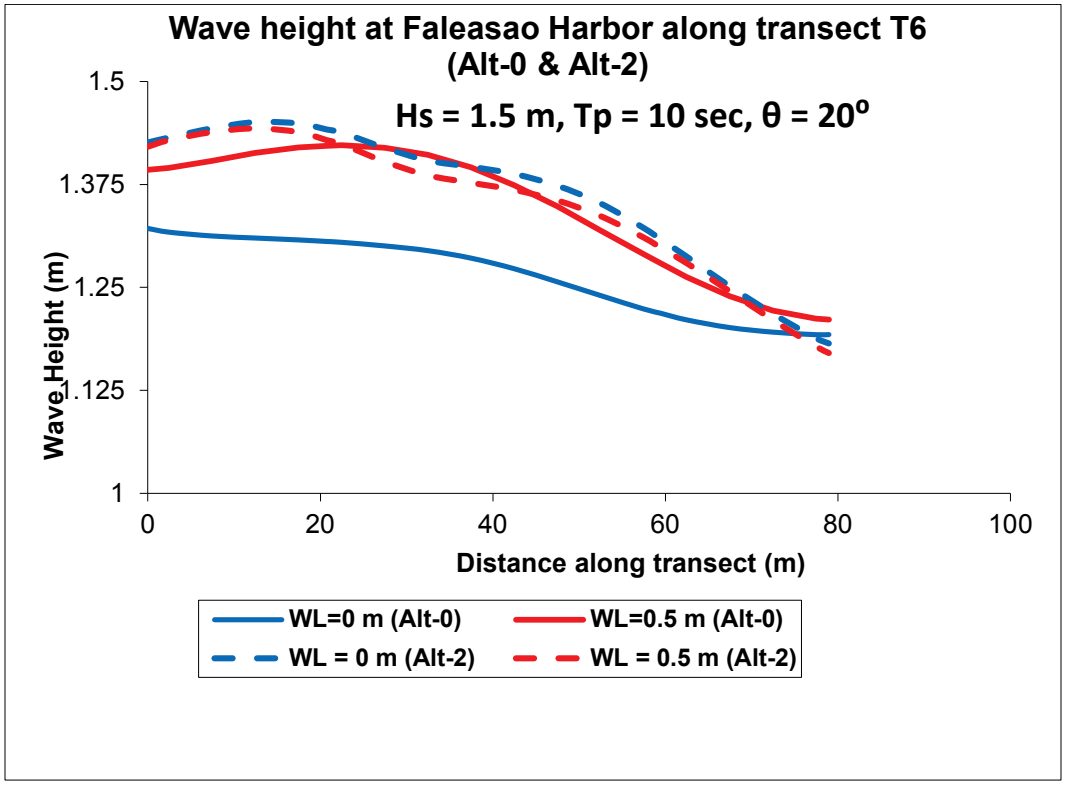

Figure 4-85. Comparison of Alt-0 and Alt-2 wave heights along transect T7 (θ = 20°).

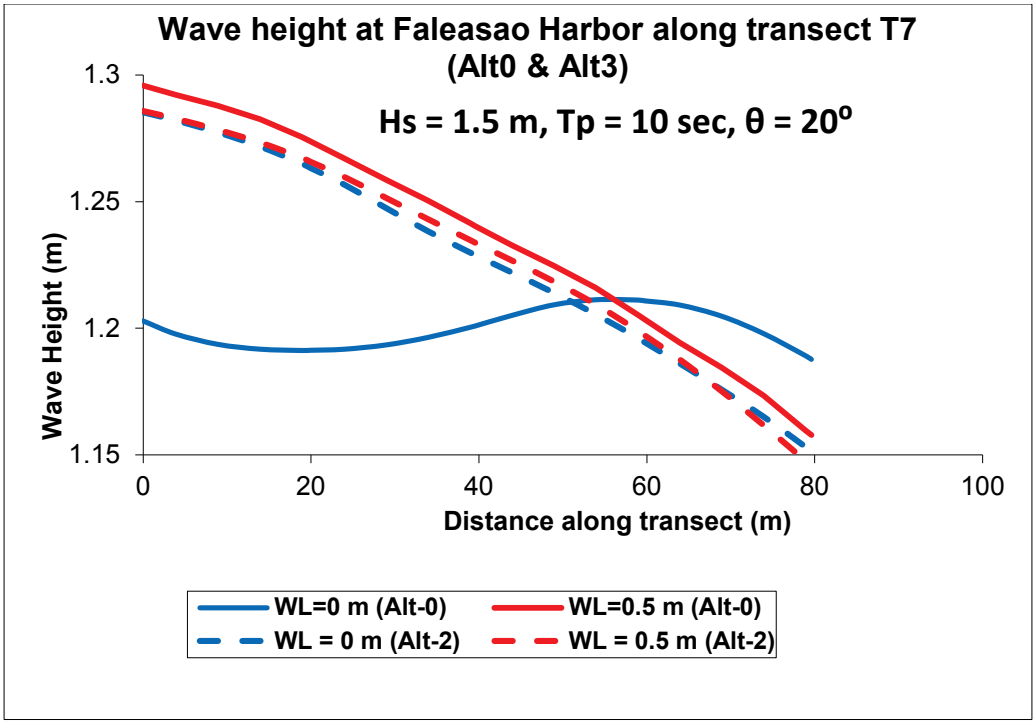

Figure 4-86. Comparison of Alt-0 and Alt-2 wave heights along transect T8 (θ = 20°).

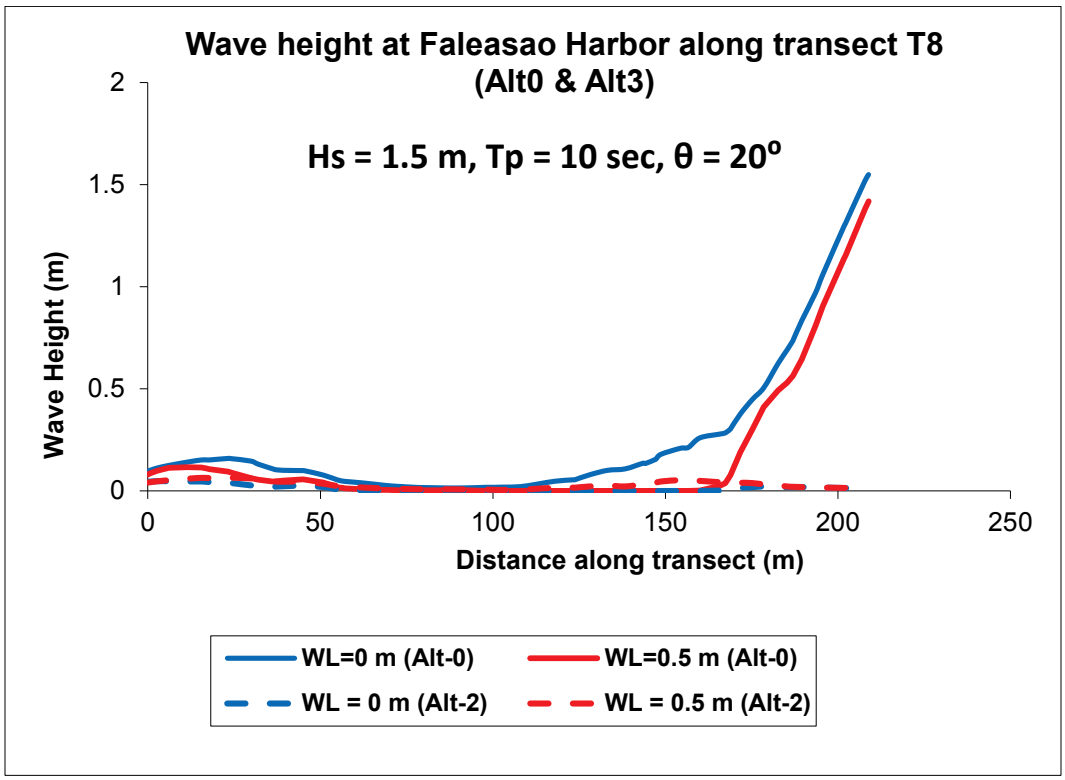

Figure 4-87. Comparison of Alt-0 and Alt-2 wave heights along transect T9 (θ = 20°).

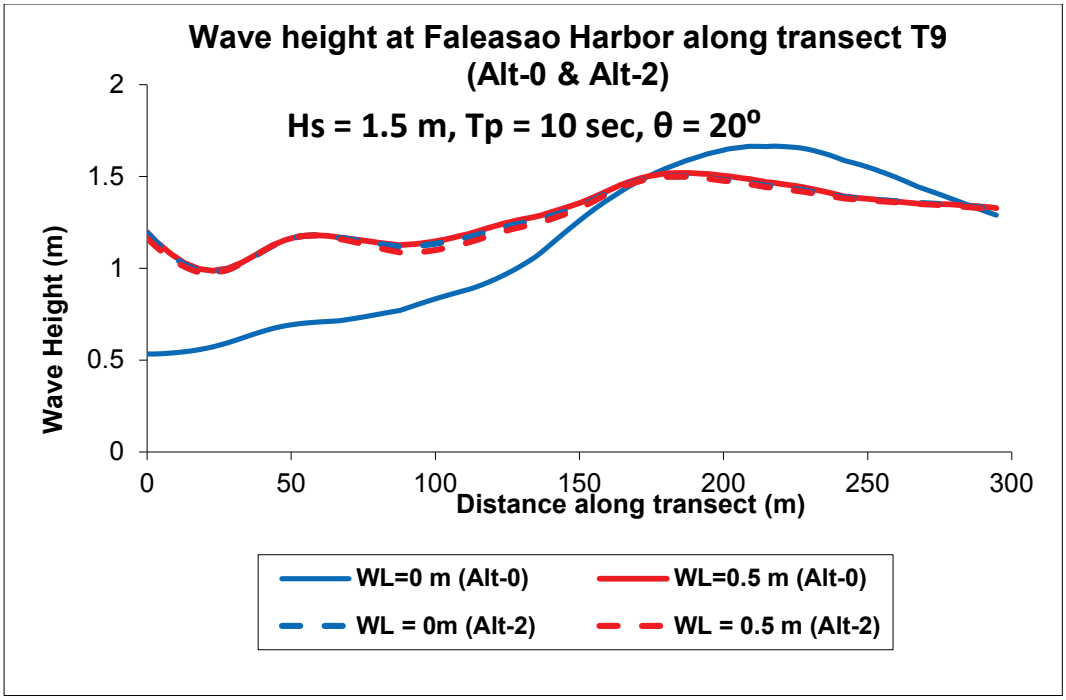

Alt-2 results for a 340° incident average wave condition are compared to the existing harbor (Alt-0) in Figures 4-88 to 4-96 to show local wave height variation along the nine transects which cover the areas of interest in the harbor.

Figure 4-88. Comparison of Alt-0 and Alt-2 wave heights along transect T1 (θ = 340°).

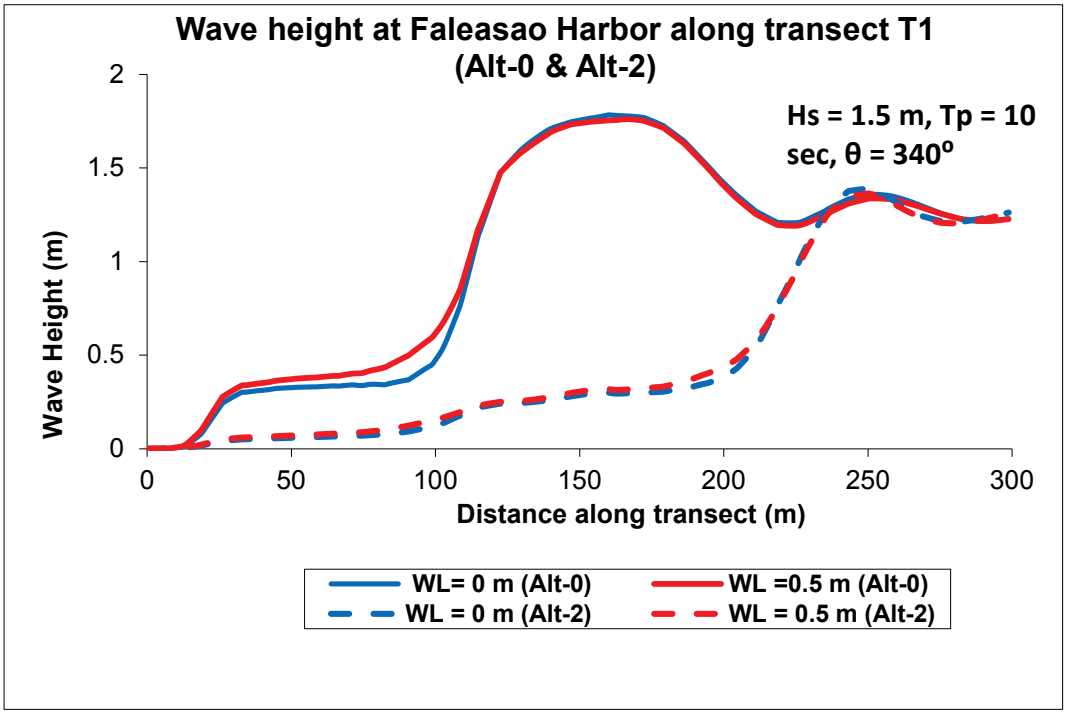

Figure 4-89. Comparison of Alt-0 and Alt-2 wave heights along transect T2 (θ = 340°).

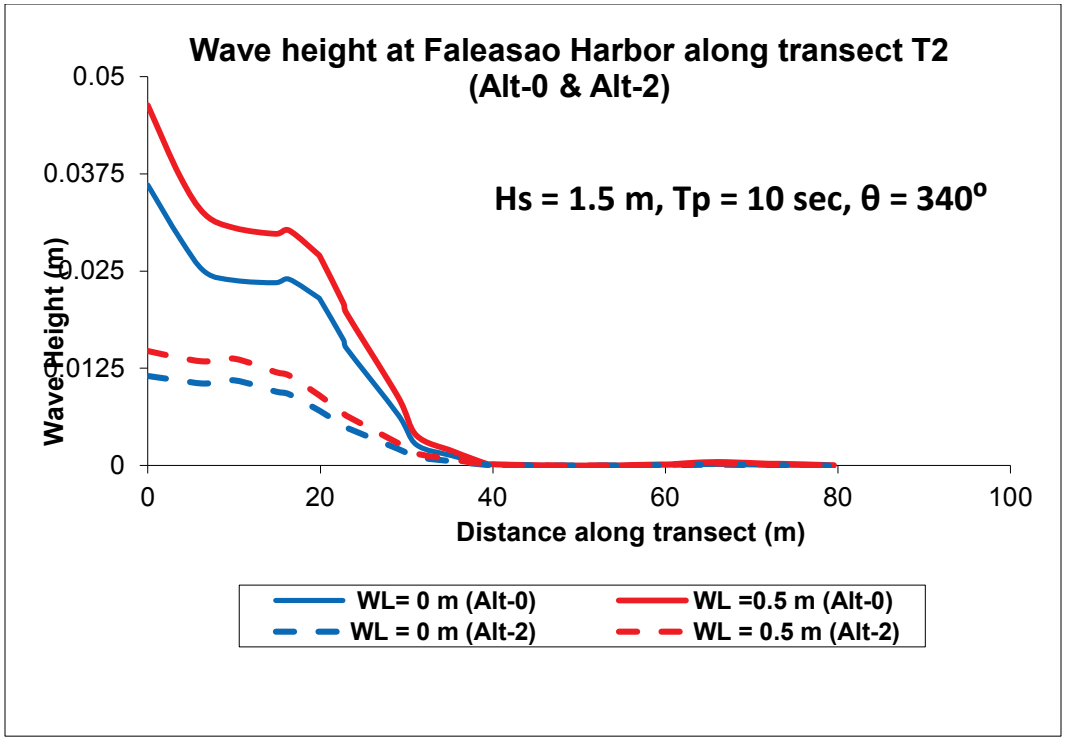

Figure 4-90. Comparison of Alt-0 and Alt-2 wave heights along transect T3 (θ = 340°).

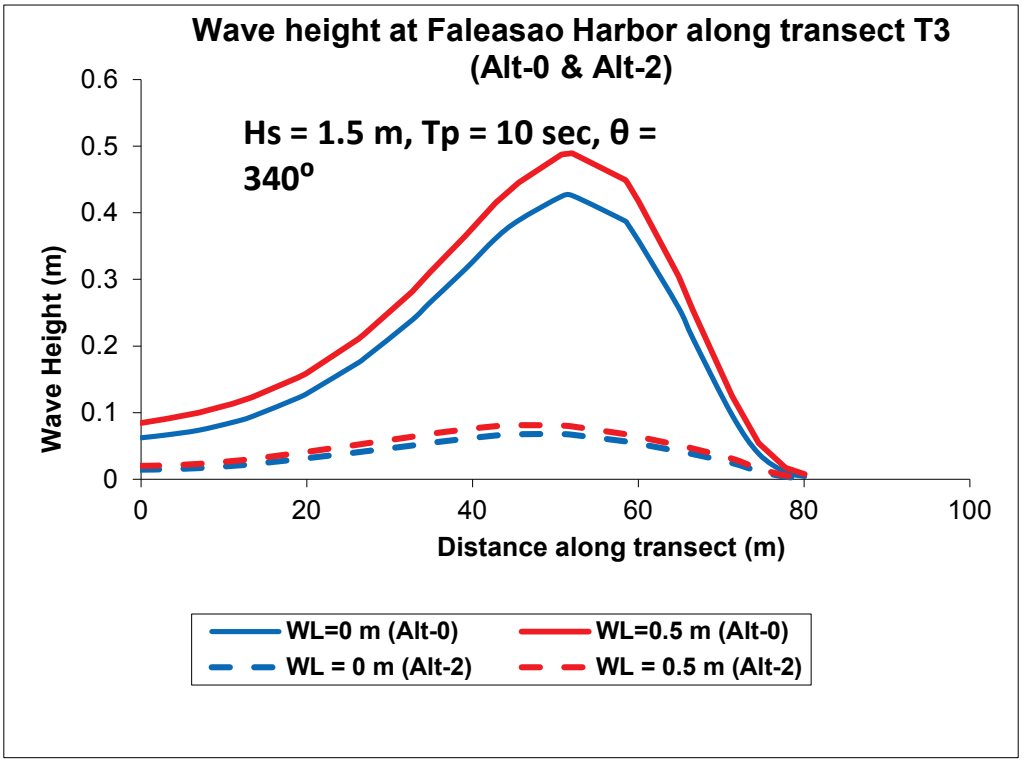

Figure 4-91. Comparison of Alt-0 and Alt-2 wave heights along transect T4 (θ = 340°).

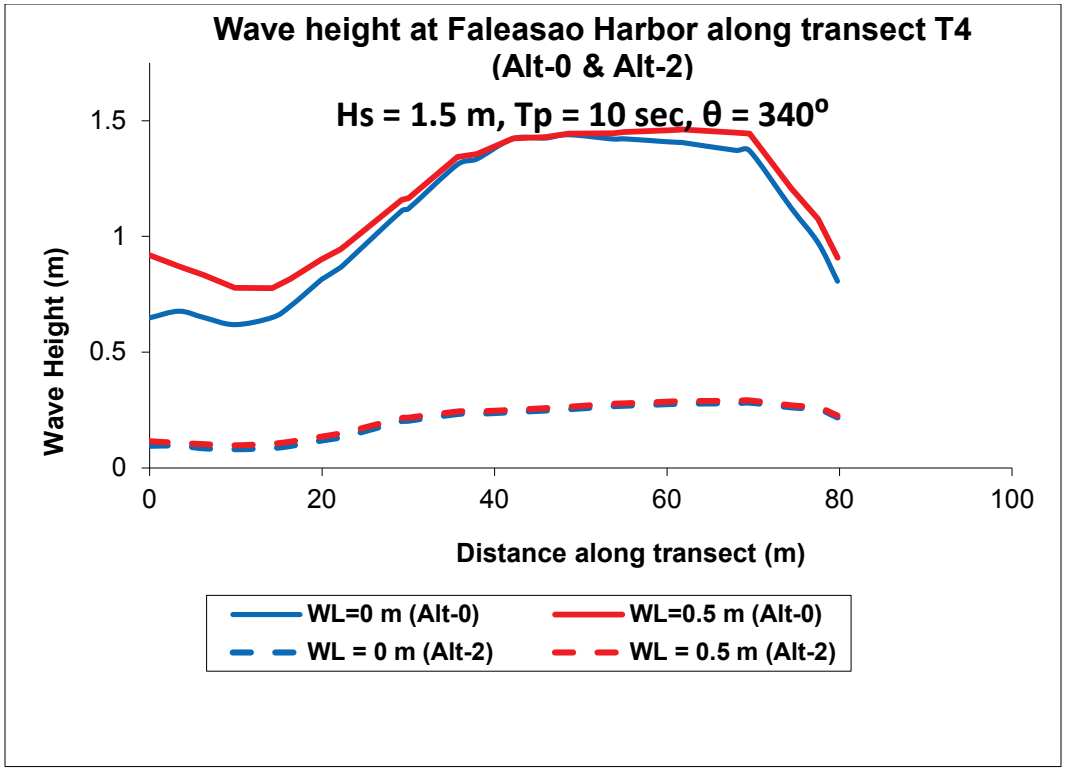

Figure 4-92. Comparison of Alt-0 and Alt-2 wave heights along transect T5 (θ = 340°).

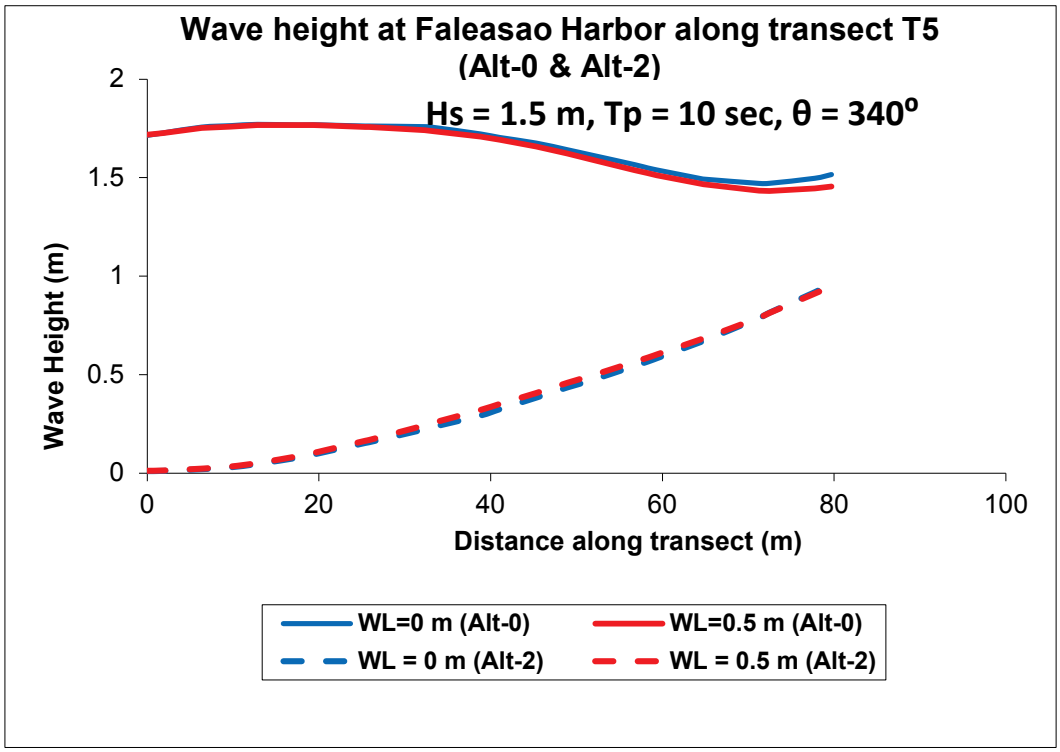

Figure 4-93. Comparison of Alt-0 and Alt-2 wave heights along transect T6 (θ = 340°).

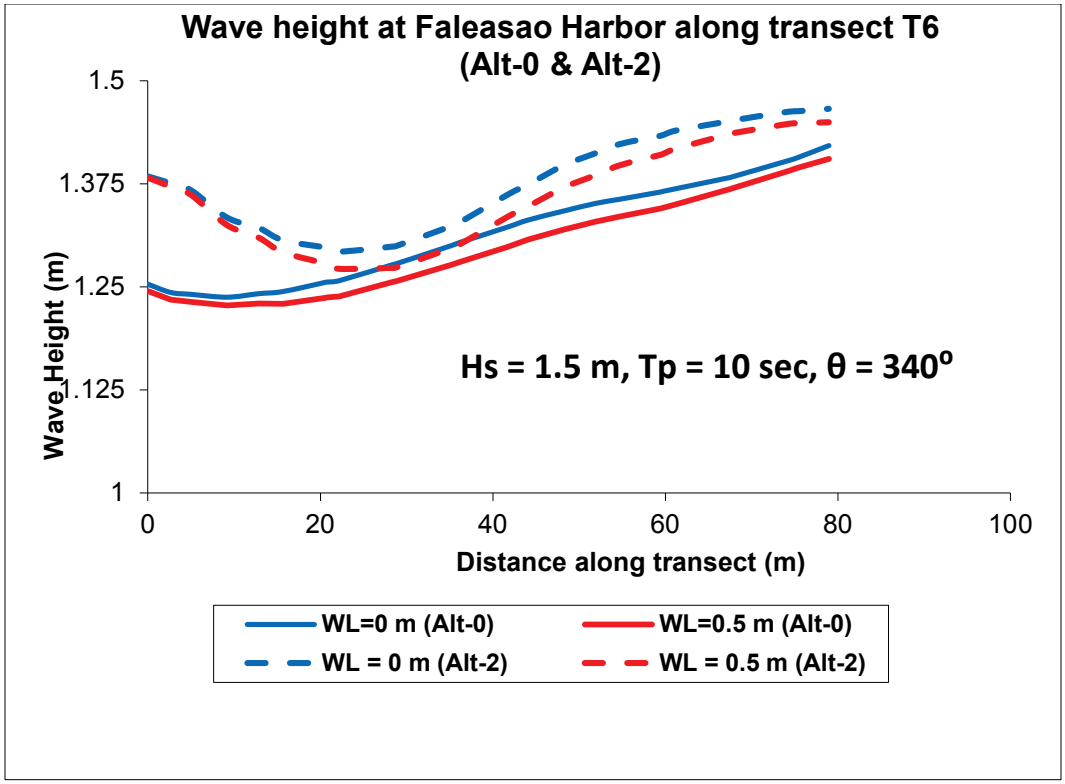

Figure 4-94. Comparison of Alt-0 and Alt-2 wave heights along transect T7 (θ = 340°).

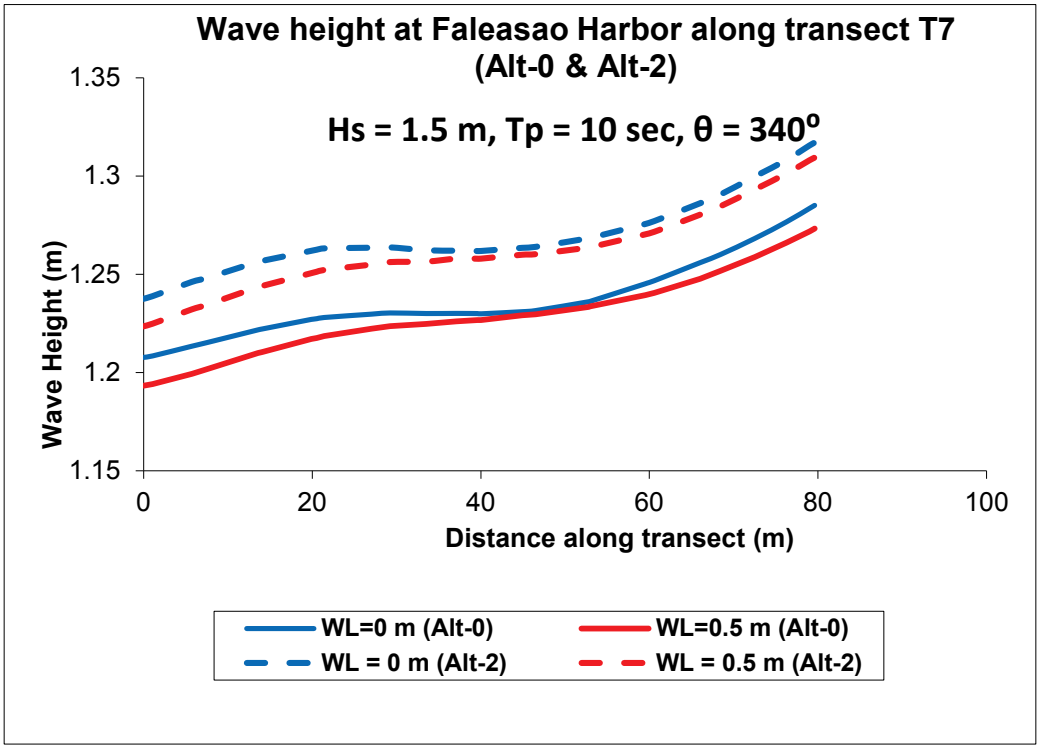

Figure 4-95. Comparison of Alt-0 and Alt-2 wave heights along transect T8 (θ = 340°).

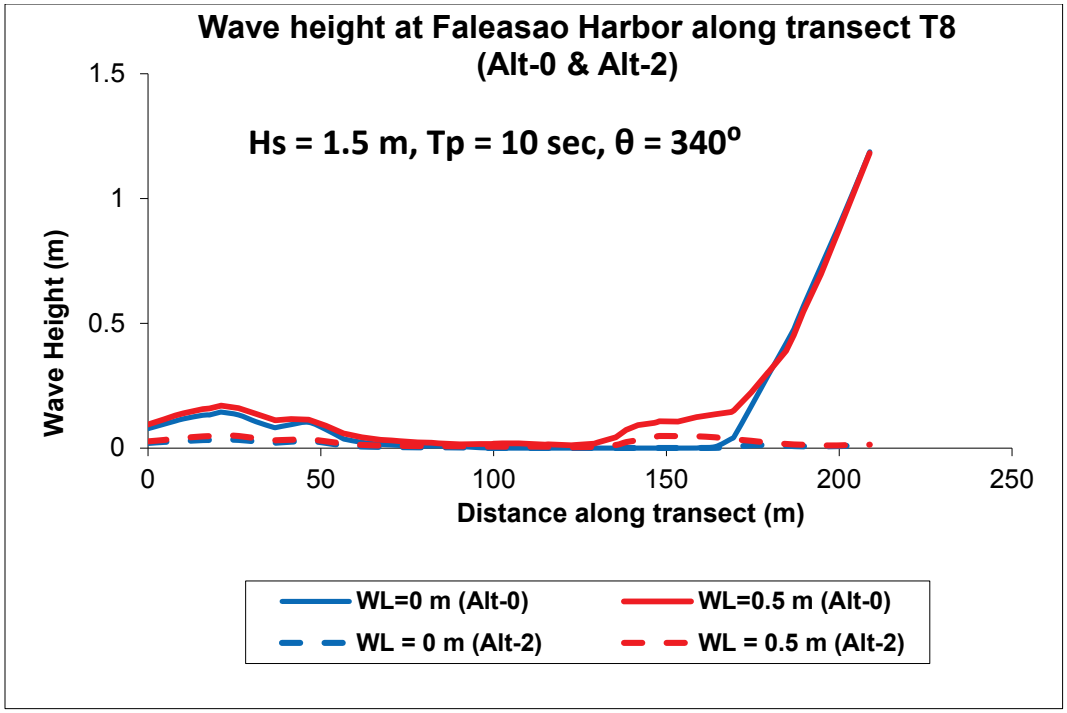

Figure 4-96. Comparison of Alt-0 and Alt-2 wave heights along transect T9 (θ = 340°).

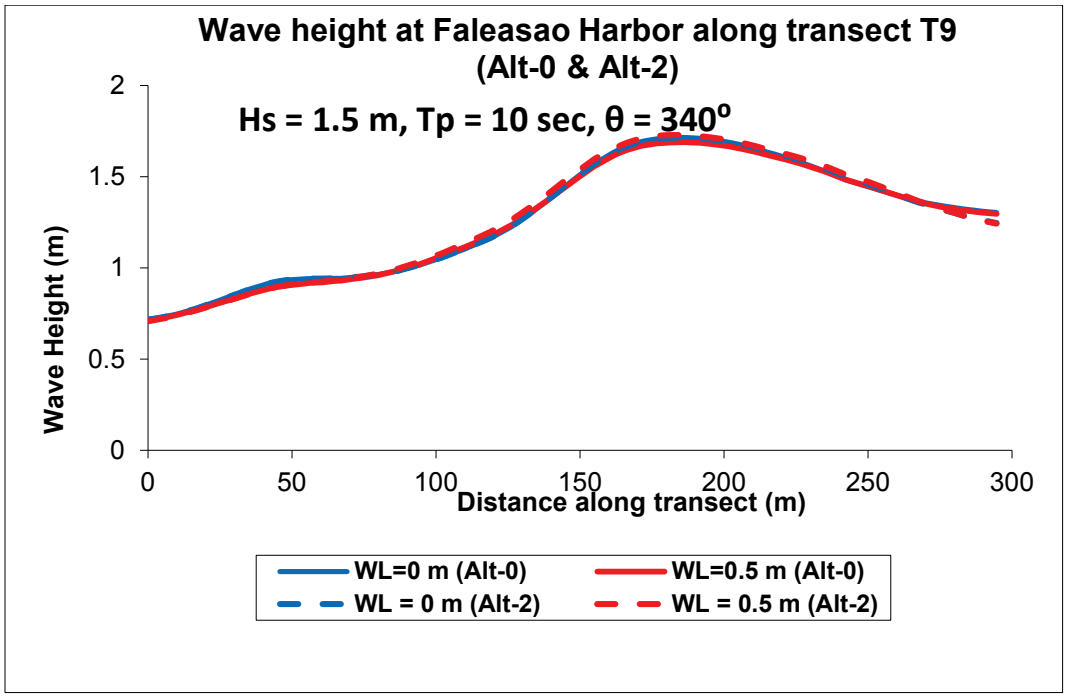

Alt-2 results for a 320° incident average wave condition are compared to the existing harbor (Alt-0) in Figures 4-97 to 4-105. These show the local wave height variation along the nine transects covering the areas of interest in the harbor.

Figure 4-97. Comparison of Alt-0 and Alt-2 wave heights along transect T1 (θ = 320°).

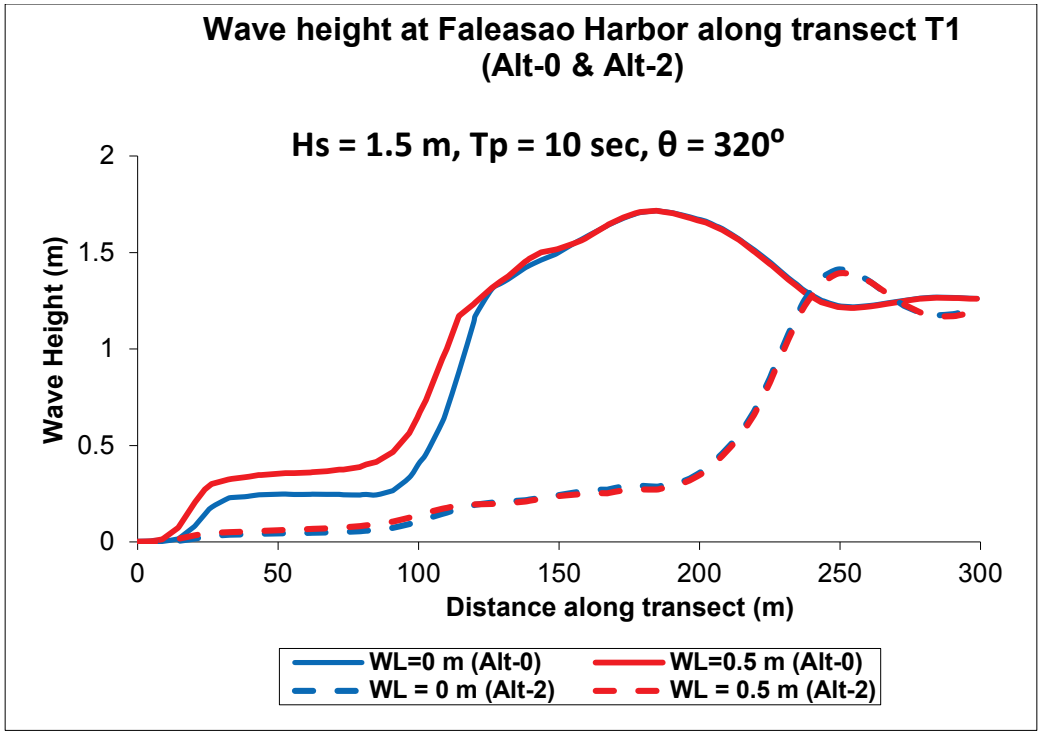

Figure 4-98. Comparison of Alt-0 and Alt-2 wave heights along transect T2 (θ = 320°).

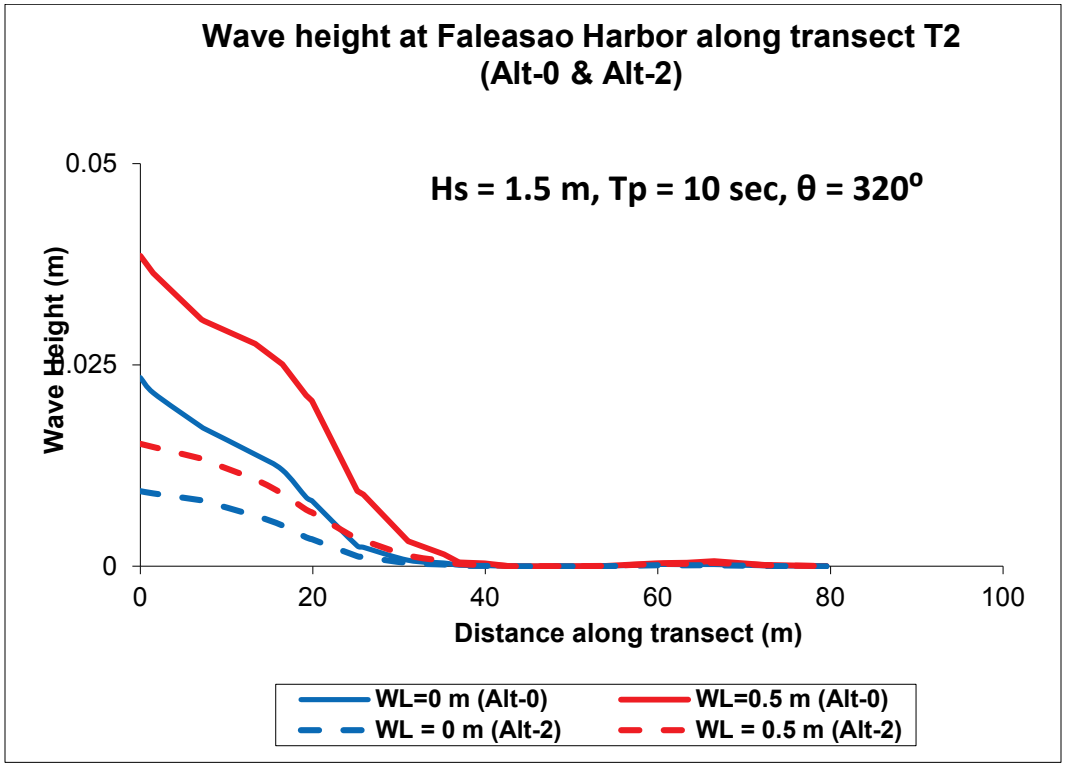

Figure 4-99. Comparison of Alt-0 and Alt-2 wave heights along transect T3 (θ = 320°).

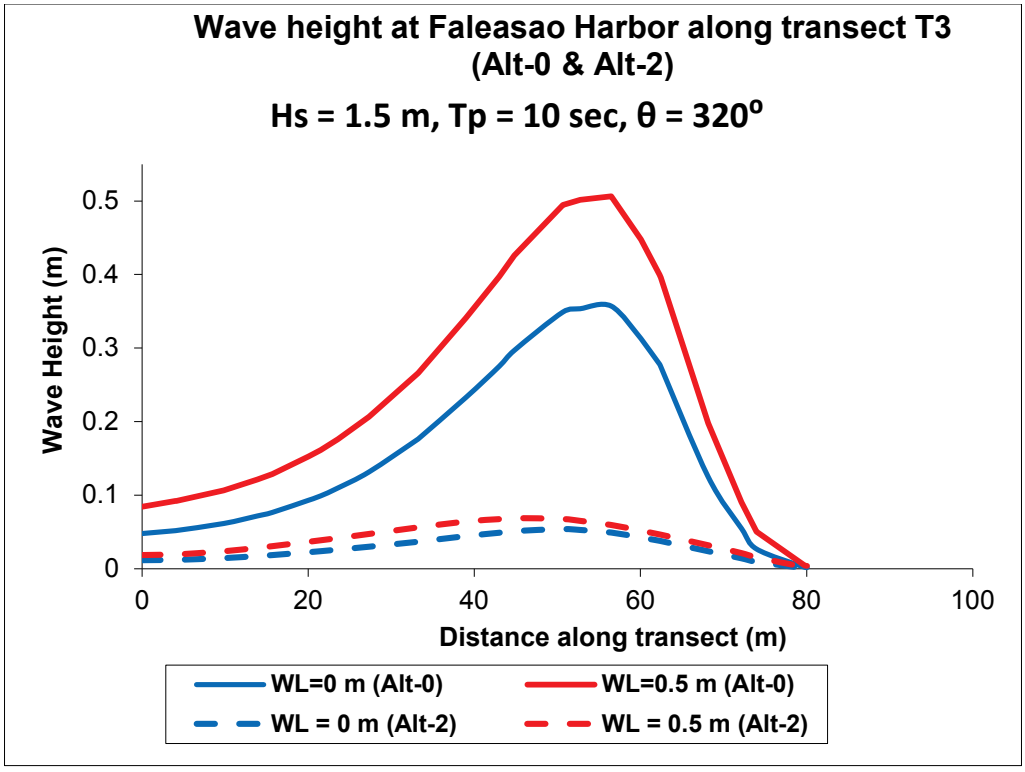

Figure 4-100. Comparison of Alt-0 and Alt-2 wave heights along transect T4 (θ = 320°).

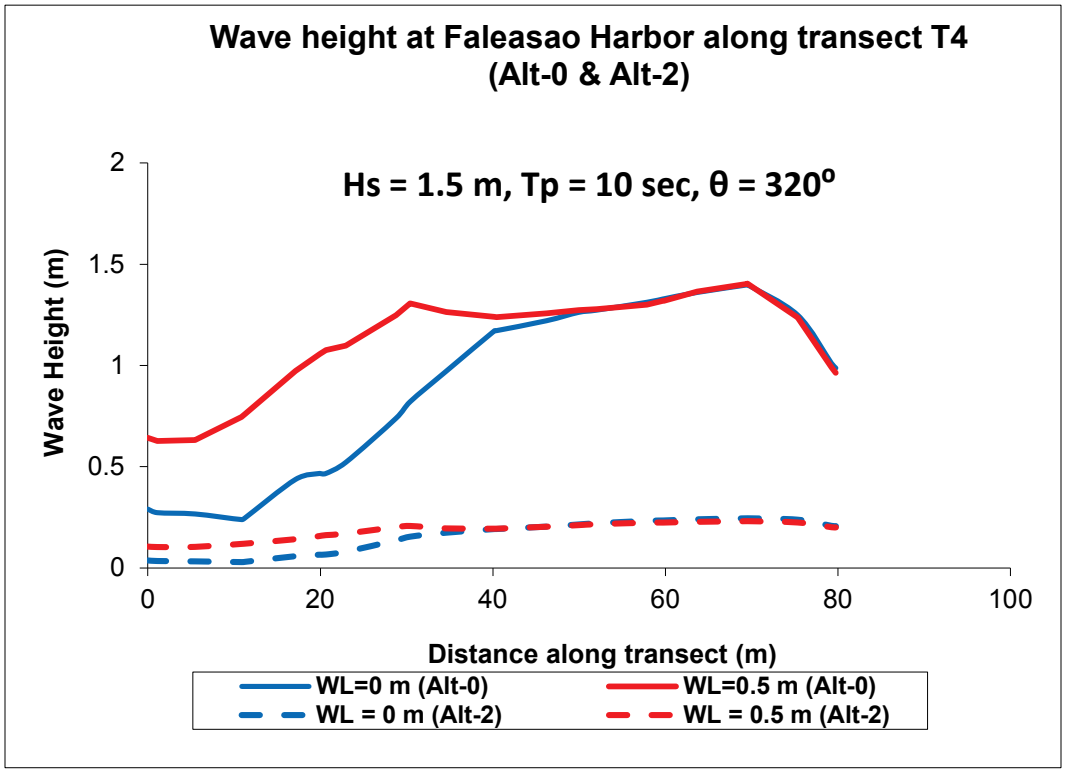

Figure 4-101. Comparison of Alt-0 and Alt-2 wave heights along transect T5 (θ = 320^0).

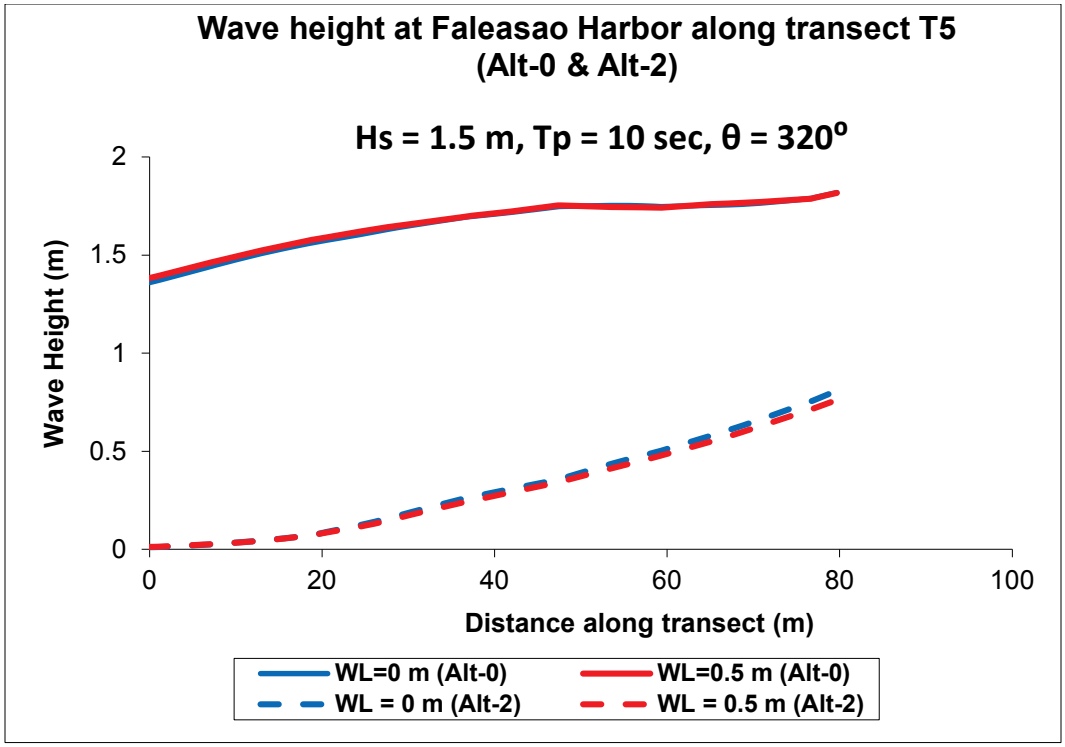

Figure 4-102. Comparison of Alt-0 and Alt-2 wave heights along transect T6 (θ = 320^0).

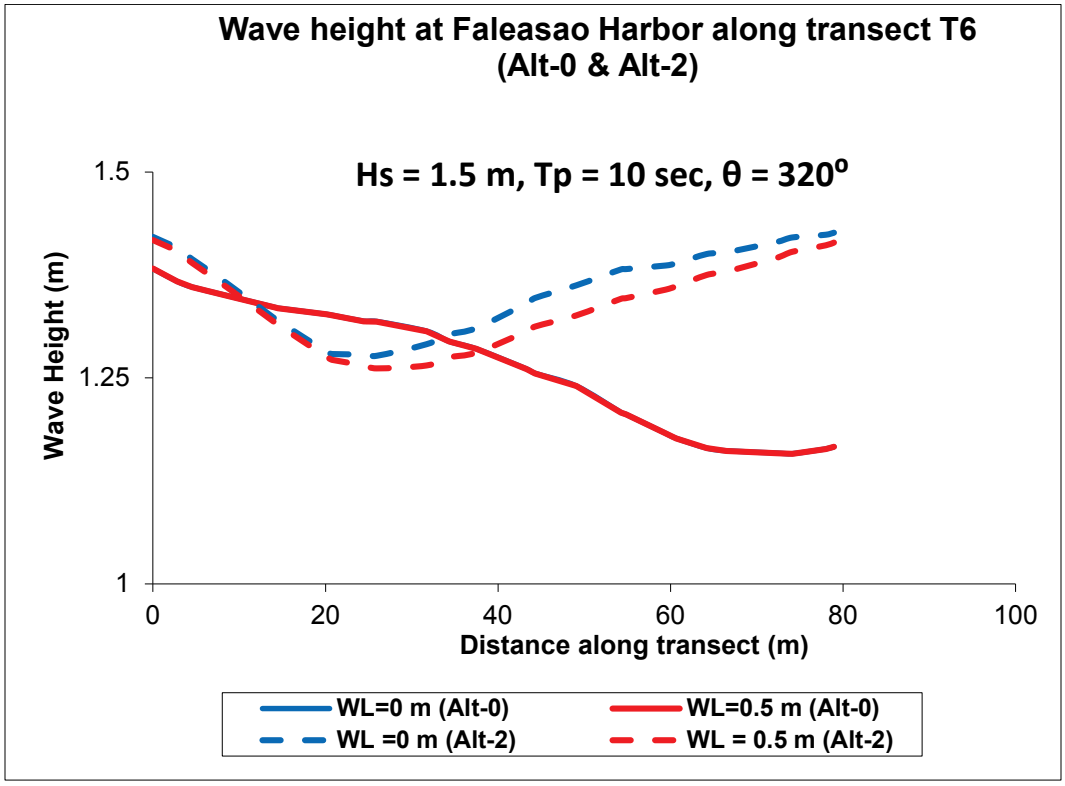

Figure 4-103. Comparison of Alt-0 and Alt-2 wave heights along transect T7 (θ = 320°).

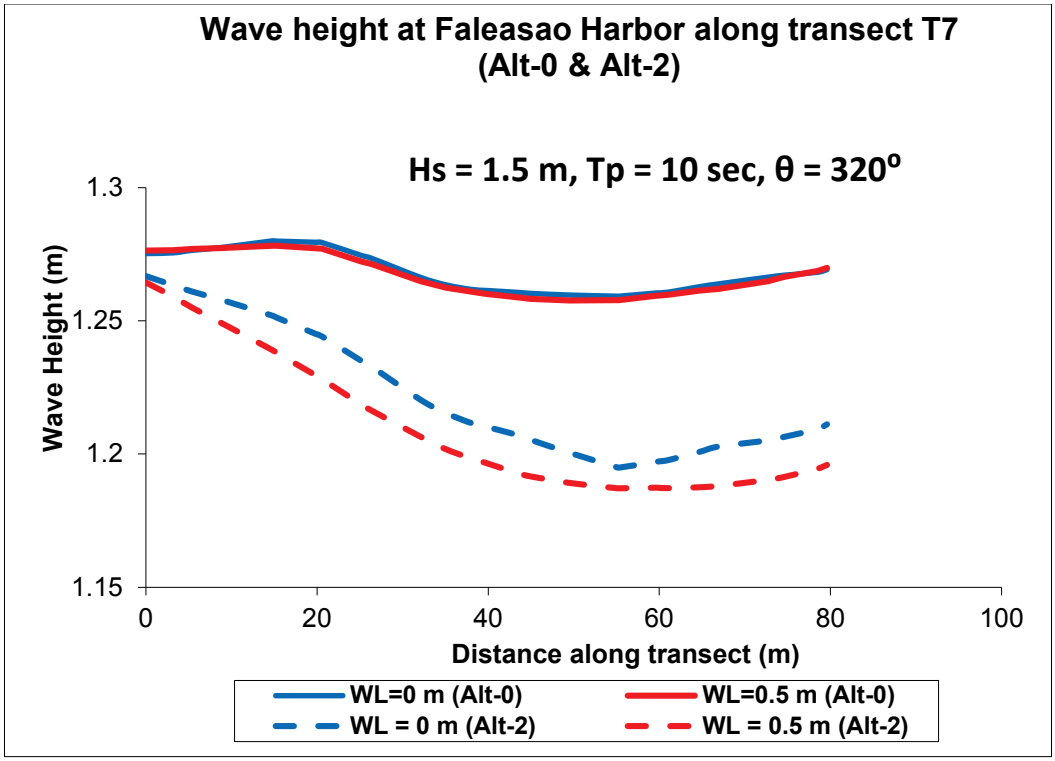

Figure 4-104. Comparison of Alt-0 and Alt-2 wave heights along transect T8 (θ = 320°).

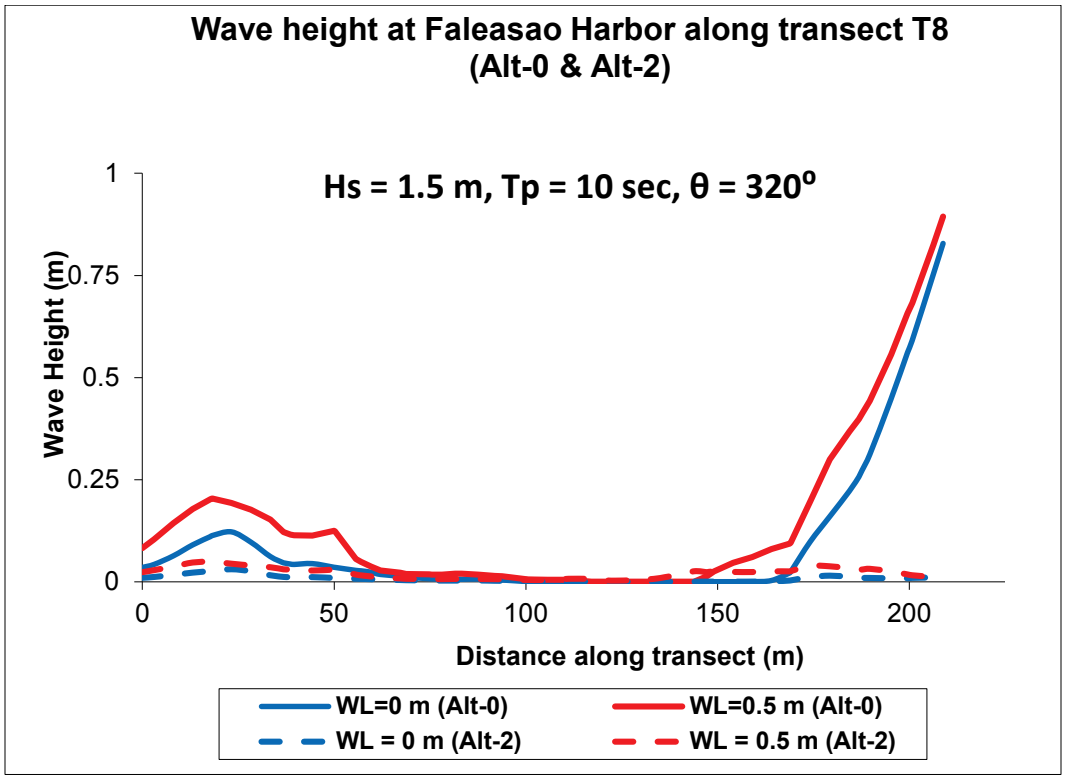

Figure 4-105. Comparison of Alt-0 and Alt-2 wave heights along transect T9 (θ = 320^0).

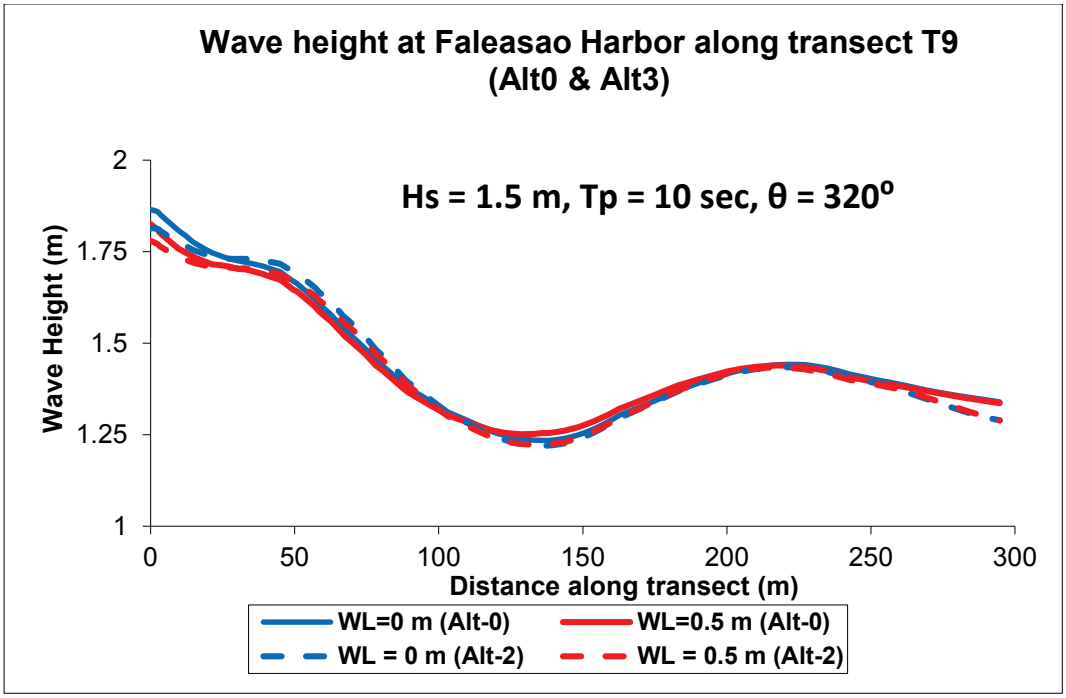

4.6 Model results for Alt-3

Alt-3 results for 0° incident wave direction are compared to the existing harbor (Alt-0) in Figures 4-106 to 4-114, for a 20° incident wave in Figures 4-115 to 4-123, for 340° (-20°) in Figures 4-124 to 4-132, and for 320° waves in Figures 4-133 to 4-141. These comparative results indicate a significant reduction in wave heights by Alt-3.

Although the geometries of Alt-0, Alt-1, Alt-2, and Alt-3 were different, similar model parameters were used in Alt-3 simulations to control numerical stability and convergence of model solutions. Alt-3 results indicate this breakwater geometry is very effective in protecting the harbor. The wave height reduction varies along transects located in different areas both inside and outside the harbor. The local variation in wave heights along the nine transects for the two water levels for incident waves from four directions is described next.

In Figure 4-106, the values of the average wave height for Alt-0 and Alt-3 are approximately 0.6 m and 1.2 m along T1, respectively. This is a 50% wave height reduction by Alt-3, and a 5% change can be expected based on sensitivity tests done for Alt-2. The Alt-3 results are compared to the existing harbor (Alt-0) to quantify the local wave height variation along the nine transects covering some key areas of interest to navigation in Faleasao Harbor.

Figure 4-106. Comparison of Alt-0 and Alt-3 wave heights along transect T1 (θ = 0°).

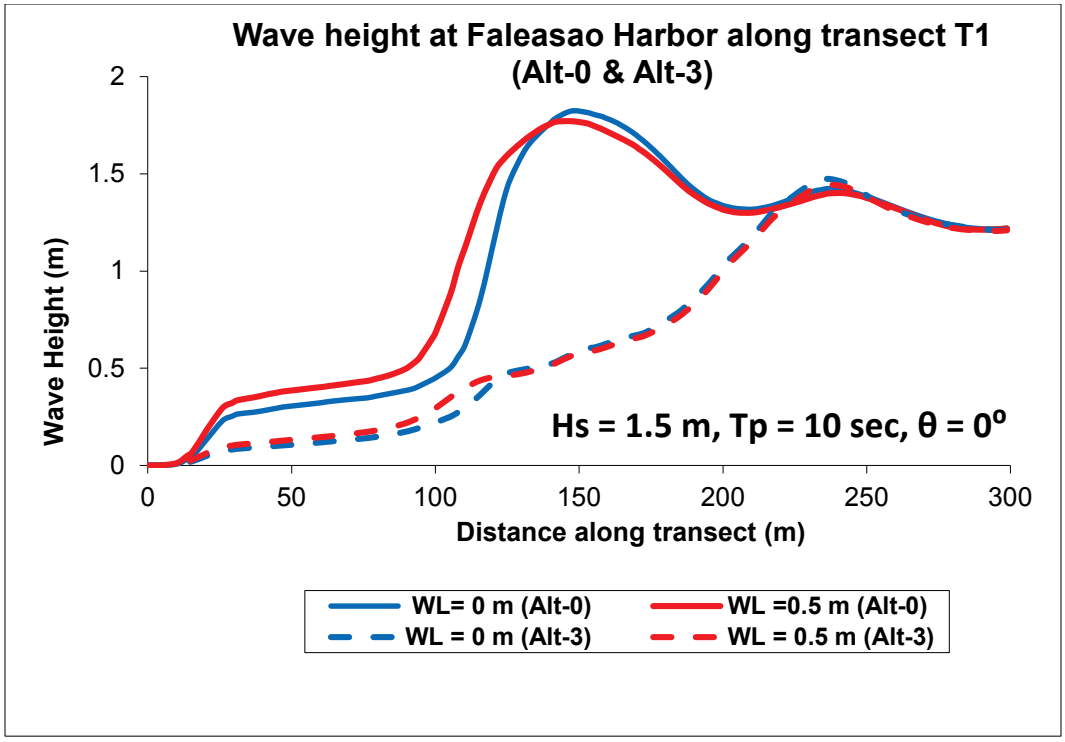

Figure 4-107. Comparison of Alt-0 and Alt-3 wave heights along transect T2 (θ = 0°).

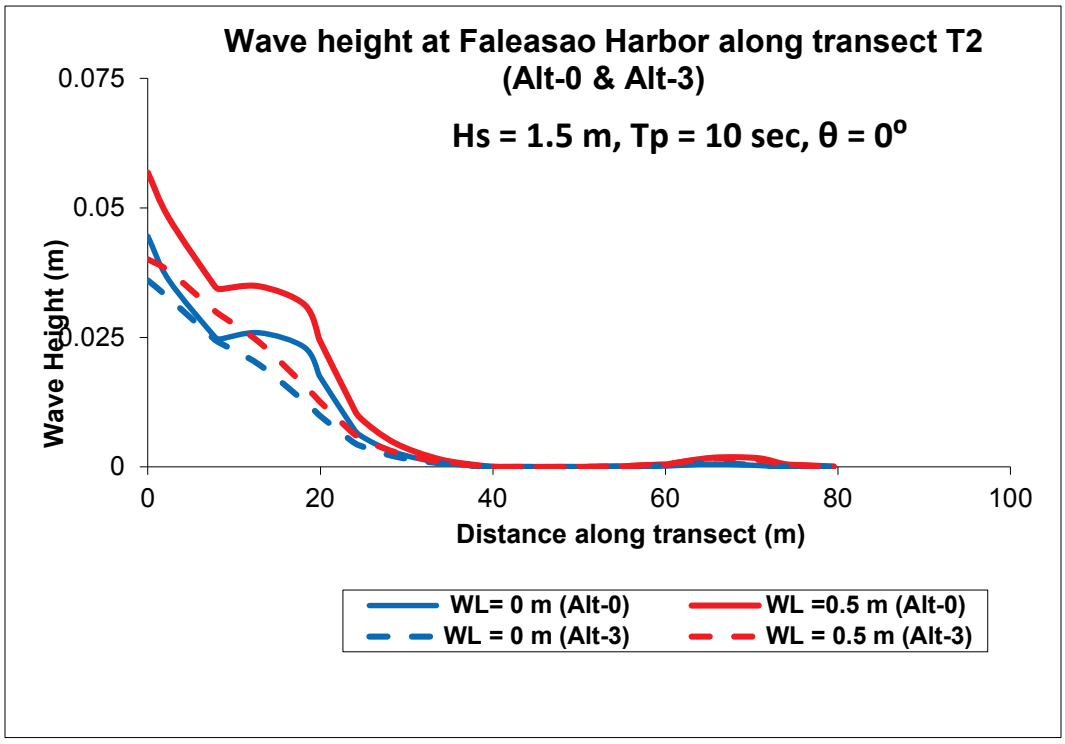

Figure 4-108. Comparison of Alt-0 and Alt-3 wave heights along transect T3 (θ = 0°).

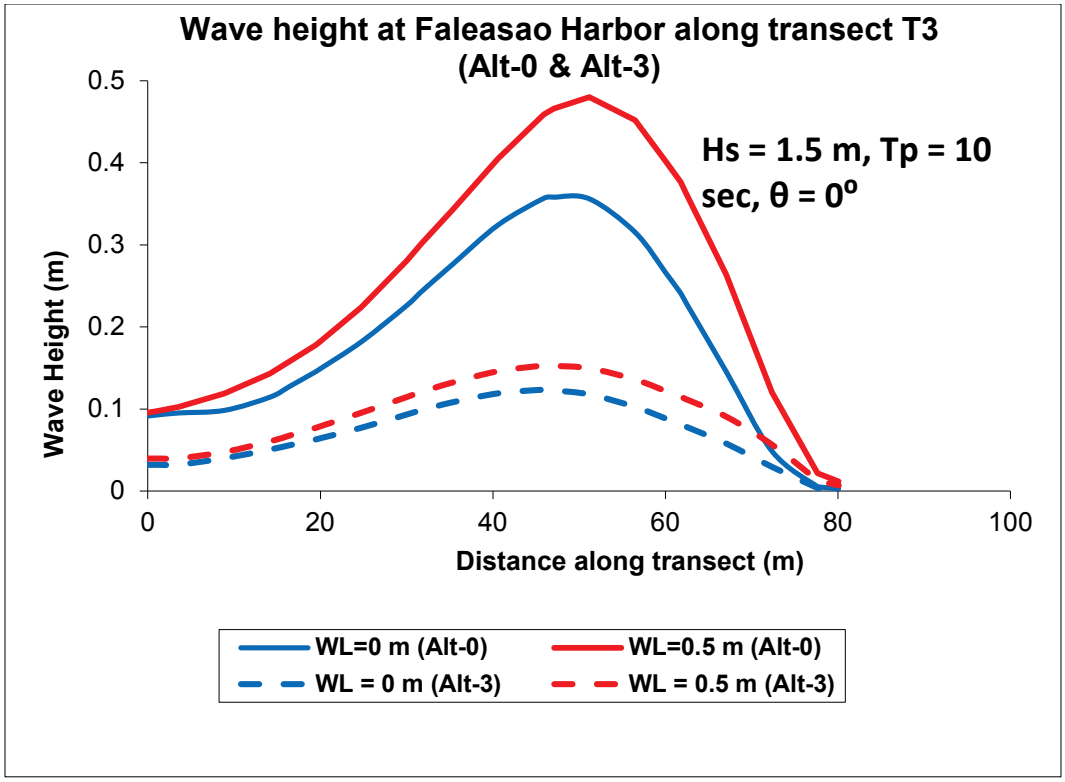

Figure 4-109. Comparison of Alt-0 and Alt-3 wave heights along transect T4 (θ = 0°).

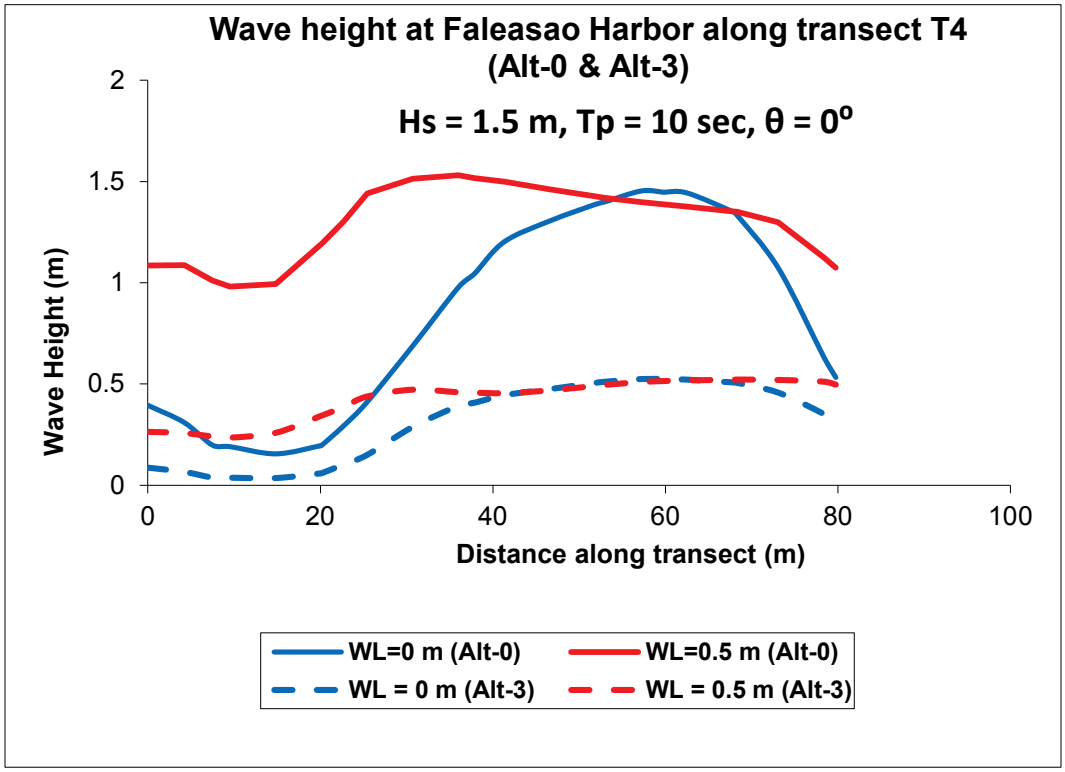

Figure 4-110. Comparison of Alt-0 and Alt-3 wave heights along transect T5 ($\theta = 0^o$).

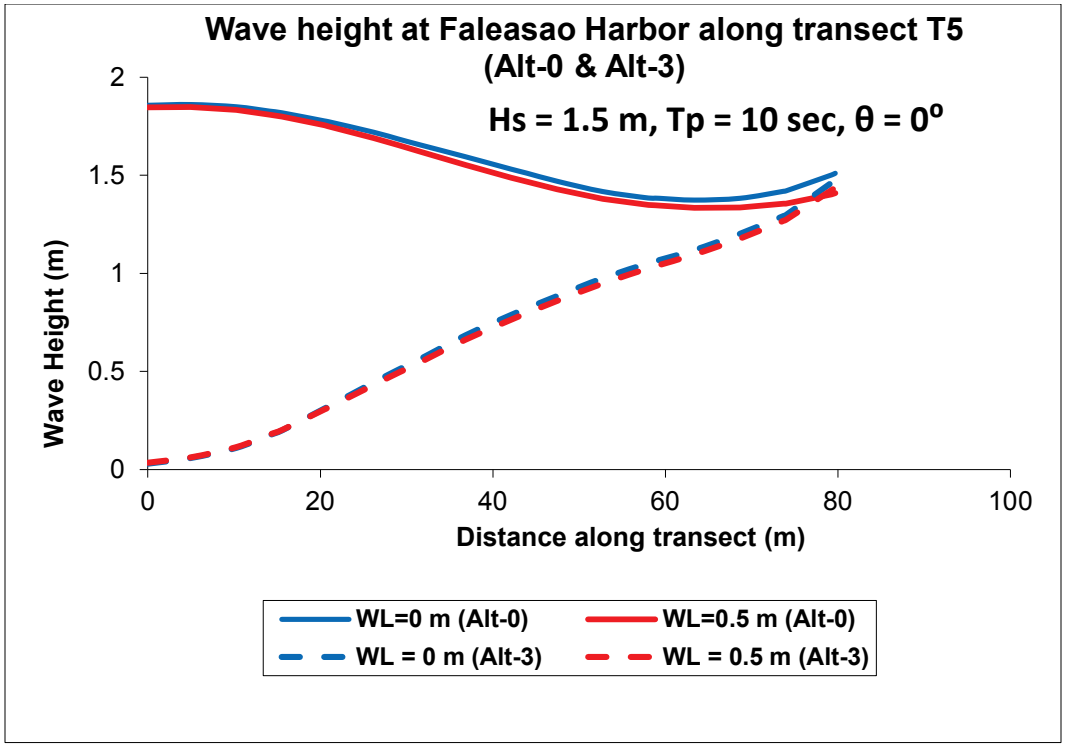

Figure 4-111. Comparison of Alt-0 and Alt-3 wave heights along transect T6 ($\theta = 0^o$).

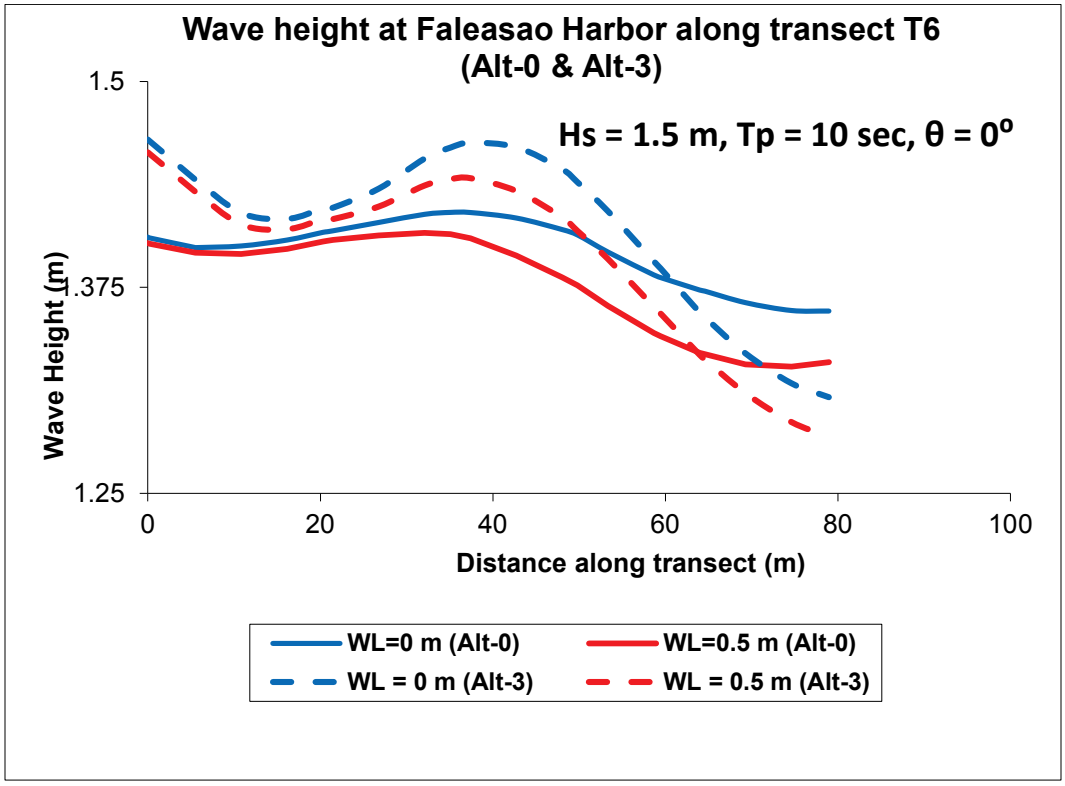

Figure 4-112. Comparison of Alt-0 and Alt-3 wave heights along transect T7 (θ = 0°).

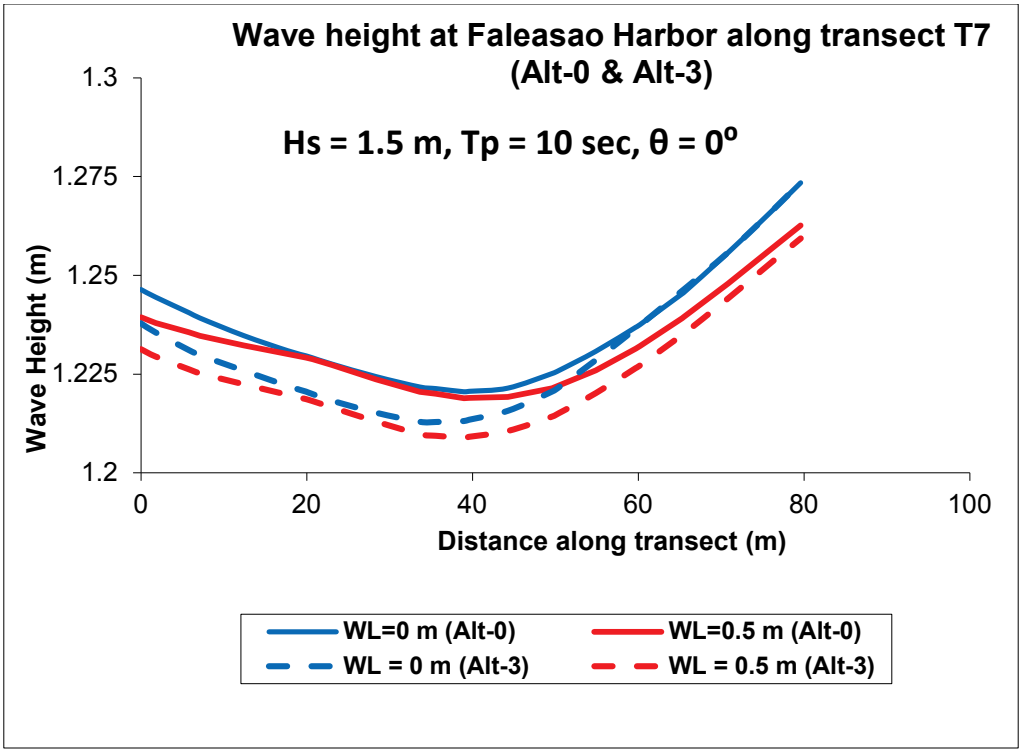

Figure 4-113. Comparison of Alt-0 and Alt-3 wave heights along transect T8 (θ = 0°).

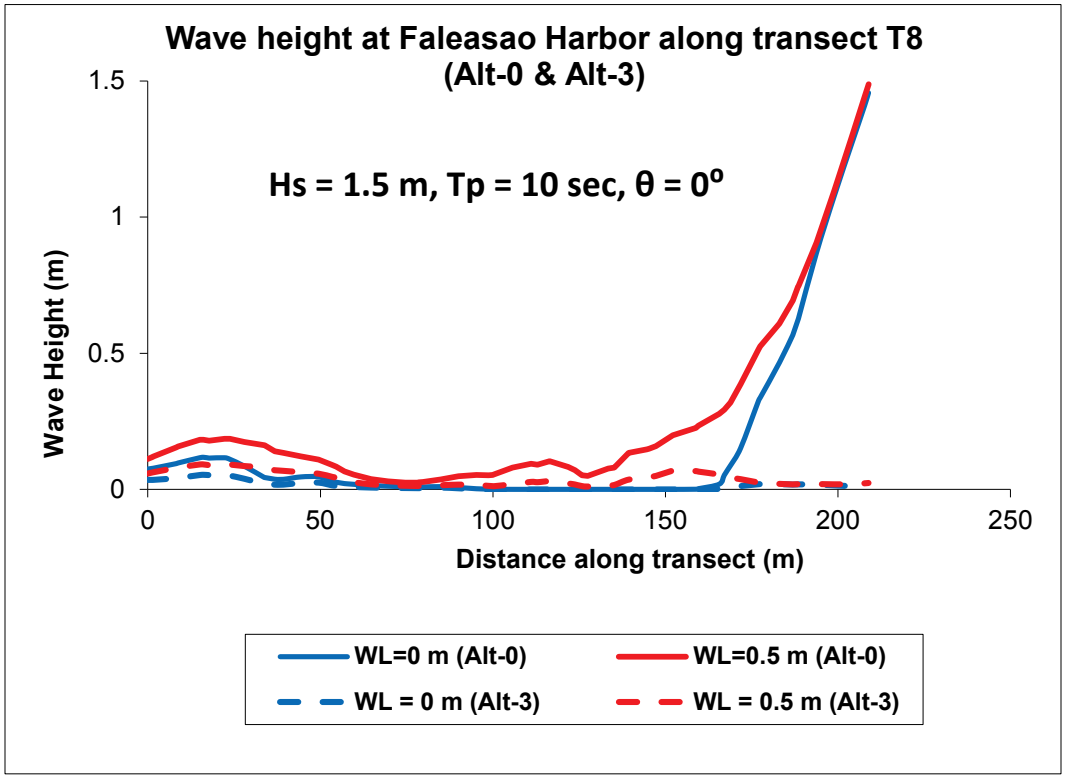

Figure 4-114. Comparison of Alt-0 and Alt-3 wave heights along transect T9 (θ = 0°).

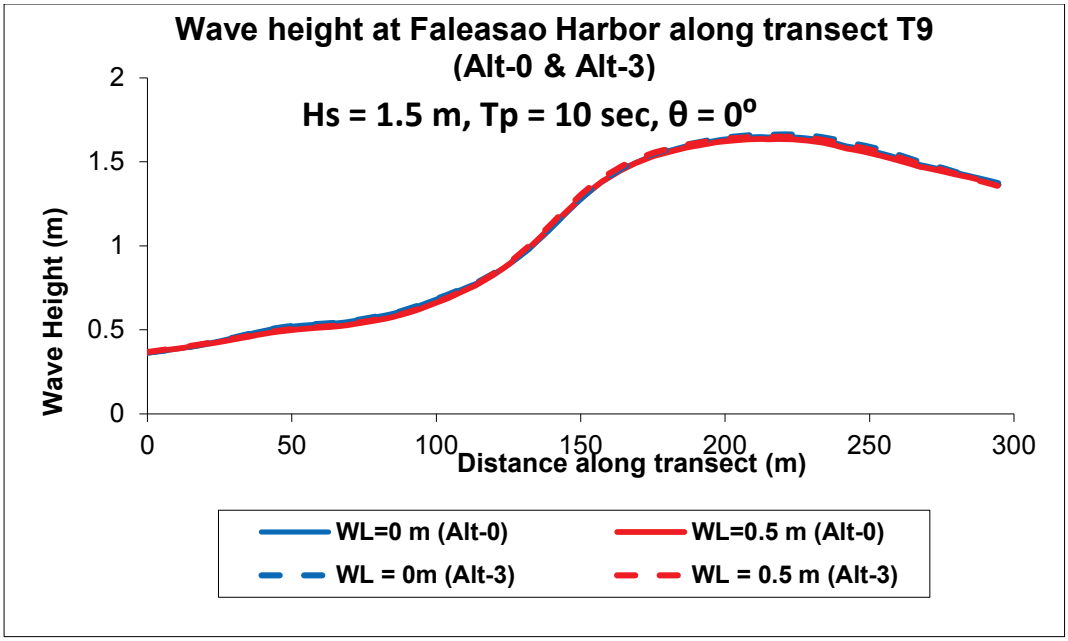

Alt-3 results for the 20° incident average incident wave condition (from NNE direction) are compared to the existing harbor (Alt-0) results in Figures 4-115 to 4-123. It is noteworthy that although wave heights have increased along parts of T2, this is not a concern because wave heights are too small to affect navigation (e.g., less than 0.1 m) in these extremely shallow, unnavigable areas.

Figure 4-115. Comparison of Alt-0 and Alt-3 wave heights along transect T1 (θ = 20°).

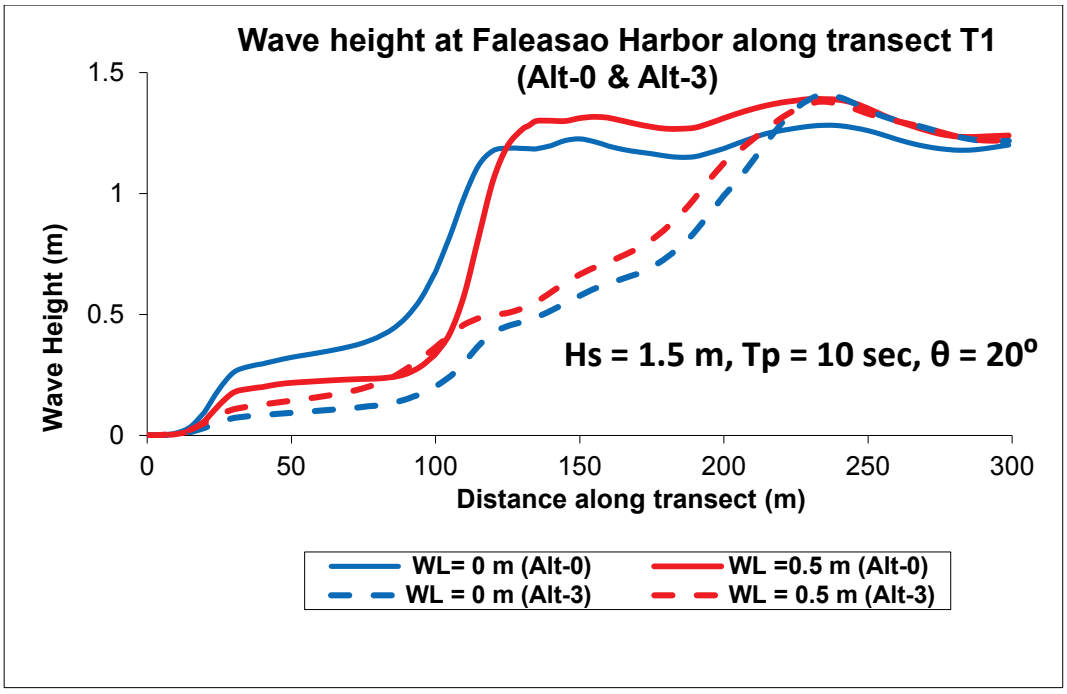

Figure 4-116. Comparison of Alt-0 and Alt-3 wave heights along transect T2 ($\theta = 20^0$).

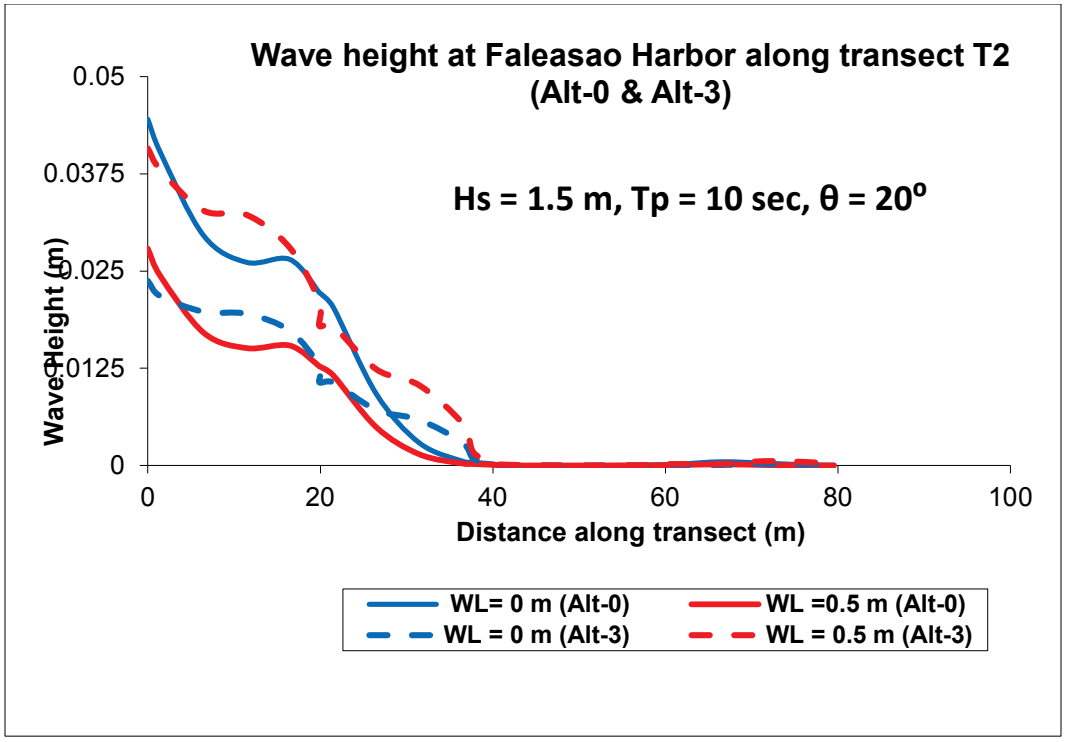

Figure 4-117. Comparison of Alt-0 and Alt-3 wave heights along transect T3 ($\theta = 20^0$).

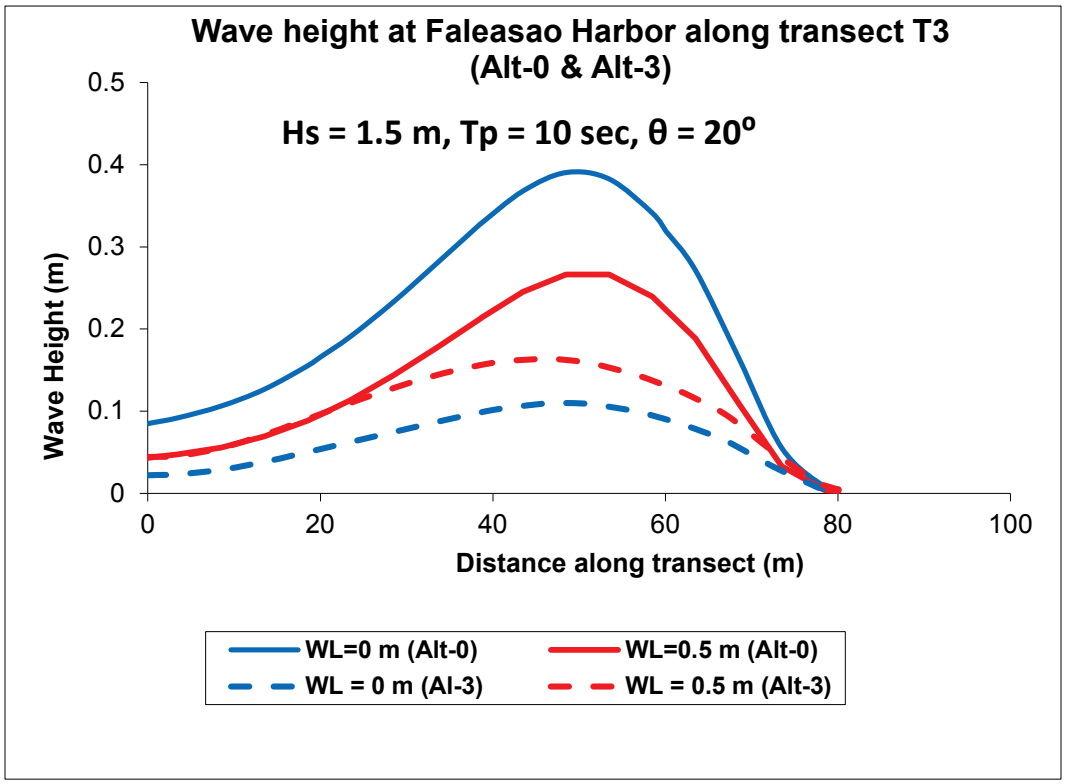

Figure 4-118. Comparison of Alt-0 and Alt-3 wave heights along transect T4 ($\theta = 20^0$).

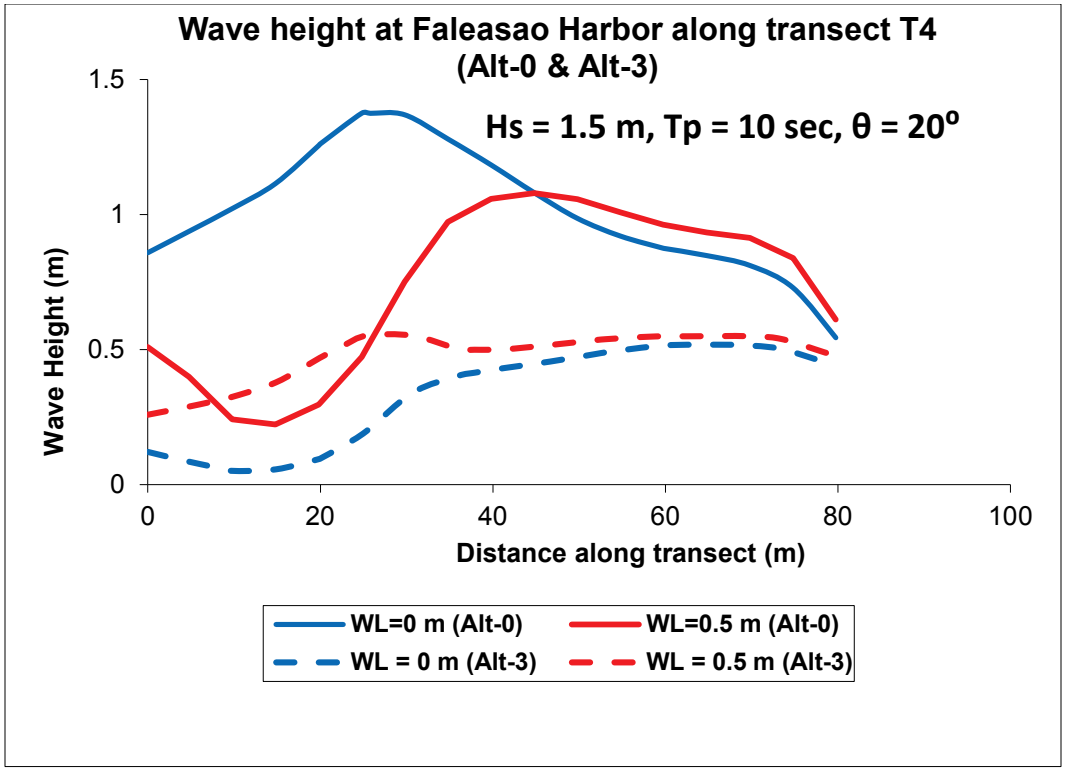

Figure 4-119. Comparison of Alt-0 and Alt-3 wave heights along transect T5 ($\theta = 20^0$).

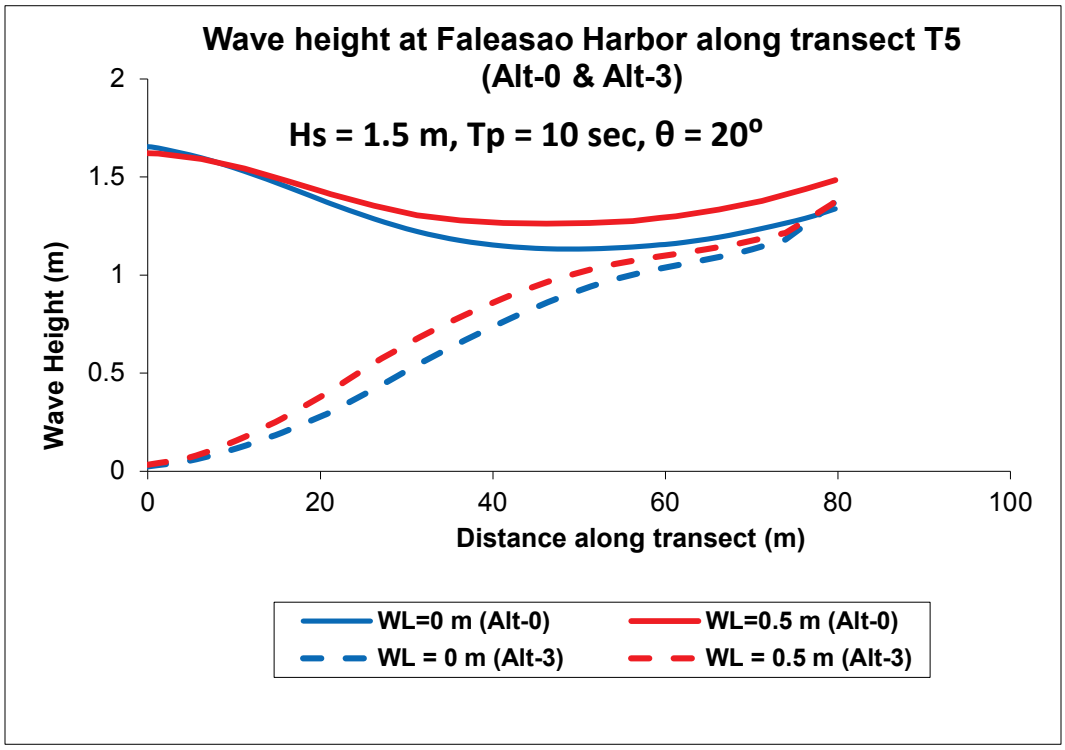

Figure 4-120. Comparison of Alt-0 and Alt-3 wave heights along transect T6 ($\theta = 20^0$).

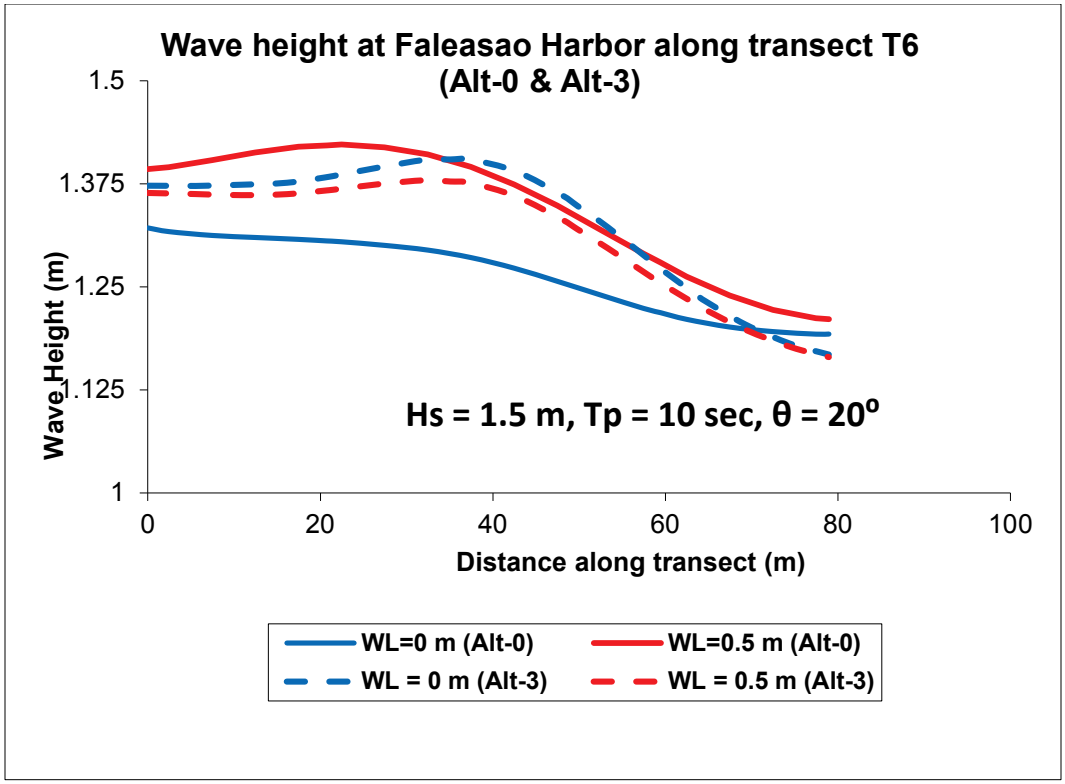

Figure 4-121. Comparison of Alt-0 and Alt-3 wave heights along transect T7 ($\theta = 20^0$).

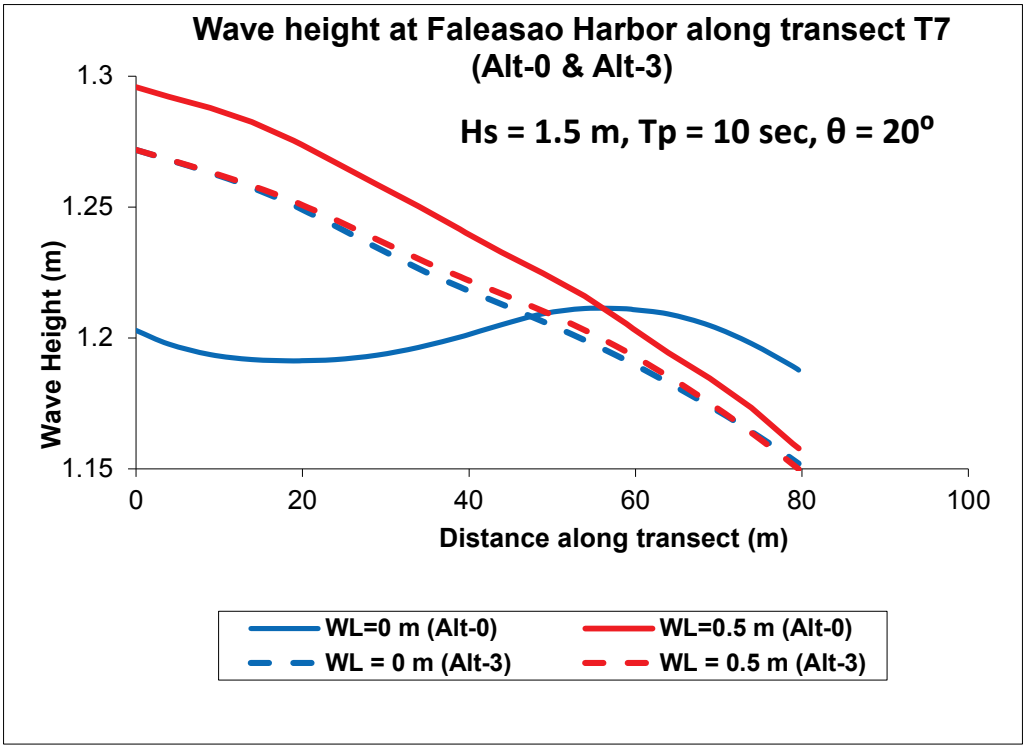

Figure 4-122. Comparison of Alt-0 and Alt-3 wave heights along transect T8 ($\theta = 20^0$).

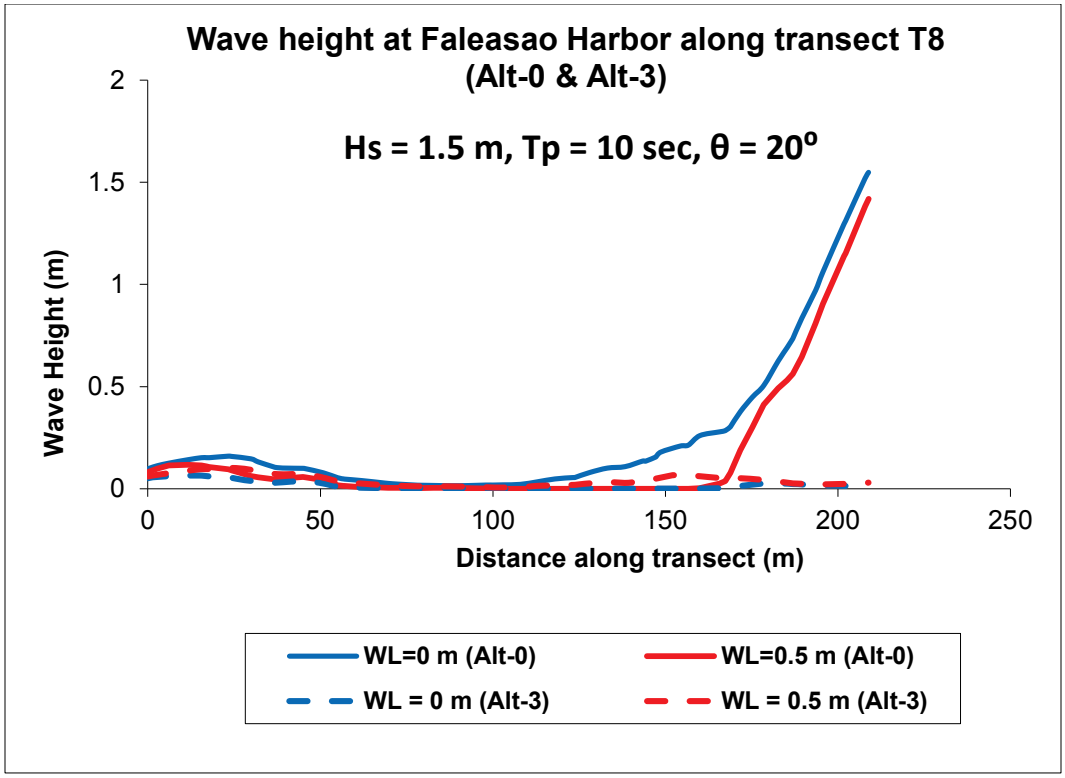

Figure 4-123. Comparison of Alt-0 and Alt-3 wave heights along transect T9 ($\theta = 20^0$).

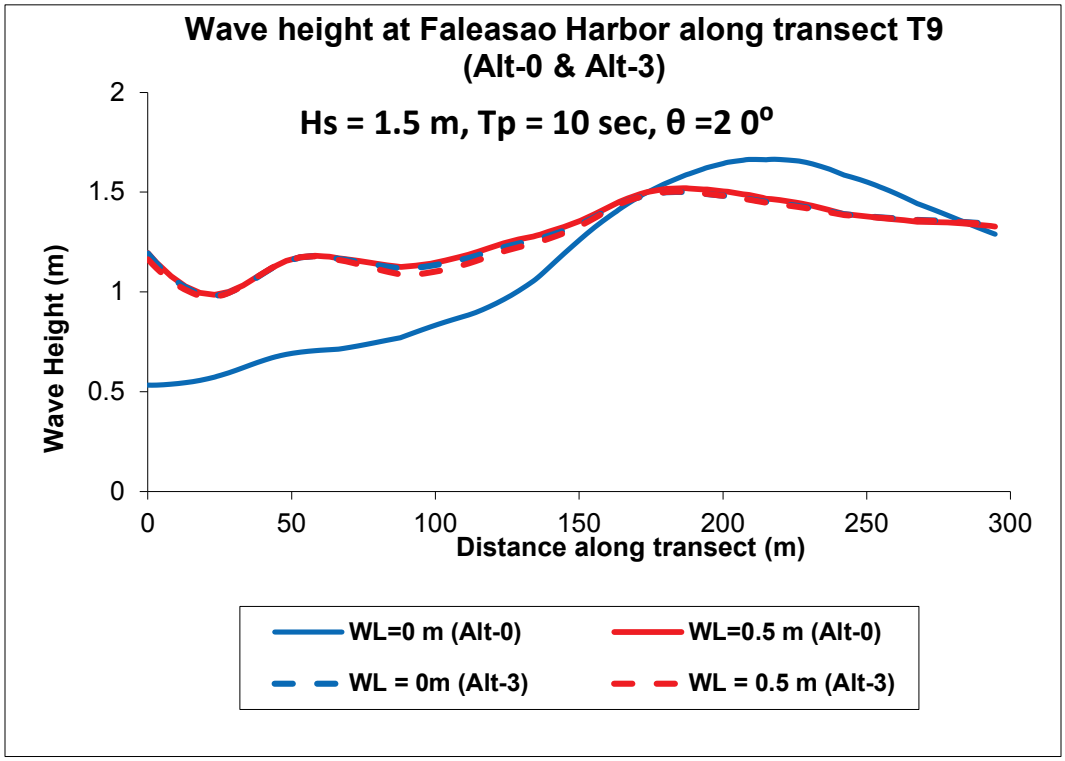

Alt-3 results for a 340° average incident wave (from NNW direction) are compared to the existing harbor (Alt-0) in Figures 4-124 to 4-132 to determine the wave height reduction attainable by Alt-3. As was noted for two previous incident wave directions, even though wave heights may have increased along some sections of some transects, this is not of concern because either wave heights are extremely small (e.g., inconsequential to affect navigation) or some of these areas are not navigable.

Alt-3 results for a 320° average incident wave (from WNW direction) are compared to the existing harbor (Alt-0) in Figures 4-133 to 4-141 to calculate the magnitude of wave height reduction achievable by Alt-3. Similar to the three previous incident wave directions, an increase occurs in the wave height along parts of some transects, which is again not of concern because the wave heights are either very small and would not affect navigation or these areas are unnavigable.

Figure 4-124. Comparison of Alt-0 and Alt-3 wave heights along transect T1 ($\theta = 340^0$).

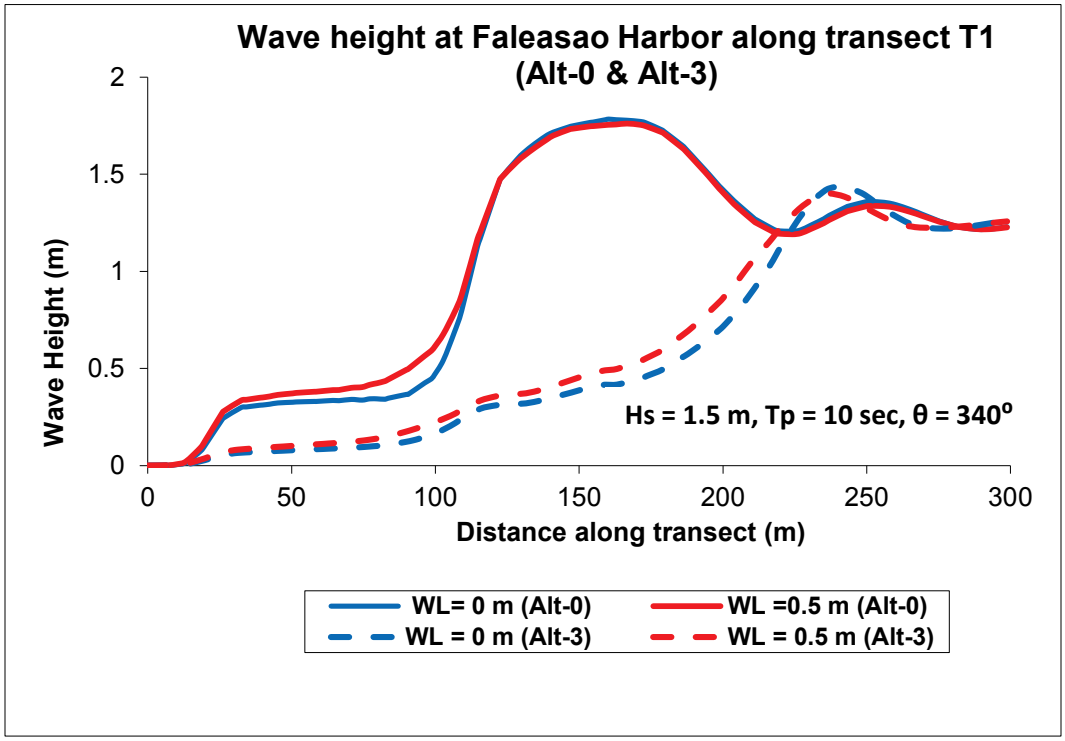

Figure 4-125. Comparison of Alt-0 and Alt-3 wave heights along transect T2 (θ = 340^0).

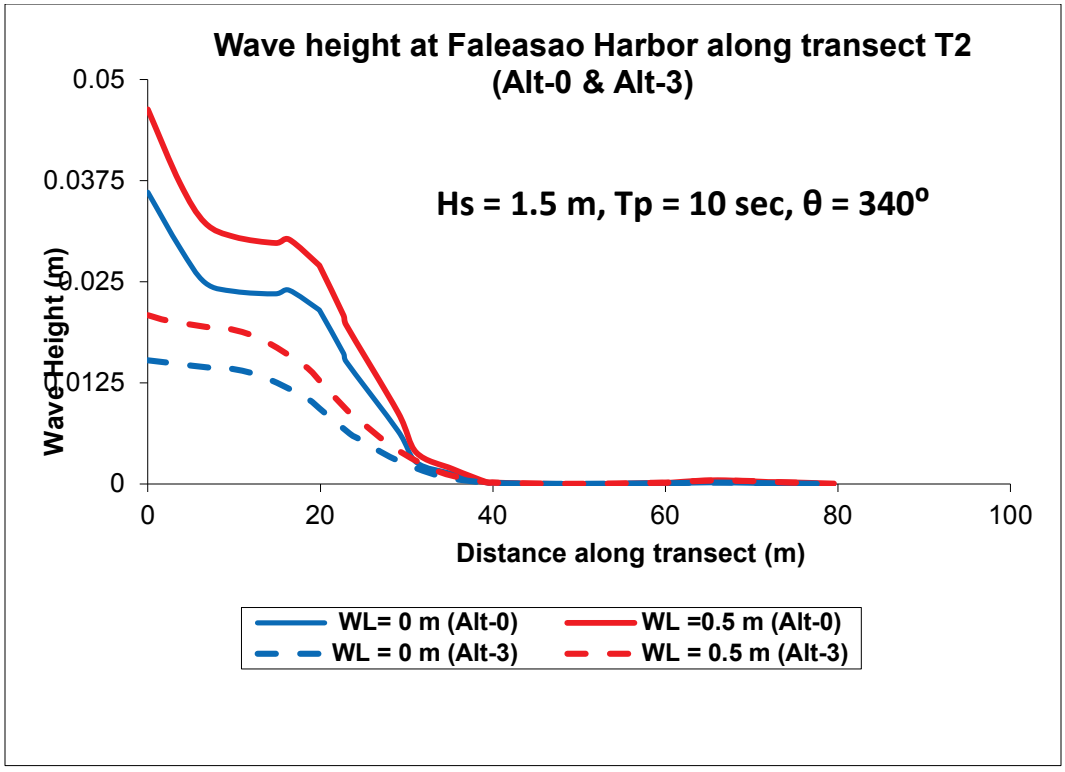

Figure 4-126. Comparison of Alt-0 and Alt-3 wave heights along transect T3 (θ = 340^0).

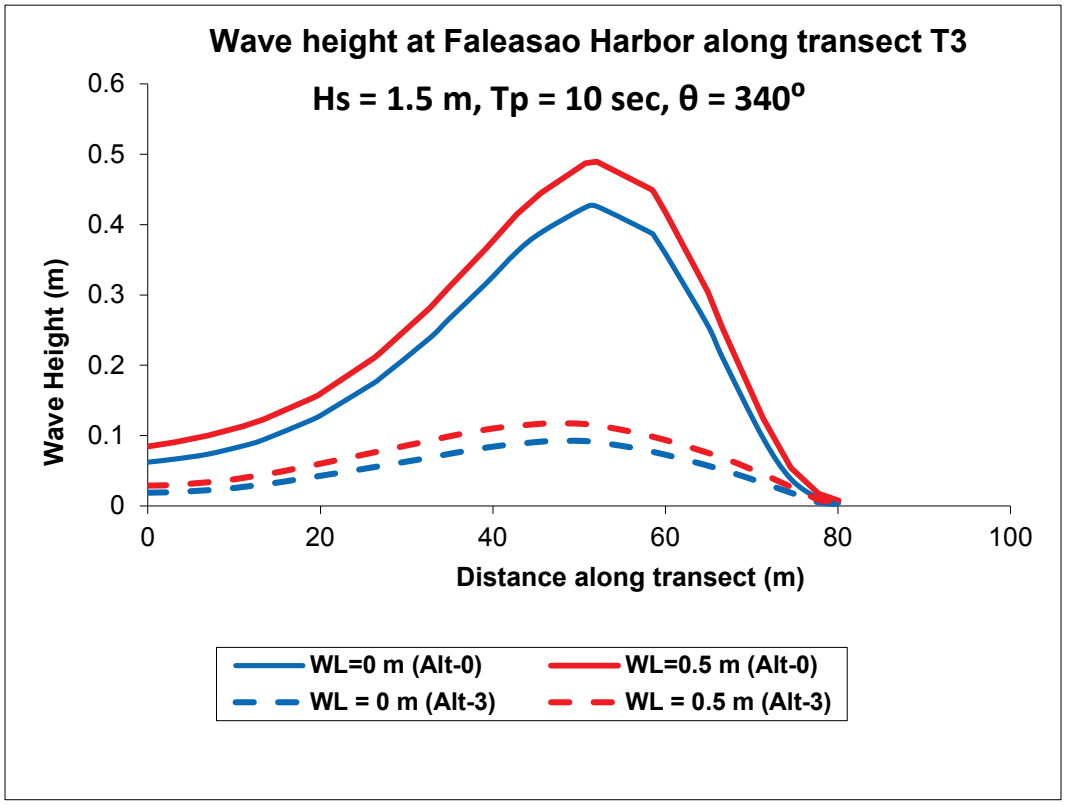

Figure 4-127. Comparison of Alt-0 and Alt-3 wave heights along transect T4 (θ = 340^0).

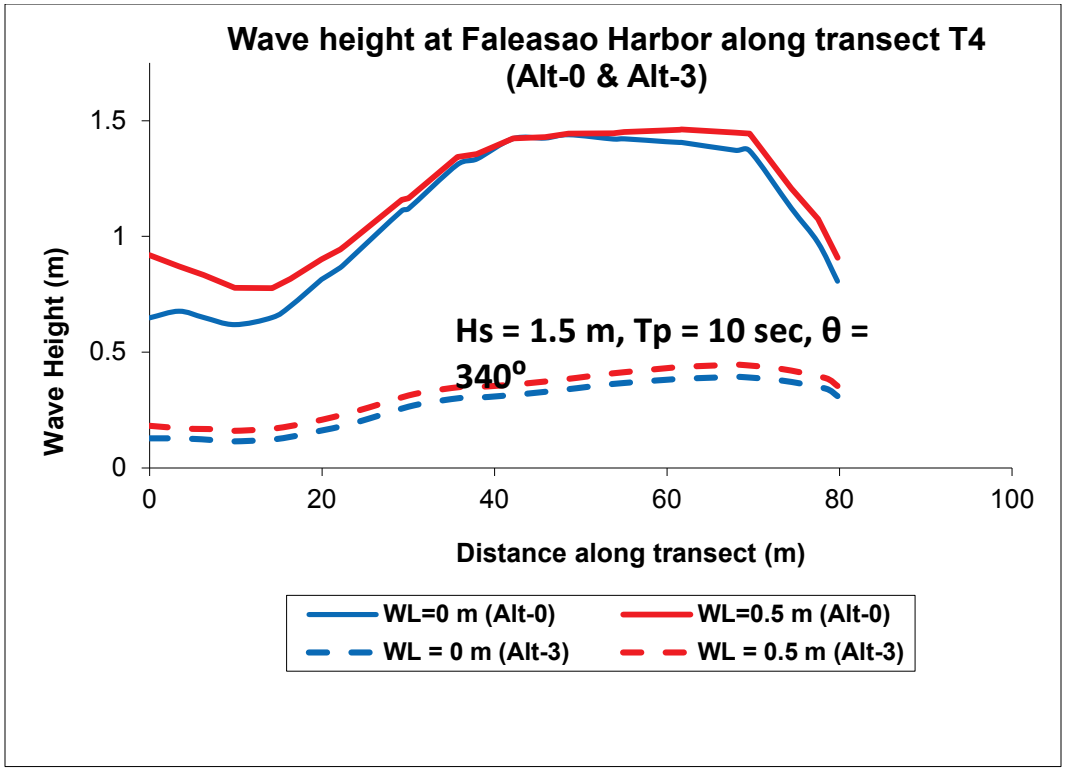

Figure 4-128. Comparison of Alt-0 and Alt-3 wave heights along transect T5 (θ = 340^0).

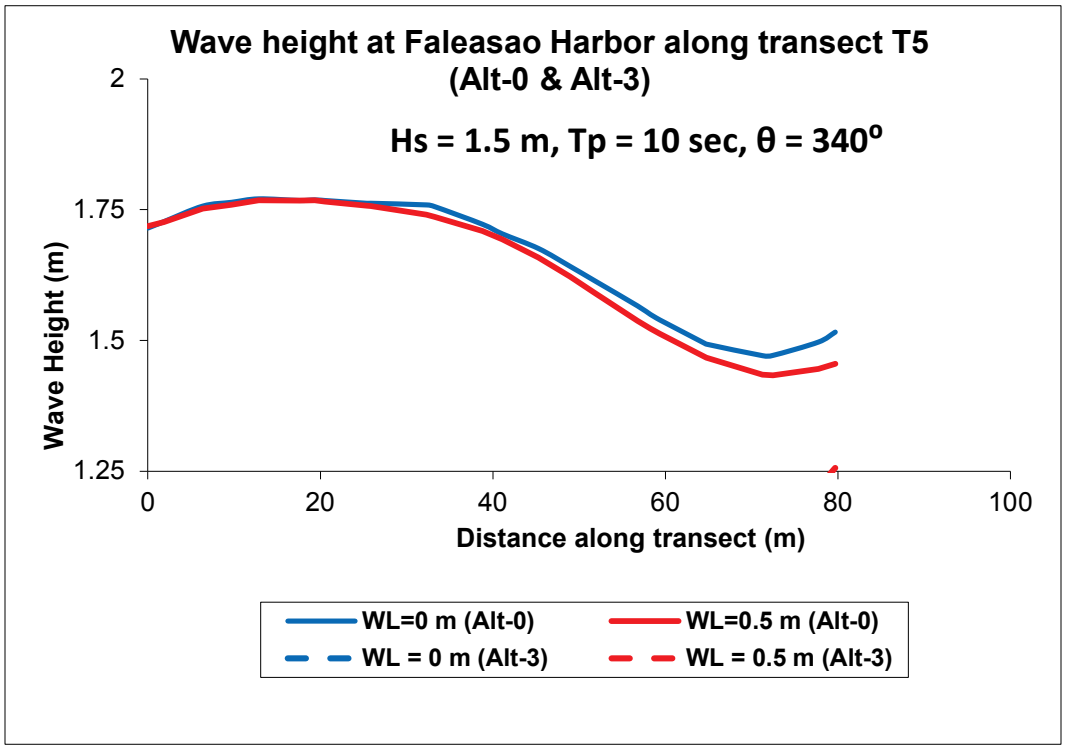

Figure 4-129. Comparison of Alt-0 and Alt-3 wave heights along transect T6 (θ = 340^0).

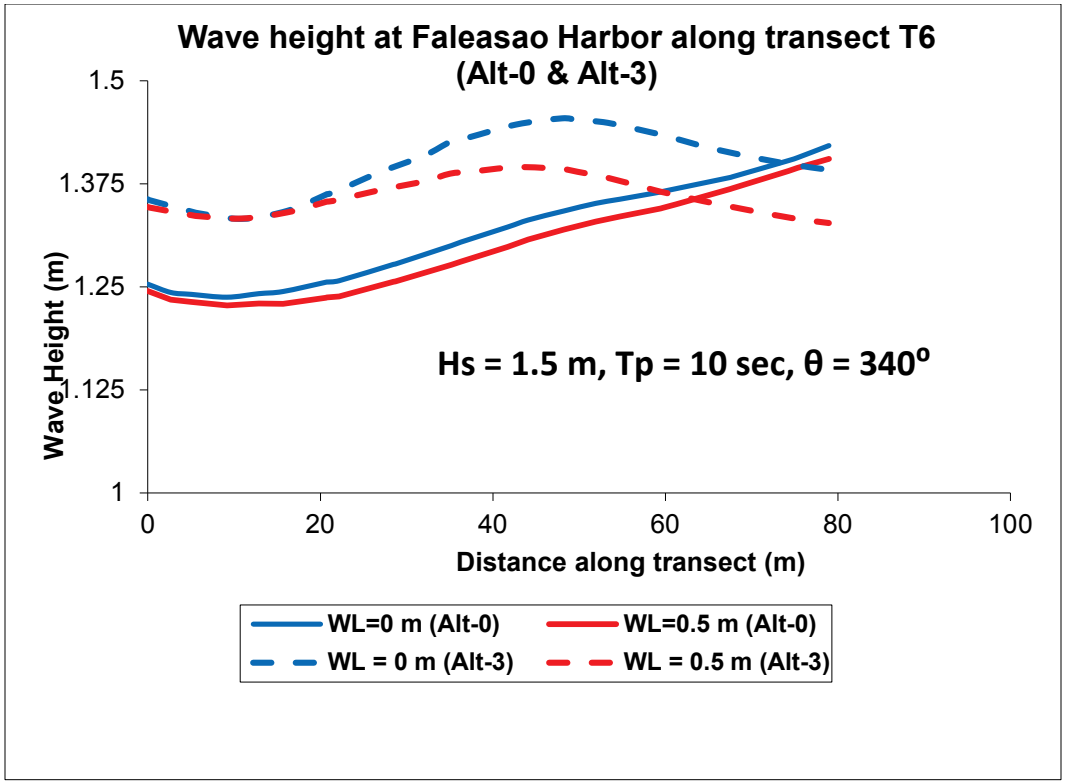

Figure 4-130. Comparison of Alt-0 and Alt-3 wave heights along transect T7 (θ = 340^0).

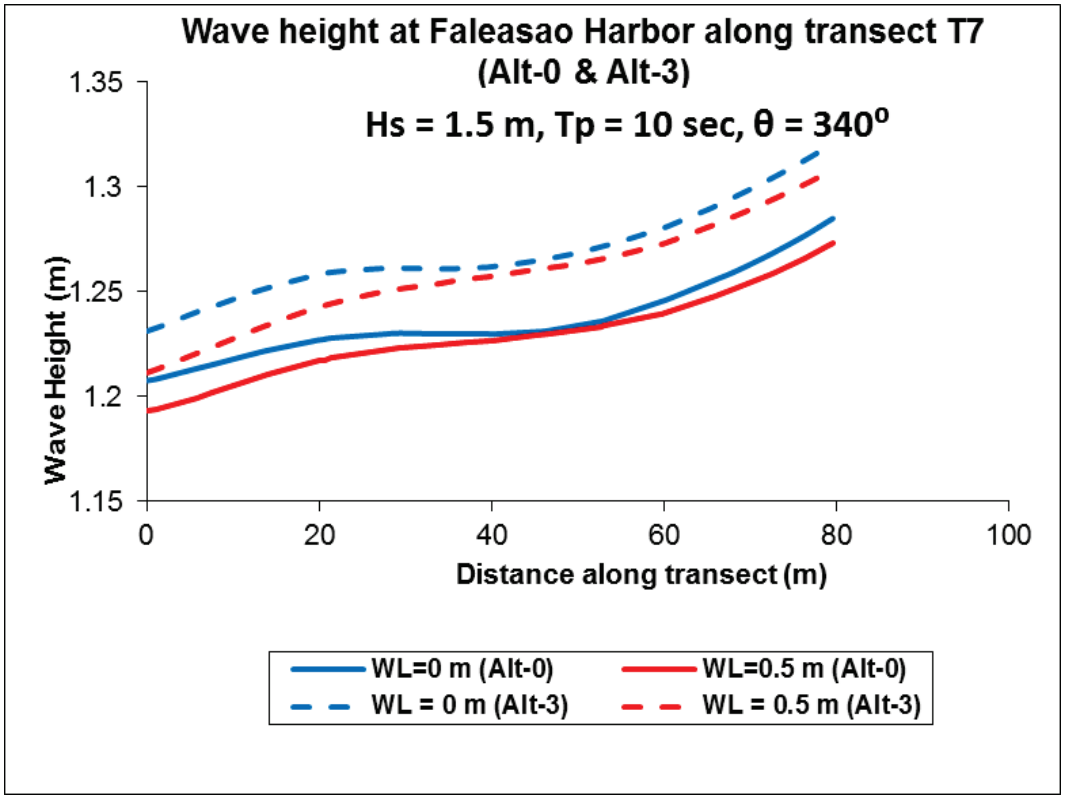

Figure 4-131. Comparison of Alt-0 and Alt-3 wave heights along transect T8 (θ = 340^0).

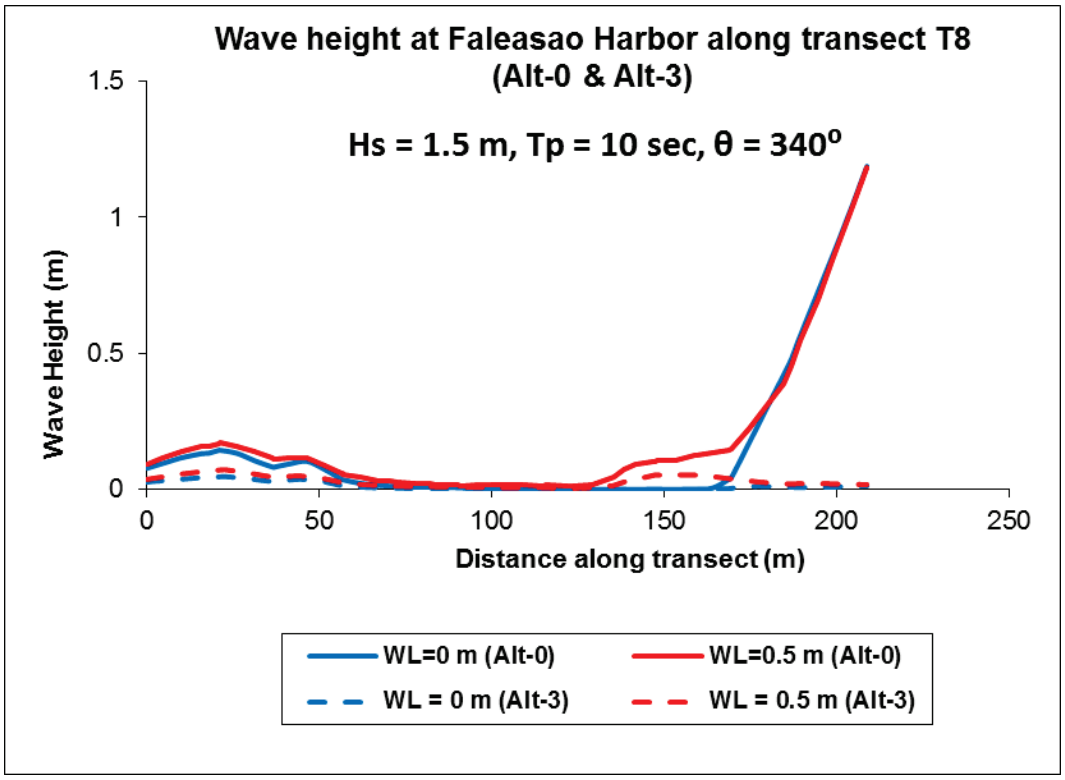

Figure 4-132. Comparison of Alt-0 and Alt-3 wave heights along transect T9 (θ = 340^0).

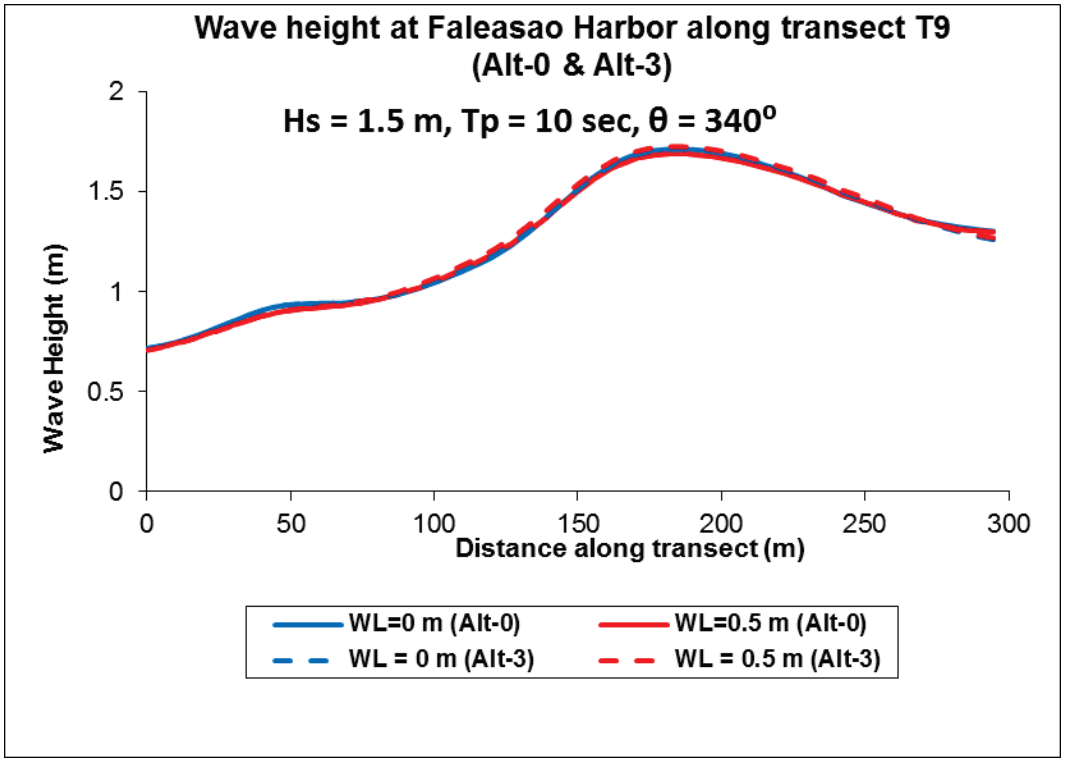

Figure 4-133. Comparison of Alt-0 and Alt-3 wave heights along transect T1 (θ = 320°).

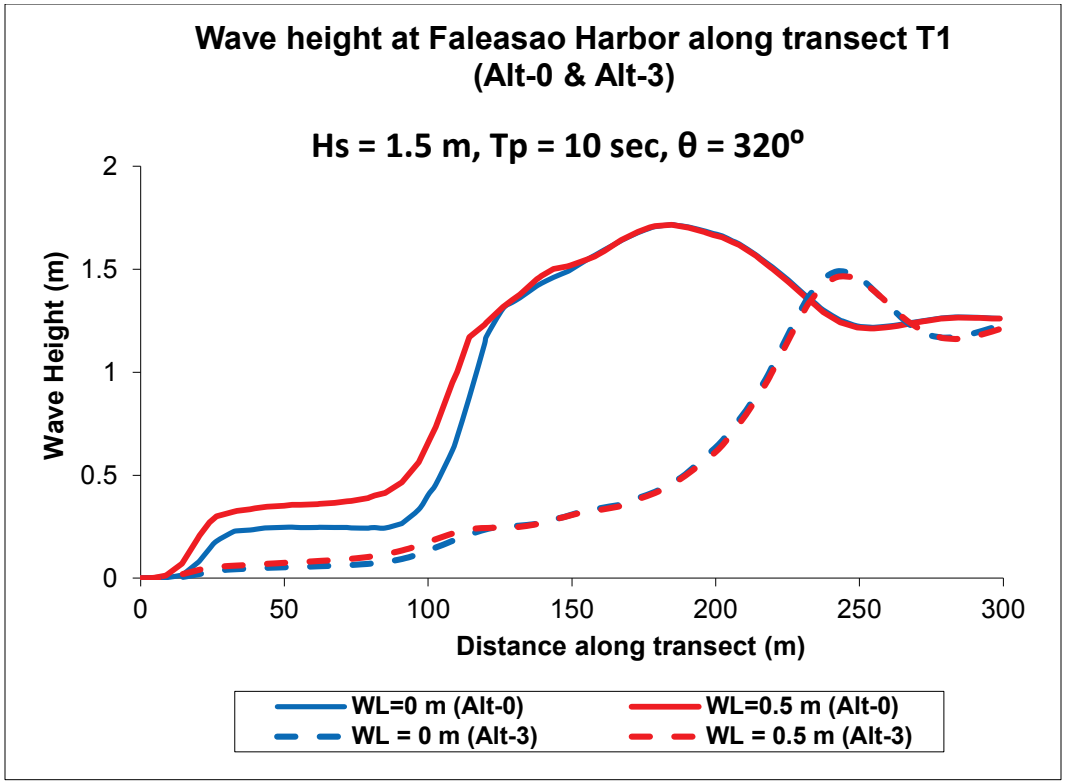

Figure 4-134. Comparison of Alt-0 and Alt-3 wave heights along transect T2 (θ = 320°).

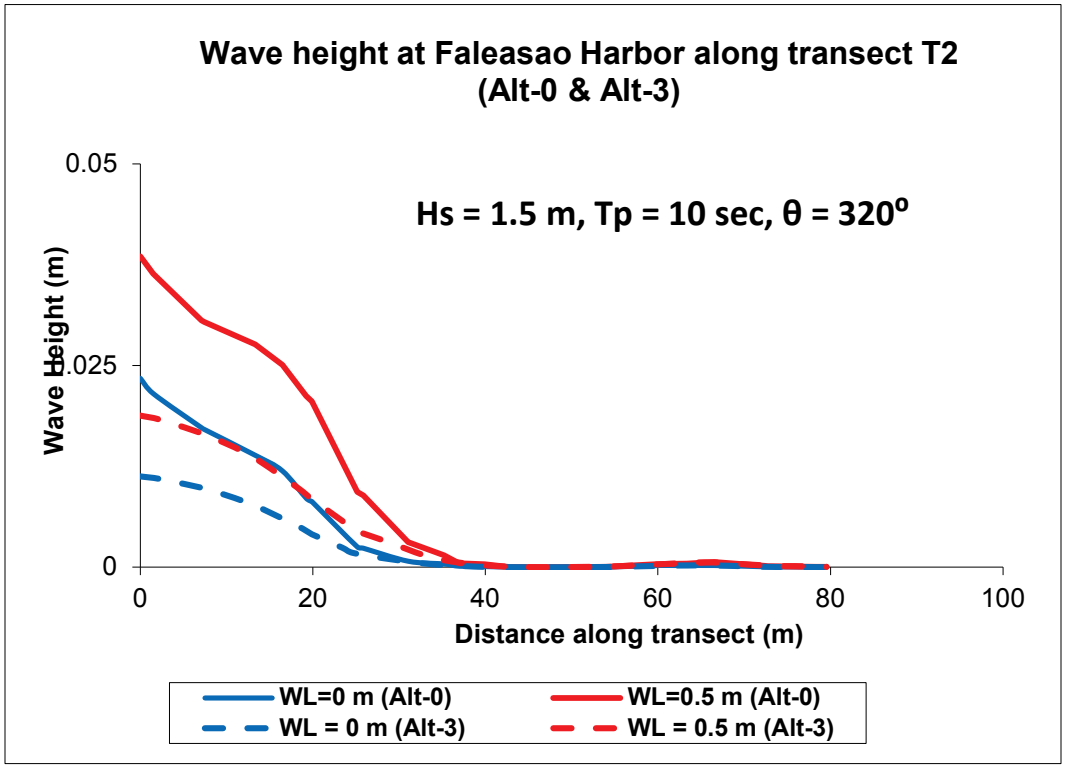

Figure 4-135. Comparison of Alt-0 and Alt-3 wave heights along transect T3 (θ = 320°).

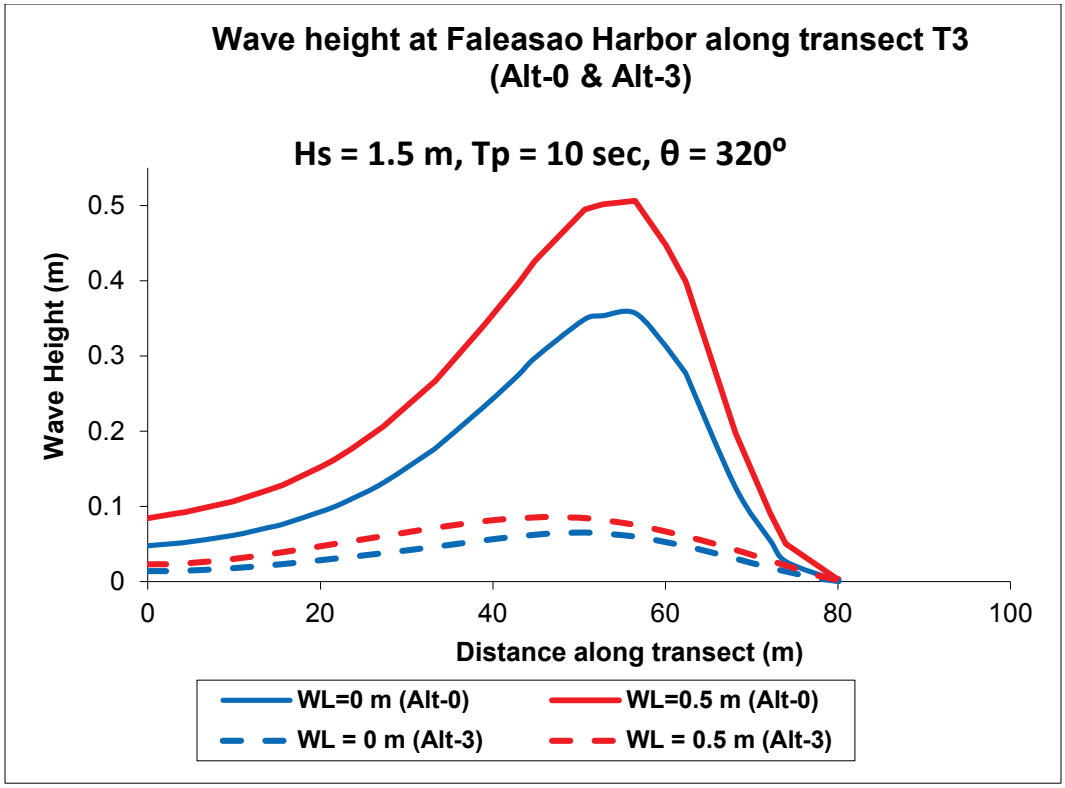

Figure 4-136. Comparison of Alt-0 and Alt-3 wave heights along transect T4 (θ = 320°).

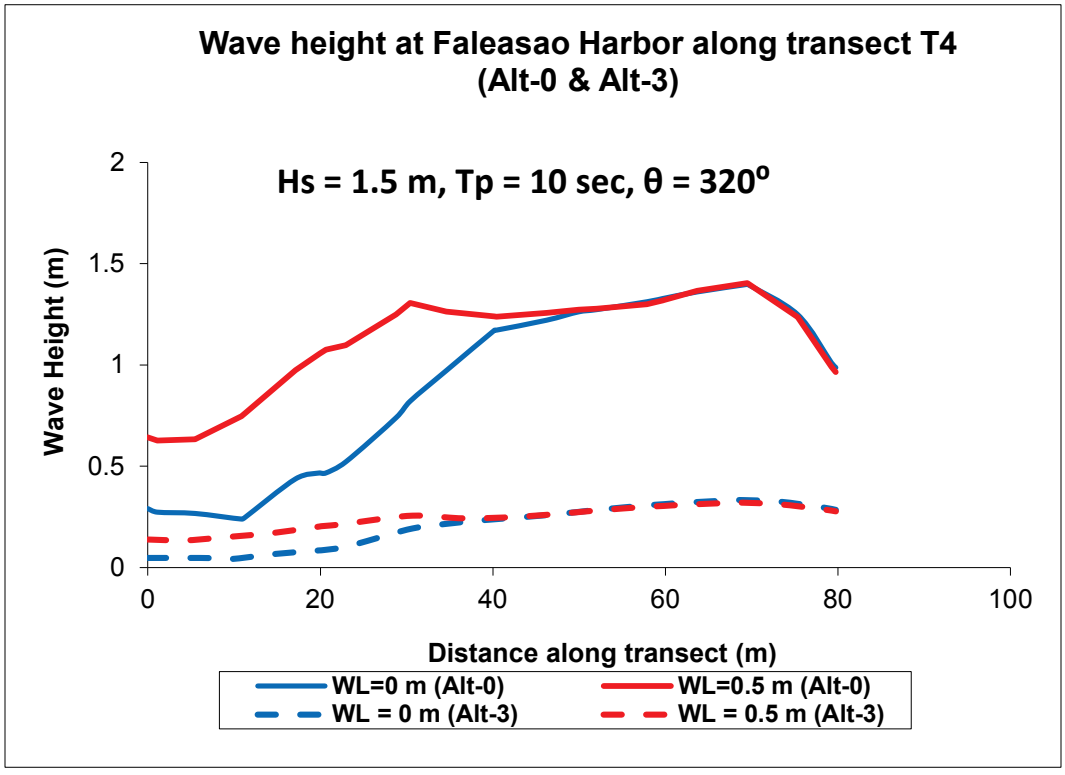

Figure 4-137. Comparison of Alt-0 and Alt-3 wave heights along transect T5 (θ = 320^0).

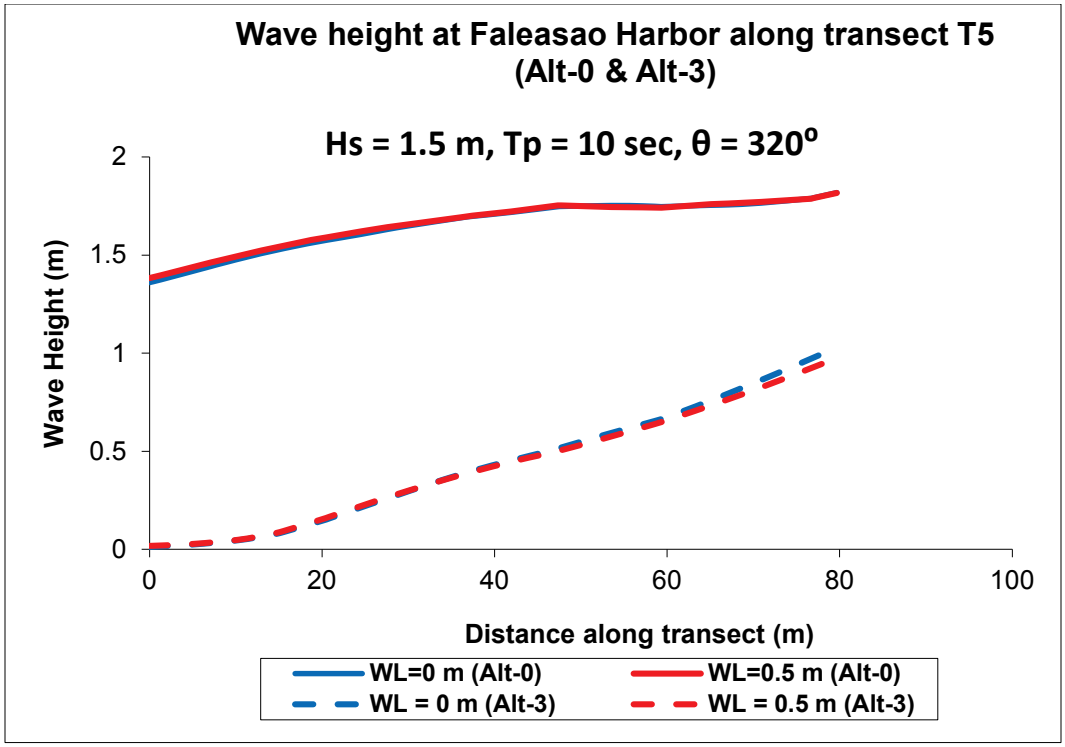

Figure 4-138. Comparison of Alt-0 and Alt-3 wave heights along transect T6 (θ = 320^0).

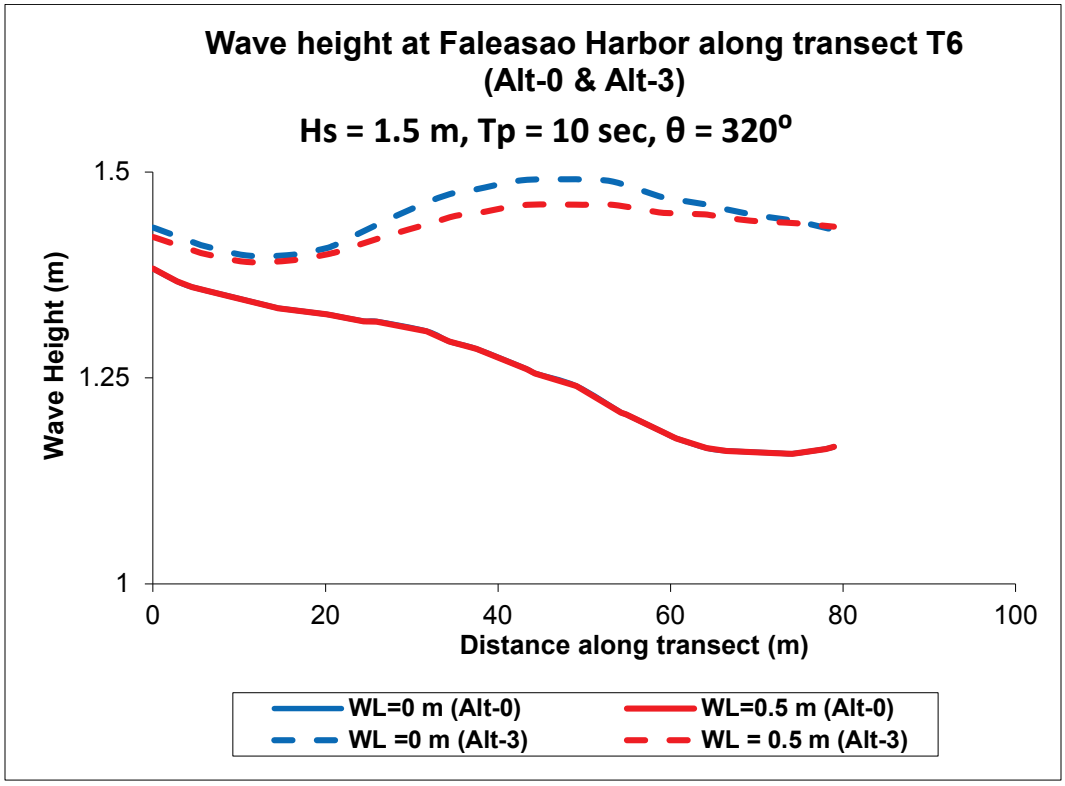

Figure 4-139. Comparison of Alt-0 and Alt-3 wave heights along transect T7 (θ = 320°).

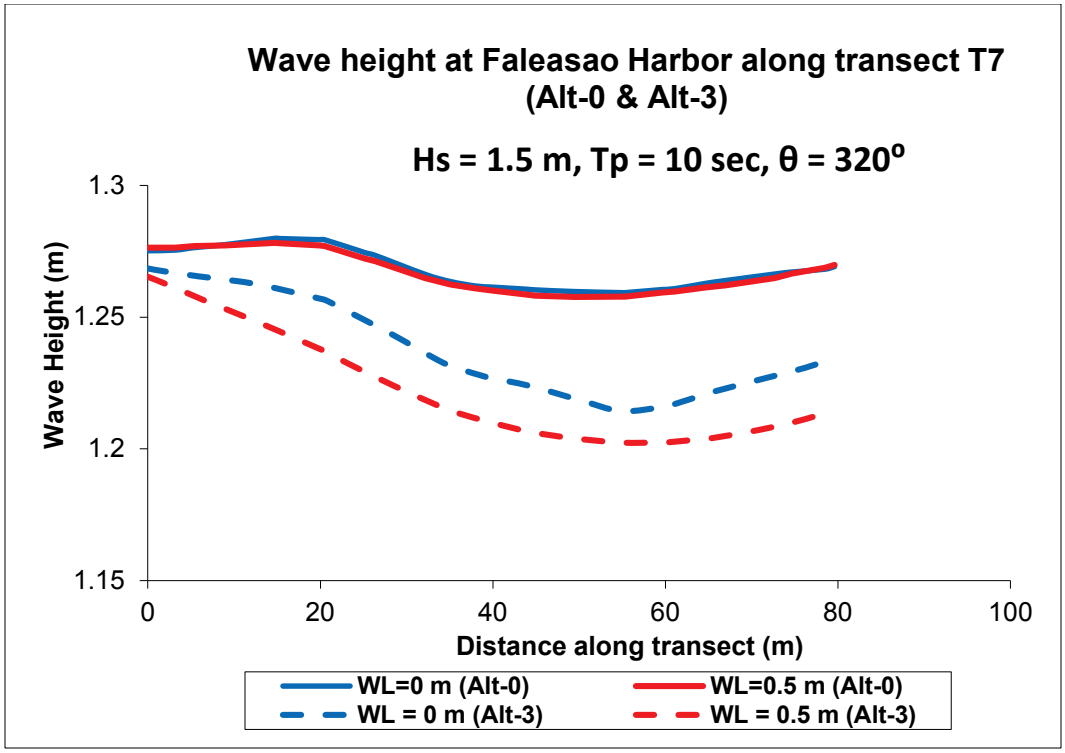

Figure 4-140. Comparison of Alt-0 and Alt-3 wave heights along transect T8 (θ = 320°).

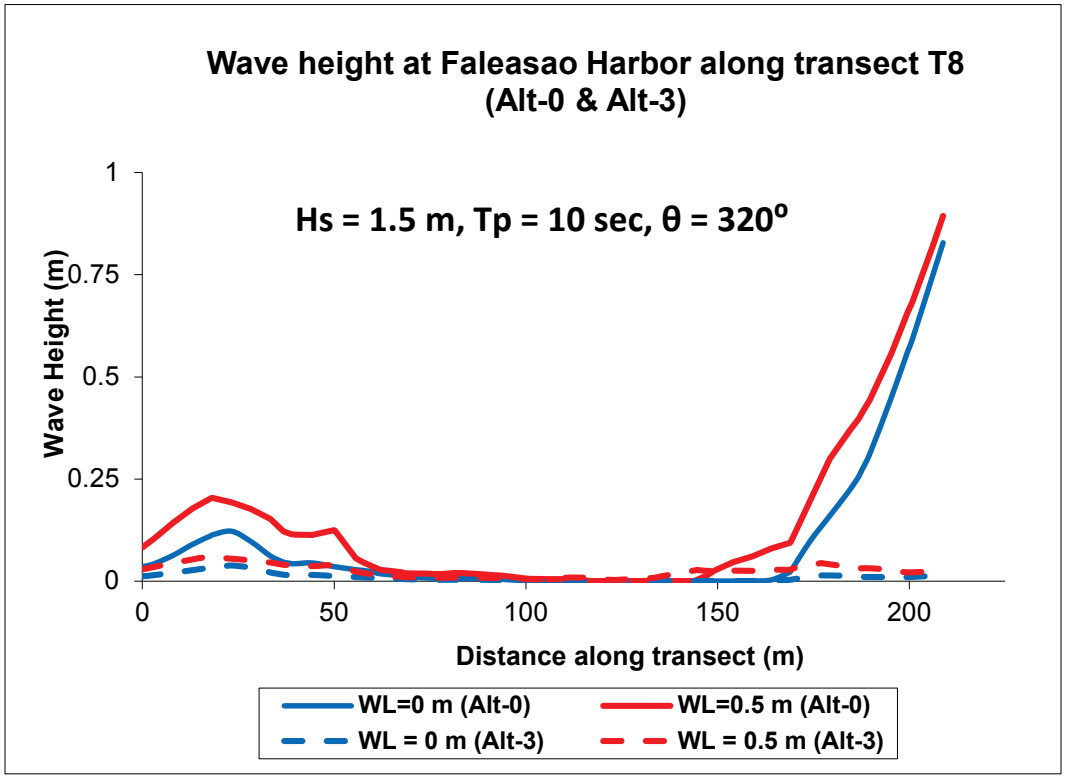

Figure 4-141. Comparison of Alt-0 and Alt-3 wave heights along transect T9 (θ = 320°).

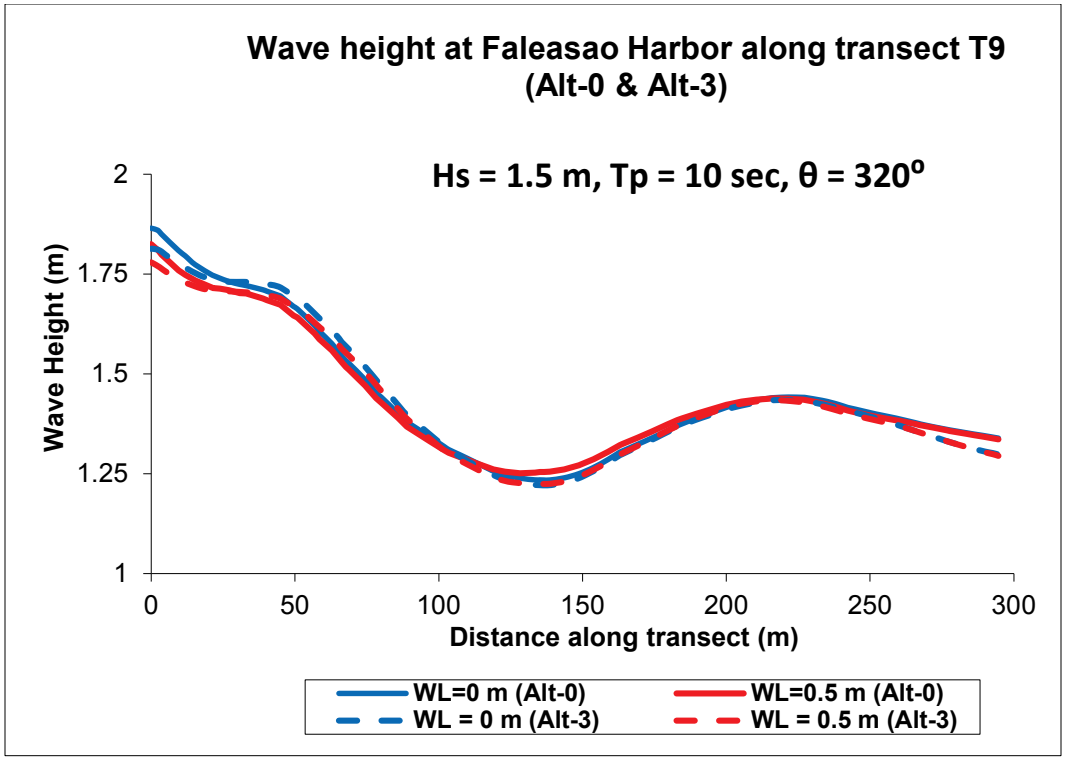

4.7 Comparison of Alternatives

The B2D model provides estimates of wave height, period, direction, wave-induced current, and time series data. One or more of these outputs, or other engineering parameters derived by postprocessing model results, could be used in evaluation of improvements to harbor utilization and for checking navigation safety. Engineering parameters selected from the B2D model, when checked against operational criteria, will determine pros and cons of a proposed Alternative. For consistency with the original design project, the wave height was selected in the present study as the primary parameter to use in comparing the Alternatives. The reduction of wave energy was the ultimate goal for improving conditions in the existing harbor, which was used as the baseline in evaluation of the three Alternatives investigated.

A total of 32 simulations was performed (4 Alternatives, 4 directions, 2 water levels). In Figures 4-8 through 4-15, examples of model results for Alt-0 are presented as 2D color contours of wave height that show the spatially varying wave fields with low and high wave energy areas. B2D model results are provided in groups for each of four incident wave directions. The grouped presentation is used for Alt-0, Alt-1, Alt-2, and

Alt-3 to see clearly the performance of each Alternative with respect to the existing harbor. In Figures 4-15 through 4-141, the four groups provide wave heights along nine transects for waves from north (N = 0°), north-northeast (NNE = 20°), north-northwest (NNW = 340°), and west-northwest (WNW = 320°) at two water levels (MLLW = 0 m and MHHW = 0.5 m).

The calculated wave heights along the transect T1 through the channel centerline and extending into the turning/mooring basin and dock area are used to compare and rank the Alternatives. For each incident wave direction at two water levels, Tables 4-3 through 4-6 provide statistics of the simulated wave height (maximum and average) from B2D simulations along T1. These wave statistics are compared for Alt-0, Alt-1, Alt-2, and Alt-3. The Alternative with the best wave height reduction is marked by an asterisk (*) in each table. Overall, Alt-3 has the largest wave height reduction along T1 for all four incident wave directions.

It is emphasized that Alternatives have been ranked based on calculated average wave-height statistics along transect T1, a transect that covers the navigation channel and mooring basin areas, for incident-wave directions from the north-northeast, north, north-northwest, and west-northwest. Based on this method, Alt-3 is the top ranking Alternative with the smallest average wave height along T1. Furthermore, B2D simulations showed that incident waves coming from the northern direction penetrated farthest into the interior of the harbor, even impacting the inner harbor areas. However, results show that Alt-2 also offers a very good reduction of wave energy inside the harbor. Consequently, Alt-2 has the potential to be considered as a long-term solution for improving conditions inside the existing harbor. The costs associated with design, construction, and environmental impacts of Alt-3 and Alt-2 are other factors which will have to be considered in the selection of an Alternative for improving future navigation conditions to increase the utilization of Faleasao Harbor.

Table 4-3. Wave-height statistics along T1 for incident waves from N ($\theta = 0^0$).

Alternatives	Max Hs (m)		Ave Hs (m)	
	MLLW (0 m, MSL)	MHHW (0.5 m, MSL)	MLLW (0 m, MSL)	MHHW (0.5 m, MSL)
Alt-0	1.82	1.77	1.00	1.05
Alt-1	1.60	1.55	0.95	0.97
Alt-2	1.47	1.44	0.66	0.67
Alt-3	1.43	1.40	0.53	0.53 *

Table 4-4. Wave-height statistics along T1 for incident waves from NNE ($\theta = 20^0$).

Alternatives	Max Hs (m)		Ave Hs (m)	
	MLLW (0 m, MSL)	MHHW (0.5 m, MSL)	MLLW (0 m, MSL)	MHHW (0.5 m, MSL)
Alt-0	1.28	1.39	0.88	0.88
Alt-1	1.39	1.28	0.81	0.80
Alt-2	1.41	1.38	0.65	0.71
Alt-3	1.39	1.38	0.53	0.54 *

Table 4-5. Wave-height statistics along T1 for incident waves from NNW ($\theta = 340^0$).

Alternatives	Max Hs (m)		Ave Hs (m)	
	MLLW (0 m, MSL)	MHHW (0.5 m, MSL)	MLLW (0 m, MSL)	MHHW (0.5 m, MSL)
Alt-0	1.78	1.76	1.00	1.01
Alt-1	1.65	1.64	0.93	0.95
Alt-2	1.44	1.40	0.62	0.66
Alt-3	1.39	1.36	0.46	0.47 *

Table 4-6. Wave-height statistics along T1 for incident waves from WNW ($\theta = 320^0$).

Alternatives	Max Hs (m)		Ave Hs (m)	
	MLLW (0 m, MSL)	MHHW (0.5 m, MSL)	MLLW (0 m, MSL)	MHHW (0.5 m, MSL)
Alt-0	1.72	1.72	1.10	1.14
Alt-1	1.74	1.71	0.91	0.94
Alt-2	1.49	1.46	0.57	0.58
Alt-3	1.41	1.39	0.44	0.45 *

5 Harbor Access and Usability Analysis

The USACE guidance in EM 1110-2-1100 Part V specifies that for small boat harbors, the maximum allowable wave height in the entrance channel and at the dock is 2 ft and 1 ft, respectively. The terms *accessibility* and *usability* are used in this study interchangeably for simplicity, although strictly speaking these two terms have a different meaning in harbor engineering. With this in mind, an estimate of harbor usability is provided for each Alternative based on two assumed operational thresholds for safe navigation. Calculation of these estimates requires knowledge of the long-term offshore wave conditions. The recent 32-year (1980–2011) update of the WIS hindcast data at Sta 81137 was used to develop these estimates. Deep-water conditions at Sta 81137 were transformed to the project site using CMS-Wave. The wave rose plot for Sta 81137 in Figure 2-4 (Chapter 2) provides the percent occurrence for significant wave height (H_s) for different wave directions clustered into 22.5° directional bins.

An example of the percent occurrence of deep-water waves for the 0° bin is provided in Table 5-1. The spectral model CMS-Wave was used to transform individual wave height, peak period, and direction (H_s, T_p, and D_p) combination from the offshore WIS station to the nearshore area. This was done to determine if the H_s values in the entrance channel and at the dock meet or exceed the above-mentioned 2 ft and 1 ft thresholds. Next, the exceedance probabilities of waves arriving in the channel and at the dock were calculated to develop a probabilistic usability index by summing up the occurrence probabilities of individual waves (H_s, T_p, and D_p combination) at these locations. These estimates were used to calculate the percentage of time the harbor was accessible. Details of the selection of deep-water wave conditions, transformation of these with CMS-Wave, and the calculation procedure used are described in this Chapter. Using this approach, the calculated percent occurrences of the significant wave height and peak period for D_p = 0° (true north) are listed in Table 5-1.

Table 5-1. Percent occurrence (x1000) of Hs and Tp for Dp = 0° (true north).

Hs (m)	Peak period, Tp (sec)										Total
	<5.0	5.0-5.9	6.0-6.9	7.0-7.9	8.0-8.9	9.0-9.9	10.0-11.9	12.0-13.9	14.0-25.9	16+	
0.00-0.49	.	.	.	.	3	12	37	146	93	25	0
0.50-0.99	.	8	25	18	119	262	462	796	1322	904	0
1.00-1.49	.	.	31	39	39	56	167	92	193	454	789
1.50-1.99	.	.	1	24	22	5	15	1	21	55	5829
2.00-2.49	.	.	.	5	14	7	2	1	.	4	7079
2.50-2.99	.	.	.	.	5	3	.	1	.	1	3751
3.00-3.49	.	.	.	.	3	1	.	.	.	.	1617
3.50-3.99	.	.	.	.	.	.	.	.	.	.	565
4.00-4.49	.	.	.	.	.	.	1	.	.	.	206
4.50-4.99	.	.	.	.	.	.	2	.	.	.	55
5.0+	.	.	.	.	.	.	.	.	.	.	6
TOTAL	0	8	57	86	205	346	686	1037	1629	1443	19897

5.1 Selection of deep-water wave conditions

If all values of H_s and T_p in each 22.5° directional bin were considered (e.g., 11 wave heights, 10 wave periods, and 16 directions), a total of 1,760 CMS-Wave simulations would be required for each Alternative. This equates to 5,280 simulations for four Alternatives, which are too many to consider. To reduce the number of simulations, the deep-water wave conditions were analyzed by excluding wave conditions which had little or no impact on Faleasao Harbor. Also, small wave heights not affecting access to the harbor and waves of statistically insignificant probability of occurrence were excluded from the calculated percent occurrences. It is noted that the location and geometry of the existing Faleasao Harbor on northwest corner of Tau Island provides a natural sheltering to incident waves from 112.5° to 247.5° sector. This includes approximately 40% of all waves at the WIS Sta 81137. Consequently, waves from this sector were also excluded from the present analysis. Last, waves approaching from 270° and 292.5° direction bins were also excluded because the probabilities of occurrence of these waves were 0.1% and 0.2%, respectively.

This elimination process resulted in seven incident H_s values (1.0 m, 1.5 m, 2.0 m, 2.5 m, 3.0 m, and 3.5 m) approaching from seven wave directions (315°, 337.5°, 0°, 22.5°, 45°, 67.5°, and 90°). This reduced set of offshore input conditions was used in CMS-Wave simulations to check two exceedance thresholds in the entrance channel and at the dock. Further

analysis of the WIS hindcast data indicated that the most common wave period for incident waves was 10 sec. This represents the average wave period of the 32-year hindcast data at Sta 81137, which was also used in the B2D modeling. The 10 sec period is also a conservative estimate of a wave period appropriate for harbor usability.

Two additional observations were noted, and associated actions were utilized in the present analysis. The first was that offshore wave periods greater than 10 sec generally had higher offshore wave heights for selected directions. These were expected to result in higher wave heights in the entrance channel and therefore were not considered because these conditions would make the entrance channel and harbor inaccessible. Second, H_s values greater than 3.5 m were not considered because the probability of occurrence of these incident wave heights for the directional bins 315° to 90° was negligible (~0.2%). These observations were further confirmed by the pilots using Faleasao Harbor. These users indicated that the existing harbor was inaccessible and unusable when offshore wave heights were greater than 3.5 m. Note that this and other wave conditions which were not considered in the present analysis were tied closely to the harbor operability limits and verified by mariners who are familiar with the harbor. This careful filtering of the offshore incident wave climate greatly reduced the number of wave conditions from 1,760 to 42. The final simulations for calculating the overall harbor usability estimates for each Alternative were made with seven significant wave heights, one wave period, and six directions. This filtering method resulted in a total of 168 CMS-Wave simulations performed for the four Alternatives (Alt-0, Alt-1, Alt-2, and Alt-3). These simulations are described next.

5.2 CMS-Wave simulations and results

Figure 5-1 shows the bathymetry used in CMS-Wave. Figure 5-2 shows the CMS-Wave calculated wave height fields for Alt-0, Alt-1, Alt-2, and Alt-3 for the most typical average wave conditions (Hs = 1.5 m and Tp = 10 sec) for 0° wave direction . The wave fields show small differences for Alt-0 and Alt-1. In Alt-2 and Alt-3, there is significantly more energy focusing along the toe of the breakwater (dark red) and less wave energy in the entrance channel and turning basin. This is shown in these figures by the lighter green and blue colors landward of the breakwater alignment in Alt-2 and Alt-3 as compared to Alt-0 and Alt-1.

Figure 5-1. CMS-Wave model bathymetries for (a) Alt-0, (b) Alt-1, (c) Alt-2, and (d) Alt-3.

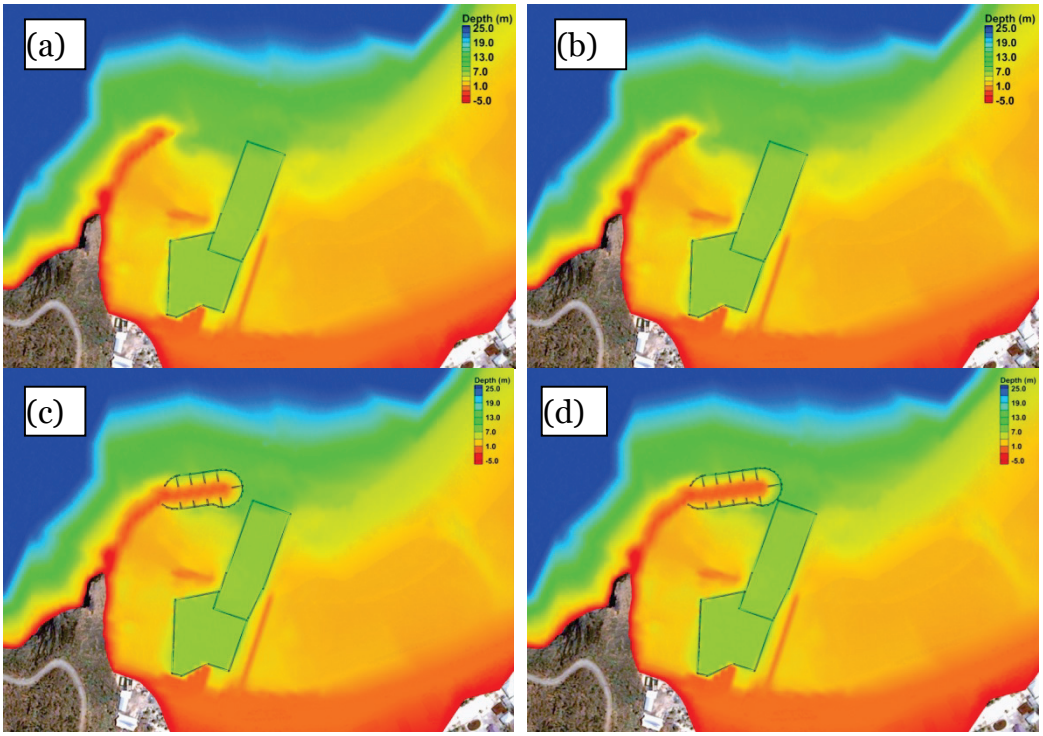

Figure 5-2. Model calculated wave heights for (a) Alt-0, (b) Alt-1, (c) Alt-2, and (d) Alt-3 for an average wave condition (Hs = 1.5 m, Tp = 10 sec, Dp = 0°).

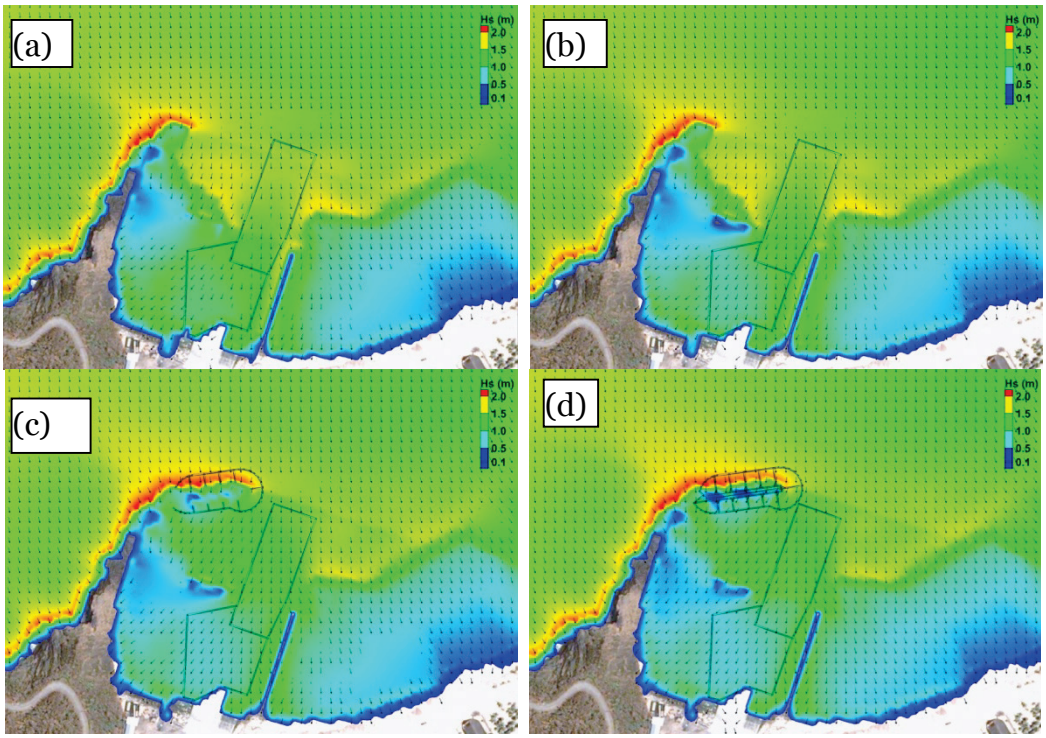

Figures 5-4, 5-6, and 5-7 show the simulated values of H_s along the channel centerline transect (as shown in Figure 5-3) for waves approaching from 315°, 337.5°, 0°, and 22.5° directions for the typical wave conditions of H_s = 1.5 m and T_p = 10 sec. The CMS-Wave results along this transect show a small reduction in wave heights along the channel centerline for Alt-0 and Alt-1 and a greater reduction for Alt-2 and Alt-3. Alt-0 and Alt-1 results show constant wave heights from Sta 0+00 to Sta 1+00, which drop off gradually beyond Sta 1+00. Alt-2 and Alt-3 results show a gradual reduction in wave heights between Sta 0+00 and Sta 3+00 and constant wave heights beyond Sta 3+00. The cross-shore wave height profiles for offshore wave heights of 1.0 m, 2.0 m, 2.5 m, 3.0 m, and 3.5 m are similar for each Alternative and wave direction as shown in Figures 5-4, 5-5, 5-6, and 5-7.

Figure 5-3. Stationing for Hs output transect along the channel centerline.

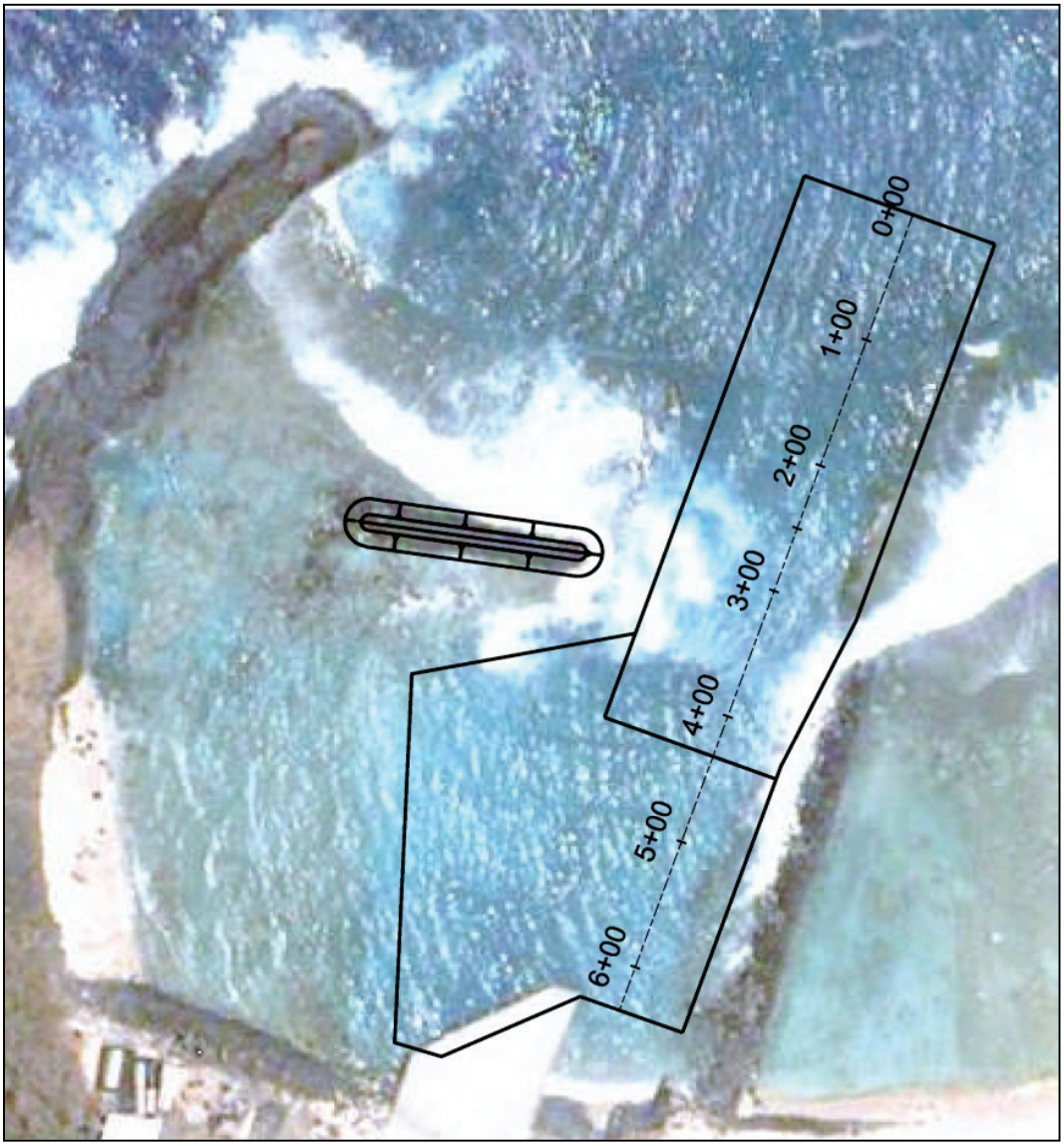

Figure 5-4. Comparison of significant wave heights along the channel centerline for Alt-0, Alt-1, Alt-2, and Alt-3 for waves approaching from 315°.

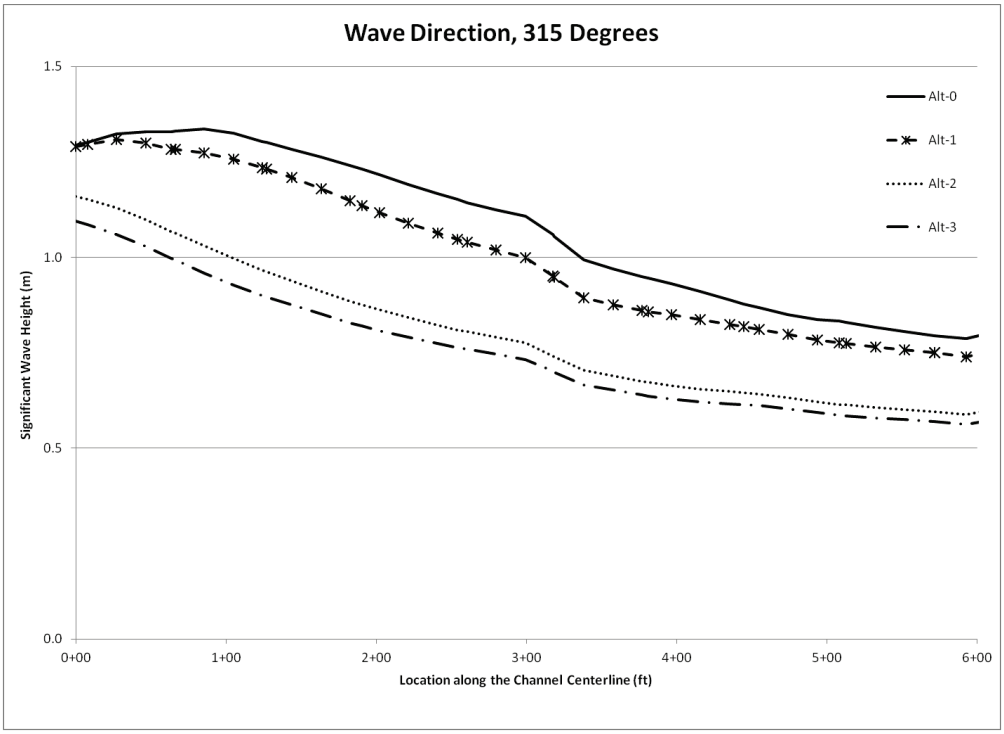

Figure 5-5. Comparison of significant wave heights along the channel centerline for Alt-0, Alt-1, Alt-2, and Alt-3 for waves approaching from 337.5°.

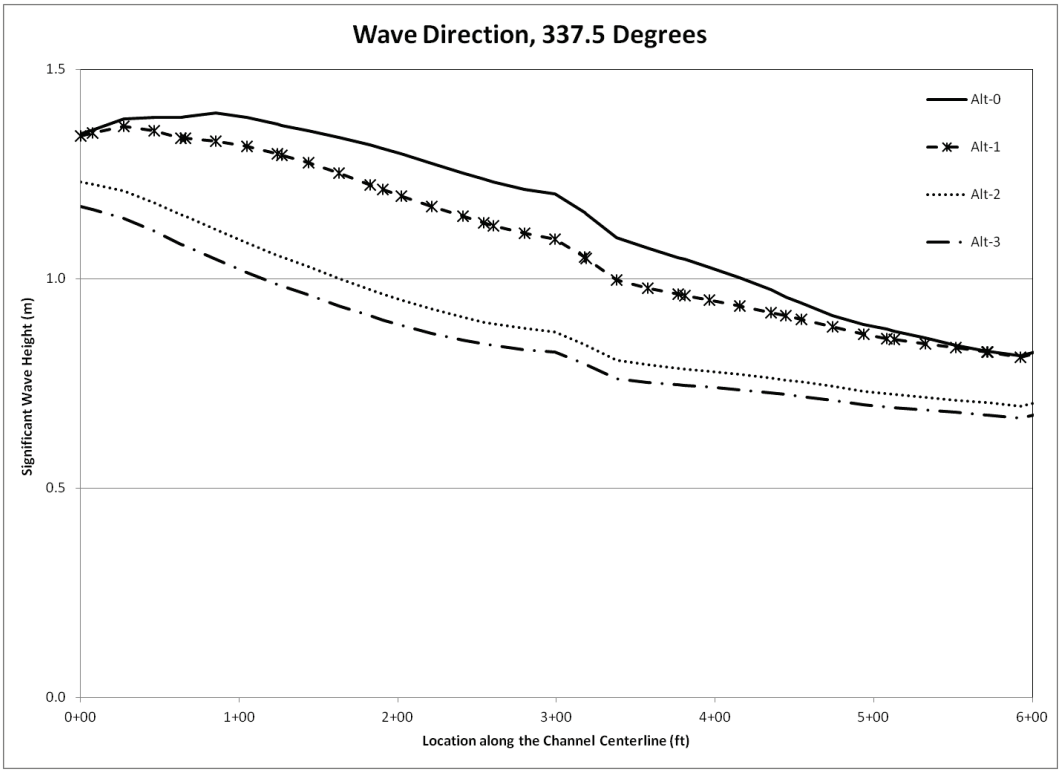

Figure 5-6. Comparison of significant wave heights along the channel centerline for Alt-0, Alt-1, Alt-2, and Alt-3 for waves approaching from 0°.

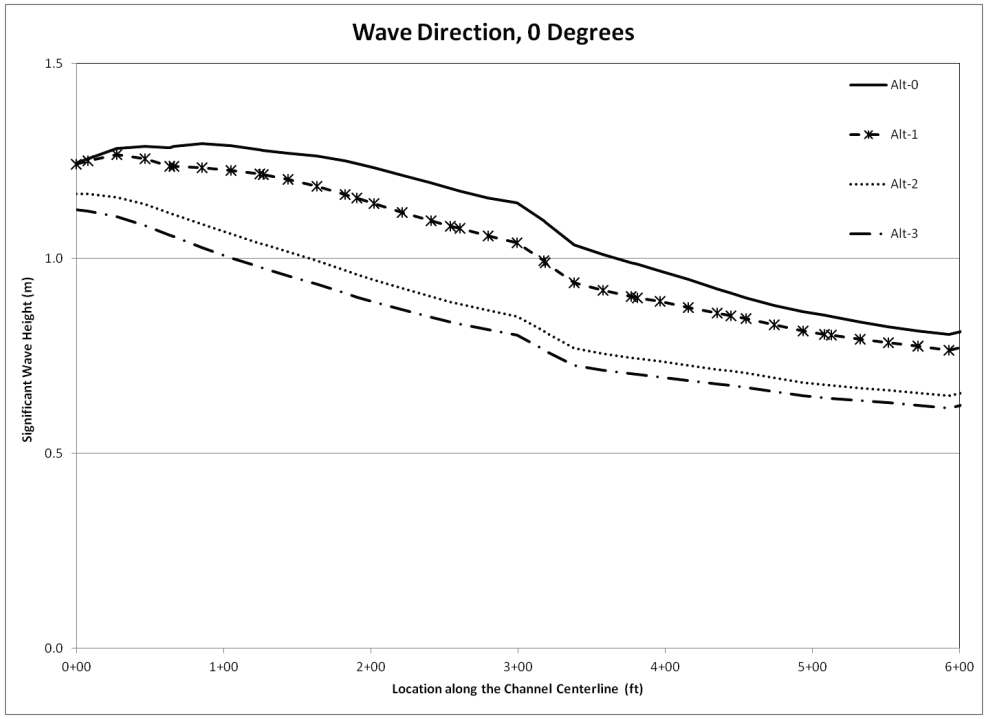

Figure 5-7. Comparison of significant wave heights along the channel centerline for Alt-0, Alt-1, Alt-2, and Alt-3 for waves approaching from 22.5° degrees.

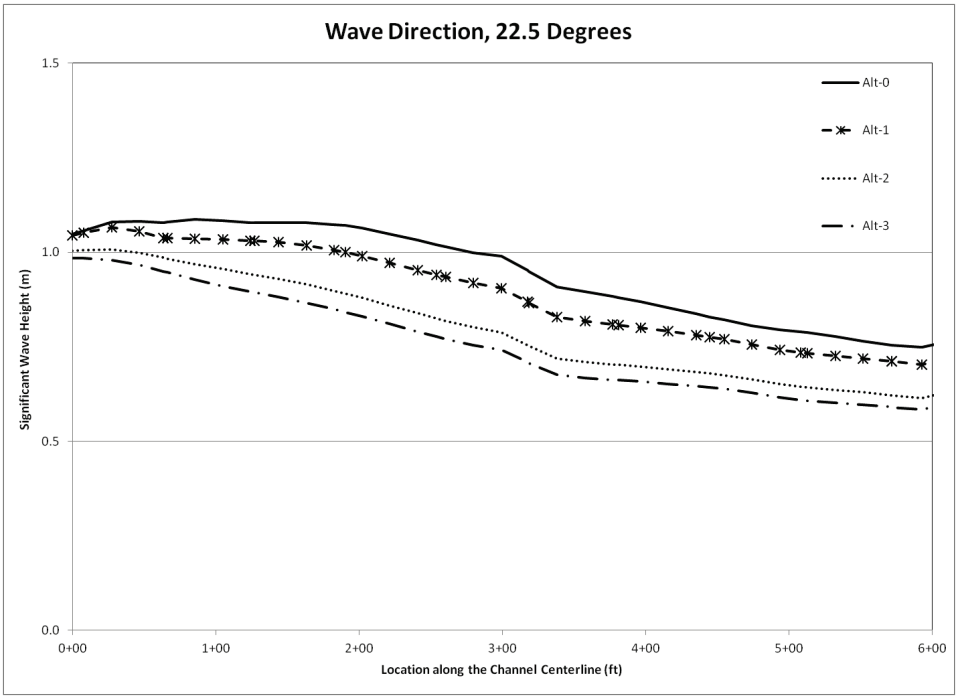

Simulated wave heights along the face of the dock on a transect are shown in Figure 5-8. Figures 5-9 through 5-12 show significant wave heights along the dock face, where the distance 0 m represents the western end of the dock and 30 m the eastern end of the dock. These transect plots show a small reduction in wave heights along the channel centerline for Alt-0 and Alt-1, and Alt-2 and Alt-3 provide a greater reduction in wave heights. Wave heights generally appear to be greater along the western edge of the dock and smaller in the middle of the dock face. The cross-shore wave height profiles for offshore wave heights of 1.0 m, 2.0 m, 2.5 m, 3.0 m, and 3.5 m all are similar for each Alternative and wave direction as shown in Figures 5-9, 5-10, 5-11, and 5-12.

Figure 5-8. Location of Hs output transect (red line) along the face of the dock.

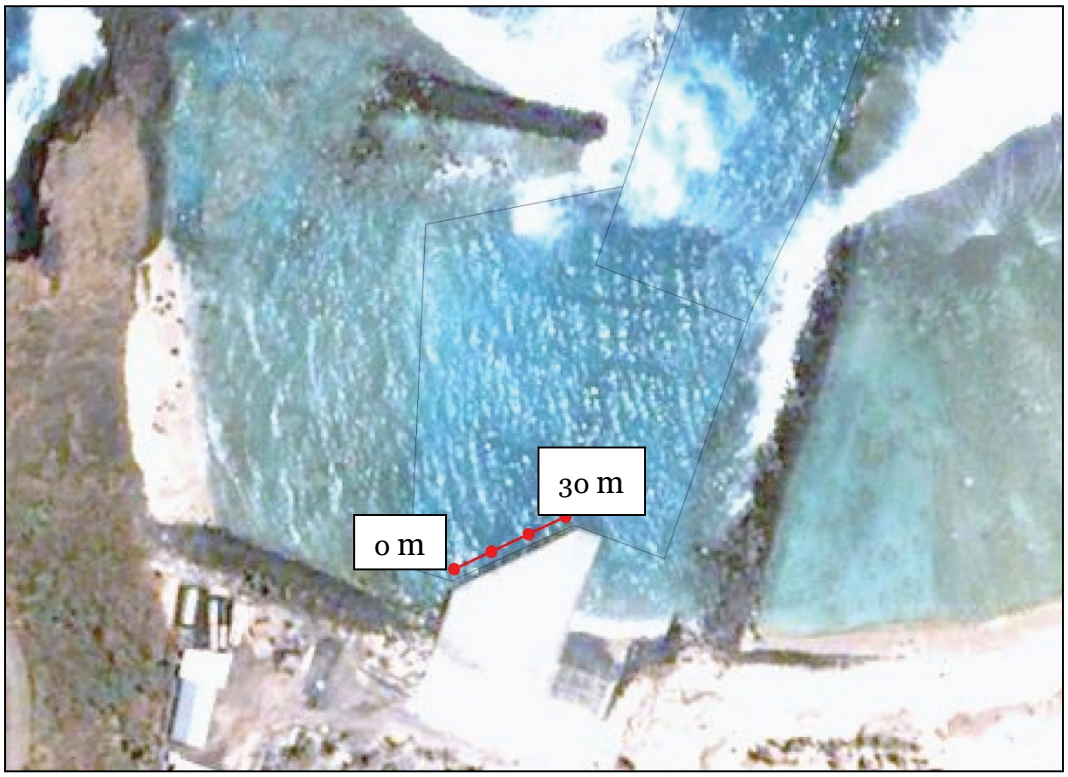

Figure 5-9. Comparison of significant wave heights along the dock face forAlt-0, Alt-1, Alt-2, and Alt-3 for waves approaching from 315° degrees.

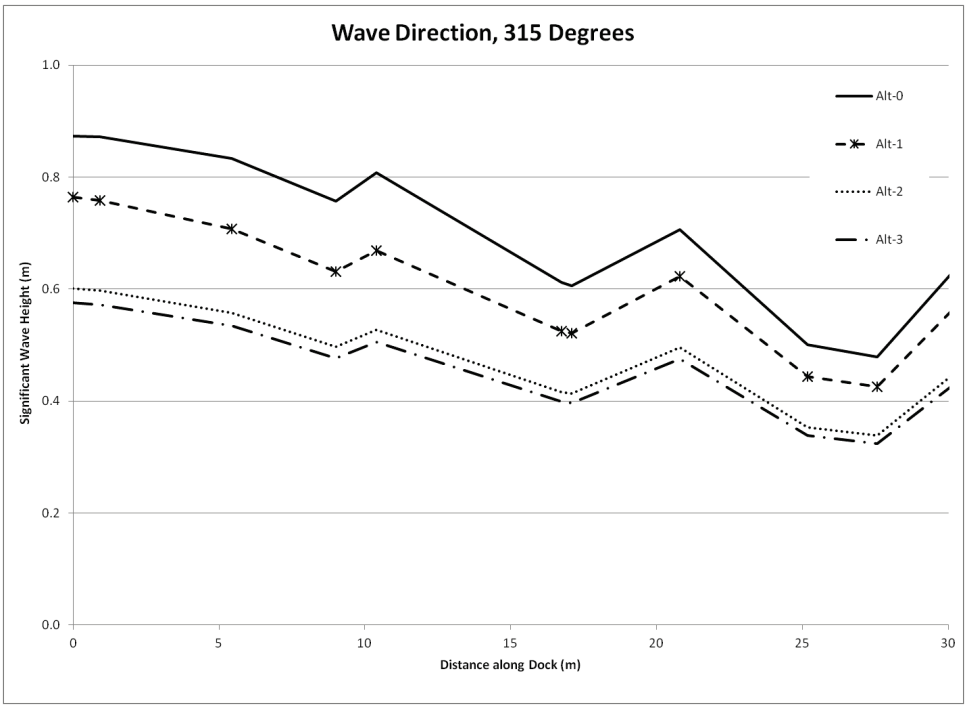

Figure 5-10. Comparison of significant wave heights along the dock face for Alt-0, Alt-1, Alt-2, and Alt-3 for waves approaching from 337.5°.

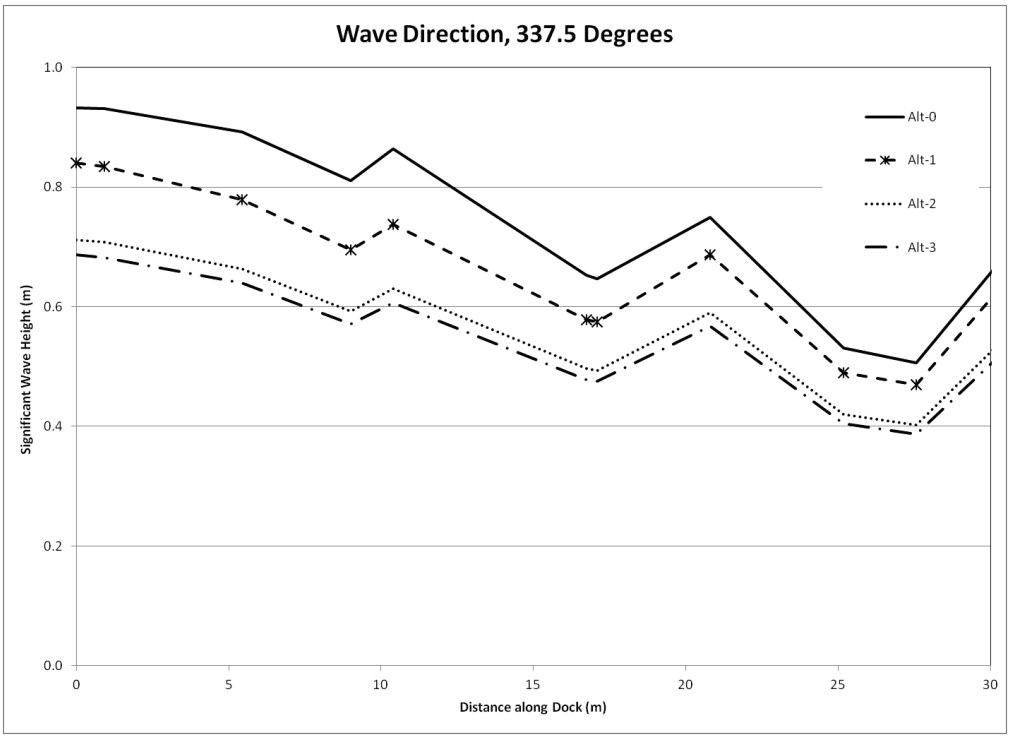

Figure 5-11. Comparison of significant wave heights along the dock face for Alt-0, Alt-1, Alt-2, and Alt-3 for waves approaching from 0° degrees.

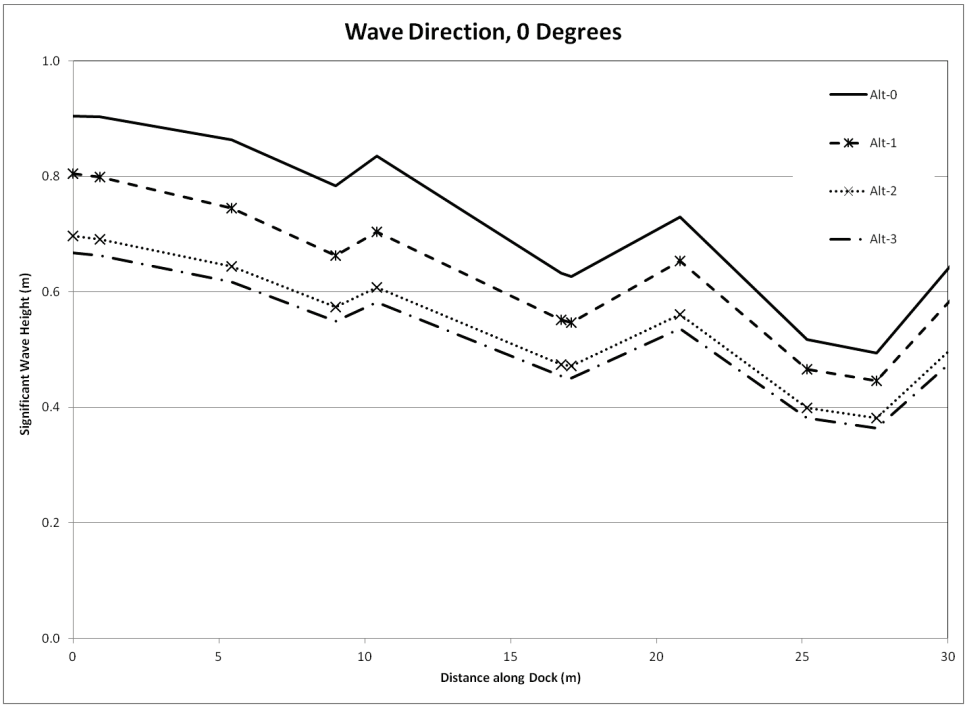

Figure 5-12. Comparison of significant wave heights along the dock face for Alt-0, Alt-1, Alt-2, and Alt-3 for waves approaching from 22.5°.

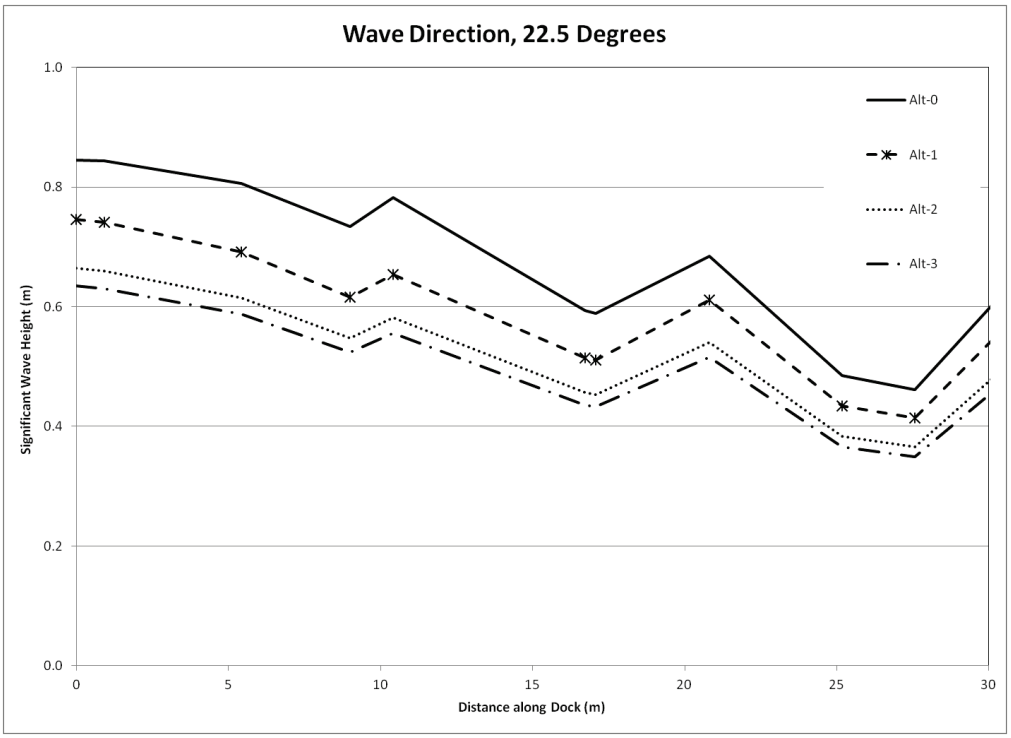

5.3 Comparison of Alternatives for harbor usability

Table 5-2 provides a comparison of the percent average wave height reduction from different wave directions along the channel centerline and along the face of the dock for all four Alternatives. The average percent wave height reduction was used because varying the offshore wave height produced a small change with a standard deviation of approximately 1% to 2% in the wave height reduction.

Table 5-2. Average wave height reduction for Alt-1, Alt-2, and Alt-3 as compared to Alt-0 along the channel centerline and dock.

	Channel Centerline			Dock		
θ	Alt-1	Alt-2	Alt-3	Alt-1	Alt-2	Alt-3
315°	6%	25%	30%	12%	27%	30%
337.5°	6%	25%	28%	11%	25%	29%
0°	6%	21%	26%	15%	24%	28%
22.5°	6%	17%	22%	14%	24%	27%

The proposed channel deepening in Alt-1 reduced wave heights within the entrance channel centerline by 6% and along the dock face by 11%–15%. For typical wave conditions (H_s = 1.5 m and T_p = 10 sec) within the entrance channel (Sta 0+00 to Sta 4+35), there was minimal wave height reduction for all wave directions (0.0 to 0.03 m) between Sta 0+00 to 0+50. There is greater wave height reduction between Sta 0+50 and Sta 4+35, with a maximum wave height reduction of 0.1 m occurring near Sta 3+00 for the modeled offshore wave directions. Within the turning basin (Sta 4+35 to Sta 6+00), wave height reduction is generally less than 0.05 m, with minimal variability in wave height reduction between different locations within the entrance channel and offshore wave directions. Along the dock face wave heights varied from 0.05 to 0.14 m for the modeled wave directions of the typical wave conditions.

Alt-2 reduced wave heights within the entrance channel centerline by 17%–25% and along the dock face by 24%–27%. For typical wave conditions (H_s = 1.5 m and T_p = 10 sec) within the entrance channel the wave height reduction varied from 0.1 to 0.4 m for 315°, 0.1 to 0.4 m for 337.5°, 0.1 to 0.3 m for 0°, and 0.1 to 0.3 m for 22.5°. The smallest amount of wave height reduction was near the start of the entrance channel, and the greatest amount was near Sta 2+00. Within the turning basin, the wave height reduction varied between 0.1 to 0.2 m for the modeled wave

directions. The new breakwater has a greater effect in reducing wave heights from the northwest, reducing waves as they begin to approach from the north and northeast directions. Along the dock face wave heights varied between 0.1 to 0.3 m for the modeled wave directions for typical conditions, with the largest wave height reductions occurring along the western edge of the dock.

Alt-3 reduced wave heights by 22%–30% along the entrance channel centerline and by 27%–30% and along the dock face. For typical wave conditions (H_s = 1.5 m and T_p = 10 sec), the wave height reduction within the entrance channel varied from 0.2 to 0.4 m for 315°, 0.1 to 0.4 m for 337.5°, 0.1 to 0.3 m for 0°, and 0.1 to 0.3 m for 22.5°. The smallest amount of wave height reduction was near the start of the entrance channel, and the greatest amount was near Sta 2+00. The wave height reduction within the turning basin varied from 0.1 to 0.3 m for the modeled wave directions. The wave height reduction with the new breakwater has a greater effect in reducing wave heights from the northwest. The reduction decreases as waves approach from the north and northeast directions. Wave heights along the dock face varied from 0.1 to 0.3 m for the modeled wave directions for typical conditions, with the largest wave height reductions occurring along the western edge of the dock.

The breakwater proposed in Alt-2 and Alt-3 had the greatest wave sheltering effect for the northwestern waves and was less effective for more easterly wave directions. Overall, Alt-3 was 3%–5% more effective than Alt-2 at reducing the wave heights along the entrance channel centerline and along the dock face.

For calculation of the estimates of harbor usability, it was assumed that the harbor is inaccessible (unusable) if either H_s exceeded 2 ft in the entrance channel or 1 ft at the dock area. Table 5-3 lists example results for Alt-0 for waves approaching from 0° (north). For Alt-0, offshore wave heights greater than 1.0 m yielded maximum H_s of 4.8 ft, which exceeded both the 2 ft limit in the entrance channel and 1 ft at the dock. Consequently, based on the two values of thresholds used as harbor operability criteria, the Faleasao Harbor would be unusable for offshore wave heights greater than 1.0 m incident from 0° (true north). The estimated time for harbor inaccessibility is 5.5% for waves from 0° based on the percent occurrence of offshore waves from 0° which exceed the 2 ft height in the entrance channel and 1 ft height at the dock. The same analysis was repeated for Alt-1, Alt-2, and Alt-3, and a total

of 168 simulations were conducted to determine percent estimates of harbor accessibility (usability) for these Alternatives. Detailed results for Alt-0 are listed in Tables 5-2 and 5-3. Summary results for all Alternatives are listed in Tables 5-4, 5-5, and 5-6.

Table 5-3. Summary results for Alt-0 (0° incident wave direction).

		Channel Centerline			Dock		
Incident Hs (ft)	Percent Occurrence	Max Hs (ft)	Max Hs > 2 ft	Unusable Percentage	Max Hs (ft)	Max Hs > 1 ft	Unusable Percentage
<3.3	0.0%	2.9	yes	0.0%	1.78	yes	0.0%
3.3-4.9	0.3%	4.2	yes	0.3%	2.39	yes	0.3%
4.9-6.6	3.9%	5.6	yes	3.9%	2.99	yes	3.9%
6.6-8.2	1.1%	6.9	yes	1.1%	3.44	yes	1.1%
8.2-9.8	0.1%	8.3	yes	0.1%	3.73	yes	0.1%
9.8-11.5	0.0%	9.6	yes	0.0%	4.01	yes	0.0%
Total	5.5%	Total Percent Unusable		5.5%	Total Percent Unusable		5.5%

Table 5-4 provides a summary of the cumulative harbor usability estimates for wave directions which impact Faleasao Harbor. The results indicate 61% usability of the harbor for Alt-0 and Alt-1, 72% for Alt-2, and 75% for Alt-3, respectively.

Table 5-4. Harbor usability for 2 ft allowable maximum wave height in the entrance channel.

	Percent inaccessibility of harbor for different wave directions								
Alternative	315°	337.5°	0°	22.5°	45°	67.5°	90°	Total	Usability (%)
Alt-0	0.8%	2.5%	5.5%	6.8%	9.7%	10.3%	3.1%	38.7%	61.3%
Alt-1	0.8%	2.5%	5.5%	6.8%	9.7%	10.3%	3.1%	38.7%	61.3%
Alt-2	0.8%	2.5%	5.5%	6.8%	9.7%	0.0%	3.1%	28.3%	71.7%
Alt-3	0.8%	2.5%	5.5%	6.8%	9.7%	0.0%	0.2%	25.5%	74.5%

Results listed in Tables 5-3 and 5-4 are highly dependent on the assumed threshold H_s values. The ASG considers 4 ft as the upper limit of wave height for safe navigation in the entrance channel. According to the ASG representatives and pilots, wave heights less than 4 ft in the entrance channel pose no maneuverability issues in the entrance channel and at the dock. For a 4 ft threshold wave height criterion, the percent usability of harbor increases significantly and becomes 85% for Alt-0 and Alt-1 and 86% for Alt-2 and Alt-3.

Because the existing dock is aligned with the entrance channel, it is directly exposed to incoming waves coming through the entrance channel. Based on the 1 ft allowable maximum wave height at the dock, Table 5-5 results indicate the percent usability at the dock is 41% for Alt-0 and Alt-1 and 54% for Alt-2 and Alt-3, respectively.

Table 5-5. Harbor usability for 1 ft allowable maximum wave height at the dock.

	Harbor Inaccessibility Percentage by Wave Direction								
Alternative	315°	337.5°	0°	22.5°	45°	67.5°	90°	Total	Usability (%)
Alt-0	0.8%	2.5%	5.5%	6.8%	9.7%	12.9%	21.1%	59.2%	40.8%
Alt-1	0.8%	2.5%	5.5%	6.8%	9.7%	12.9%	21.1%	59.2%	40.8%
Alt-2	0.8%	2.5%	5.5%	6.8%	9.7%	0.0%	21.1%	46.4%	53.6%
Alt-3	0.8%	2.5%	5.5%	6.8%	9.7%	0.0%	21.1%	46.4%	53.6%

5.4 Future studies

According to ASG, hazardous navigational issues arise when offshore waves exceed the 4 ft threshold in the entrance channel, making access to harbor extremely difficult and challenging. Overall, if navigation in the entrance channel is safe, then the dock is accessible. Because the usability of the dock for the 1 ft maximum wave criterion is very low, consideration should be given to relocating the dock westward and expanding the turning basin to meet the USACE standard criteria. These measures will allow the MV *Sili* to access the dock or safely moor in the more sheltered turning basin area.

The present analysis with the stated assumptions and limitations shows that the percent usability of the harbor is dependent on the two threshold wave heights assumed for safe navigability in the entrance channel and dock area. The preliminary estimates developed for this conceptual-level study cannot be used in design, and a more systematic sensitivity of harbor usability should be performed by using other values of the two threshold wave criteria.

The additional study should be a refined and detailed investigation of waves within the channel and turning basin, and in close proximity of the dock and adjacent areas. The finding of the detailed modeling study should also help to determine whether or not structural modifications (e.g., Alt-2 and Alt-3) are necessary, and optimize the geometries and

dimensions of the proposed breakwaters to improve navigability in Faleasao Harbor.

A sensitivity analysis is necessary to determine a definitive cost/benefit for the proposed structural modifications to harbor. Once an alternative is chosen based on the two operability requirements (1-ft and 2-ft wave height limits mentioned earlier in this chapter), the sensitivity analysis should be used to size and fine-tune the dimensions of structures involved in order to develop reliable cost estimates for final engineering design and construction. A sensitivity study is required because it could produce a significant cost savings by optimizing the structural design issues affecting navigation in the channel and interior areas of harbor.

6 Summary and Conclusions

This report describes details of a numerical wave modeling study conducted for Faleasao Harbor, one of the two harbors on the island of Tau. It is a federally constructed, light- and shallow-draft harbor located on the northwest side of Tau Island in American Samoa. Because of poor navigation conditions at the other harbor (Tau Harbor) caused by large swell waves from south and west during the winter and spring months, Faleasao Harbor is a relief and backup harbor for vessels that need to seek shelter along the west side of Tau. However, the small turning basin and docking space at Faleasao Harbor have limited the use of this harbor by larger vessels, including the largest American Samoa Government boat named MV *Sili*. Three Alternatives were investigated as described herein, each with different types of modifications, to improve navigation at the harbor. In Alt-1 (Figure 3-3), the navigation channel and parts of turning basin were deepened. In addition to the deepening of the channel and mooring basin in Alt-1, two breakwaters were added to the west side of harbor to improve navigation in the harbor. The Alt-2 (Figure 3-3) included a 230 ft breakwater, and Alt-3 had a 280 ft longer breakwater; both were added to the west side of harbor. On the west side, the harbor is protected by a headland peninsula and a breakwater. The peninsula is shore connected, but the breakwater is not since it was damaged by strong currents generated by wave overtopping the peninsula. There is also a short rubble-mound jetty that extends on the east side halfway along the edge of the channel.

Wide coral fringing reefs covering the north and northwest ocean sides of the harbor extend to approximately a 250 ft (70 m) depth before transitioning to deeper water, where offshore depths drop sharply into a deep ocean canyon. Consequently, incident waves are not affected by the bathymetry until they move over the reefs, which serve as natural protection to the harbor. Water depths over the reef decrease as waves propagate over the reef and reach the adjacent shorelines. Shoaling and breaking waves over the reefs generate wave-induced currents that can affect vessels coming into and out of the harbor through the navigation channel.

Two numerical models, CMS-Wave and BOUSS-2D (B2D), were used to develop wave estimates necessary for evaluating the efficacy of proposed Alternatives to improve navigation in the harbor. Chapters 2–4 include description and details of the numerical modeling study, including data

and types of conditions simulated and analyses performed, modeling results, and study findings. Wave estimates inside and outside the harbor were provided for the existing condition (Alt-0) and three Alternatives (Alt-1, Alt-2 and Alt-3). Two structural modifications with the deepening of channel and turning basin were investigated. Estimates of waves at the harbor were developed using the available bathymetric surveys, winds, water levels, and wave hindcast data. CMS-Wave was used in this study to develop incident wave input conditions for B2D model. Wave heights calculated in different areas inside and outside the harbor were used to determine effects of modifications on the usability of Faleasao Harbor. Details of the calculated wave estimates were described in Chapters 3 and 4. The effects of proposed structural Alternatives on waves were quantified in the channel and inner harbor. Impacts of these modifications on harbor usability were described in Chapter 5.

Several improvements to CMS-Wave were made to develop model inputs as well as to address this project's other needs. Implementation of the model improvements was funded by the Coastal Inlets Research Program. They included (a) analysis of wave hindcast, wind, and water level data for simulations of three tropical storms and nonstorm waves in a full-plane mode, (b) modeling of a dual-peaked wave spectrum with seas and swells from different directions, (c) development of pre- and postprocessing analysis codes for improving model setup, (d) development of Fortran and Matlab programs to provide B2D input conditions as wave parameters (height, period, direction) and 2D wave spectra, (e) development of a number of Fortran and Matlab utilities to facilitate the coupling of the two wave models, analyses of models results in time and frequency domain, and (f) development of Matlab codes for comparison of wave spectra plots from solution files of both models.

The utilization of two wave models was necessary to address the needs of this project. In addition to differences between models' theoretical and numerical formulations, different extent and resolution of model grids were necessary to model waves properly for the needs of this project. Despite the stated differences between the wave models, where possible general comparison of outputs from the two models is provided.

The combination of two models was necessary to address the needs of this project. In addition to differences between models' theoretical and numerical formulations, different extents and model grid resolutions were

necessary to investigate waves properly for the needs of this project. Based on model results for Alt-0, Alt-1, Alt-2, and Alt-3, calculated wave heights inside the harbor near structures were generally larger than wave heights calculated in other areas inside the harbor. Outside the harbor to the north and west and in the channel, CMS-Wave calculated wave heights were greater than B2D estimates. These differences in wave height estimates are due to shallow-water wave processes which affect propagation of waves in shallower areas of interior harbor.

B2D results were obtained for the corresponding geometries and bathymetries using finer resolution grids required to model nonlinear wave processes in the harbor. There are differences in wave height between alternatives and existing harbor in the channel, turning basin, and close to the dock. The results indicate that by adding a west breakwater about 250-ft length as in Alt-2 or Alt-3 would significantly reduce wave energy reaching the dock and mooring basin. However, the degree of reduction depends on incident wave direction. The modeling indicates that a 50% reduction in wave height is attainable. Counter to the expectations of ASG representatives, deepening of the channel and turning basin did not increase wave energy near the dock and in the turning basin. Wave height reduction of approximately 10% was obtained by deepening the channel and mooring basin an additional 6 ft. A slight increase in wave energy in the entrance channel occurs near where the breakwater in Alt-2 and Alt-3 comes close to the west side of the channel. The primarily impact of the Alternatives is increased wave diffraction and reflection from the breakwater. Additional impacts of the alternatives include increased wave shoaling, refraction, diffraction and reflection from the channel sides. Effects of structures are evident in B2D results provided in Chapter 4.

In summary, there was a major change in wave heights throughout the harbor for Alt-1 as a result of the channel deepening. An increase in wave heights occurred in the entrance channel for Alt-2 and Alt-3 near the tip of added breakwater. There was no significant increase in wave height in the turning basin or at or near the dock. For Alt-2 and Alt-3, aside from a slight increase of wave height in the entrance channel near the tip of added breakwater, these Alternatives produced a substantial reduction in wave energy in the rest of channel, turning basin, and vicinity of the dock.

Generally, larger wave heights resulted inside the harbor for incident waves from north. For three oblique incident wave directions from NNE,

NNW and WNW, wave heights in the channel, turning basin, and near the dock were comparatively less than normal incident waves from the north. The largest calculated wave heights were obtained over the reefs to the north and northwest, and in the outer half of the entrance channel (along a length of approximately 150 m). Incident waves from N and NNW penetrated into the inner harbor, potentially affecting maneuverability and berthing. Because both Alt-2 and Alt-3 result in a significant reduction of wave energy inside the harbor, either alternative could potentially be a long-term solution for improving navigation in harbor.

Based on B2D model results, in addition to the extent of wave height reduction criterion for improving navigation in Faleasao Harbor, another key factor to consider is the effect of proximity of structures to navigation channel. When a structure is constructed adjacent to a channel, the effects of wave diffraction and reflection must be thoroughly evaluated. The distinct possibility exists that local wave heights will increase. Chapter 4 results indicate a significant increase in wave height in the channel near where structures were situated. This effect is visible for all incident wave directions. Consequently, if the existing breakwater on the west side of the harbor were removed, material from this structure could be used in the construction of the selected Alternative, either Alt-2 or Alt-3. Although model results did not show any detrimental effects of the east breakwater along the channel, this structure could also be removed and material from it used in the construction of the selected Alternative. Moreover, the removal of either or both existing structures would further provide additional maneuvering space within the harbor. Removing these structures would enable widening of the channel to accommodate access to harbor by larger vessels and potentially reduce accidents, collisions, and groundings.

Aside from the impacts of dredging on the reefs inside and outside the harbor, the implementation of Alt-1 is straightforward. Sedimentation in the harbor historically has not been a concern. Channel deepening is neither expected to increase maintenance dredging costs or create increased harbor shoaling. However, the implementation of Alt-2 or Alt-3 presents a few challenges and consequences. The three potential concerns which are worthy of mentioning are: (1) increase in wave action in the entrance channel, (2) reduced maneuvering space in the entrance channel, and (3) risk of boat collisions with the structure. These concerns arise because the structure proposed in Alt-2 or Alt-3 is expected to reflect more wave energy into the channel. Depending on characteristics of superposition of

incident and reflected waves, wave heights in the channel could increase or decrease. An optimization study is necessary to determine appropriate dimensions of the structure and its alignment, and material properties if Alt-2 or Alt-3 is selected. Furthermore, Alt-2 or Alt-3 may reduce the maneuvering area available to the boats in the channel close to the tip of the structure. Minor channel realignment eastward could provide more maneuvering room to avoid grounding and collision of boats with adjacent structures. The channel realignment should be considered together with the structural optimization study to make it a viable option. In addition, Alt-2 or Alt-3 would require the placement of rocks in water depths up to 10 m to 15 m. This can increase construction cost significantly depending on size of structure involved, requiring building the breakwater from an ocean-based platform such as a barge.

In conclusion, two Alternatives (both incorporating structural and channel modifications) were considered in this conceptual-level study to investigate details of waves at Faleasao Harbor. Results clearly show that each Alternative has trade-offs between potential improvements and consequences.

References

Demirbilek, Z., L. Lin, O. Nwogu, W. C. Butler, K. K. Hathaway, and T. D. Smith. 2015. *Kikiaola light-draft harbor monitoring plan, part 2 –Numerical wave modeling for evaluation of alternatives*. ERDC/CHL TR-14-9. Vicksburg, MS: U.S. Army Engineer Research and Development Center.

Demirbilek, Z., L. Lin, and A. Zundel. 2007. *WABED model in the SMS: Part 2. graphical interface*. ERDC/CHL CHETN-I-74. Vicksburg, MS: U.S. Army Engineer Research and Development Center.

Demirbilek, Z., O. G. Nwogu, D. L. Ward, and A. Sanchez. 2009. *Wave transformation over reefs: Evaluation of one-dimensional numerical models*. ERDC/CHL TR-09-1. Vicksburg, MS: U.S. Army Engineer Research and Development Center.

Demirbilek, Z., L. Lin, and O. G. Nwogu. 2008. *Wave modeling for jetty rehabilitation at the mouth of the Columbia River, Washington/Oregon, USA*. ERDC/CHL TR-08-3. Vicksburg, MS: U.S. Army Engineer Research and Development Center.

Demirbilek, Z., and O. G. Nwogu. 2007a. *Boussinesq modeling of wave propagation and runup over fringing coral reefs: Model evaluation report*. ERDC/CHL TR-07-12. Vicksburg, MS: U.S. Army Engineer Research and Development Center.

Demirbilek, Z., O. G. Nwogu, and A. K. Zundel. 2007b. *Infra-gravity wave input toolbox (IGWT): User's guide*. ERDC/CHL CHETN-I-73. Vicksburg, MS: U.S. Army Engineer Research and Development Center.

Demirbilek, Z., O. G. Nwogu, D. L. Ward. 2007c. *Laboratory study of wind effect on runup over fringing reefs. report 1: Data report*. ERDC/CHL TR-07-4. Vicksburg, MS: U.S. Army Engineer Research and Development Center.

Demirbilek, Z., and J. Rosati. 2011. *Verification and validation of the coastal modeling system, report 1: Summary report*. ERDC/CHL TR-11-10. Vicksburg, MS: U.S. Army Engineer Research and Development Center.

Demirbilek, Z., and C. L. Vincent. 2010. Water wave mechanics. In *Coastal Engineering Manual*, Part 2, Chapter 1. EM 1110-2-1100. Washington, DC: U.S. Army Corps of Engineers.

Demirbilek, Z., A. Zundel, and O. Nwogu. 2005a. *BOUSS-2D wave model in SMS: I. graphical interface.*ERDC/CHL CHETN-I-69. Vicksburg, MS: U.S. Army Engineer Research and Development Center.

Demirbilek, Z., A. Zundel, and O. Nwogu. 2005b. *BOUSS-2D wave model in SMS: II. tutorial with examples*. ERDC/CHL CHETN-I-70. Vicksburg, MS: U.S. Army Engineer Research and Development Center.

El Asmar, W., and O. Nwogu. 2006. Finite volume solution of Boussinesq-type equations on an unstructured grid. In *Proceedings 30th International Conference on Coastal Engineering, San Diego, CA*, 73–85.

Lin, L., and Z. Demirbilek. 2005. Evaluation of two numerical wave models with inlet physical model. *Journal of Waterway, Port, Coastal, and Ocean Engineering* ASCE 131(4):149–161.

Lin, L., and Z. Demirbilek. 2012. *Coupled BOUSS-2D and CMS-Wave modeling approach for harbor projects*. ERDC/CHL CHETN-IV-84. Vicksburg, MS: U.S. Army Engineer Research and Development Center.

Lin, L., Z. Demirbilek, H. Mase, and F. Yamada. 2008. *CMS-Wave: A nearshore spectral wave processes model for coastal inlets and navigation projects*. ERDC/CHL TR-08-13. Vicksburg, MS: U.S. Army Engineer Research and Development Center.

Lin, L., Z. Demirbilek, and H. Mase. 2011a. Recent capabilities of CMS-Wave: A coastal wave model for inlets and navigation projects. In Proceedings, Symposium to honor Dr. Nicholas Kraus. *Journal of Coastal Research* Special Issue 59:7–14.

Lin, L., Z. Demirbilek, R. Thomas, and J. Rosati. 2011b. *Verification and validation of the Coastal Modeling System, report 2: CMS-Wave*. ERDC/CHL TR-11-10. Vicksburg, MS: U.S. Army Engineer Research and Development Center.

Nwogu, O. G., and Z. Demirbilek. 2001. *BOUSS-2D: A Boussinesq wave model for coastal regions and harbors*. ERDC/CHL TR-01-25. Vicksburg, MS: U.S. Army Engineer Research and Development Center.

Nwogu, O., and Z. Demirbilek. 2004. Numerical modeling of ship-induced currents in confined waterways. In *Proceedings, 29th International Conference on Coastal Engineering, Lisbon, Portugal*, 256–268.

Nwogu, O., and Z. Demirbilek. 2006. Nonlinear wave interaction with submerged and surface-piercing porous structures. In *Proceedings, 30th International Conference on Coastal Engineering, San Diego, CA*, 287–299.

Nwogu, O., and Z. Demirbilek. 2008. Nonlinear wave transformation and runup over fringing coral reefs. In *Proceedings, 31st International Conference on Coastal Engineering, Hamburg, Germany*.

Nwogu, O., and Z. Demirbilek. 2010. Infragravity wave motions and runup over shallow fringing reefs. *ASCE Journal of Waterway, Port, Coastal, and Ocean Engineering*. (http://dx.doi.org/10.1061/(ASCE)WW.1943-5460.0000050)

Nwogu, O. 1993a. On the generation of infragravity waves by shoaling multidirectional waves. In *Proceedings, 2nd International Symposium on Ocean Wave Measurement and Analysis, ASCE, New York*, 1–14.

Nwogu, O. 1993b. Alternative form of Boussinesq equations for nearshore wave propagation. *Journal of Waterway, Port, Coastal and Ocean Engineering*, ASCE 119(6):618–638.

Nwogu, O. 1994. Nonlinear evolution of directional wave spectra in shallow water. In *Proceedings, 24th International Conference on Coastal Engineering, Kobe, Japan, Vol. 1*, 467–481.

Nwogu, O. G. 1996. Numerical prediction of breaking waves and currents with a Boussinesq model. In *Proceedings,. 25th International Conference on Coastal Engineering, Orlando, Vol. 4*, 4807–4820.

Nwogu, O. G. 2000. Time domain simulation of long-period oscillations in harbors. In *Proceedings, 27th International Conference on Coastal Engineering, Sydney, Australia, Vol. 4*, 3643–3654.

Nwogu, O. 2006. Boussinesq modeling of landslide-generated waves and tsunami runup. In *Advanced Numerical Models For Simulating Tsunami Waves and Runup Advances in Coastal and Ocean Engineering* (ed. P.L.-F Liu, H. Yeh and. C. Synolakis) 10:273–278.

Nwogu, O. 2007. Numerical modeling of waves generated by high-speed vessels in shallow water with a coupled Boussinesq-Panel method. In *Proceedings, 9th International Conference on Numerical Ship Hydrodynamics, Ann Arbor, MI*, 331–343.

Nwogu, O. G. 2009.Interaction of finite-amplitude waves with vertically sheared current fields. *Journal of Fluid Mechanics* 627:179–213.

Sanchez, A., W. Wu, T. M. Beck, H. Li, J. D. Rosati, Z. Demirbilek, and M. Brown. 2011a. *Verification and validation of the Coastal Modeling System, report 4: Sediment transport and morphology change*. ERDC/CHL TR-11-10. Vicksburg, MS: U.S. Army Engineer Research and Development Center.

Sanchez, A., W. Wu, T. M. Beck, H. Li, J. Rosati III, R. Thomas, J. D. Rosati, Z. Demirbilek, M. Brown, and C. Reed. 2011b.*Verification and validation of the Coastal Modeling System, report 3: Hydrodynamics.* ERDC/CHL TR-1-10. Vicksburg, MS: U.S. Army Engineer Research and Development Center.

Appendix A: Description of CMS

The CMS-Wave module of the Coastal Modeling System (CMS) was used for the numerical modeling estimates of waves at Faleasao Harbor. A brief description of the CMS is provided here for completeness.

As shown in Figure A-1, the CMS is an integrated suite of numerical models for waves, flows, and sediment transport and morphology change in coastal areas. This modeling system includes representation of relevant nearshore processes for practical applications of navigation channel performance, and sediment management at coastal inlets and adjacent beaches. The development and enhancement of CMS capabilities continues to evolve as a research and engineering tool for desk-top computers. CMS uses the Surface-water Modeling System (SMS) interface for grid generation and model setup, as well as plotting and post-processing. The Verification and Validation (V&V) Report 1 (Demirbilek and Rosati 2011) and Report 2 (Demirbilek et al. 2007; Lin and Demirbilek 2012, 2005; Lin et al. 2011a, 2011b, 2008).

Figure A-1. The CMS framework and its components.

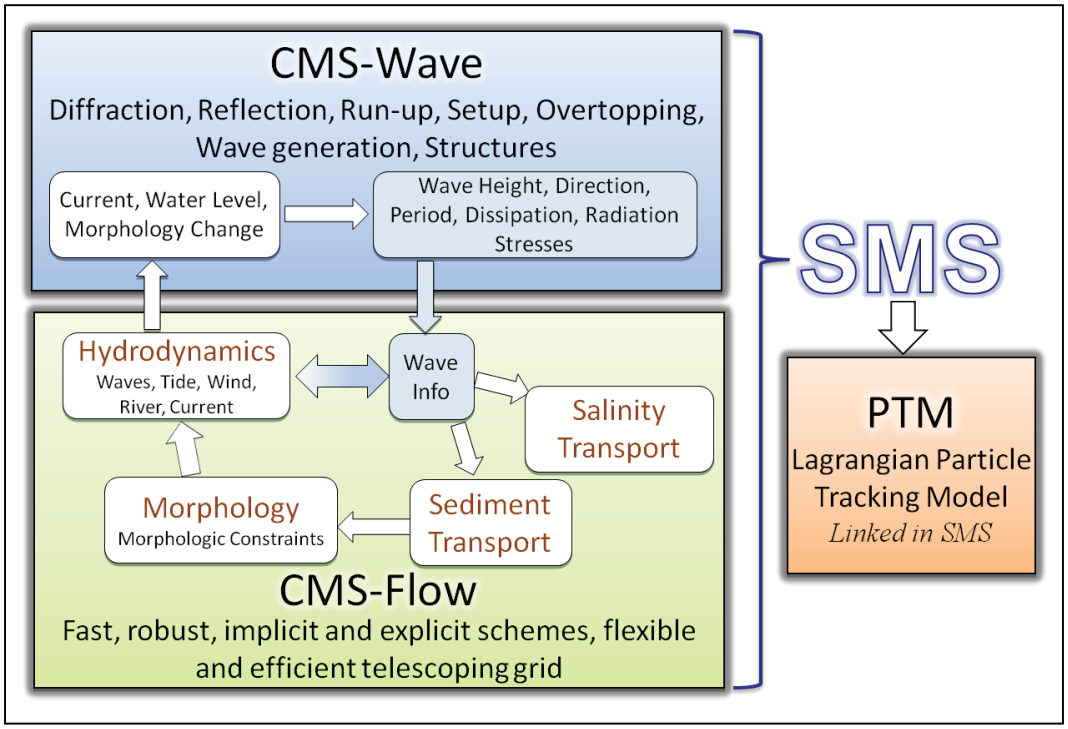

CMS uses the Surface-water Modeling System (SMS) interface for grid generation and model setup, as well as plotting and postprocessing. The

Verification and Validation (V&V) Report 1 (Demirbilek and Rosati 2011) and Report 2 (Lin et al. 2011) have detailed information about the CMS-Wave features and evaluation of model's performance skills in a variety of applications. Report 3 and Report 4 by Sanchez et al. (2011a and 2011b) describe coupling of wave-flow models and hydrodynamic and sediment transport and morphology change aspects of CMS-Flow. The performance of the CMS for a number of applications is summarized in Report 1, and details are described in the three companion V&V Reports 2, 3, and 4.

The CMS-Wave, a spectral wave model, is used in this study given the large extent of modeling domain over which wave estimates were required. Details of the wind-wave modeling are described in Chapter 3 of this report. The main wave processes included in the CMS-Wave are wind-wave generation and growth, diffraction, reflection, dissipation due to bottom friction, white-capping and breaking, wave-current interaction, wave runup, wave setup, and wave transmission through structures. The height and direction of waves approaching the Faleasao Harbor entrance channel change due to wave shoaling, refraction, diffraction, reflection, and breaking. Waves propagating through the entrance interact with bathymetry, surrounding land features, currents and coastal structures. These changes to waves affect waves propagating into the access channel and interior of harbor and bed shear stresses and sediment mobility in these areas.

CMS-Wave model solves the steady-state wave-action balance equation on a nonuniform Cartesian grid to simulate steady-state spectral transformation of directional random waves at and around the Faleasao Harbor. CMS-Wave is designed to simulate wave processes with ambient currents in navigation channels, coastal inlets, and harbors. The model can be used either in half-plane or full-plane mode for spectral wave transformation (Lin et al. 2008; Demirbilek et al. 2007b). The half-plane mode is default because in this mode CMS-Wave can run more efficiently as waves are transformed primarily from the seaward boundary toward shore. See Lin et al. (2011, 2008) for features of the model and step-by-step instructions with examples for application of CMS-Wave to a variety of coastal inlets, ports, structures, and other navigation problems. Publications listed in the V&V reports and this report provide additional information about the CMS-Wave and its engineering applications. Additional information about CMS-Wave is available from the CIRP website:

http://cirp.usace.army.mil/wiki/CMS-Wave

Since the flow model was not used in this study, only brief information is provided. The CMS-Flow is a 2D, shallow-water wave model that can be used for hydrodynamic modeling (calculation of water level and current). Both the explicit and implicit versions of flow (circulation) model are available to provide estimates of water level and current given the tides, winds, and river flows as boundary conditions. CMS-Flow calculates hydrodynamic (depth-averaged circulation) sediment transport and morphology change and salinity due to tides, winds, and waves.

The hydrodynamic model solves the conservative form of the shallow-water equations that includes terms for the Coriolis force, wind stress, wave stress, bottom stress, vegetation flow drag, bottom friction, wave roller, and turbulent diffusion. Governing equations are solved using the finite volume method on a nonuniform Cartesian grid. Finite-volume methods are a class of discretization schemes, and this formulation is implemented in finite-difference for solving the governing equations of coastal wave, flow, and sediment transport models. See the V&V Reports 3 and 4 by Sanchez et al. (2011a and 2011b) for the preparation of the flow model at coastal inlet applications. Additional information about CMS-Flow is available from the CIRP website:

http://cirp.usace.army.mil/wiki/CMS-Flow

Although hydrodynamic, sediment transport, and morphology change modeling were not considered in this study, it is noted for future reference that there are three sediment transport models available in CMS-Flow: a sediment mass balance model, an equilibrium advection-diffusion model, and a nonequilibrium advection-diffusion model. Depth-averaged salinity transport is simulated with the standard advection-diffusion model and includes evaporation and precipitation. The V&V Reports 1 through 4 describe the integrated wave-flow-sediment transport and morphology change aspects of CMS-Flow. The performance of CMS-Flow is described for a number of applications in the V&V reports.

Appendix B: Description of BOUSS-2D

The Boussinesq wave model BOUSS-2D (abbreviated as B2D) is an advanced modeling approach for nonlinear wave propagation nearshore (Nwogu and Demirbilek 2001). This technology was developed and implemented in the Surface-water Modeling System (SMS) in 1990s through early 2000 and has since been used by Districts for navigation channels, inlets, harbors, coastal structures, moored vessels, floating breakwaters, and wave runup and overtopping on revetments, shorelines, and levees. Recent publications describe different applications of B2D model (Demirbilek et al. 2015, 2009, 2008, 2007a, 2007b, 2007c, 2005a, 2005b; Nwogu and Demirbilek 2010, 2008, 2006, 2004; Nwogu 2009, 2007, 2006, 2000, 1996, 1994, 1993a, 1993b; El Asmar and Nwogu 2006). Additional information about B2D is available from these and other related publications in the References section of this report.

B.1 Types of problems for B2D application

The list below shows types of wave problems that can be simulated using Boussinesq wave models:

- harbor/port/marina problems: harbor resonance, harbor and marina infrastructure modifications
- generation of wave sub- and superharmonics
- wave dissipation over porous media
- wave reflection and diffraction from structures, shorelines, and variable surfaces
- wave-wave interactions in shallow water
- channel deepening/widening/realignment
- wave-structure interactions: levees, flood walls, barriers, revetments, seawalls, groins, and breakwaters design and repair (coastal and inland)
    - wave runup/overtopping
    - structure loading (wave forces)
    - structure freeboard requirements
    - frictional dissipation (i.e., waves on vegetated surfaces)
    - wave interaction with array of structure types
    - embankment stability
    - wave interaction with complex geometries of levees, navigation channels and canals, ports/harbors, etc.

- inundation mapping: overland propagation and runup
- bore propagation through rivers and canals
- transient waves (tsunamis, sneaker waves)
- vessel-generated waves and ship wakes
    - vessel-generated waves and effect on shorelines
    - vessel-generated bed velocities and shear stresses
    - vessel interactions with other vessels and with locks and dams.

A few example applications are shown at the end of Appendix B.

B.2 Background

B2D model was used for numerical modeling of wave estimates at Faleasao Harbor. The POH study plan in Chapter 1 described the purpose of numerical modeling tasks while the implementation details of the wave modeling tasks were provided in Chapter 4. Only a brief description of the B2D features is provided here for completeness because details of model theory, numeric, and examples are available from the references listed.

Boussinesq models are essentially shallow-water models with extra dispersive and nonlinear terms. They excel under conditions of nonlinearity (large and/or long waves in shallow depths). Processes modeled well by Boussinesq models include nearshore wind-wave propagation, harbor resonance, nonlinear shoaling, runup and inundation, nearshore circulation, and tsunami. Because Navier-Stokes models are not practical for field-scale problems, Boussinesq models presently are the computational tools for calculating runup and overtopping of vertical or near-vertical walls or impulsive forces on structures. Boussinesq models can propagate vessel-generated waves if a source term is added for generation (i.e., moving pressure source or internal boundary). Boussinesq models are much better at this than shallow-water models because they include both short- and long-waves whereas shallow water wave equations (SWWEs) can only represent the long-wave component of the vessel-induced disturbances.

The B2D computes changes to waves caused by shoaling and refraction over variable bathymetry, reflection, and diffraction from shorelines and structures, and nonlinear wave-current and wave-wave interactions. The internal Boussinesq equations defining the B2D do not contain adjustable parameters. Potential errors are introduced in numerical discretization of

mathematical equations, imperfect boundary conditions, and physical processes that contain process-specific parameters, such as wave turbulence, dissipation, bottom friction, and boundary reflectivity. The B2D needs field data because it can simulate processes that cannot be properly scaled in physical models, and consequently, these B2D model parameters are best calibrated with field data since they may not be estimated well by physical models (i.e., laboratory experiments) due to scaling effects. In the absence of field data, physical model data if available could be used in B2D for validation and calibration of boundary conditions, material parameters, and numerical algorithms. Generally, errors in the nearshore wave estimates come from two sources: input to the model and the model itself, including errors in the incident wave conditions, bathymetry, and boundary specifications. The largest errors are associated with the specification of incident wave parameters and simplification of wave breaking, dissipation processes, and contamination from model boundaries.

The B2D provides spatially and temporally varying wave, current, and water level parameter estimates for engineering problems. Estimates include significant wave height, peak period and direction, wave spectrum, time-series of surface elevation, velocity and pressure, and wave-induced circulation. B2D model interface is operational in the SMS for grid generation and visualization of model results. The custom-built SMS interface of B2D allows users to set up and run the model in an intuitive manner, with built-in safeguards (Demirbilek et al. 2005a, 2005b). The B2D can be run on PCs, workstations, and super-computers.

The B2D consists of a set of comprehensive numerical modeling systems based on a time-domain solution of Boussinesq-type equations for simulating waves (wind-waves and vessel-generated waves) and their propagation in coastal regions, harbors, and waterways. The B2D represents most of wave phenomena of interest in the nearshore zone for navigation projects, inlets, harbors, levees, structures, reefs, wetlands, ship wakes, wave-ship-bank interactions, and wave-current-structure interactions. The B2D-based engineering analysis systems may be used in navigation infrastructure design with a risk-based probabilistic design approach to evaluate life-cycle cost of Alternatives, operation, and maintenance of coupled systems in deciding the benefit or negative consequences of structures in projects. The B2D has capability of replacing considerably more expensive physical models, with flexibility and generality for extension

to sediment transport and morphology change, channel infilling, and water-quality issues. The Corps Operation and Maintenance (O&M) budget for dredging navigation channels and expansion of ports/harbor economic capacity will continue to increase with calls for deepening and widening channels and harbors to accommodate future fleets having larger vessels and drafts and larger and faster boats. Vessel-to-vessel and vessel-to-bank interactions and risk of accidents will also increase with these demands. Aging and natural deterioration of navigation structures increases vessel transit and maneuvering risks along the high-traffic shipping routes, channels, and ports.

Numerical models that solve Boussinesq-type water-wave evolution equations are commonly used to investigate surface wave propagation and transformation in coastal regions. Most of the models use finite difference schemes to discretize the equations over uniformly spaced rectangular grids (i.e., Nwogu and Demirbilek 2001). The popularity of finite difference schemes is largely based on their simplicity and ease of implementation. However, the use of structured grids can severely restrict the potential application of such models to complex boundary problems such as coastal flooding over complex topography, wave propagation in curved channels, wave interaction with coastal structures of arbitrary shape, and wave agitation in harbors of arbitrary shape. Because unstructured grids provide users the flexibility of modeling complex geometries, and the grid resolution can be refined where needed such as near structures or in shallow regions, it was therefore highly desirable to develop an unstructured-grid version of the finite-difference B2D model used in civil and military works. The development of an unstructured-grid, finite-volume version of B2D has been completed. This new model is being tested on super-computers, and its interface in SMS is under development.

The B2D is designed to simulate wave processes with ambient currents at coastal inlets and in navigation channels. The model can be used for spectral wave transformation. See Lin and Demirbilek (2012) for step-by-step instructions for examples of coupled B2D and CMS-Wave modeling approach to harbor projects and other applications to coastal inlets, ports, structures, and other navigation problems. See Nwogu and Demirbilek (2001), Demirbilek et al. (2005a and 2005b), and other publications listed in the References for further information about the B2D and its engineering applications. Additional information about CMS-Wave is also available from these websites:

http://cirp.usace.army.mil/wiki/BOUSS-2D

http://www.xmswiki.com/xms/SMS:BOUSS-2D

In this study, the coupled B2D model was used for wave modeling nearshore to evaluate merits of eight proposed Alternatives to improve conditions inside the Existing Harbor. Details of B2D modeling are described in Chapter 4 of this report.

B.3 Example applications

The images in Figures B-1 through B-10 show some recent examples of B2D model applications. See References for other types of applications.

Figure B-1. BOUSS-2D calculated wave-induced current field for Pillar Point Harbor, CA.

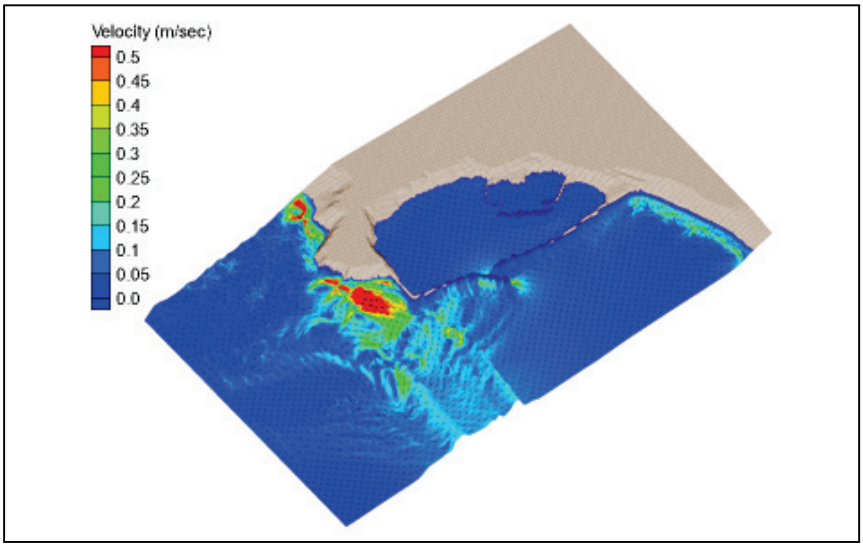

Figure B-2. Calculated wave fields by (a) BOUSS-2D, and (b) CMS-Wave at Point Judith Harbor, RI, for incident wave from SSE.

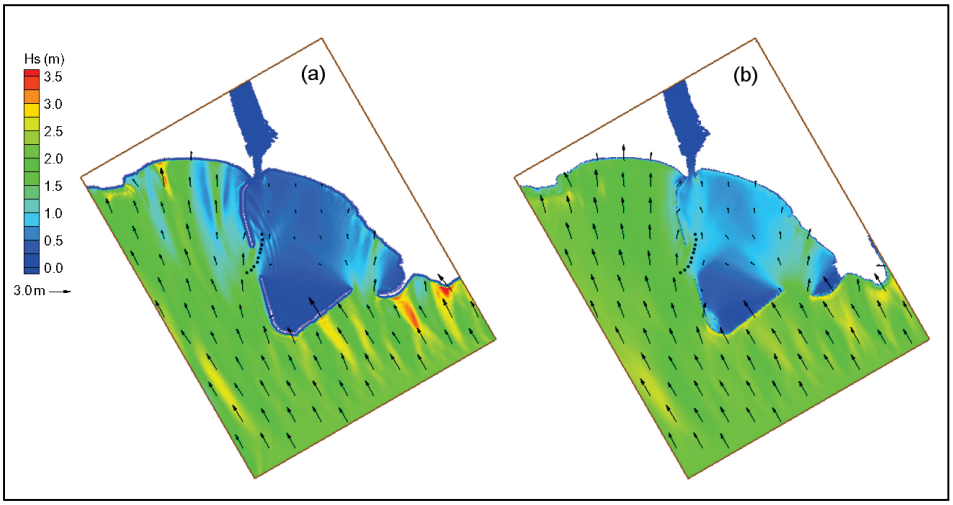

Figure B-3. Wave propagation inside a bay.

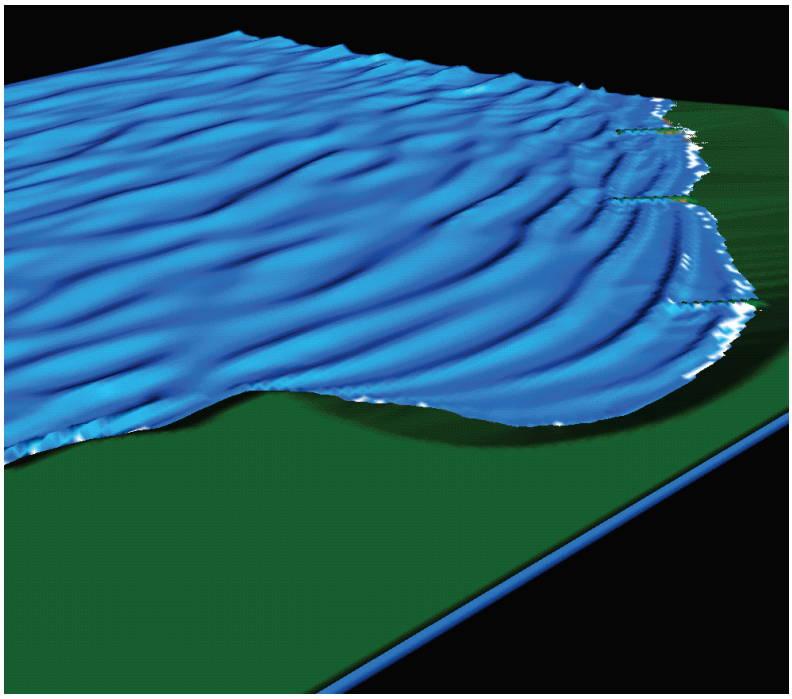

Figure B-4. Wave field around a detached breakwater.

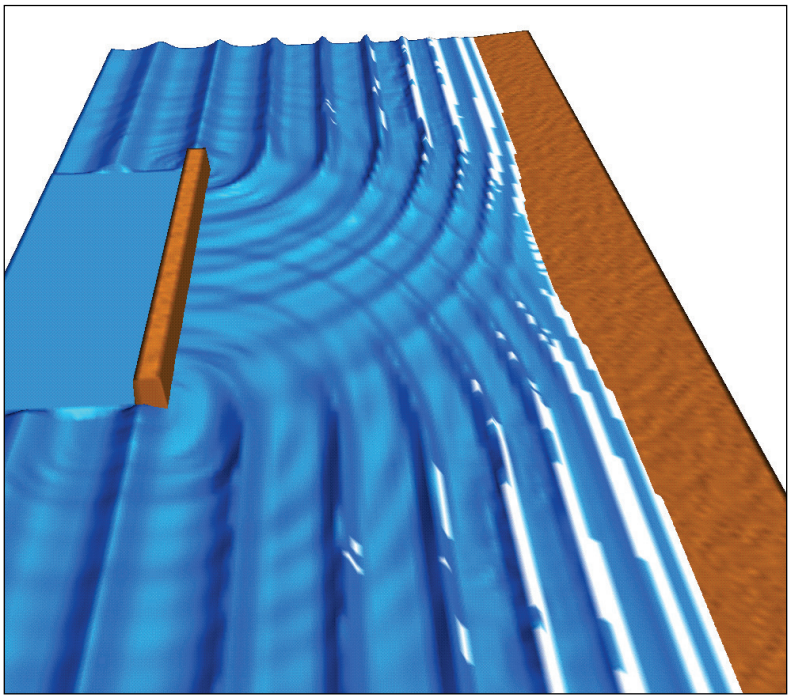

Figure B-5. Waves, wave-induced current, and circulation near a reflective jetty of an inlet.

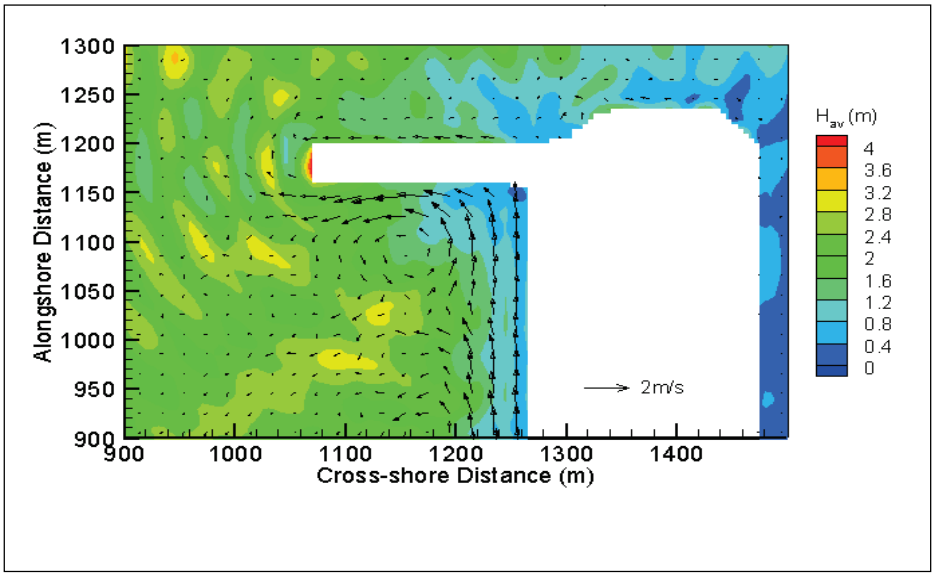

Figure B-6. Wave-induced current field developed between two groins placed on a beach.

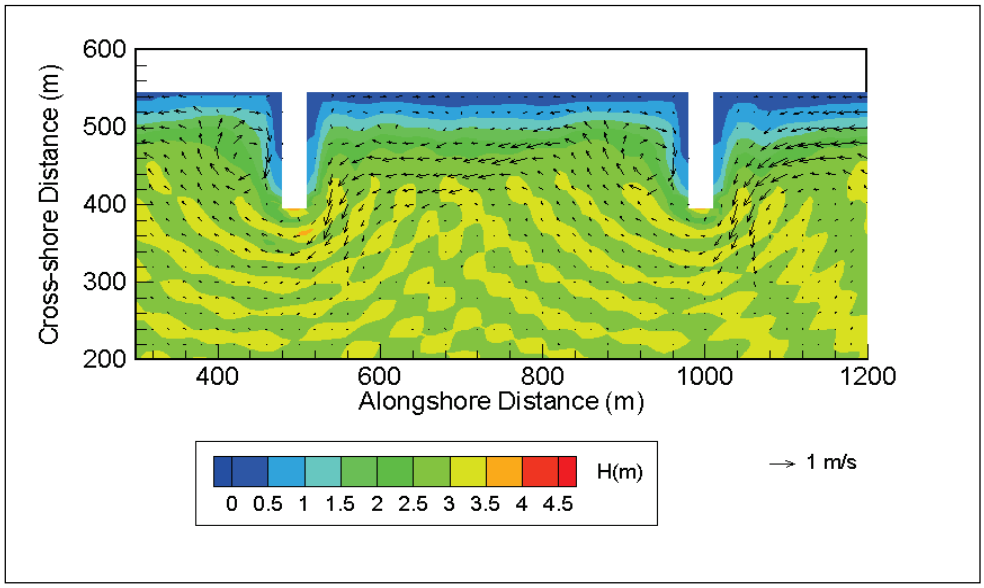

Figure B-7. Multiple ships moving (in transit) in a harbor.

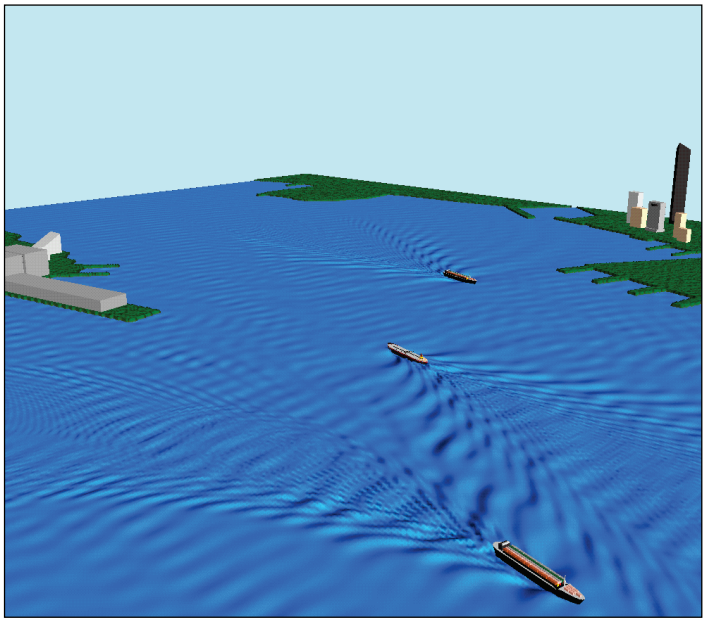

Figure B-8. BOUSS-2D domain for the Oyster Point Marina, CA, entrance and east marina.

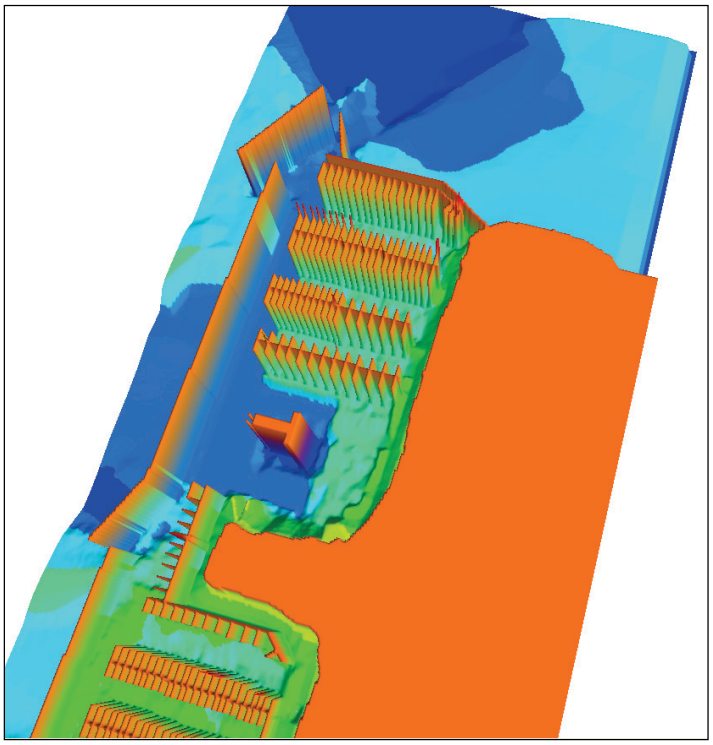

Figure B-9. BOUSS-2D grid for changes to entrance of Diversey Harbor, MI.

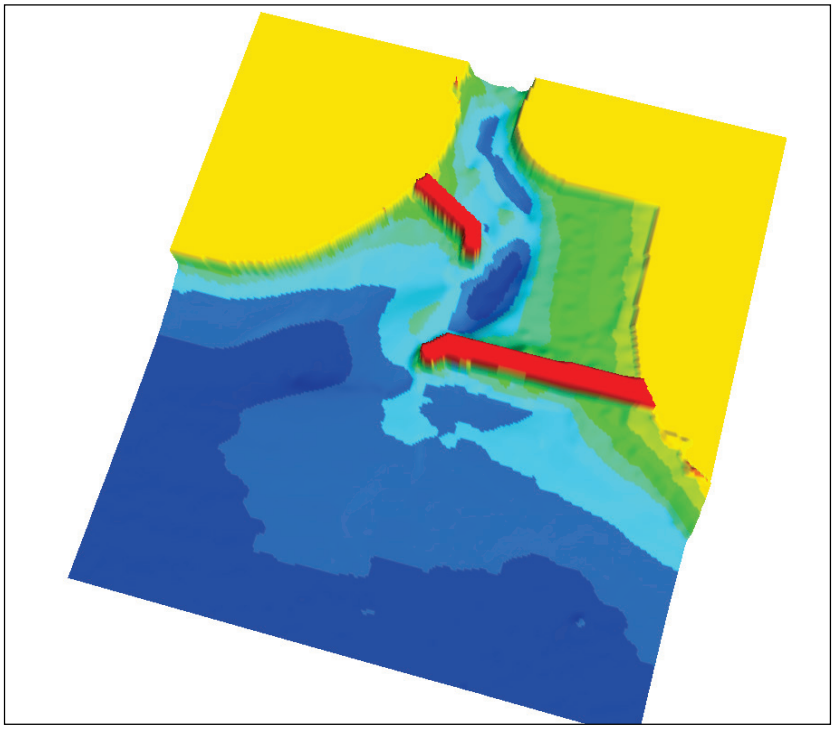

Figure B-10. BOUSS-2D runup/overtopping toolbox in SMS for a fringing reef application.

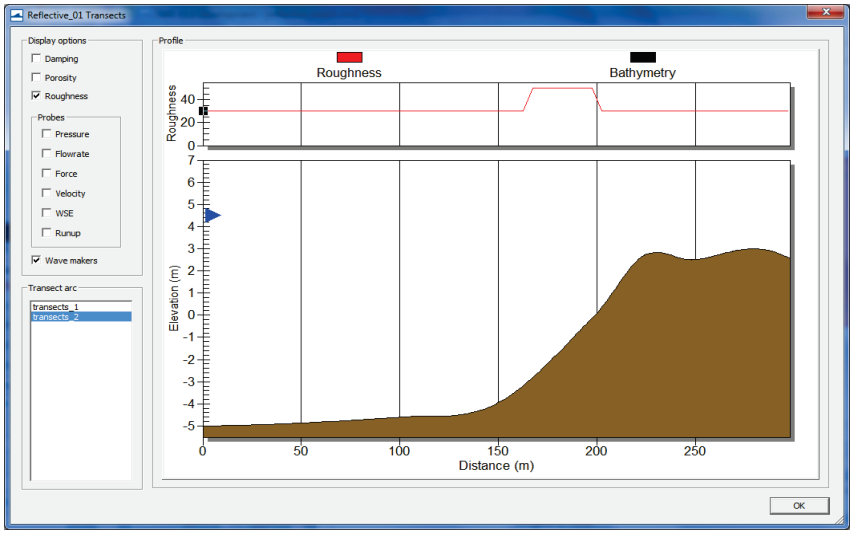

REPORT DOCUMENTATION PAGE

Form Approved OMB No. 0704-0188

1. REPORT DATE	2. REPORT TYPE	3. DATES COVERED *(From - To)*
November 2015	TR	

4. TITLE AND SUBTITLE
Infrastructure Modification for Improving Navigation at Faleasao Harbor in American Samoa

5a. CONTRACT NUMBER

5b. GRANT NUMBER

5c. PROGRAM ELEMENT NUMBER

6. AUTHOR(S)
Zeki Demirbilek, Lihwa Lin, Okey G. Nwogu, Justin A. Goo, and Thomas D. Smith

5d. PROJECT NUMBER

5e. TASK NUMBER

5f. WORK UNIT NUMBER

7. PERFORMING ORGANIZATION NAME(S) AND ADDRESS(ES)
Coastal and Hydraulics Laboratory
US Army Engineer Research and Development Center
3909 Halls Ferry Road
Vicksburg, MS 39180-6199

8. PERFORMING ORGANIZATION REPORT NUMBER
ERDC/CHL TR-15-15

9. SPONSORING/MONITORING AGENCY NAME(S) AND ADDRESS(ES)
U.S. Army Engineer District, Honolulu
Building T223 Fort Shafter, HI 96858

10. SPONSOR/MONITOR'S ACRONYM(S)

11. SPONSOR/MONITOR'S REPORT NUMBER(S)

12. DISTRIBUTION/AVAILABILITY STATEMENT
Approved for public release; distribution is unlimited

13. SUPPLEMENTARY NOTES

14. ABSTRACT

This report describes details of a numerical modeling study conducted to evaluate impacts of infrastructure modifications for improving navigation in Faleasao Harbor in American Samoa. The existing harbor and three proposed infrastructure modifications (Alternatives) were investigated. This small, federally constructed, shallow-draft harbor is located on the northwest coast of Tau Island, the largest island in the American Samoa islands chain. Navigation in the harbor is affected by waves passing over reefs located to the north and northwest of the harbor. Swells from the north and northwest undergo shoaling and breaking on the reefs, which generate unfavorable conditions to boats entering and leaving the harbor. The shallower harbor entrance area is flanked on the west by a rocky natural headland and an unraveling detached west breakwater that is now a disconnected spur. A jetty along the east side of the navigation channel extends a short distance northeast from the boat launching ramp. These structures protect the harbor interior from waves and currents and reduce sedimentation. Smaller vessels access the harbor through a narrow navigation channel approximately 300 m long, 40 m wide, and 4 m deep. The south end of the channel connects to a small turning/mooring basin where vessels can turn or moor at the dock. Wave processes in both exterior and interior areas of the harbor were investigated in this scoping-level study to determine benefits and consequences of three proposed infrastructure modifications for improving navigation in the harbor. These include deepening of the navigation channel and turning basin and adding structures to the tip of west peninsula. Modeling results indicated that the modifications reduced wave energy in the harbor and improved navigation in the channel, turning basin, and dock areas, thereby ensuring access by larger vessels to the harbor. Under typical weather conditions with the proposed modifications, wave estimates obtained indicated that the American Samoa Government's (ASG) largest vessel MV *Sili* would be able to access the harbor. Preliminary wave estimates for design and repair of infrastructures were also provided.

15. SUBJECT TERMS

Navigation, Small-boat harbor, Wave modeling for planning and operations, Harbor access/usability, CMS-Wave, BOUSS-2D model, Structural design

16. SECURITY CLASSIFICATION OF:			17. LIMITATION OF ABSTRACT	18. NUMBER OF PAGES	19a. NAME OF RESPONSIBLE PERSON
a. REPORT	b. ABSTRACT	c. THIS PAGE			ZEKI DEMIRBILEK
UNCLASSIFIED	UNCLASSIFIED	UNCLASSIFIED	UNCLASSIFIED	181	19b. TELEPHONE NUMBER *(Include area code)* 6016343226